# Institut für Wasserbau · Universität Stuttgart

Mitteilungen

Heft 203   Oinam Bakimchandra

Integrated Fuzzy-GIS approach for
assessing regional soil erosion risks

Integrated Fuzzy-GIS approach for assessing regional soil erosion risks

Von der Fakultät Bau- und Umweltingenieurwissenschaften der
Universität Stuttgart zur Erlangung der Würde eines
Doktor-Ingenieurs (Dr.-Ing.) genehmigte Abhandlung

Vorgelegt von
Oinam Bakimchandra
aus Imphal, Manipur, India

Institut für Wasserbau der Universität Stuttgart
2011

Heft 203   Integrated Fuzzy-GIS approach
for assessing regional soil
erosion risks

von
Dr.-Ing.
Oinam Bakimchandra

D93   Integrated Fuzzy-GIS approach for assessing regional soil erosion risks

Acknowledgements

Table of contents

List of Figures

List of Tables

Abbreviations

AERI	Actual Erosion Risk Index
AHP	Analytical Hierarchy Process
CASiMiR	Computer Aided Simulation Model for Instream flow Requirements
CPC	Climate Prediction Centre
CoG	Centre of Gravity
DBF	Database File
DoF	Degree of Fulfilment
EEA	European Environment Agency
ETM	Enhanced Thematic Mapper
ESDI	Earth Science Data Interface
ESB	European Soil Bureau
EPIC	Erosion Productivity Impact Calculator
EVI	Enhanced Vegetation Index
EHRS	Ethiopian Highlands Reclamation Study
FMWR	Federal Ministry of Water Resources, Ethiopia
FAO	Food and Agriculture Organization (United Nations)
F-WERCAM	Fuzzy-Water Erosion Risk Classification and Assessment Model
FEWS-NET	Famine Early Warning System- Network
GLFC	Global Land Cover Facility
GLASOD	Global Assessment of Human Induced Soil Degradation
GIS	Geographical Information System
GPS	Global Positioning System
HILK	Highly Interpretable Linguistics Knowledge
ILRI	International Livestock Research Institute
ITCZ	Inter Tropical Convergence Zone
IDW	Inverse Distance Weighting
LADA	Land Degradation Assessment in Dry Lands
LULC	Land Use and Land Cover
MLC	Maximum Likelihood Classifier
MSS	Multi Spectral Sensor
MCDM	Multi Criteria Decision Making Technique
MUSLE	Modified Universal Soil Loss Equations
MODIS	Moderate Resolution Imaging Spectroradiometer
NOAA	National Oceanic and Atmospheric Administration
NMSA	National Meteorological Services Agency, Ethiopia
NDVI	Normalized Difference Vegetation Index
PERI	Potential Erosion Risk Index
RB	Rule Base
ROI	Region of Interest
RFE 2.0	Rainfall Estimates ver.2.0
RS	Remote Sensing
RUSLE	Revised Universal Soil Loss Equations
SPI	Soil Protection Index

SRTM Shuttle Radar Topography Mission
SBRE Satellite Based Rainfall Estimates
TRMM Tropical Rainfall Measuring Mission
TOVAS TRMM Online Visualization and Analysis System
TWI Topographic Wetness Index
USGS United State Geological Survey
UTM Universal Transverse Mercartor
USLE Universal Soil Loss Equation
WGS World Geodetic System

Abstract

Modelling a dynamic and physical process, such as soil erosion, is prone to errors and problems. The availability of the right kind of data source, quality of data used, scale issues in modelling, measurement errors etc. and the complexity of the model in itself are some of the issues that are explicitly addressed and reported in soil erosion research studies. Existing soil erosion models based on physical processes are very data demanding in both their amount of variables and their temporal and spatial resolution requirements. Hence, data scarcity and lack of reliable data tend to pose a problem for successful application of physical based erosion models. On the other hand, less data demanding empirical based models are developed for a certain environmental set up using erosion plot studies and thus their applicability is restricted to regions where they were developed. Another significant aspect that is overlooked in many past soil erosion risk assessment studies is the nature of the various environmental control parameters involved in modelling, which are fuzzy in reality. When mapping erosion risk, the introduction of fuzzy sets instead of crisp sets to define classes (i.e. degree of hazard or risk) will help to incorporate a degree of fuzziness within each class of the governing parameters. It is found that various existing soil erosion risk models consider each feature and spatial units present on the landscape or catchment as having distinct boundaries. In reality, the existing natural boundaries are much more complex. To cope with such problems of class boundaries and to incorporate the expert knowledge that can represent the processes under investigation, there is a need of fuzzy logic based modelling approach.

A large amount of datasets that represent climate, topographic and anthropogenic factors are a basic requirement for environmental modelling, regardless of the types of processes to be modelled in a landscape. With the advancement in technology, remote sensing data products provide the necessary data in regional and global scale, and act as a complementary dataset with reference to ground measured data. The development in geospatial technology gives the flexibility to integrate, analyze and visualize various data in a spatial and temporal scale. GIS provides the framework to spatially model and deliver the results in a more interpretable manner to the end user. Hence, a fuzzy logic based modelling approach using remote sensing data products along with limited ground data in a GIS environment is attempted in this PhD research to address the issues of water induced soil erosion risk in a regional landscape environment.

In this PhD research, a simple and efficient fuzzy logic-based soil erosion risk model for monitoring the soil erosion risk distribution over a regional landscape is developed. The developed model is known as **F**uzzy-**W**ater **E**rosion **R**isk **C**lassification and **A**ssessment **M**odel (F-WERCAM). As the name indicates, this model is intended for water based soil erosion risk classification and their assessment using a fuzzy logic modelling concept in a GIS platform. The model is designed or set up in such a way that it has minimum input data requirements for model execution, provided the considered input parameters are the main primary governing factors that influence the soil erosion risk of a region.

Every soil erosion assessment model must represent how the governing parameters of climate, soil, topography, and land use affect soil loss and related variables. Land Use and Land Cover (LULC) map, Normalized Difference Vegetation Index (NDVI) as proxy for vegetation cover distribution,

annual rainfall erosivity map, soil erodibility map and slope gradient are used as the input model parameters. The identification of the influential parameters considered in this model is based on literature and expert knowledge. Since the developed model is based on the underlying principle of fuzzy logics, accessing the knowledge base related to the soil erosion process and developing the corresponding fuzzy sets and fuzzy rules becomes one of the most important tasks in this study. In this aspect, detailed literature review of the soil erosion processes over a regional landscape and expert-based questionnaires obtained from various scientific professionals in soil erosion research provides the background for the formulation of fuzzy sets and fuzzy rules.

One of the salient features in the F-WERCAM is the multi-stage modelling approach. It consist of 3 stages namely, Stage 1- mapping of the Soil Protection Index (SPI), Stage 2- mapping of the Potential Erosion Risk Index (PERI) and Stage 3- mapping of the Actual Erosion Risk Index (AERI).This set up allows for the simplification of the fuzzy rule bases by reducing the number of input parameters at each stage of the modelling. In addition, this approach allows for a step-by-step evaluation of the intermediate results. For instance, Stage 1 of the modelling approach allows for the evaluation of the SPI of a region, before integrating with the PERI of Stage 2, to obtain the final AERI of a region (Stage 3). The final soil erosion risk map provides qualitative based information on the distribution pattern of the soil erosion risk classes over a region. Apart from the qualitative based spatial information on soil erosion risk obtained from this model, the possibility of transferring the output erosion risk index into quantitative soil loss values (in t/ha/yr) is explored and discussed in this study. The model is successfully tested in Upper Awash Basin in Ethiopia and further used to produce a soil erosion risk map of Italy.

First hand information on land cover characteristics and their distribution are required for many scientific studies, natural resource management and development of various local and regional policies. This makes the land use and land cover information an indispensable asset for monitoring various environmental problems and their associated risks. Within the context of this PhD research study, an initial assessment of LULC classes of the Upper Awash Basin for two different time periods is carried out by setting up an LULC model in ArcGIS. Using the post-classification method of change detection, the dynamics of LULC pattern are analyzed. The result reveals that there is an appreciable increase of agricultural and settlement area by 60 % and 222 % from 1973 to 2000. In addition, a large reduction of 78 % in grassland from 1973 to 2000 is observed. Both deforestation and reforestation occurs spatially throughout the region. The dynamics of forest cover in Upper Awash Basin is attributed to the possibility that a part of the region is being cleared, while other parts previously pertaining to other classes are found to be regenerating into forest and therefore counterbalancing each other. It can be concluded that this study is able to provide a vehicle to understand the dynamics of LULC change and land degradation processes over the Upper Awash Basin. In addition, this type of assessment can provide first hand information to the policy makers and the architects of land use to identify the potential regions where prioritization for land use management, soil conservative measures and closer overall monitoring is needed.

Another important issues addressed in this PhD research work is the assessment of Satellite based Rainfall Estimates (SBRE). This part of the research work is to provide an insight to the scientific and user community about the potential and possibility of utilizing the right kind of satellite based indirect rainfall estimates for environmental and hydrological process monitoring. This is potentially attractive for data-scarce regions of the world. In this study, due to the sparse number of rainfall stations in the

study area, an indirect estimate of rainfall from various satellite based algorithms is analyzed and compared to the data available from ground measured rainfall. Dekadal time-steps of rainfall estimates from the CPC-NOAA RFE 2.0 algorithm and that of TRMM 3B43 V6 monthly precipitation from 2001-2003 are used for the assessment purpose. In general, the degree of agreement between the reference data and the satellite estimates, i.e. RFE 2.0 and TRMM 3B43 V6 estimates, varied with temporal scale, that is, dekadal, monthly and seasonally. A better degree of agreement and statistical significance are found in larger time-steps than in smaller time-steps (i.e. monthly better than dekadal). The analysis of 3B43 V6 monthly estimates yields very low bias, ME and RMSE despite its coarser resolution of 0.25 degree, in comparison to the finer resolution of the RFE 2.0 results. A significant R^2 of 0.90 and coefficient of efficiency of 0.90 on the monthly basis from the 3B43 data is observed. It is apparent that the TRMM product performed relatively better than RFE 2.0 on the basis of statistical measures that are used in this study for comparison. The SBRE data is used further for computing the annual rainfall erosivity of the region. Then, the computed rainfall erosivity maps from SBRE data are used as input fuzzy parameters to compute the PERI of the region using F-WERCAM. This assessment procedure helps us to test the applicability of SBRE data for soil erosion risk mapping of the region.

The multi-stage modelling framework of the F-WERCAM is tested in Upper Awash Basin in Ethiopia. The stage-1 of F-WERCAM maps the Soil Protection Index (SPI) of the region. It is defined as the function of land use practices and intensity of vegetation cover. LULC and NDVI map are considered as the input parameters to produce the SPI map of the region. The output fuzzy sets that correspond to SPI is set up by considering a relative scale from 0-1 (0 being "Very Low" protection and 1 being "Very High" protection) for the lower and upper threshold. The output SPI map is qualitatively evaluated and it is found that locations which are mapped with "Low" and "Very Low" SPI classes at different time periods of the year have a high potential land degradation risk. In general, the assessment of SPI shows the importance of vegetation cover and land use practices as a resisting factor to soil erosion. Socio-economic data and other environmental parameters are also used to correlate with the SPI map. It is found that population and livestock density explained 68% of the spatial distribution pattern of predicted SPI. Furthermore, the SPI distribution for two different time periods correlated positively (R^2Jan = 0.41 and R^2July = 0.51) with the soil erodibility of the region. The SPI derived from this model can be utilized by decision makers to locate and point out the zones of extreme need for special treatment. Such series of maps will help policy makers to initiate steps towards the prioritization of the landscape for proper land management practices, land use and soil conservation measures. For example, maps which have 29 administrative zones within the study area are used here for illustration. It is found from our model results, that out of 29 administrative units three units, namely Wenchi, Sodo and Addis Abeba need immediate attention for a proper land management in order to prevent the loss of valuable soil. On the other hand, Dodata (West) and Sululta region are found to have relatively "High" SPIs, which indicates regions of highly vegetated cover and forest zones with low potential land erosion. This simple example shows how the SPI map can effectively be used as a tool for prioritization and decision making purposes.

Stage-2 of F-WERCAM mapped the PERI of the Upper Awash Basin using the slope, soil erodibility and annual rainfall erosivity parameters. The output fuzzy sets of PERI are set up considering the concept of tolerable soil loss limit (i.e. 1-16 t/ha/yr) and using the reported range of soil loss value within the Awash Basin. The output PERI map indicates the degree of potential risk of erosion by classifying the region into 5 risk classes ranging from VL to VH. In the absence of vegetation cover,

the potential erosion risk map of the region indicates a varying degree of erosion risk: higher erosion risk is located in region of steeper slopes and corresponds to soils units having sandy clay loam, clay, sandy loam and clay loam. On the other hand, low erosion potential risk is concentrated in plain areas in the central part of the Upper Awash where most of the region is dominated by leptosols type of soil. Some dispersed spots on the central eastern part of the Upper Awash Basin are associated with "High" to "Very High" erosion risk. These areas correspond to mountainous regions that have steep slopes and therefore higher potential for erosion risk. The low lying area of the Upper Awash located in south eastern part is found to be associated with a "Very Low" potential risk.

Stage-3 of F-WERCAM mapped the AERI of the Upper Awash Basin using the intermediate output from Stage-1 and Stage-2 of the model. SPI and PERI are used as the input fuzzy parameters for producing the Actual Erosion Risk Index (AERI) map of the region. The integration of the intermediate parameters at this stage of modelling is done by considering the importance and effect of each parameter on the overall assessment of soil erosion risk of the region. The importance of each parameter is reflected and incorporated when setting up the fuzzy rule base. For instance, two fuzzy rule bases are setup and employed - the initial rule base, RB1 considered the SPI to have higher influence than PERI when determining the actual erosion risk of the region and the later one, RB2 considered both the parameters to be of equal importance when determining the actual soil erosion risk.

From the assessment of AERI map, it is seen that about 50 % and 16 % of the Upper Awash Basin is found to be within the VL and L soil erosion risk, respectively. These regions correspond to the "tolerable soil loss" limit of Upper Awash Basin which is below 16 t/ha/yr. The areas of high slope gradient and less vegetation cover correspond to "High" and "Very High" erosion risk zones. These comprise about 14 % of the Upper Awash Basin. The areas with "Medium" risk of erosion (i.e. 14 % of the region) are found in north-western and the southern part of the study area. Overall, the actual erosion risk map of the Upper Awash Basin indicates higher erosion risk in regions of higher PERI and lower SPI and these areas need immediate prioritization measures. Such qualitative maps provide a way to compare the degree of erosion risk associated with different regions within the study area.

From the fuzzy logic perspective, different combinations of fuzzy rule bases and output fuzzy sets using the fuzzy inference tool are tested to map the soil erosion risk of Upper Awash Basin. The resulting erosion risk map is found to be more sensitive to a slight change in the fuzzy rule base than the change in the adopted output membership functions. It is observed that the influence of different membership functions on the output erosion risk distribution is quite low and insensitive. Nevertheless, it should be kept in mind that changing the shape of the membership functions has some influence on the overlapping region of the adjacent fuzzy sets. Through this, their effects are translated on the output soil erosion risk class distribution. On the other hand, the effect of the fuzzy rules on the output risk distribution is found to be quite significant and high. For instance, the fuzzy rules base i.e. RB1 and RB2 used for mapping AERI are found to be quite sensitive when classifying the extreme erosion risk classes. From this analysis it is evident that the combination of the different rule bases with different fuzzy sets produces a number of dissimilar erosion risk distribution maps of the region. Hence, in a fuzzy based modelling approach, it is imperative to choose the right fuzzy rule base that reflects the process under investigation as the modelling output is very sensitive to fuzzy rule system.

The absence of ground observed spatial distributed soil loss data over the Upper Awash Basin limited the study from ground-based validation of the fuzzy based erosion risk map. In addition, for determining which output soil erosion risk map can be considered as representative map of the Upper Awash, further assessment of the model results is carried out in this study. One of the approaches adopted is by comparing the output from F-WERCAM with the RULSE model output of the region. The assessment is made by constructing the error matrix or confusion matrix, which provides the degree of agreement between the two different model outputs. The results of the F-WERCAM outputs as compared to the RUSLE based predicted erosion risk map indicated a satisfactory performance of F-WERCAM in predicting the soil erosion risk classes. Different scenarios are tested using different combinations of fuzzy rule bases and output fuzzy sets and the accuracy assessment of the results is performed by constructing the "error matrix" using RUSLE-based output maps as the reference maps. From the results, significant agreement between F-WERCAM and RUSLE model is found i.e. the range of overall accuracy varies from 54.64 % to 71.30 %, having corresponding kappa values of 0.34 to 0.52. For instance, the AERI map produce using RB1, corresponding to Stage 3 of F-WERCAM, is found to map the erosion risk distribution in a similar degree to the RUSLE-based output.

It is difficult to make a straight forward conclusion whether the F-WERCAM-based modelling approach represents the soil erosion risk distribution pattern of Upper Awash Basin more accurately than the RUSLE based erosion risk map. Differences in the risk classes from the model outputs are observed. One of the main reasons behind it is that- in fuzzy based modelling, the slope is considered to be the only parameter influencing the effect of topography on soil erosion, whereas for RUSLE, slope length and slope gradient are taken into account in the form of the LS factor. It is evident that the difference in risk classes is found to be concentrated in areas of higher elevation having higher slope length and gradient. In case of the plain areas which are subject to lower slope gradient and slope length, the influence of LS is minimized, resulting in a more similar distribution of risk classes, i.e. VL to L between the two model outputs. In addition, the inherent differences between fuzzy-based and empirical-based modelling concepts may also be a contributing factor for the differences in the output soil erosion risk. For example, the accuracy of the predicted erosion risk is largely influenced by the adopted fuzzy rule base for F-WERCAM, whereas it is the multiplication of the input parameters that produce the erosion risk distribution for RUSLE. Nevertheless, considering the input parameters i.e. slope gradient compared to LS factor, the representation of vegetation cover dynamic in form of SPI and the flexibility of fuzzy logic to incorporate additional expert knowledge in the form of fuzzy rules, made F-WERCAM an innovative approach for assessment of soil erosion risk in a regional scale.

Furthermore, the F-WERCAM-based assessment is carried out in order to understand the effect of temporal parameters like vegetation cover in the form of SPI, on erosion risk distribution patterns of the region. This temporal analysis provides a framework to understand the distribution of erosion risk pattern. It serves as a basis for the development of future options for more sustainable land use over a large landscape. The effectiveness of utilizing SBRE in this fuzzy based modelling approach is also studied. The results from the analysis shows that satellite-based rainfall datasets like RFE 2.0 and TRMM 3B43 V6 estimates can be effectively used to compute the annual rainfall erosivity index and used as an input parameter for soil erosion risk assessment. It is to be noted that, when computing the PERI of the region before integrating with SPI maps to obtained the AERI maps, only the annual rainfall erosivity index, R is taken into account. The variability of temporal or seasonal rainfall erosivity is not taken into account due to lack of rainfall intensity data for the computation purpose. Nevertheless, it is found that the effect of rainfall is greatly muted by the vegetation cover distribution

in Upper Awash Basin. This can be deduced from the fact that with an increasing in monthly rainfall during the year, there is a tendency of increasing vegetation cover which is reflected by distribution of NDVI within the region. Even though there is a high amount of precipitation during the main rainy period, the increases in vegetation cover provide the protection layer of soil from being eroded. This comparatively decreases the percentage coverage of higher soil erosion risk class of the region during this period when compared with other period of the year. Hence, the influence of the vegetation cover on the soil erosion risk of the Upper Awash Basin is arguably found to be the most important temporal parameter. Further temporal based assessment is necessary by taking into account the monthly rainfall erosivity in addition to temporal vegetation cover as it may provide additional results concerning the additive or synergetic influence of both parameters on the temporal soil erosion risk distribution of Upper Awash Basin.

Two different approaches are tested in this research that focuses on the possibility of quantifying the output erosion risk index of the F-WERCAM model. The initial approach considers the domain of the output fuzzy sets, i.e. the defuzzified output range of the model which is set as the actual observed soil loss range within the study area. The latter of the approaches then quantifies the soil erosion risk by establishing a relationship between the F-WERCAM output risk indexes and the actual soil loss range as predicted by RUSLE. The main focus in this approach is to see whether the qualitative erosion index (0-100) by F-WERCAM can be quantified with actual soil loss as observed from ground or predicted from other models by setting up a relationship between them. Due to the absence of ground measured spatially referenced soil loss data, the predicted soil loss values of the study area by RUSLE at different locations is considered as the proxy or test data to establish a relationship with the F-WERCAM index scale. The assessment and analysis indicates that this is a reliable approach for cases where a qualitative-based erosion risk index can be quantified relatively in terms of actual soil loss in a regional scale. These approaches serve as an indirect method to evaluate the F-WERCAM-based soil erosion risk map. Additionally, this assessment shows the promising performance of the fuzzy sets and rule base system adopted for erosion risk modelling in a regional scale. With ground observed soil loss data, more detailed assessment on the quantification procedure could be developed, implemented and tested.

The implementation of the F-WERCAM model is carried out for Italy using geospatial datasets obtained from JRC, European commission. Fuzzy rules developed for the Upper Awash Basin are tested to produce an erosion risk map of Italy. For the fuzzy rules to be applied effectively, it is required that similar input parameters adopted for the Upper Awash Basin are considered for Italy, too. The SPI and AERI maps of Italy are evaluated by comparing them to the existing soil erosion risk map of Italy. The response of the SPI to the erosion risk distribution of the region is assessed and it is found that SPI is negatively correlated with the annual soil loss of the region. This assessment shows that the produced SPI map of Italy, using the fuzzy rules of Upper Awash Basin, is able to capture quite well the variability of the soil erosion risk distribution predicted by the European Soil Bureau. The erosion risk map produced by the F-WERCAM model is found to represent the general trend of the erosion risk distribution as predicted in the existing erosion risk map. When comparative analysis is performed, it is found that there are areas with similar and dissimilar erosion risk classes but a good overall agreement between the two maps is shown. Even though the existing soil erosion risk map used here for comparison is ground validated, possible errors involved in the model application resulting from both, model simplification and input errors, need to be taken into consideration when evaluating the two erosion risk maps. This assessment provides an understanding of the erosion risk

distribution as predicted by different modelling approaches. In addition, it shows the potential and capability of implementing the F-WERCAM model under different environmental conditions. There is a possibility to carry out a more detailed assessment and mapping by adding other input parameters (depending on data availability) and implementing new expert-based fuzzy rules that reflect the local conditions.

The F-WERCAM framework is unique as it adopts the underlying principle of fuzzy logic for erosion risk classification and analysis in a multi-stage approach. The multi-stage modelling framework allows handling the problem of dimensionality when formulating the fuzzy rule bases. Fewer input fuzzy parameters at each stage allow for simpler rule bases and evaluation of the model at each intermediate stage. In addition, implementation of the framework within GIS allows the handling of both spatial and non-spatial data with ease and it allows for an efficient decision making through spatial analysis. This kind of model is intended for a quick appraisal or monitoring of erosion risk over a large landscape and should help towards prioritization of the landscape or identifying the hotspot zones for further detailed assessments.

However, there are certain limitations of this modelling approach that need further investigation. Due to lack of ground measured soil loss data at a large regional scale, proper model validation remains a key question, apart from the various model evaluation approaches presented in this research. Hence, the model is still open for further assessment and improvement with regard to its validation. The question of subjectivity is still a concern in such expert based modelling approaches. For instance, the model results are found to be more or less dependent on the design of the fuzzy sets and the fuzzy rule base adopted. To address such problem in future, further quantification approaches of the model output in addition to the approaches tested in this research should be examined. The possibility of generating fuzzy rules from numerical or ground observed data should be investigated. Specifically, the possibility of applying the data driven fuzzy rules optimization techniques or a combination of both, the expert based and automatic rule based algorithm approach is recommended. The developed F-WERCAM framework can be enhanced or upgraded by incorporating additional stages that focus on identifying large gullies and mapping of the depositional area within the region.

The ability of fuzzy logic to describe and transform the knowledge in a descriptive human like manner in the form of simple rules using linguistic variables has provides a new direction and opening to explore and develop a simple and well structured framework for soil erosion risk assessment. Overall, the integration of fuzzy logic within GIS using remotely sensed data in this research tries to address the problems of data scarcity, uncertainty in the input model parameters and handling of large spatial data effectively. From the various assessments and evaluations presented in this research, it is found that such an expert based fuzzy logic model has the potential to be used as a practical tool for assessment of regional soil erosion risk by policy makers and scientists.

Zusammenfassung

Die Modellierung von dynamischen und physikalischen Prozessen, wie zum Beispiel die Bodenerosion, beinhaltet zahlreiche Fehlermöglichkeiten und Fragestellungen. Die Verfügbarkeit von sicheren Datenquellen, die Datenqualität, verschiedenste Skalierungseffekte, Fehler in der Datenaufnahme sowie die Modellkomplexität sind nur einige Aspekte, die explizit in wissenschaftlichen Studien über Bodenerosion zu berücksichtigen sind. Des Weiteren beinhalten zahlreiche Modellparameter eine gewisse Unschärfe und Unsicherheit, die in vorangegangen Studien über Risikobewertungen hinsichtlich Bodenerosion weitestgehend vernachlässigt wurden. Diesbezüglich bietet die Einteilung von Parametern in überlappende Klassen mittels fuzzy-logischer Ansätze, anstatt scharf getrennter Parameterbereiche, eine Art Unsicherheitsbetrachtung je Parameterklasse an. In verschiedenen existierenden Modellen zur Bewertung des Erosionsrisikos sind die berücksichtigen den zu Parameter und deren räumliche Zuordnung in einem Einzugsgebiet als feste Grenzen definiert, wobei in Realität diese natürlichen Grenzen weitaus komplexer sind. Für Fragestellungen hinsichtlich der Definition von Klassengrenzen und um Expertenwissen, welches die maßgeblichen Prozesse repräsentiert in die Untersuchungen einzubinden, eignet sich hingegen ein fuzzy-logischer Modellierungsansatz.

In dieser Doktorarbeit wird ein einfaches aber effizientes fuzzy-logisches Modell entwickelt, um die Verteilung von Bodenerosionsrisiken für regionale Gebiete zu erfassen. Das entwickelte Modell nennt sich „**F**uzzy-**W**ater **E**rosion **R**isk **C**lassification and **A**ssessment **M**odel" (F-WERCAM) und zielt auf die Simulation niederschlagsinduzierten Bodenerosion sowie deren Bewertung im Rahmen einer GIS-Umgebung ab. Das Modellkonzeption strebt möglichst geringe Anforderungen an die Eingangsdaten an und beinhaltet für die Simulation des Bodenerosionsrisikos auf regionaler Ebene folgende dominierende Variablen: Landnutzung und Landbedeckung (LULC), den normierten Vegetationsunterschieds index (NDVI), jährliche Niederschlagserosivität (R), Bodenerodierbarkeit (K) und Geländeneigung (%).

Die Bestimmung der dominierenden Modellparameter basiert auf einer detaillierten Literaturstudie und Expertenwissen. Da das entwickelte Modell auf Fuzzy-Logik beruht, ist die zur Verfügungstellung von Expertenwissen und die entsprechende Definition von Fuzzy-Sets und Fuzzy-Regeln einer der wichtigsten Aufgaben in dieser Studie. Die wissenschaftliche Basis zur Formulierung dieser Fuzzy-Sets und Fuzzy-Regeln basiert einerseits auf Fachliteratur über Bodenerosionsprozesse und zum anderem auf einer Befragung von mehreren fachlich anerkannten Wissenschaftlern aus dem Forschungsbereich der Bodenerosion.

Einer der wichtigsten Eigenschaften des F-WERCAM ist der mehrstufige Modellierungsansatz. Er besteht aus insgesamt 3 Stufen: Stufe 1 beinhaltet die den Bodenschutz Index (SPI), Stufe 2 den index des potenziellen Erosionsrisikos (PERI) und die Stufe 3 den index des tatsächlichen Erosionsrisikos (AERI). Das mehrstufige Konzept erlaubt eine Vereinfachung der Fuzzy-Regeln durch Reduzierung der Input-Parameter je Modellstufe sowie eine schrittweise Beurteilung der einzelnen Modellstufen mit entsprechenden Zwischenresultaten. Zum Beispiel bewertet die Stufe 1 den SPI einer Region bevor er mit dem PERI der zweiten Stufen kombiniert wird, um anschließend das Endergebnis (AERI) einer Region zu bestimmen. Das Endergebnis (Bodenerosionsrisiko) gibt qualitativ das räumliche Verteilungsmuster der Bodenerosion in Risikoklassen wieder. Des Weiteren wird im Rahmen dieser Studie untersucht und diskutiert, inwiefern die erhaltenen Resultate in quantitative Werte der Bodenerosion (in t/ha/yr) umgewandelt werden können.

Das entwickelte Modell wurde erfolgreich im dem Einzugsgebiet des Oberen Awash in Äthiopien getestet und wird in einer zusätzlichen Fallstudie zur Ermittlung des Bodenerosionsrisikos für Italien angewendet.

Im Falle der F-WERCAM Anwendung im Oberen Awash Becken beinhaltet die erste Stufe von F-WERCAM den Bodenschutz Index (SPI) der Region. Die Ergebnisse belegen, dass SPI-Bereiche, die mit „Niedrig" und „Sehr Niedrig" klassifiziert wurden, ein hohes Risikopotential hinsichtlich Bodenerosion zu unterschiedlichen Zeiträumen innerhalb eines Jahres aufweisen. Im Allgemeinen zeigt die Auswertung der SPI-Klassen die Bedeutung der Vegetationsbedeckung und Landnutzung als Widerstandsfaktor gegenüber der Bodenerosion. Die Ergebnisse aus der ersten Stufe helfen unter anderem Entscheidungsträgern Maßnahmen hinsichtlich Landnutzung und Bodenerhaltung zu priorisieren. Die zweite Stufe von F-WERCAM untersucht den PERI des Einzugsgebiets des Oberen Awash unter Verwendung der Geländeneigung, Bodenstabilität und der erosivität infalse des jährlichen Niederschlags. Das Ergebnis der PERI-Simulation gibt den Risikograd von potentieller Bodenerosion in 5 Risikoklassen von „Sehr Niedrig" bis „Sehr Hoch" an. Bei Nicht berücksichtigung der Vegetationsbedeckung ergeben sich variierende Erosionsrisiken: z.B. tritt hohes Risiko in Gebieten mit hoher Geländeneigung und den Bodenzusammensetzungen wie ZB. Sand/Schluff/Lehm, Schluff, Sand/Lehm und Schluff/Lehm auf. Andererseits besteht ein geringes Erosionsrisiko in flachen Regionen des Oberen Awash Einzugsgebietes, in dem die Bodenzusammensetzung von Leptosolen dominiert ist. Die dritte Stufe von F-WERCAM simuliert den AERI des Oberen Awash Einzugsgebiets unter Verwendung der Zwischenergebnisse aus Stufe 1 und Stufe 2, wobei für die Berechnung des index der tatsächlichen Erosionsrisikos (AERI) die zuvor ermittelten SPI und PERI als unscharfe Eingangsparameter berücksichtigt werden. Die Integration dieser Zwischenergebnisse in der dritten Stufe berücksichtigt die Bedeutung und Wirkung der Eingangsdaten auf die Gesamtbewertung des Bodenerosionsrisikos in der Region. Die Bedeutung und Gewichtung der einzelnen Parameter ist in der Erstellung des Fuzzy-Regelwerks berücksichtigt. Der AERI des Oberen Awash Einzugsgebiets zeigt ein hohes Erosionsrisiko in Bereichen von hoher PERI und geringer SPI. Das Oberen Awash becken wird somit als Gebiet identifiziert, in dem sofortige Maßnahmen notwendig wären. Diese qualitativen Simulationsergebnisse ermöglichen somit den Vergleich der Erosionsrisiken in unterschiedlichen Bereichen des Untersuchungsgebietes.

Aufgrund fehlender beobachteter räumlicher Bodenerosionsdaten im Oberen Awash Einzugsgebiet war eine Validierung des fuzzy-logischen Ansatzes zur Ermittlung des Erosionsrisikos nur schwer realisierbar. Eine Möglichkeit der Validierung besteht im Vergleich der Resultate von F-WERCAM mit den Ergebnissen des sogenannten RUSLE-Modells. Die Ergebnisse in Form von Bodenerosionsrisikoklassen in F-WERCAM geben im Vergleich zu den prognostizierten Bodenerosionsrisiken mit RUSLE eine zufriedenstellende Übereinstimmung. Insgesamt wurden unterschiedliche Szenarien mit verschiedenen Fuzzy-Sets und Regelwerken getestet, um die Genauigkeit der Ergebnisse anhand einer „Fehler-matrix" den Simulationsergebnissen des RUSLE-Modells anzupassen. Die Auswertung der verschiedenen Szenarien ergibt eine gute Übereinstimmung mit dem RUSLE-Modell, z.B. variiert die Genauigkeit zwischen 54.64% und 71.30%. Die AERI-Ergebnisse unter Verwendung von RB1 (Stufe 3 von F-WERCAM) ergibt eine ähnliche Verteilung des Bodenerosionsrisikos wie die simulierten Werte im RUSLE-Modell.

Anhand der Ergebnisse ist es schwierig zu beurteilen, ob die F-WERCAM basierten Simulationsergebnisse das Bodenerosionsrisiko im Oberen Awash Becken genauer prognostizieren als das RUSLE-Model. Aber unter Betrachtung der Eingangsparameter wie z.B. der Geländeneigung gegenüber dem LS-Faktor, die Berücksichtigung der Vegetationsbedeckung in Form von SPI und insbesondere die Flexibilität des Fuzzy-Ansatzes zur Berücksichtigung von Expertenwissen in Form

von Fuzzy-Regeln gestalten das F-WERCAM-Modell zu einem innovativen Ansatz, um das Risiko von Bodenerosion auf einer regionalen Skala zu bewerten.

Des Weiteren ermöglicht F-WERCAM die Bewertung des Einflusses von zeitlich veränderlichen Variablen wie z.B. der Vegetationsbedeckung in Form von SPI auf Bodenerosionsrisikoverteilungen in einem Untersuchungsgebiet. Ein weiterer Aspekt dieser Arbeit untersucht wie effektiv satellitenbasierte Niederschlagsabschätzungen(SBRE) in dem Fuzzy-Ansatz berücksichtigt werden können. Die Ergebnisse der Analyse belegen, dass satellitenbasierte Niederschlagsdaten wie RFE 2.0 und TRMM 3B43 V6 effektiv in der Simulation des durch den jährlichen Niederschlag verursichten Erosionsgeschehens verwendet und somit als Eingangsparameter in die Bewertung des Bodenerosionsrisikos einbezogen werden können.

Zwei unterschiedliche Ansätze wurden im Rahmen dieser Forschungsarbeit getestet, um mittels des F-WERCAM-Modells quantitative aussagen über Erosionsmengen zu generieren. Die Ausarbeitungen und Bewertungen zeigen, dass, der Fuzzy-Ansatz eine zuverlässige Methode ist wenn die Klassengrenzen des Erosionsrisiko faktors verläaalich mit Erosionsraten (in Mengeneinheiten prozeiteinheit) assoziiert werden können. Solche Ansätze dienen als indirekte Evaluierungsmethoden für das simulierte Bodenerosionsrisiko mit F-WERCAM. Zusätzlich zeigt diese Untersuchung die vielversprechende Modellausführung des Fuzzy-Ansatzes für die Modellierung des Erosionsrisikos auf einer regionalen Skala.

Durch die freundliche Bereitstellung von räumlichen Daten von der JRC, European Commission, konnte das F-WERCAM-Modell für die Berechnung des Erosionsrisikos in Italien eingesetzt werden, wobei das entwickelte Fuzzy-Regelwerk für das Oberen Awash Einzugsgebiet eingesetzt und getestet wurde. Diese zusätzliche Ausarbeitung in einem anderen Testgebiet führt zu einem erhöhten Verständnis hinsichtlich verschiedener Modellierungsansätze und den räumlichen Verteilungen des Erosionsrisikos. Zusätzlich konnten mit dieser Untersuchung die Möglichkeiten des F-WERCAM-Modells für verschiedene Eingangsdaten getestet werden.

Das F-WERCAM-Modell, als ein auf den Prinzipien der Fuzzy-Logik basierendes Konzept mit einem mehrstufigen Ansatz zur Simulation von Bodenerosion ist bislang einzigartig. Insbesondere der mehrstufige Fuzzy-Ansatz ermöglicht die Handhabung unterschiedlichster Dimensionalität bei der Erstellung von Fuzzy-Regelwerken. Weniger Eingangsparameter in jeder Stufe vereinfachen in den einzelnen Modellstufen das Regelwerk und die Auswertung. Durch die Implementierung des Modells in einer GIS-Umgebung können raumbezogene und nicht-raumbezogene Daten gehandhabt werden um damit räumlich Analysen durchführen zu können, die im Sinne von Maßnahmen entscheidungsunterstützend wirken können. Diese Art der Modellierung dient vornehmlich einer schnellen Einschätzung der Erosionsrisiken in großen Einzugsgebieten und erlaubt die Identifikation und Priorisierung von „Hotspots" für anschließende Detailuntersuchungen. Jedoch beinhaltet der Modellierungsansatz einige Limitierungen, die es zu zukünftig untersuchen gilt. Durch das Fehlen von Bodenerosionsmessungen auf regionaler Ebene besteht weiterhin die Frage nach einer gründlichen Validierung des Modellansatzes, obwohl der Ansatz anhand von verschiedenen anderen Modellierungsansätzen überprüft wurde. Des Weiteren sollte die Möglichkeit der Erstellung eines Fuzzy-Regelwerks anhand numerischer oder gemessener Werte untersucht werden. Insbesondere Techniken zur daten-basierten Regelwerk-Optimierung oder eine Kombination von Expertenwissen und Algorithmen zur automatischen Regelerstellung könnten zu einer Ergebnisoptimierung führen. Das im Rahmen dieser Arbeit entwickelte F-WERCAM kann beliebig weiterentwickelt werden, z.B. durch die Implementierung von weiteren Modellstufen, die zusätzlich Erosionsrinnen und Ablagerungsbereiche in einer Region berücksichtigen.

Insgesamt betrachtet, bietet der Fuzzy-Ansatz in der GIS-Umgebung unter Verwendung von Daten aus der Fernerkundung eine zuverlässige Lösung, um mit Problemen wie unzureichende Datenbasis, Unsicherheit der Eingangsdaten oder große räumliche Datenmengen umzugehen. Aus den verschiedenen Bewertungen und Beurteilungen, die in dieser Arbeit präsentiert sind, lässt sich schließen, dass experten-basierte fuzzy-logische Modelle ein praktisches Simulationswerkzeug zur Bewertung von Bodenerosionsrisiken für Wissenschaftler und Entscheidungsträger bieten.

1   Introduction

"Most of the fundamental ideas of science are essentially simple, and may, as a rule, be expressed in a language comprehensible to everyone."

- Albert Einstein

1.1   General Introduction

Land is considered to be the most fundamental geographical element in the development and growth of other biophysical resources of the earth. All the patterns and dynamic activities on the earth's surface are largely determined and controlled by the factors of surface configuration, mainly altitude, slope, soil characteristics and consequent factors of water, climate and natural vegetation. In various parts of the world, the cultivation and agricultural activities are now being pushed to forested areas, marginal lands, floodplain areas and up slopes without taking into account the suitability of these lands for agriculture; and the vegetal cover is being lopped and cleared for fuel and fodder. This unscientific and irrational land transformation process has brought about very serious environmental crisis in terms of erosion of topsoil, increase in sediment discharge in streams and reduction in ground water recharge which in turn results in sedimentation, contaminations, habitat degradation and altered flow of regimes. Focusing on the soil erosion problem at different parts of the world, it is evident and widely known that erosion by water greatly affects the productivity of soils, thereby reducing the potential of vegetation growth. Such effect on a long term period can lead to the degradation and desertification of the landscape.

In today's world, a comprehensive and scientific study on quantitative and qualitative variations of land resources and their reasonable exploitation and utilization to bring their potential into full play for meeting the needs of sustainable development is one of the most important challenges to resource managers and the scientific community. Studies focus on the impact of changes in land use patterns to environmental degradation i.e. detrimental effects of land use practices on soil erosion at various spatial and temporal scales over watershed needs to be realized using various new approaches and methodologies. In such a procedure the aim is to see any difference in results from related past studies and models and adopt them to different regions of the world for the present and future time.

Modelling a dynamic and physical process, such as soil erosion, is prone to errors and problems. The availability of the right kind of data source, quality of data used, scale issues in modelling, measurement errors etc. and the complexity of the model in itself are some of the issues that are explicitly addressed and reported in soil erosion research studies. Existing models based on physical processes like WEPP (Nearing et al., 1989); ANSWERS (Beasley et al., 1980); EUROSEM (Morgan et al., 1998a); AGNPS (Young et al., 1987), to name a few, are very data demanding in both their amount of variables and their temporal and spatial resolution requirements. Hence, data scarcity and lack of reliable data tend to pose a problem for successful application of physical based erosion models. On the other hand, less data demanding popular empirical based models like USLE

(Wischmeier and Smith, 1978); RUSLE (Renard et al.,1991) and MUSLE (Williams, 1975) are developed for a certain environmental set up using erosion plot studies and thus applicability is restricted to regions where they were developed.

Soil erosion risk modelling involves various environmental control parameters which are fuzzy in reality. When mapping erosion risk, the introduction of fuzzy sets instead of the crisp sets to define classes (i.e. degree of hazard or risk) will help to incorporate the degree of fuzziness within each class of the governing parameters. Overall, the ability of fuzzy logic to describe and transform the knowledge in a descriptive human like manner in the form of simple rules using linguistic variables can provide a new direction and opening to explore and develop a simple and well structured framework for erosion risk assessment.

This PhD research aims to develop a fuzzy logic methodological framework for soil erosion risk assessment over a large regional landscape. The developed framework helps to measure the degree and magnitude of the association between the changing patterns of land use and the influence of these changes on the soil erosion risk distribution patterns. The spatial distribution of the Soil Protection Index (SPI) and erosion potential (or the actual erosion risk) should be the result of the fuzzy modelling. An in-depth analysis is carried out at a regional level using the developed framework by incorporating literature and expert knowledge on soil erosion in the form of fuzzy rules and sets. Satellite remote sensing based datasets are primarily explored in this study to bridge the gap in data scarcity problem. Moreover, such datasets help to analyze the temporal change of patterns and to asses the interaction of various parameters influencing soil loss risk at the regional landscape. To implement the developed Fuzzy-Water Erosion Risk Classification and Assessment Model (F-WERCAM) framework, a fuzzy-GIS interface system is customized using ArcGIS. The fuzzy inference engine and calculator used in this study is mainly adopted from the earlier research work by Schneider (2001) and Kopecki (2008).

1.2   Research Need and Directions

This research focuses on understanding the non-linear processes of soil erosion, its assessment and effect on a landscape using an integrated tool based on Fuzzy logics, GIS and Remote Sensing. In reality, parameters such as land use and land cover, vegetation distribution, soil type distribution etc. influence natural conditions and this becomes a main drawback when modelling natural processes using the crisp Boolean logic. Various existing modelling approaches consider each feature and spatial units present on the landscape as having distinct boundaries. In reality, the existing natural boundaries are much more complex. To cope with such problems of class boundaries and to associate the expert knowledge that can represent the processes under investigation, a fuzzy linguistic concept is realized in this study. Generally, a large amount of datasets that represent climate, topographic and anthropogenic factors are a basic requirement for environmental modelling, regardless of the types of processes to be modelled in a landscape. With the advancement in technology, remote sensing data products provide the necessary data in regional and global scale, and act as a complementary dataset with reference to ground measured data. In addition, various data products derived from remote sensing can be utilized to bridge the gap of data scarcity in many regions in the world. The development in geospatial technology gives the flexibility to integrate, analyze and visualize various data in a spatial and temporal scale. The GIS provides the framework to spatially model and deliver the result in a more interpretable manner to the end user. Hence, a fuzzy logic based modelling

approach using remote sensing data products along with limited ground data in a GIS environment is attempted in this research to address the issues of water induced soil erosion risk in a regional landscape environment.

Thus, the proposed soil erosion risk assessment using a fuzzy logic approach and remote sensing datasets in a GIS environment is justifiable due to the following factors:

- need of simplified and easily understandable models that incorporate human knowledge and experience,

- applicability of existing data-driven physical models is still a problem on a regional scale (calibration and prediction accuracy),

- provide a way to explore the applicability of remotely sensed data to bridge the gap of data scarcity in erosion risk modelling,

- most end-users and policy makers rely on transparent and easily interpretable results for implementation and prioritization,

- a fuzzy linguistic modelling approach can handle the uncertainty in environmental factors unlike the crisp logic, thereby representing the actual ground (soil composition) more accurately.

1.3   Research Objectives and Questions

The main research objective is to '*develop a simple and efficient erosion risk model and study its feasibility for monitoring the landscape soil erosion risk (spatially and temporally) using an integrated approach of fuzzy logic and satellite remote sensing datasets within a GIS framework.*'

Specific objectives of this study are:

a. Development of a framework or model for soil erosion assessment based on fuzzy logic and remote sensing input datasets.

b. Devise an appropriate GIS approach to interface and utilize the fuzzy inference system or fuzzy calculator[*] within ArcGIS as a new tool for soil erosion risk mapping (i.e. *identification of an approach for raster data integration, spatial analysis and visualizations of the results*).

c. Assessment and analysis of different primary parameters influencing soil erosion, based on literature and expert knowledge, thus providing the background for the development of fuzzy sets and fuzzy rules applicable in regional erosion risk assessment.

---

[*] *Fuzzy Inference originally used in the CASiMiR (**C**omputer **A**ided **S**imulation **M**odel for **I**nstream flow **R**equirements) model developed at IWS, Stuttgart.*

d. Mapping of land-use and land-cover classes in the study region using the multi-temporal satellite data and to analyze the effect of temporal land use change in erosion risk distribution patterns.

e. Investigation of the potential of indirect satellite precipitation estimates by comparing with the reference gauging data, and to utilize them as an input parameter for erosion risk mapping.

This study aims to answer some of the following research questions as outlined below:

- Can simple linguistic fuzzy rules which are based on literature and expert knowledge capture the soil erosion risk distribution patterns as efficiently as other existing erosion models in a regional landscape?

- Which factors can explicitly represent the variability of vegetation cover distribution and their significance on erosion risk classification and assessment over the basin?

- Is there an approach for the quantitative assessment in addition to qualitative assessment of the soil erosion risk using the developed model framework?

- What is the accuracy of mapped erosion risk when satellite rainfall estimates are used as a climatic parameter instead of gauged measured rainfall?

1.4   Research Hypothesis

- 'Integrating Remote sensing, GIS and a soft computing technique like fuzzy logic will improve the assessment of the soil erosion risk (both spatially and temporally) and thereby provide information for prioritization needs within a landscape.'

- 'Incorporation of expert knowledge and rules about the water erosion processes using fuzzy concepts will result into a simplified and easily understandable model.'

- 'Satellite based rainfall estimates can be used effectively as a complementary dataset toward erosion risk mapping in data scarce regions of the world.'

- 'The proposed model framework can be easily modified and tuned for application in different geographical regions using a limited number of input variables freely available for public access globally.'

1.5   Overview of the PhD thesis

This section provides an overview of the content of each chapter and the logical flow of the accomplished task carried out in this PhD research. This provides a quick snapshot and understanding of the various topics and discussions presented in this research.

Chapter 1: This chapter provides the fundamental background on the research proposal development. A general introduction with focus on the problem statement of the research, research objectives and questions is highlighted. In addition, the hypotheses to be tested in this research work are explicitly presented.

Chapter 2: This chapter aims to provide and discuss the background behind land degradation and the soil erosion problem in a global perspective. A review on various types of existing soil erosion risk assessment tools and models is also discussed along with their strengths and weaknesses. In addition, this chapter provides the understanding and basic fundamentals on the fuzzy logic principles, and the use of this approach in environmental monitoring. A brief overview on existing soil erosion risk assessment studies using fuzzy logic approach is given. The need for satellite remote sensing environmental data and the GIS approach in this type of research is also discussed briefly.

Chapter 3: This chapter deals with the development of the F-WERCAM framework for water erosion risk assessment. An explanation on the identification of primary governing parameters that influence erosion risk is also discussed. In addition, this chapter provides a background on the technical flow and the description on the fuzzy inference calculator used. The additional customization process in GIS for implementation of the F-WERCAM is also discussed.

Chapter 4: An overview of the area under investigation, the Upper Awash Basin, Ethiopia focusing on the physical and environmental setting of the region is provided. The current status of land degradation and the soil erosion problem of the region are also highlighted. The source of the dataset used along with the acquisition method are presented and discussed at the end of this chapter.

Chapter 5: This chapter deals with developing a Land Use and Land Cover (LULC) map of the Upper Awash Basin using satellite imagery. An overview on LULC change detection analysis is provided to understand the effect of LULC change on land degradation in the Upper Awash Basin.

Chapter 6: This chapter compares the indirect satellite estimates rainfall product with gauged measured rainfall over the Upper Awash Basin. This study is made to provide the scientific community an insight into the potential and possibility of utilizing the right kind of satellite indirect rainfall estimates for environmental monitoring, especially in data scarce regions of the world.

Chapter 7: This chapter discusses the procedure of the estimation of input parameters for F-WERCAM. Parameters analysis, classification and fuzzification i.e. defining the input-output membership functions, along with developing the fuzzy rules for each stage of modelling are also discussed.

Chapter 8: This chapter discusses the result and analysis of Stage 1 of F-WERCAM, i.e. mapping the Soil Protection Index (SPI) of the Upper Awash Basin. A discussion of the results and analysis of the Stage 2 and 3 of F-WERCAM, that is the mapping of the Potential Erosion Risk Index (PERI) and Actual Erosion Risk Index (AERI) of the Upper Awash Basin is presented here. The analysis on the comparative assessment of RUSLE based predicted erosion risk map with F-WERCAM output risk map is also discussed. Results and analysis on the effect of temporal SPI and LULC on the erosion risk distribution of Upper Awash basin is presented. The applicability of the satellite estimates rainfall data for the soil erosion risk assessment is also discussed.

Chapter 9: This chapter provides an attempt to quantify the Actual Erosion Risk Index (AERI) obtained from F-WERCAM where the basis is the actual soil loss of the region by different approaches. A discussion is also provided in this chapter regarding the feasibility of adopting such a quantification method presented in this research. In addition, other probable methods are also suggested for obtaining the quantified soil loss from such modelling approach.

Chapter 10: This chapter provides an outlook on the applicability of the fuzzy rules developed for the Upper Awash Basin also for mapping the soil erosion risk of Italy. The output SPI and AERI map of Italy is compared with the existing soil erosion risk map of Italy. Such assessment gives an initial indication of the applicability of the developed fuzzy model in different climatic zones and environments.

Chapter 11: This chapter addresses the original research questions and provides the overall achievement of this research. Specifically, some of the major advantages and limitations of such developed methodology is discussed. A research outlook and recommendations are also given.

2 Theory, Concept and Literature Review

"Gravity is one variable in a lot of scientific processes. If you can remove gravity or minimize its effect, then you can understand the other processes that are going on."

- Laurel Clark

2.1 Land Degradation and Soil Erosion: A Global Perspective

From the beginning of cultivation by mankind, soil forms are the basic platform to provide food and nutrients and have a great influence on the growth and development of civilization. With the transition from hunter-gatherer to settled agricultural activities in the last 10,000 years, human dependence and impact upon soils have become more direct and obvious (McNeill and Winiwarter, 2004).

Land degradation and soil erosion occur naturally and persist through the geologic ages in almost all parts of the earth. Increase in interventions by human activities aggravate the situation of soil erosion to a greater extent in recent times (~ past 60 years) and disturb the balance of the ecosystem to unprecedented levels. According to a recent study by FAO (2008) using data taken over a 20- year period, it is found that land degradation is intensifying in many parts of the world. At present, more than 20 % of all cultivated areas, 30 % of forests and 10 % of grasslands all over the world is undergoing degradation process. It is also estimated that 1.5 billion people, representing a quarter of the world's population, depend directly on degraded land. The first Global Assessment of Human Induced Soil Degradation, or 'GLASOD', carried out by the International Soil Reference and International Centre (ISRIC) for UNEP in 1990 produced a map containing soil degradation, which indicates that basins with the highest levels of water erosion are found in China, Southeast Asia, India and Madagascar. The basins located in Africa, Europe, Central and South America are found to have more than 15% of their land area exposed to moderate to extreme water erosion (Oldeman et al., 1990). Similarly, a map of the global distribution of water erosion vulnerability produced by USDA-NRCS (United States Department of Agriculture; Natural Resource Conservation Services) in 1998 (see Figure 2-1) clearly shows that most parts of the world are highly vulnerable to water erosion risk ranging from "moderate to very high".

Deforestation is identified to be the main cause of degradation of soil in most Asian (40 %), South American (41 %) and Eastern European countries (38 %). On the other hand, overgrazing is identified to be the main factor that causes the degradation of soil in most African countries (50 %) (Oldeman et al., 1990). Hence, deforestation, overgrazing, improper agricultural management, over exploitation of vegetation cover and human activities are considered to be the main causative factors of land degradation. Land degradation problems threaten the food security and economic development of many developed and developing nations. Various international organizations like FAO, ISRIC and EU (European Union) have highlighted the importance of preventive soil ecosystem management and point out the necessity to find a solution for various types of land degradation experienced in different parts of the world.

For instance, a new environmental legislation and policy is implemented by the European parliament in 2007 for the protection of soils and to prevent further degradation (European Commission, 2007).
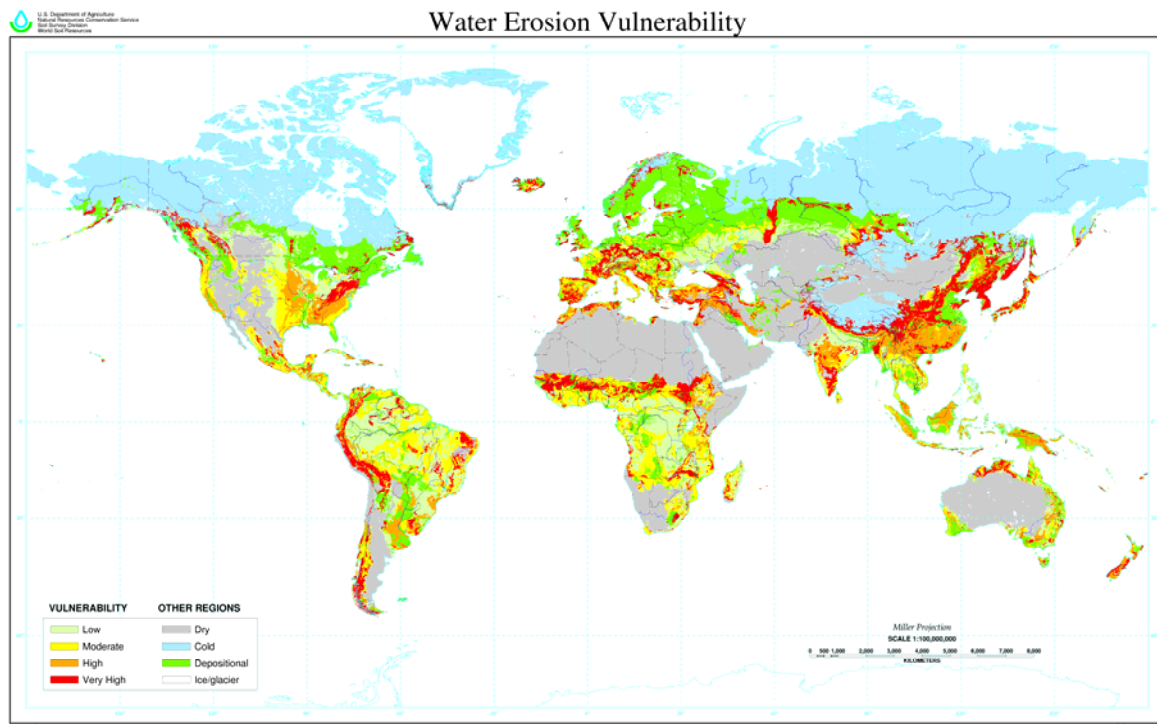
Figure 2-1: Map of the water erosion vulnerability (USDA-NRCS, 1998)

Only when the causes and the impacts of the resulting pressure on the system are identified and known, adequate response and prioritization measures can be formulated (FAO, 2003). Hence, understanding and analysing the spatial processes of land degradation can help us to determine the underlying environmental or cultural factors that cause the change in the patterns over time. For any geographical phenomenon, it is often needed to study both its spatial patterns and the spatial processes associated with those patterns (Lee and Wong, 2001). Expert groups on LADA (Land degradation Assessment in Dry Lands) indicate the importance of identifying hot spot regions for cost-effective and timely land degradation assessment.

2.2   Overview on Soil Erosion Risk Assessment and Modelling

2.2.1   An Insight into the Soil Erosion Processes and Modelling Aspects

"Soil erosion is the process by which the land surface is worn away by the action of wind, water, ice and gravity. Geological (also known as natural erosion) and accelerated erosion are the two types of soil erosion that is distinguished in water erosion studies. Geological erosion is defined as the inexorable and continuous process of evolution of the Earth's surface by such geological agents as rainfall, overland flow, snow melt, stream etc. On the other hand, as the name indicates, accelerated erosion is considered to be a more rapid and intense process that is largely induced by anthropogenic activities like clearing of forest, improper land use practices and construction activities etc"(El-Swaify et al., 1982).

Generally, the classification of erosion processes is based on a concept of progressive erosion severity (Toy et al., 2002). In other words, water based erosion classification is based on the spatial context in which the erosion takes place. Sheet erosion is considered to be the first phase of the erosion process and its rate is assumed to be low. As the erosion rate increases, rill erosion is assumed to begin, thereby progressing to gully erosion where the rates are considered to be very severe and leads to deeply incised channels. More specifically, overland erosion occurs on denuded slopes as a result of raindrop splash and runoff. It includes sheet (inter-rill), rill, and gully erosion. Since stream channels are also an integral part of the landscape, erosion that occurs in the streams is termed as "stream channel erosion". It happens when the volume and velocity of flow increase sufficiently to cause movement of the streambed and bank materials. Toy et al. (2002) provide a simple rule of thumb to identify the dominant erosion type, based on the amount of average soil loss per year. For instance, rill erosion is considered to start when the sheet erosion rate reaches 15 tons/ha per year.

A clear understanding of the model is important for its effective utilization. Various methodologies are available from past and recent studies on the assessment of soil erosion (Gobin et al., 2002). Some of these are based on field observations while others are based on an assessment and combination of parameters which influence the rate of soil erosion. Vente and Poesen (2005) indicate that the different erosion models should be classified by time and space scale, system approach and details of the input parameters. From these criteria, erosion models can be categorized as physical based, conceptual, empirical/regression or semi-quantitative. For instance, a semi-quantitative model is considered to be "Holistic" with less input data requirement; physical based models are considered to be "Reductionistic" and have high data requirement (see Figure 2-2). Blinkov and Kostadinov (2010) also summarize different types of modeling approaches to identify areas at risk which have been mainly adopted in various countries of Europe.
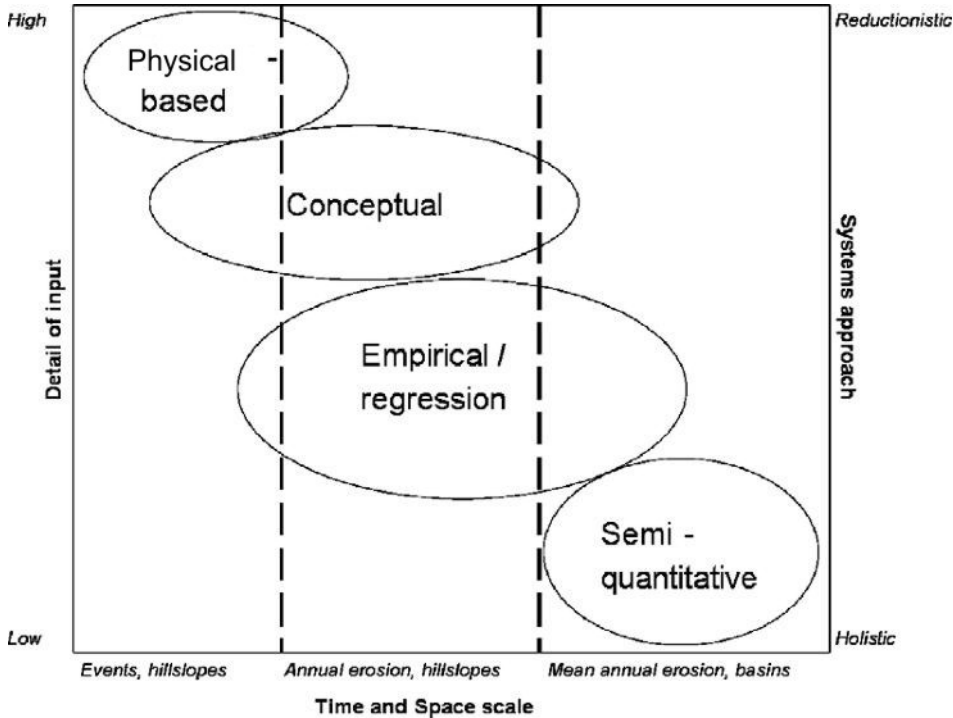
Figure 2-2: The different types of erosion modelling approach (adopted from Vente and Poesen, 2005)

When studying the soil erosion problem in different parts of the world, the lack of observed and measured erosion data always pose a problem for model evaluation. To circumvent such lack of ground data at large spatial locations, many earlier and present studies that employed physical and conceptual soil erosion models used to extrapolate observations of plot studies or even small watersheds to determine average annual soil loss rates for large regional landscapes. However, such extrapolation is controversial and is proven to be unsatisfactory (Renschler and Harbor, 2002). Vente and Poesen (2005) reports that soil erosion rates measured at one scale level are not representative for sediment yield at another. So, the issues on how the data on erosional processes at one scale can be extrapolated to processes operating at other scales become one of the major challenges to various scientists dealing with erosion problems. The "scale" of modelling dictates and influences the model development and selection as well as availability of data and its quality. Depending on the scale of interest, different groups of erosion processes are found to be dominant. This indicates that the effective focus of the model also changes with scale (Renschler and Harbor, 2002). In addition, the availability of temporal and spatial data is extremely important for the assessment of erosion risks, as erosion processes in a landscape are highly non-linear and inter-dependent on various parameters. It is difficult to choose and judge one model over another, but one can always focus and examine whether the model serves its intended purpose and goal. Toy et al. (2002) provide a basic overview of erosion prediction technology and suggest that erosion models should be used as a guide to decision making and models should not dictate the decision.

Another common approach to evaluate the soil erosion problem is to identify the area at risk using indicator variables that influence the soil erosion processes. The chance of the occurrence of some undesirable events at a certain location is the associated "*risk*" of that particular location. In general, risk assessment used in various disciplines involves identification of the risk and the measurement of the exposure to that risk. In the case of soil erosion risk assessment, it is the combination of parameters which influence the erosion processes in the landscape that provide the necessary steps to measure the intensity of the associated risk. The magnitude of erosion risk and its distribution patterns at various locations is determined by the weights of the influential parameters and their unique combinations. Past studies on soil erosion problems identify and proposed *erosion risk* or *erosion hazard* as an important indicator or the surrogate parameter of actual soil erosion. For example, the European Environment Agency (EEA) used a soil erosion risk assessment approach to evaluate the problem of soil erosion in large regions and for decision making purposes. Moreover, a qualitative based model, in general, should be considered as the tool for understanding the spatial and temporal degree of erosion risk over a large area and for identification of hot spot regions. However, it should not be consider as a replacement of physical and conceptual based models. Basically, most of the available erosion risk assessment models have qualitative outputs but some of them have the capability to quantify the associated risk into actual soil loss. Such models are considered to be "semi-quantitative".

To summarize, erosion modelling approaches, ranging from simple to complex ones, are developed for various parts of the world. The decision to adopt a certain approach depends on various factors like data requirements, underlying assumptions of the model, components of the model which reflect models' capabilities and the hardware requirement of the model (Merritt et al., 2003). In general, there is no model which is "best" for all applications. A brief discussion about state of the art of empirical and physical based models along with expert risk assessment erosion models is given in the subsequent section.

2.2.2 Empirical and Physical based Models

A comprehensive review on the different types of soil erosion and sediment transport models is reported by Merritt et al. (2003). Their study focuses on the comparison of the models' complexity, their inputs and requirements, the processes they represent and the manner in which the processes are represented. Their review also covers the scale of various models intended for use and the types of output information the models provided to the end user. Another review of modern watershed scale hydrologic and non-point-source pollution models is published by Borah and Bera (2003). Similar studies focusing on semi-quantitative erosion models for basin scale are reviewed by Vente and Poesen (2005). These authors conclude that most of the semi-quantitative models might benefit from a more quantitative description of the factors used to characterize the basin. Modelling and prediction provide a mean for a quantitative and consistent approach to estimate erosion risk under a wide range of conditions. In this section, two model categories are presented: firstly, empirical and, secondly, physical-based models.

Empirical based models are based primarily on the analysis of observations and seek to characterize response from these data. Common empirically based models like Universal Soil Loss equation (USLE) (Wischmeier and Smith, 1978), the Modified Universal Soil Loss Equation (MUSLE) (Williams, 1975) and the Revised Universal Soil Loss Equation (RUSLE) (Renard et al., 1991) are frequently used for the estimation of surface erosion and sediment yield from catchment areas because of their limited data requirement and ease of application (Bhattarai and Dutta, 2007; Kothyari et al., 2002; Lim et al., 2005). The USLE and RUSLE models estimate the average annual gross erosion as a function of rainfall energy which is represented by R, rainfall erosivity index, together with the soil erodibility factor (K), slope-length and steepness factor (LS), and CP which represent the land cover and support practices factor. The RUSLE model maintains the basic form of USLE with a modification of the equations to derive the input factors. For example, the improved equation to compute slope length L in RUSLE incorporates the concept of basin contributing area which takes into account the flow direction and accumulation of the region. This allows RUSLE to predict the soil loss due to Hortonian overland flow in 3-D terrains with convergent and divergent slope (Merritt et al., 2003). In MUSLE the rainfall erosivity index is replaced with a runoff factor (Q). This improves the sediment yield prediction and eliminates the need for delivery ratios (Zhang et al., 2009).

Although these empirical models may not replicate real world erosion processes, they are extensively applied all over the world as they provide the first step in identifying sources of sediment and nutrient generation (Merritt et al., 2003). In spite of their popularity and acceptance, they are often criticized for relying on unrealistic assumptions, i.e. the assumption of stationarity ignoring the heterogeneity of catchment inputs and characteristics. Nevertheless, empirical based model are still preferred over conceptual and physical-based models as they have the capabilities to model erosion using limited input data. Rapid development in the field of erosion modelling, change and improve common empirical models in its components make them more process oriented. Most of the empirical models, especially USLE and MUSLE, are found to be used as a model component in physical or process based models for the computation of overland sediment and erosion processes.

Physical-based models are considered to have the capability of representing the physical processes involved and assessing both the spatial and temporal variability of the natural erosion processes. The major drawback is the necessity for a large amount of input data and parameters to run the model as

the models have different sub-models related to hydrology, hydraulics, meteorology and soil mechanics. A brief description on the overland erosion processes or overland sediment modeling concept for some of the common physical based models is provided in Table 2-1 (taken from Borah and Bera, 2003).

Table 2-1: Some of the common watershed scale hydrologic and non-point source pollution models

Models: C (continuous); S (single event)	Overland Sediment (erosion processes)
AnnAGNPS (C)	Uses RUSLE to generate sheet and rill erosion daily; sediment deposition based on size distribution and particle fall velocity
WEPP (C)	Process oriented continuous simulation erosion prediction field or watershed scale model. Calculates erosion from rill and inter-rill areas and uses the concept that detachment and deposition rates in rills are a function of transport capacity which is filled by sediment; uses a steady state sediment continuity equation as the basis for describing the movement of suspended sediment in a rill.
ANSWERS (C)	Raindrop detachment using rainfall intensities and USLE factors, transport and deposition of sediment sizes using modified Yalin's equation.
HSPF (C)	Rainfall splash detachment and wash-off of the detached sediment based on transport capacity as a function of water storage and outflow plus scour from flow using power relation with water storage and flow.
SWAT (C)	Sediment yield calculated from the Modified Universal Soil loss equations; expressed in terms of runoff volume, peak flow and USLE factors.
AGNPS (S)	Soil erosion using USLE and routing based on steady state continuity, effective transport capacity from a modification of Bagnold's stream power equation, fall velocity, and Manning's equations.
ANSWERS (S)	Raindrop detachment using USLE factors, flow erosion and transport of four sizes (0.01 mm to 0.30 mm) using a modified Yalin's equation and a explicit numerical solution of steady state continuity equations.
CASC2D (S)	Soil erosion and sediment deposition are computed using a modified Kilinc-Richardson equation with a USLE factor and conservation of mass.
DWSM (S)	Raindrop detachment and sediment transport, scour and deposition of user specified particle size groups based on sediment transport capacity and approximate analytical solution of temporarily and spatially varying continuity equations.
KINEROS (S)	Raindrop detachment and sediment transport, scour and deposition of one particle size based on sediment transport capacity and explicit numerical solution of temporarily and spatially varying continuity equation.

Considering the large spatial heterogeneity of the landscape and complex interdependence of variables that influence the erosion process, physical- and complex conceptual-based models are found to be inappropriate and rather disappointing for estimating overland erosion and catchment exports. Merritt et al. (2003), in their comprehensive review of erosion models, identifies the reasons that made the physical-based models quite limited in their application. Specifically, they bemoaned the lack of sufficiently spatial distributed input data to drive the models, the paucity of calibration data in space and time to define an appropriate parameter set for the models and hence reliable output. They are also critical of the over-dependency of model results on the experience of the user and the high computational requirements at larger scale. Hence, despite their capability to represent the physical

processes involves in soil erosion and sediment transport, a large mass of older results from physical-based models are found to be rather unsatisfactory when compared with measured data at catchment and basin scale.

2.2.3 Expert-based Erosion Risk Assessment Model

With the advancement in the understanding of physical processes involved in soil erosion and increasing expert knowledge about the process of erosion, expert based approach of soil erosion assessment in a regional and basin scale is found to be adopted in many recent erosion risk assessment studies (Vente and Poesen, 2005; Gobin et al., 2002) . Such approaches of assessment are categorized as "semi-quantitative" and "qualitative" modelling approaches, e.g. factor or indicator mapping, expert based mapping or scoring method.

Table 2-2: A comparative summary of common expert-based models (semi-quantitative methods) to assess soil erosion at regional and basin scale (Vente and Poesen, 2005)

Models	Input parameters (Soil, Climate, Topography, Vegetation)	Combination or evaluation method	Distributed modeling approach	On-site/Off-site	Validated
PSAIC	lithology, soil texture, stoniness, rainfall amount, slope, % cover and % cultivation	sum	no	off-site	yes
FSM	lithology, slope and % cover	multiplication	no	off-site	yes
CORINE	soil texture, depth, stoniness, Fournier index, Bagnouls-Gaussen aridity index, average slope, % cover	multiplication	yes	on-site	no
EHU	lithology, kinetic energy (total rain), average slope, % cover	multiplication	yes	on-site	no
FKSM	soil texture, Fournier index, slope, vegetation type	multiplication	no	on-site	yes

Key: PSAIC: Pacific Southwest Inter-Agency Committee; FSM: Factorial Scoring Model; CORINE: Coordination of Information on the Environment; EHU: Erosion Hazard Unit; FKSM: Fleming and Kadhimi Scoring Model.

Expert judgments are identified to be a potential and valuable source of information in soil erosion and land degradation assessment, especially in areas where data paucity impedes the use of quantitative models (Sonneveld, 2003). The main concept behind the expert-based erosion assessment model is quite simple and in most of the cases it tends to generalize and simplify the soil erosion process. Generally, once the factors that influence the rate of erosion are identified it is possible to rank and give weights to each individual factor for susceptibility to erosion. Then, by various methods like multiplication, sum of scores or simple overlay analysis one can deduce that a high susceptibility for all the identified factors indicates a "high erosion risk" and a low susceptibility for all the factors indicates a "low erosion risk".

Apart from the models summarize in Table 2-2 there are further models such as Hot Spots approach, RIVM approach, GLASOD approach. These can be used for erosion risk assessment on large regional, national and global scales (Gobin et al., 2002).

Similar to other empirical and process models, the expert-based modelling approach has its own advantages and limitations. The main advantage is the modest data requirement. The expert-based models can be widely applied at different geographical settings using appropriate data of the local conditions. Such an approach provides a method to represent available knowledge on sources of sediments i.e. high erosion risk areas. This type of model provides a clear understanding on the erosion risk distribution for a whole area under investigation, which in turn provides first hand information for decision making and prioritization of the landscape.

The main limitation of this modelling approach is the assignment of weights, ranking of parameters and their combination methods (addition, multiplication etc.) that influence soil erosion. There is a degree of subjectivity involved when the assessment of weights for each factor is carried out with expert knowledge or the available information in the literature. Nevertheless, it should be pointed out that even a complex physical-based model seems to have a strong degree of subjectivity in the calibration exercises, in that *a priori* knowledge of the area prevails in the selection of parameters (Favis-Mortlock, 1998; Sonneveld, 2003). One of the identified problem areas with methods based on scoring and weighting is that the results are affected by the way the scores or weights are defined. In addition, classifying the source data results in information loss and the results of the analysis may be dependent on the class limits and number of classes used (Gobin et al., 2002). Another major drawback with such an approach is the evaluation of model results, i.e. a correct way of interpretation and explicit validation. Hence, the results from such modelling approaches should be indicative of a general pattern of the relative differences rather than providing accurate absolute erosion rates.

2.3 Need of Fuzzy Logic Modelling in Environmental Assessment

2.3.1 Fuzzy Logic: An introduction of the underlying concepts

In the real world all the elements and features present are perturbed by imperfection and thus form the central idea of the platonic philosophy, for example, there exists no object that is perfectly round. We are associated with "inexact structures" in the real world while "perfect notions" and "exact concepts" correspond to things that are envisaged in pure mathematics (Kandel, 1986). The term "fuzzy" is introduced by Zadeh in 1962 and is followed by a technical exposition in 1965 which started to be termed as the theory of FUZZY SETS (after Zadeh, 1965). The concept of fuzzy sets is defined as a *class* with a continuum of "grades of membership". The basic concept of a membership grade, defined by a crisp set and a fuzzy set, is shown in Figure 2-3.

The central basic concept of fuzzy systems is that truth values or membership values (in fuzzy sets) are indicated by a value on the range [0, 1], with 0 representing absolute falseness and 1 representing absolute truth (Brule, 1985). The ability to describe the knowledge in a descriptive human like manner in the form of a simple rules using linguistic variables allow any fuzzy model to be simple, efficient and more flexible.
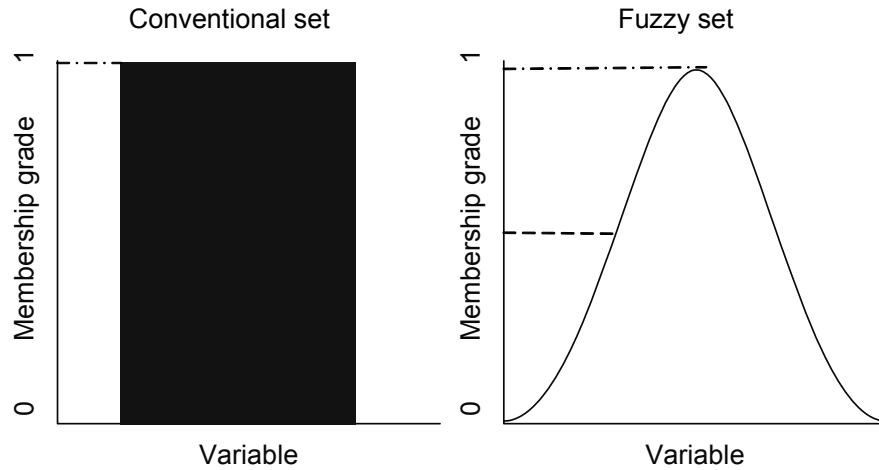
Figure 2-3: Schematic description of a membership grade of an object (crisp set: left picture; fuzzy set: right picture)

In general, a fuzzy set (class) A in X, where X is a space of points (objects) with a generic element of X denoted by x having, X = {x}, is characterized by a membership function f_A(x) which associates with each point in X, a real number in the interval [0, 1]. The value of f_A(x) represents the grade of membership (or certainty factor) of x in A. The closer the value of f_A(x) is to unity, the higher is the grade of membership of x in A. When A is set to an ordinary set of a term, its membership takes only two values, i.e. 0 and 1, with f_A(x) = 1 or 0 according to if x does or does not belong to A. Thus, in this case, f_A(x) reduces to the familiar characteristic function of a set A. Such a set is referred to as ordinary sets or simple sets, according to Zadeh (1965).

Fuzzification, inference and defuzzification are the three basic steps of fuzzy logic systems (see Figure 2-4). Any fuzzy expert system is composed of three primary elements, namely fuzzy sets, membership functions and fuzzy rules.
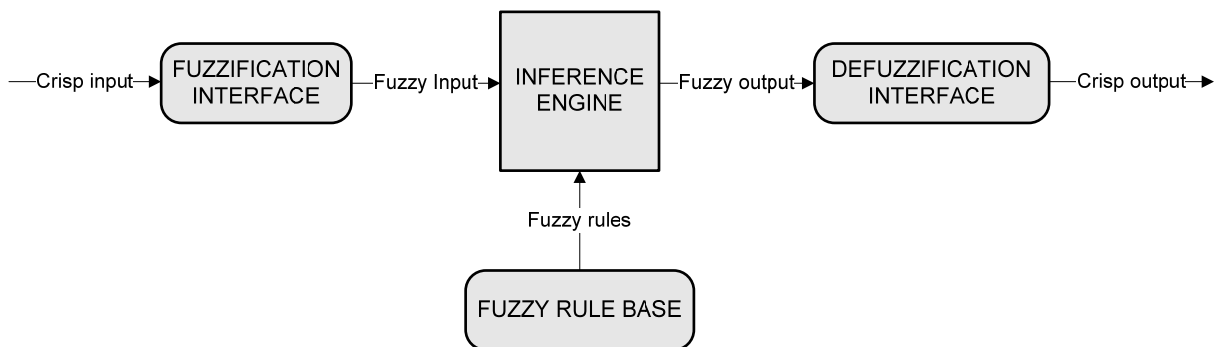
Figure 2-4: Basic architecture of a fuzzy expert system

Fuzzy sets are quantitatively defined by membership functions. Typically simple functions like triangles and trapezoids are used and cover the specified domain of the value of the input parameter. Set up of the fuzzy rules is in the form of 'IF-THEN' statements with the knowledge of experts. Linguistic terms are ordinary language description like high, moderate, very high etc. taken by linguistic variables that are used to represent a particular fuzzy set with an associated degree of

membership in the set (Zadeh, 1965; Kandel, 1986; Bardossy and Duckstein, 1994; Mendel, 1995; Ross, 2004).

Both the process of fuzzification and fuzzy rules development involve a certain amount of uncertainty. This concerns the definition of linguistic classes from the crisp input range of the variables and the applicability of defined fuzzy rules on the basis of expert knowledge and literature. However, this process of membership assignment and fuzzy rules development is problem dependent. The accuracy of design rules and sets can be assesses by means of evaluation of each function and the modification of rules. Above all, experience, expert judgments and knowledge about the process under investigation plays an important role in the determination of fuzzy sets and rule base (Murtha, 1995). Hence, fuzzy logic is a technique which uses fuzzy sets and an expert rule system that defines the processes toward logical processing.

One of the main purposes of fuzzy logic is the development of a methodology for the formulation and solution of problems that are too complex or ill defined to be analyzes by conventional techniques (Kandel, 1986). Therefore, fuzzy logic can be found in fields varying from electronic power systems to environmental applications (Metternicht and Gonzales, 2005).

2.3.2   Application of Fuzzy Logic in Soil Erosion Risk Assessment

Fuzzy logic aids in precise representation of vague and imprecise environmental factors. There is a wide use of fuzzy logic in environmental assessment and ecological research (Salski, 1999; Salski et al., 2008). The application of fuzzy logic for environmental assessment especially in watershed management, hydro-ecological modelling, habitat modelling, hydrological processes, water quality problems and flood forecasting is extensively reported (Yu and Yang, 2000; Raj and Kumar, 1998; Mitra et al., 1998; Zhu and Mackay, 2001; Xiong et al., 2001; Kisi et al., 2006). Studies focusing on using fuzzy logic concepts to improve the existing soil erosion models, developing a exploratory soil erosion model and about general assessment of soil erosion in different geographical regions of the world are also reported (Mitra et al., 1998; Adinarayana et al., 1999; Ahamed et al., 2000; Tran et al., 2002; Bahrami et al., 2005; Tayfur et al., 2003; Gournellos et al., 2004; Metternicht and Gonzalez, 2005; Cohen et al., 2008). These studies give the impression that the advantages of using fuzzy logic are its flexibility, allowing easy improvement of the model output and process in comparison to empirical- and physical-based models. Previous soil erosion prediction studies using fuzzy logic tend to employ a limited number of input variables that influence the soil erosion processes. The prediction and output is governed, therefore, by the limited set of variables in their models. Hence, there is a need to further devise a fuzzy-based methodological framework that is simple, robust and relies on common erosion influencing parameters that are easily available for modelling. In addition, the modelling framework should be set up to overcome certain limitations of fuzzy logic systems, i.e. the problem of increased dimensionality of rules with increased numbers of fuzzy input parameters. For instance, a multi-stage fuzzy approach for erosion risk assessment can be developed where each stage can be evaluated independently or in combination with different modelling stages. This will provide the user and experts in the formulation and assessment of the fuzzy rule base with ease, due to lesser rule dimension at each stage of modelling.

Environmental assessment such as risk mapping of regions prone to erosion processes generally involves the incorporation of expert knowledge at various levels of decision making. It is clear from

this that a certain level of ambiguity exists when making the final project decision (Prakash, 2003). Hence, uncertainty and imprecision involves in expert knowledge can be well addressed using fuzzy logic concepts. Researchers in the past have used fuzzy models to incorporate the level of uncertainty involved in the input data when dealing with environmental modelling. There is less or no account of studies which are related to uncertainties that are associated with expert knowledge. Involvement of multiple criteria and factors make it difficult for the expert to judge and correlate from the literature to arrive at a precise decision on the importance of each criteria. In such situations, all considered criteria can be compared, weighted and ranked using MCDM techniques (Multi-Criteria Decision Making Techniques) such as AHP (Analytical Hierarchy Process) described in Saaty (1980) and Al-Harbi (2001).

It is a well known fact that soil erosion risk modelling at watersheds or basin scale involves various environmental parameters which are fuzzy in reality. Hence, the ability of fuzzy logic to transform the knowledge in a descriptive human-like manner in the form of simple rules using linguistic variables provides a new direction to explore and develop an efficient, simple and well structured model. Incorporation of knowledge in the form of simple rules provides a mechanism to understand the process easily and update the rules, whenever additional knowledge about the process is available. Such capability of fuzzy systems will make the model more dynamic and help in easy interaction with different users, i.e. scientists, policy- and decision-makers.

2.4   Need of Geospatial Data for Environmental Assessment

A large body of literature on the application of Remote Sensing (RS) and Geographical Information Systems (GIS) to various environmental issues pertaining to domains like water resources management, forest sustainability assessment and land cover assessment is available. However, listing them here is beyond the focus of this thesis. One of the most recent and comprehensive reviews of satellite remote sensing for water erosion assessment is made by Vrieling (2006). This review summarizes the methodologies and the contribution of satellite remote sensing in the field of erosion research by providing necessary spatial data at various scales. On the other hand, Renschler and Harbor (2002) discusses the need of developing a model which is user-friendly, scientifically sound and has the capability of spatial analysis and visualization in a GIS environment.

One of the main concerns in regional-based environmental studies is the scarcity of data for the assessment and validation of the model. Many existing models for evaluation of the regional soil erosion risk have a high data demand and need an extensive collection of field data. With the advancement in remote sensing technology, it is now clear that remotely sensed platform provides the necessary data in regional and global scale and acts as a complementary dataset with reference to ground measured data. The development of RS and GIS technology has given the flexibility and opportunity to gather, analyze and produce information that can identify the characteristics of landscape features. It helps to observe changing patterns, processes and structures at various spatial and temporal scales (Mesev, 2007). Geo-spatial layers obtained from RS satellite sensors can be used as thematic input parameters required for the assessment of simple to complex environmental problems like LULC change analysis and soil erosion risk mapping in various regions of the world. In addition, the dynamic changes in landscape patterns and processes can be monitored and mapped on the spatial and temporal domains.

In this research, geospatial data is used to quantify and analyze the various parameters influencing soil erosion processes. The GIS provides the necessary framework to integrate the process of erosion and represents the associated varying degree of risk in a spatial domain. Such an approach can provide a spatial erosion risk distribution map that in turn will help for further analysis and decision making purposes. One of the significant advantages of GIS is that it is not limited to displaying spatial data (Lee and Wong, 2000). Shifting from spatial data management systems to spatial decision support systems, GIS can provide the necessary functions for spatial queries, dynamic mapping, geo-coding and even simulating alternative scenarios of future regional development.

3 F-WERCAM (Fuzzy-Water Erosion Risk Classification and Assessment Model) Framework

This chapter provides the methodology of water erosion risk classification and the assessment by the fuzzy logic concept. A brief description of the fuzzy inference calculator tool used and its interface within ArcGIS is also provided. The customized tool in ArcGIS is used for implementing the developed F-WERCAM framework.

3.1 Identification of Parameters Controlling the Soil Erosion Process in a Landscape

It is imperative to take into account the primary variables that influence the soil erosion risk of a region, when developing an erosion model. Every soil erosion assessment model must represent how the governing parameters of climate, soil, topography, and land use affect soil loss and related variables. Any external disturbance of short-term factors such as a change in climatic condition or land use patterns can intensify the erosion process. Many of the present day erosion models (empirical-, conceptual-, physical-based etc.) rely on these primary parameters. According to the literature on past and present studies on soil erosion, the primary parameters that are considered to be important for the erosion risk assessment can be summarized as follows in Table 3-1.

Table 3-1: Main governing parameters for the water erosion risk assessment study

Category	Primary parameters	Source
Topography	Digital Elevation Model (DEM) derived slope gradient (%), slope-length	Contour map, topographical map and geospatial based SRTM DEM, ASTER DEM
Climate	Rainfall, temperature and wind	Ground measured and satellite estimates of rainfall data
Soil	Soil type and texture, soil organic carbon content (soil erodibility factor)	Soil map, experimental and documented results
Land use and land cover	Land use and cover practices, vegetation coverage in temporal scale	Satellite imagery like LANDSAT data, classified LULC map , NDVI map as a proxy for vegetation cover

In this study, five important parameters are identified and incorporated in the formulation and the development of the F-WERCAM framework. Descriptions of these main factors that are considered in this water erosion modeling framework are as follows:

1. **Slope**: A terrain parameter that accounts for the topographic setting of the region, such as the influence of slope gradient on the soil erosion risk.

2. **LULC** (**Land Use and Land Cover**): This is considered to be one of the most dynamic factors that can be readily manipulated to produce wide variations in rates of erosion and the corresponding risk. It is generally considered as the "anthropogenic factor" as it tends to be affected by the influence of human activities.

3. **NDVI (Normalized Difference Vegetation Index)**: This represents a proxy for the vegetation cover distribution within each LULC class. This factor can be used as an indicator of vegetation growth and when comparing different periods of a year it can provide the temporal change in vegetation cover. This in turn will help to study the influence of vegetation growth patterns on the erosion risk of the region.

4. **Soil erodibility (K)**: This factor takes into account for the inherent resistance of soil to erosive forces. This factor reflects the sensitivity of different soil types to erosion. It is considered as an inherent soil property with a constant value for a given soil type of particular physical and chemical composition (texture, depth and organic carbon content, etc). This factor is used widely in many existing erosion prediction models as one of the important governing factors (Wischmeier and Smith, 1978; Renard et al., 1997). Soil information on organic carbon and particle size distribution is required to calculate a soil erodibility map of a region. A positive aspect of this erodibility factor is that it tries to reflect the complexity of inherent physical and chemical properties of different types of soils and their response to water erosion.

5. **Rainfall erosivity** (R): This index accounts for the spatial and temporal distribution of rainfall. "Erosivity" is defined as the potential ability of precipitation to cause erosion and is a function of the physical characteristics of rainfall. This function is termed the rainfall erosivity index, R. The higher the rainfall, the greater the surface runoff will be, thereby increasing the susceptibility of soil particles detachment and transportability. Hence, the rainfall erosivity index is considered in this study as an important input parameter for the fuzzy rule base erosion model.

3.2   Development of the F-WERCAM Framework

The whole methodology is set up considering the most important primary factors that control the water erosion. A multi-stage framework is considered to take into account the dimensionality problem during the fuzzy rules development at the later stage. All considered parameters are initially grouped under two broad categories. The definition of each category used in this research is defined as:

a) Dynamic factors

Factors and criteria that are dynamic in both spatial and temporal scale, i.e. a small variation within these factors can induce high variability of erosion risk within a short interval of time. The factors that are within this category are rainfall amount, intensity, duration (represented by R factor of USLE; RUSLE), land use configuration of a region and the intensity of vegetation cover distribution within each LULC class. These factors tend to produce wide variations in rates of erosion and its corresponding erosion risk in temporal scale in addition to their spatial variability.

b) Static factors

These are factors that are insignificant in short temporal scale (as opposed to geologic time scale) but have significant spatial variability. The changes in these factors in temporal scale can be assumed as static when studying the soil erosion process and its effect on seasonal, monthly and dekadal time scales. For instance, slope gradient of a region may undergo a significant change when considering in a geologic time scale but within a short temporal scale there may not be any significant changes. These factors can induce as well as resist the erosion process due to its specific material composition and surface configuration. The factors that belong to this category are soil texture and its properties (K, soil erodibility), slope gradient and elevation.

Integration of both the dynamic and static factors will result in an overall assessment of the water based erosion risk, experienced at certain locations with varying degrees of potential erosion risk. Initial weighting of the factors are made using expert based opinion through questionnaires about the regional soil erosion risk assessment. In addition, past and recent documented literature on soil erosion risk is reviewed and taken in account when weighting the influence of each considered variable on the overall erosion risk of the region. Another approach to rank the considered factors is done using the AHP (Analytical Hierarchical Process) technique (Saaty, 1980; Al-Harbi, 2001). Using this technique, all the influential factors can be prioritized by assigning a weight, which in turn can help in the development of fuzzy rules in addition to combining individual intermediate fuzzy-based output into a final result that would represent the overall soil erosion risk.

3.2.1   Description of the F-WERCAM framework

The general workflow of the F-WERCAM framework can be described as shown in Figure 3-1. The F-WERCAM framework is composed of three main stages: the integration of the output of the first two stages of modelling results in the overall system output, i.e. Stage 3 of the model. The model output from the initial stages can be analyzed independently to study the influence of each parameter at each stage of modelling. Stage 1 of the framework focuses on studying the influence of vegetation cover and LULC practices for the protection of top soil from being eroded by action of external agents like rainfall and overland flow. Stage 1 of the framework provides the Soil Protection Index (SPI) map, which takes into account the LULC and NDVI maps as the two input model parameters. Stage 2 of the framework determines the potential erosion risk of the region, which is basically the inherent risk of erosion, irrespective of ground cover and current land use practices. This stage takes into account the climate, topography and soil factor as input model parameters. The output from Stage 2 is the Potential Erosion Risk Index (PERI) map and it reflects or represents the worst possible scenario without ground vegetation cover. The final stage of the F-WERCAM framework is the "Actual Erosion Risk Index (AERI)" which is considered as a function of SPI and PERI, i.e. the influence of Soil Protection Index (SPI) on the Potential Erosion Risk (PERI) of the region. In short, the F-WERCAM framework provides a spatial distribution map of SPI, PERI and AERI, where the potential soil erosion risk of the region can be analyzed spatially and temporally. A more detailed description on each stage of the modelling, including the development of the fuzzy sets and corresponding fuzzy rules is given in chapter 7.

3.3 Fuzzy Logic Tool Components and its Customization for the F-WERCAM

Pertaining to the research objective of identifying an appropriate GIS approach to interface and utilize the fuzzy calculator within ArcGIS for water erosion risk classification and assessment the following procedure is adopted. The main idea behind the customization is to allow the fuzzy tool to be interactively used with ease. The tool provides additional functionalities of using grid data structure layers in addition to feature layers, shape files, DBF tables, etc. It also provides the spatial representation of the model output for further advanced analysis in GIS. The main customization is made using the ArcGIS Model Builder (ESRI; ArcGIS Release 9.2).

3.3.1 Background of the Fuzzy Logic Tool or Fuzzy Calculator

A brief introduction on the fuzzy logic system is discussed earlier in chapter 2. This section focuses on the description of the fuzzy inference system and the fuzzy calculator used in this research. The customized tool took advantage of an existing fuzzy inference calculator (Schneider, 2001; Kopecki, 2008), which is integrated within ArcGIS, thereby allowing for direct data integration from various geospatial sources as input parameters and the presentation of the output in the form of spatial and temporal maps.

Accessing the knowledge base related to the process and developing the corresponding rule base is a prerequisite for any fuzzy logic system. The knowledge base provides the foundation for setting up fuzzy sets of the input variables, i.e. the range of values of input variables are "fuzzified" into suitable linguistic values which then become the labels of fuzzy sets. This initial step of fuzzy logic, which involves conversion of crisp quantities into fuzzy ones, is termed as "fuzzification". After fuzzification is carried out, the next step of fuzzy inference requires the development of the fuzzy rule base which is characterized by a set of linguistic statements based on expert knowledge and documented literature.

a) Fuzzy Inference System (FIS)

In the inference procedure, various inference methods can be employed to combine fuzzy "IF-THEN" rules from the existing rule base into a mapping from fuzzy input sets to fuzzy output sets (Bardossy and Duckstein, 1994; Mendel, 1995; Ross, 2004). The fuzzy calculator adopted in this study has a number of pre-defined settings or options for the fuzzy system parameters such as for the selection of the inference method and the combination method.
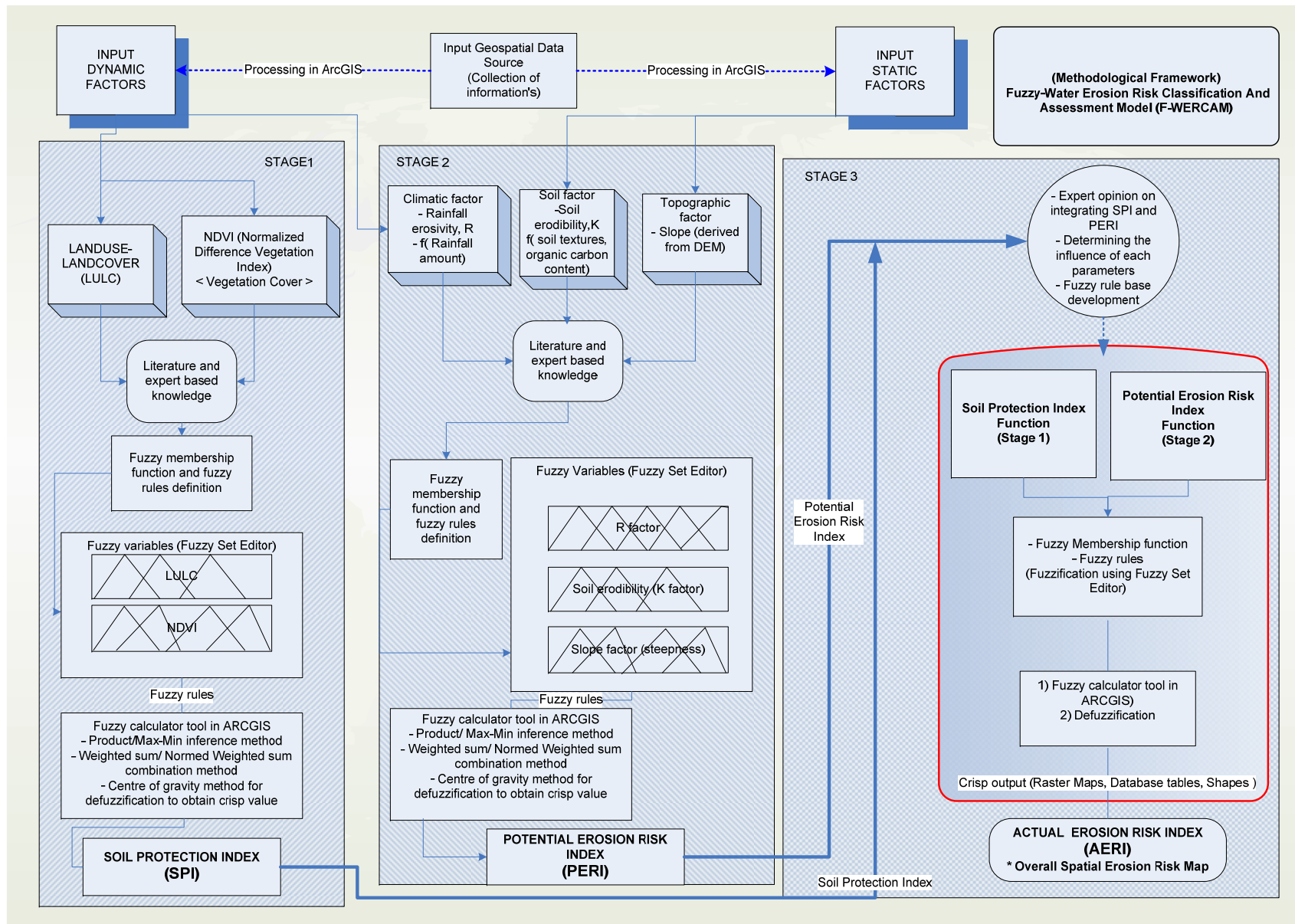
Figure 3-1: A methodological framework for water erosion risk classification and assessment by fuzzy logic approach

It is required to determine the applicability of a fuzzy rule depending on the condition of the rule in the defined rule base. The *truth value* or *truth grade* of a certain rule depends on the arguments to which the rule is to be applied. The truth value corresponding to the fulfilment of the conditions of a rule for given premises (a_1, a_2....a_k) is called the degree of fulfilment (DOF) of that rule (Bardossy and Duckstein, 1994). For the computation of the degree of fulfilment (DOF) of each rule which depends on the combination of input variables, the user can select the "product inference" or the "min-max inference" method for implementation in the fuzzy calculator. The product inference method uses the *standard product*, whereas the min-max inference method takes the *min* as the implication operator. They can be defined mathematically as follows (for two input parameters having "AND" as logical operator):

Product method: $\eta_i = \mu_A(x_1) * \mu_B(x_2)$ (3.3a)

Min-max method: $\eta_i = \min(\mu_A(x_1), \mu_B(x_2))$ (3.3b)

where η_i = degree of fulfilment of a rule i,

$\mu_A(x_1)$ = degree of membership of parameter x_1 relating to fuzzy set A,

$\mu_B(x_2)$ = degree of membership of parameter x_2 relating to fuzzy set B,

Various studies of fuzzy logic applications show that there is no great difference in the performance of rule systems with respect to the choice of the implication operator for determining the DOF (Bardossy and Duckstein, 1994). Hence, both, the product and min-max methods, are considered and implemented in the present fuzzy calculator. The product inference method is used as the standard pre-defined setting for inference but the user has the flexibility or option to select the min-max method for the computation of DOF as well.

The next step after calculating the degree of fulfilment for each rule is to combine the DOF's for each of the fired rules to obtain the total consequence output. In this tool, the weighted sum combination method, which is one of the additive combination methods, is used as the pre-defined setting and adopted for obtaining the total consequence. As defined by Bardossy and Duckstein (1994), the weighted sum combination of responses (B_i, η_i) is the fuzzy set B with the membership function:

$$\mu_B(x) = \frac{\sum_{i=1}^{I} \eta_i \mu_{B_i}(x)}{\max_u \sum_{i=1}^{I} \eta_i \mu_{B_i}(u)}$$ (3.3c)

where $\mu_{B_i}(x)$ = membership function of x in the fuzzy set B_i for rule i,

η_i = degree of fulfilment of a rule i,

I = total number of rules fired,

u = index corresponding to output fuzzy sets of the rule consequences, e.g. low, medium, high.

In this method, the division by the maximum of the sum is required to ensure that the resulting total consequence output of the membership function is not greater than 1. In addition to this described method, there is an option to choose the "normed weighted sum combination" for combining the fuzzy rule consequences. It is important to note that the appropriate choice of implication and combination method is context-dependent and largely influenced by the user experience and the type of the defined

input-output fuzzy sets of the system. A detailed discussion of these combination methods can be found in Bardossy and Duckstein (1994) and Schneider (2001).

b) Defuzzification

The last step in the fuzzy logic modelling process is to obtain a crisp output by the way of defuzzification. This is considered to be an art rather than a science and there are no scientific bases for any of the defuzzifiers proposed in literature (Mendel, 1995). It is basically the conversion of a fuzzy quantity to a precise quantity; just as fuzzification is the conversion of a precise quantity to a fuzzy quantity. Various methods of defuzzification are reported (Mendel, 1995; Ross, 2004). In the fuzzy calculator, the Centre of Gravity (CoG) method, which is a robust and widely used method in engineering applications, is adopted. Mathematically, this is represented as:

$$X_o = \frac{\int \mu_{total}(x) \cdot x \, dx}{\int \mu_{total}(x) dx} \qquad (3.3d)$$

where $\int$ denotes an algebraic integration and X_o is the defuzzified output of the system

In general, this method of defuzzification returns the centre of the area under the curve i.e. the area under the aggregation of the truncated output fuzzy subsets. This CoG method yields a unique crisp number while using all the information of the total output distribution. The output range by CoG method can approach the boundaries of its interval of definition. These are in fact the CoG of the two membership functions at the extreme of fuzzy partition.

It is important to discuss here that other methods of defuzzification like the "maximum defuzzifier" and "mean of maxima defuzzifier" are not considered in this study since they suffer from various limitations (Mendel, 1995; Panigrahi and Mujumdar, 2000). For instance, the "maximum defuzzifier" method ignores a lot of information of the output fuzzy set and does not take into account the shape of the output membership functions. In other words, the information not related to rules of maximal activation is generally ignored since only those elements of highest membership degrees in output sets are taken into account (Pham and Castellani, 2002).

c) Illustration of a Simple Fuzzy Inference System

Fuzzy systems that use a Mamdani-type inference, i.e. max-min or product inference are generally referred to as "standard fuzzy system" (Sablani et al., 2006). To demonstrate how a fuzzy inference system works, let us consider a simple two rule system where each rule comprises two conditions in the antecedent part and one conclusion in the consequent part as follows:

IF 'X1 is A_{11}' AND 'X2 is A_{21}' THEN 'Y is B_1'
IF 'X1 is A_{12}' AND 'X2 is A_{22}' THEN 'Y is B_2'

where A_{ij} is the jth linguistic term (fuzzy set) of the ith input variable and B_j is the jth linguistic term for the output variable Y.

The graphical representation of this (Figure 3-2) illustrates the process of inferencing and that of defuzzification to convert the resulting fuzzy output set to a crisp output. For each rule in the example, the minimal function ("min") is applied as the conditions in the antecedent are connected by logical "AND" connective. The minimum membership value for the antecedent propagates through to the consequent where the output membership function is truncated for the max-min method and scaled down for the product method. Then, the resulting membership functions for each rule are aggregated using the maximum combination method ("max") in the case of this example. Hence, the total consequence output or the resulted aggregated membership function is comprised of the outer envelopes of the individual truncated membership forms for each rule. Finally, the total consequence fuzzy output is defuzzificated to obtain a crisp output value by using the centre of gravity (CoG) method.
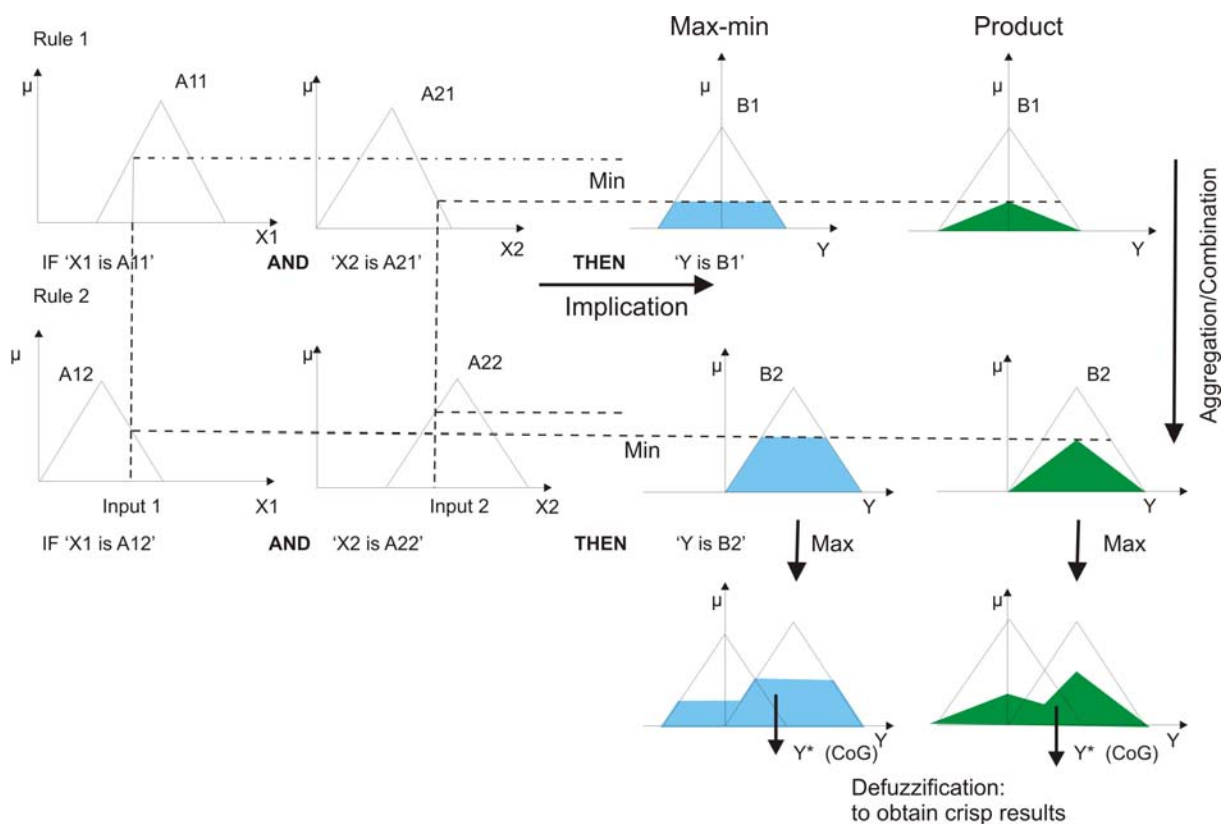
Figure 3-2: Graphical representation of a Mamdani-type fuzzy inference using max-min and product methods

3.3.2   Customization and Interface of Fuzzy Calculator using ArcGIS Model Builder

The main customization is done using the ArcGIS Model Builder (ESRI; ArcGIS Release 9.2). The schematic flow diagram of interfacing the fuzzy calculator (ArcGIS) as discussed for the implementation of the F-WERCAM framework is shown in Figure 3-3. It focuses on raster layers as input parameters using the "sample tool" in the Arc toolbox where the input raster values are extracted for each parameter and stored in the form of database tables. The integrated fuzzy inference calculator in ArcGIS then takes the DBF (database) table that contains the extracted values for each parameter as

an input along with the generated fuzzy sets and rules file. Fuzzy sets files are prepared using the "fuzzy editor tool". The desired initial output is in the form of DBF tables having an additional attribute column. This extra column contains the defuzzified value of the desired system output, for each corresponding input grid cell, along with its geographical X, Y coordinates. After this, the defuzzified output in the form of a database table is converted to a feature layer and finally maps into a raster layer using the "XY to feature event layer" and "Features to Raster" conversion tools. The final output is in the form of an interactive geo-coded map. For instance, the output spatial maps will represent the SPI, PERI and AERI of the region, thereby allowing the maps to be used interactively for advanced spatial analysis, visualization and for efficient decision making purposes. In addition, using inputs from different time periods will provide the temporal maps of SPI and the AERI of the region.
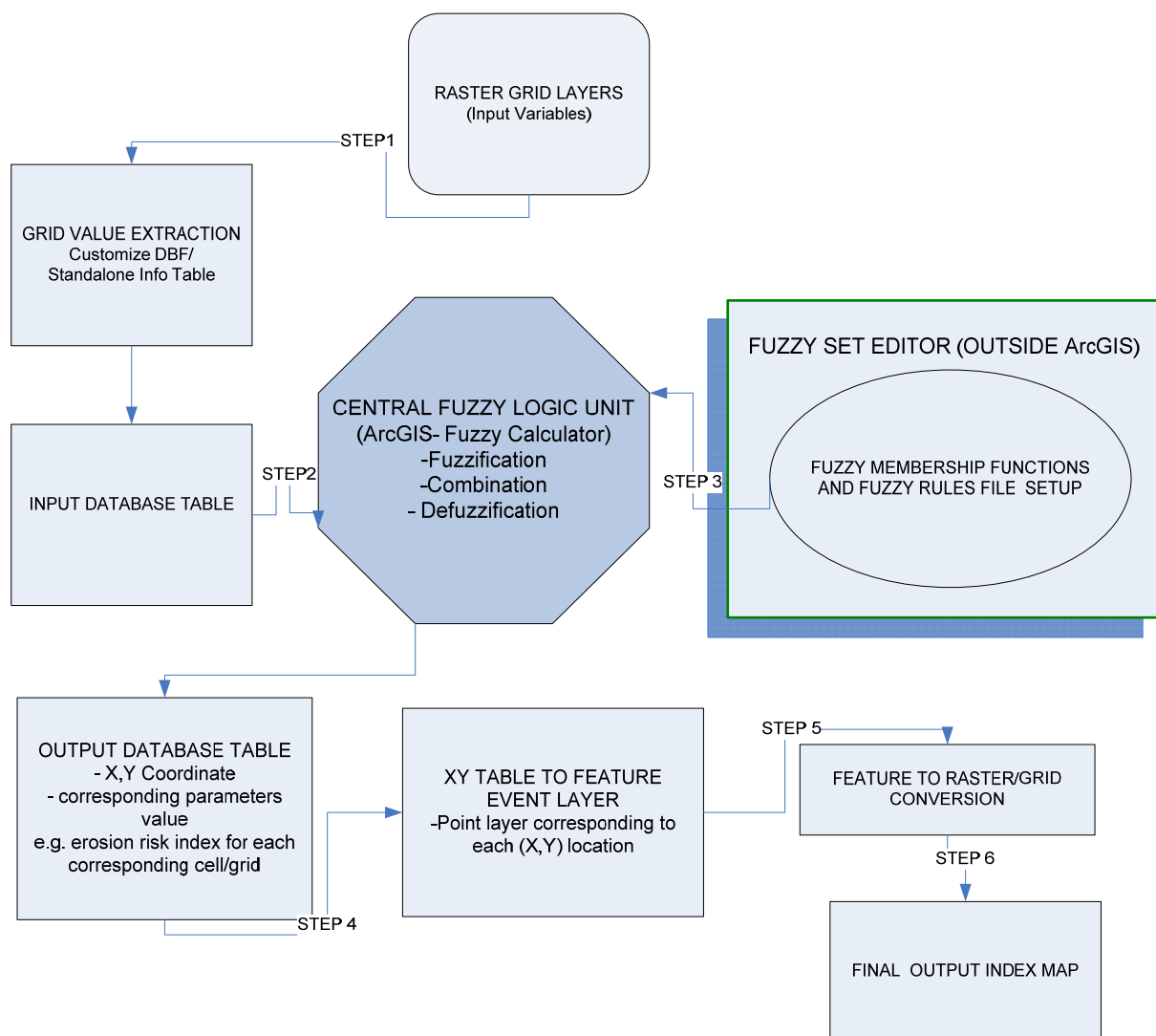
Figure 3-3: A schematic flow diagram of the customized fuzzy calculator tool in ArcGIS

A detailed flow diagram of each process implemented using the ArcGIS Model Builder is given in *Appendix 1*. The user can access the customized tool from the Arc Toolbox of ArcGIS. The tool is developed and tested successfully using the ArcGIS 9.2 and 9.3 versions. For the tool to be executed successfully, the fuzzy inference calculator module needs to be present in the Arc toolbox along with a

licence for the spatial analyst and database management module of ArcGIS. In summary, the fuzzy calculator performs all necessary fuzzy logic processing steps while the steps "grid value extraction module" and "feature to raster conversion" help in processing the input geospatial raster layers and the production of output grids or raster layers for advanced GIS based analysis.

3.4   Summary

Every soil erosion assessment model must represent how the governing parameters of climate, soil, topography and land use affect the soil loss. The developed F-WERCAM makes explicit use of the primary indicators or parameters that influence the water based soil erosion risk on a regional landscape. For instance, the LULC map, temporal NDVI maps, soil erodibility map, slope gradient and rainfall erosivity maps are the variables that are considered to be the most important ones for water erosion processes in this research. Since the F-WERCAM framework is to be implemented using a fuzzy logic system, it has become an imperative task to consider the number of primary input variables to be used in the modelling process. A trade-off or equilibrium is needed at the expense of greater accuracy when designing the model framework. This is because an increase in the number of input variables and linguistic classes leads to a dimensionality problem. In general, with an increasing number of input model parameters, the design of the fuzzy rule base tends to become more complex at a later stage. Hence, one needs to handle such problems at the initial stage when designing any fuzzy expert system. Keeping this problem in mind, the F-WERCAM is developed on the basis of a multi-stage modelling framework that primarily consists of 3 stages (i.e. SPI, PERI and AERI). This approach has the advantage of being able to make an independent assessment of each stage of the fuzzy rule base in addition to more effective handling and simplified development.

It is natural to question which method or preferred combination of fuzzy inference systems should be used for an application under consideration. Different inference, combination and defuzzification methods provide a great number of possibilities to evaluate fuzzy rules (Bardossy and Duckstein, 1994). It is important to note also that the choice of an appropriate inference, combination and defuzzification method is typically context-dependent and is largely influenced by user experience and the type of defined fuzzy input-output sets of the system. After an extensive review of the technical background of the different methods and their applicability in various engineering applications, the "min-max" and "product" as inference method, "weighted sum" as the combination method and the "centre of gravity" as the defuzzification method is adopted in this study. Bardossy and Duckstein (1994) illustrates with specific examples that the "product" inference method with additive combinations, i.e. the weighted sum combination method, and the "centre of gravity" method offer the simplest rule formulations (using the AND operator) and rule evaluations. Therefore we may consider this as one of the preferred approaches. The weighted combination, or normed-weighted-combination and the mean defuzzification method lead to simpler rule formulations. The simple combination of rule responses makes this combination-defuzzification method especially attractive for practical applications. From another perspective, the type of fuzzy inference approach adopted in this study can be considered as a "*Mamdani based fuzzy inference system*", where the rule antecedents and consequents are defined by fuzzy sets.

The fuzzy tool customization using ArcGIS Model Builder provides a user-friendly approach for the production of spatial distribution of erosion risk maps and the corresponding erosion risk values. One of the goals of this customized tool is that it should be able to produce a spatial distribution output

having visualization capabilities accessible through GIS. In other words, this means the *capability for raster data integration, spatial analysis and visualizations of the results*. Some of the salient features of this customized fuzzy tool are described below:

- The handling of large grid or raster data layers using the extraction module in addition to direct input of the DBF tables, standalone table and feature class.

- The efficient customization of the input standalone data table for direct input into the main fuzzy calculator module.

- The representation of the results in the form of a table for further analysis or in the form of a feature layer or raster layer for spatial and temporal visualization in GIS.

- An efficient processing time even of very large datasets.

- The ability to share the results in the form of an ArcGIS tool which can be linked with Arc toolbox or in the form of a script with third parties. In addition, it is able to be modified and updated easily in ArcGIS.

4 Introduction of Study Area and Datasets

"You can use all the quantitative data you can get, but you still have to distrust it and use your own intelligence and judgment."

- Alvin Toffler

4.1 Characteristic of the Upper Awash Basin, Ethiopia

To illustrate and test the F-WERCAM framework, a study site in Ethiopia is selected. Environmental datasets like precipitation, soil map, LULC map etc, and local expert knowledge for the study site is obtained from Habtamu Itefa, University of Stuttgart (which is originally obtained from Federal Ministry of Water Resources, Ethiopia). The Upper Awash catchment shown in Figure 4-1 is part of the Awash River Basin (7°53´-12°4´N; 38° 2´-43°16´ E) (Aynekulu et al., 2006). It covers a total area of approximately 11000 km^2 characterized by an upland plateau surrounded by mountains. Agriculture (crops) is the most dominant type of land use in this region. Some of the important cities and towns located within the study area are Addis Ababa, Mojo, Debre Zeyit, Adis Alem and Ginchi.
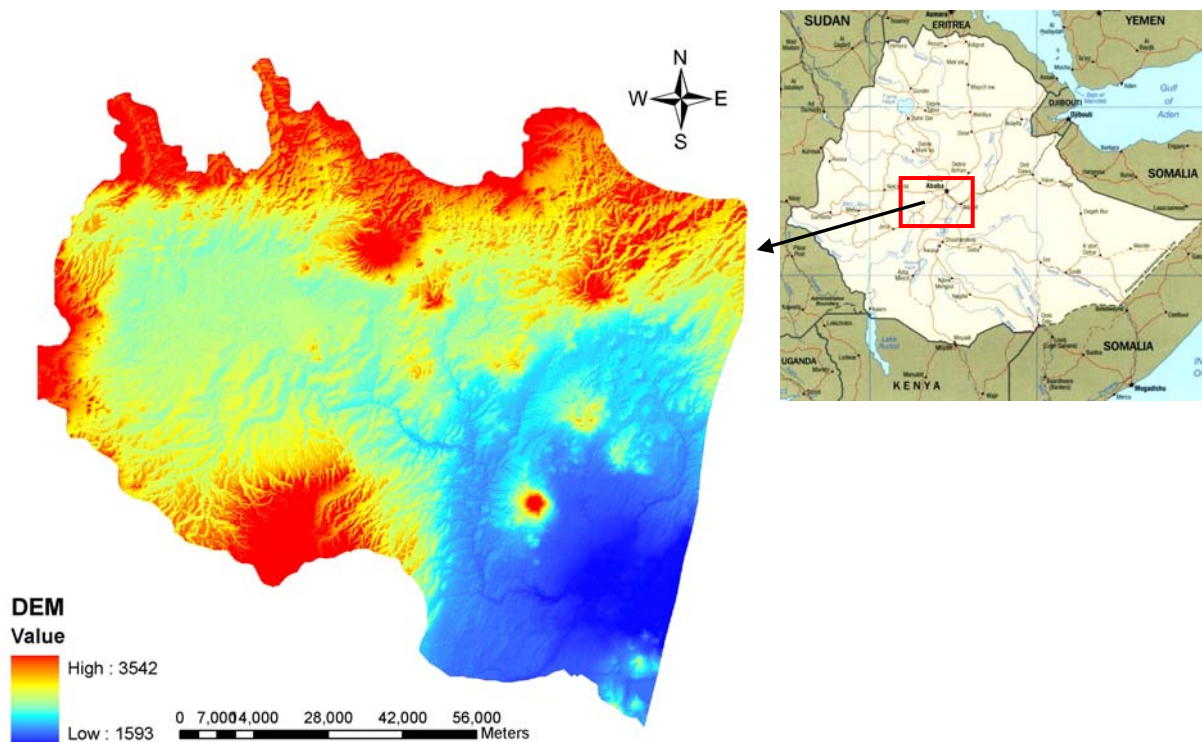
Figure 4-1: Map showing the location of the test site in Ethiopia (source: SRTM DEM)

4.1.1 Topography of the Study Region

Topography plays a significant role for the climate of Ethiopia, creating diverse microclimates ranging from hot deserts over the lowlands to cool highlands (Dinku et al., 2007). The elevation of the Upper Awash Basin ranges from 1500 to 3500 m a.s.l. Most of the northern part and extreme southern tip of Upper Awash Basin are characterized by steep and high mountains and consequently have higher slope gradients. The central area and the south eastern part are characterized by flat, low lying areas of low relief having a lower slope gradient. In the Ethiopian highlands, the slope distribution range is found to vary from 0 % to more than 60 %. Most of the regions in the study area having elevation less than 2500 m have a mean slope of 6 %, whereas the areas with an elevation higher than 2500 m have a mean slope of 15 %.

4.1.2 Climate

Figure 4-2: Rainfall regimes of Ethiopia showing location (shaded region) of the study area (USDA, 2003)

In general, annual precipitation of Ethiopia ranges from 800 to 2200 mm in the highlands and varies from less than 200 to 800 mm in the lowlands. There is a general trend of decreasing rainfall going northwards and eastwards from the high rainfall pocket area in southwest. Ethiopia has three rainfall regimes characterized by either uni-modal or bimodal rainfall patterns with two, three or four seasons as illustrated in Figure 4-2. Figure 4-2 shows that the study site (as shown in Figure 4-1) falls within the "three seasons" regime.

In the Upper Awash Basin, the range of annual precipitation is about 1400-1800 mm/a above 2500 m a.s.l. and 1000-1400 mm/a at mid-altitude between 2500 and 600 m a.s.l. The rainfall distribution, especially in the Ethiopian highland areas, is bimodal with a short rainy season from February to May and a main rainy season from June to September. Alemayehu et al. (2003) found that the variation in the seasonal distribution of rainfall in Ethiopia is attributed to its position in the Inter-Tropical Convergence Zone (ITCZ). This zone describes the relationship between upper and lower air circulation, the effects of topography, the role of local convection currents and the amount of rainfall.

4.1.3   LULC Type of the Region

The LULC of the Upper Awash primarily consists of forest area, settlement area, water bodies, grassland, agricultural land, shrubland or barrenland. These broad LULC classes are represented in the land use map of the Awash River Basin as provided by the Federal Ministry of Water Resources (FMWR), Ethiopia. It is found that Upper Awash Basin is dominated by agriculture which covers about 70 % of the region. The agricultural zone consists primarily of cropland where agriculture is practised on levelled or slightly undulated ground or on sloped land. Dense natural and protected forests of the region comprise about 6 % of the total study area.

4.1.4   Soil Type of the Region

The Upper Awash Basin is comprised of various types of soil having different properties and textural characteristics. Out of the 28 major soil groups, reflecting the main variations in the world's soil cover according to the FAO-Unesco Soil Map of the World (FAO, 1988), there are 12 major types of soil present in the Awash River Basin. Detailed information such as soil texture, organic carbon content of each soil type, etc. of the different soils are compared and cross-referenced by using the digital soil map (1:3000000) of Upper Awash Basin provided by the Federal Ministry of Water Resource (FMWR), Ethiopia.

The study area is found to be dominated largely by a type of soil which is conditioned by relief. It is called Leptosols and is present in the eroded upland areas. In general, Leptosols are characterized by their shallow depth which corresponds to less than 30 cm of soil cover over hard rock or by their high gravel content. This type of soil is reported to be highly fragile and susceptible to water and wind erosion if exposed to extensive anthropogenic events such as intensification of agricultural practices, deforestation or overgrazing, etc. Apart from this, Cambisols, Xerosols, Vertisols, Acrisols are other types of soil which are present in the region.

4.2   Land Degradation in the Upper Awash Basin

Studies and reports on land degradation by various international and national organizations highlight the problem of soil erosion, loss of agricultural productivity in the highland region of Ethiopia (EHRS-FAO, 1986; Berry, 2003). A large agriculturally productive area in Ethiopia which covers about 27 million hectares is reported to be experiencing erosion. Hakkeling (1989) reveals that the extent and the severity of soil degradation range from moderate to very severe in the Highlands region of Ethiopia. Elias (2003) identifies that the soil erosion is widespread and a serious threat for the cereal system in the highlands. The natural or tolerable rate of soil loss in the Upper Awash Basin is reported to vary between 10-16 t/ha/yr (Hurni, 1983a, b; Hawando, 1995, 1997). Agricultural lands within the Upper Awash are most vulnerable and have even higher risks of soil erosion.

The Ethiopian Highlands Reclamation Study (EHRS) estimates a total loss of two million cubic metres of top soil per year with an average annual soil loss from cultivated lands of 100 t/ha/yr (Aynekulu et al., 2006). The current erosion risk potential and associated land degradation of the region at some of the selected locations can be seen on the field photograph as shown in Figure 4-3.

Figure 4-3: Field photographs showing the problem of land degradation in the Upper Awash Basin
Source: Itefa H., IWS, Stuttgart

4.3   Available Data and Acquistion Methods

Data associated with the parameters influencing the soil erosion risk of the region (as discussed in Chapter 3) are obtained from various sources. It is to be noted that one of the focal points in this study is to develop a model that can effectively utilize the data acquired freely from remote sensing-based platforms as the main input variables. The monthly rainfall data from existing gauging stations and some limited ground-based observations or survey data on the current land degradation status in the study area are also obtained. Socioeconomic-based data on human population density (census: 2000) and livestock density data at the Wereda (administrative) level are also obtained from ILRI (International Livestock Research Institute), Addis Ababa, Ethiopia.

4.3.1   Geospatial Datasets

LULC, NDVI (vegetation cover), soil type, topography (elevation and slope), and climate (rainfall) of the Upper Awash Basin are the main primary data necessary to implement the F-WERCAM framework. The creation of the information layers or digital maps corresponding to each input data type is the first step when developing the geospatial database.

Land Use and Land Cover (LULC) map: The Geo-coded LULC map of the region for the year 2001 is obtained from the Federal Ministry of Water Resource (FMWR), Ethiopia. In addition, a thematic LULC map of the region for the year 2000 is generated by the supervised classification method using Maximum Likelihood Classifier (MLC) with the Landsat Satellite data as input source. A detailed explanation about land use and cover classification of the region is provided in Chapter 5 that deals with the temporal change assessment of LULC.

NDVI (Normalized Difference Vegetation Index) map: The source data for representing the vegetation cover of the study area is obtained from the pre-calculated periodic NDVI images supplied by the NASA Terra (AM-1) satellite's Moderate Resolution Imaging Spectroradiometer (MODIS) sensor, which contains basically a 16-day composite NDVI value. The MODIS 250 m NDVI

(MOD13Q1) provides the needed pattern of vegetation cover change, i.e. the quantification of the vegetative cover on the Earth's surface. This vegetation index is calculated from MODIS Terra surface reflectance followed by correction for molecular scattering, ozone absorption, and aerosols (Swets et al., 1999). Data corresponding to the time period of 2001 are downloaded and processed using the MRT (Modis Reprojection Tool) provided by Earth Resources Observation and Science (EROS) Center of USGS.

Rainfall data source: The gauging station rainfall data from 2001-2003 are obtained from National Meteorological Services Agency (NMSA), Ethiopia, for the 8 ground stations in and around the Upper Awash Basin, as depicted by red spots in Figure 4-4.
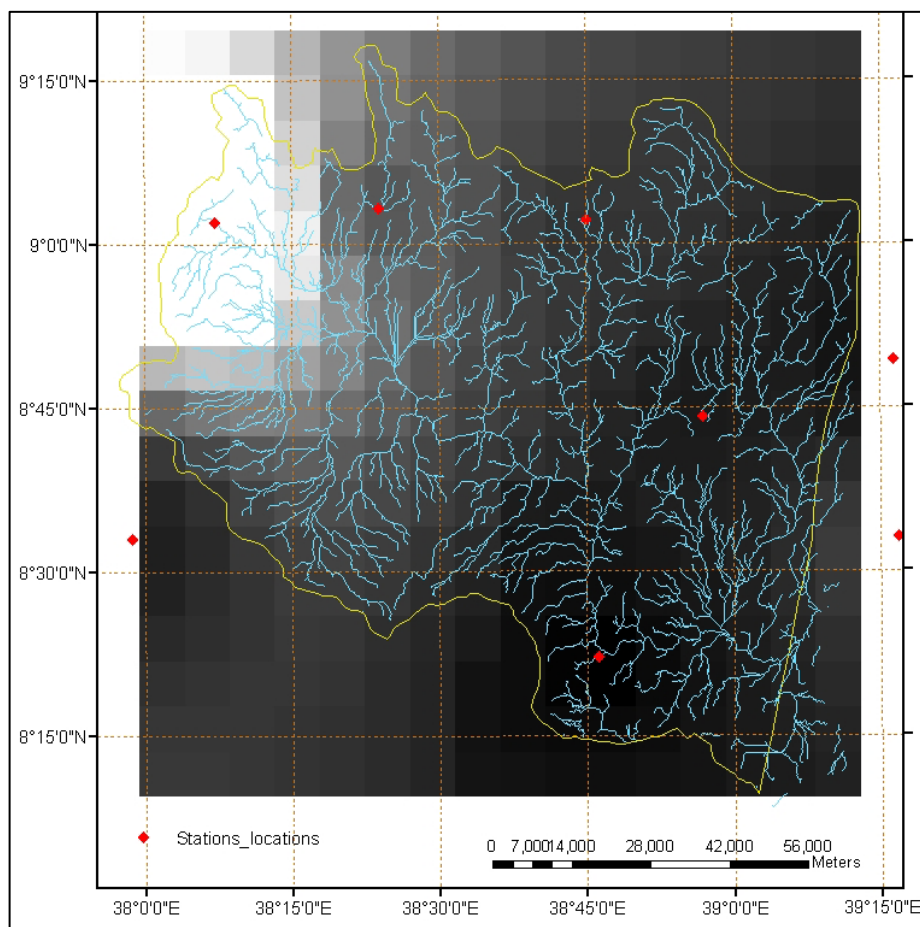
Figure 4-4: Locations of the ground rainfall stations and test site draped over a satellite estimate rainfall grid layer

In this study, the satellite rainfall estimates from two different satellite sources, having different spatial and temporal resolutions, is used for comparison with the ground measured rainfall data. The rainfall estimates obtained from the rainfall algorithm from the NOAA-Climate Prediction Centre over the African continent are downloaded from NOAA and FEWS (Famine Early Warning System) NET. The data for the Greater Horn of Africa which has a 8 km spatial resolution (original resolution 0.1° x 0.1°) and a 10 day (dekadal) time-step is obtained for the period 2001 to 2003; the rainfall estimates are processed to extract the grid cell value for the study area. For the same time period, the other data products, such as the TRMM 3B43 V6 with a spatial resolution of 0.25° x 0.25° and a monthly temporal resolution from the TRMM (Tropical Rainfall Measuring Mission) satellite are downloaded

from the TOVAS (http://lake.nascom.nasa.gov/tovas/) and processed into grid format for the area of interest. Details regarding these two specific data products and their algorithms can be accessed from:

ftp://meso-a.gsfc.nasa.gov/pub/trmmdocs/3B42_3B43_doc.pdf.
http://earlywarning.usgs.gov/adds/imgbrowses2.php?adds=&image=rf&extent=ea.

Rainfall data from these different sources are used for generating the rainfall erosivity map of the region. This erosivity map in turn is used as one of the main input parameters for the F-WERCAM modelling.

Digital Elevation Model (DEM): Data that represents the topographical setting of the region are obtained from the SRTM (Shuttle Radar Topography Mission), with a spatial resolution of 90 m. Details about the SRTM data can be seen under http://srtm.csi.cgiar.org/. The slope gradient map of the region, which is considered as another factor with regard to water erosion, is produced using the SRTM DEM.

Soil database and map of the region: The Geo-coded digital soil map (1:3000000) of the Awash Basin is obtained from the Federal Ministry of Water Resource (FMWR), Ethiopia. The regions corresponding to Upper Awash Basin are clipped out and extracted for further processing. The information on the soil texture and organic carbon content is used to compute the soil erodibility map of the region.

4.3.2   Ground and Field based Datasets

In this study, expert-based information and limited field survey data of the study area conducted during December 2009 are obtained from Itefa H. at the Institute of Hydraulic Engineering, Stuttgart University. These data helps to evaluate the current status on land use practices and intensity of land degradation of the Upper Awash Basin at 10 identified locations. The observation locations (X, Y) and a brief description about the LULC and current status of land degradation are provided in *Appendix 2-A*. Maps with locations and field photographs corresponding to the observation points are shown in *Appendix 2-B*.

5 Spatial and Temporal Change Assessment of Land Use and Land Cover Practices

"The oldest task in human history: to live on a piece of land without spoiling it."

- Aldo Leopold (1886-1948), 1938

5.1 Need for Land Use and Land Cover Monitoring

Obtaining the composition and characteristics of the land surface elements over a large area on a routine manner has only relatively recently come under consideration (Cihlar, 2000). First hand information on land cover characteristics and their distribution are required for many scientific studies, natural resource management and development of various local and regional policies. This makes the land use and land cover information an indispensable asset for monitoring various environmental problems and their associated risks. In the past, land use and land cover studies are hampered by lack of appropriate methodology, reliable technology and the cost associated with remote sensing datasets. Temporal monitoring of land cover and their studies are constrained in most of the tropical countries due to unavailability of the satellite datasets and the high cost tagged with each dataset, if available. The recent change in policy by USGS (United States Geological Survey) Landsat Satellite program, which allows an unrestricted free of charge access to the Landsat remote sensing data archive (Multi Spectral Sensor (MSS), Thematic Mapper (TM) and Enhanced Thematic Mapper Plus (ETM+)) provides the privilege to many researchers and policy makers to use the free datasets for monitoring and studying various environmental problems across the world. Landsat data from MSS, TM and ETM+ having a spatial resolution of 57-60 m and 30 m, respectively, are considered to be suitable for "Land Use and Land Cover"(LULC) assessment studies, ecosystem monitoring, land surface simulations, etc. (NASA, 2006).

According to a recent study by FAO (2008) using data from a 20-year period, it is found that land degradation is intensifying in many parts of the world. At the present status, more than 20 % of all cultivated areas, 30 % of forests and 10 % of grasslands are undergoing degradation. It is also estimated that 1.5 billion people – one quarter of the world's population – depend directly on degraded land. Hence, there is a need to understand and know the spatial dimensions of LULC so that policy makers can take better and sound decisions at all time.

In the context of this PhD research, the importance of carrying out an initial study on LULC is found to be necessary as it provides the information on the dynamics of land use and cover change over the Upper Awash Basin. It is known that the intensity of erosion risk is dependant on the type of land cover and nature of land use. Therefore, it is imperative to understand the dynamics of land use and vegetation cover of a region as this factor directly or indirectly controls the intensity and frequency of overland flow and surface wash erosion (Gobin et al., 2002). This study seeks to understand the linkage between "Land Use and Land Cover" (LULC) changes and its influence on the land degradation processes.

5.2   Data Use and Processing

Landsat satellite imageries of the study area for the year 1973 and 2000 are obtained from the GLCF (Global Land Cover Facility) and ESDI (Earth Science Data Interface). These two datasets on 31-01-1973 for Landsat-MSS and 05-12-2000 for Landsat-ETM+ respectively are selected as there was no cloud cover over the region during this period of data acquisition. Most of the free datasets for public use can be accessed from http://glcfapp.umiacs.umd.edu:8080/esdi/index.jsp

Table 5-1: Specifications of the Landsat satellite data used for Upper Awash

Satellite Name	Sensor name	Spatial resolution (m)	Spectral resolution	Temporal resolution
Landsat1-3	MSS (Multi Spectral Scanner)	50- 80 m	4 bands; *G: 0.5-0.6* *R: 0.6-0.7* *NIR: 0.7-0.8* NIR: 0.8-1.1 (2 in visible spectrum and 2 in near infrared spectrum)	18 days
Landsat7	ETM+ (Enhanced Thematic Mapper Plus)	Band 1-5 (30 m) Band 6 (60 m) Band 8 (15 m)	8 bands; *Band 1- 3 (Visible spectrum)* *Band 4,5,7 (Infrared spectrum)* Band 6 (Thermal IR spectrum) Band 8 (Panchromatic)	8 days

The downloaded data is a Level 1G standard product, i.e. it is a pre-processed (geometric and radiometric corrected), ortho-rectified product provided in GeoTiff data format. These data are converted to a compatible image (.img) and grid format for further processing. For the Landsat MSS image of 1973, the study area falls within a complete scene. In case of Landsat ETM+ of 2000, the coverage of the study area falls within two separate scenes or images. Hence, histogram equalization and matching is carried out to reduce the differences in radiometry between the two scenes (Tadesse et al., 2001). Then, the study area is extracted after mosaicking or combining the two images, which is later used for the purpose of classification. Visible and near infrared bands are considered in case of Landsat MSS, for selecting the "best band combination". This has the maximum signatures separability for the purpose of classification. Similarly, for the case of Landsat ETM+, visible and infrared spectrums are considered.

Both images have the WGS 1984 UTM Zone 37 N as the spatial reference. The datum for both images is in D_WGS_1984. Geo-coding and re-sampling in the same spatial reference and resolution is required for the post classification change assessment of the classified images of different time periods.

5.3 Methodology for LULC Classification

5.3.1 Land Use and Land Cover (LULC) Model

A simple LULC model is set up using the Model Builder of ArcGIS 9.2. The model employs the multivariate tools of spatial analyst where creation of signature file, dendrogram analysis for evaluating class and clusters and iso-data clustering or Maximum Likelihood based classification can be carried out (ESRI, 2007). It can automate the whole process of image classification and let the user interactively feed the processed input data required for the classification. It also helps to integrate various available GIS data layers such as road networks, stream and ancillary data for the correct identification and selection of features or signatures present in the region.

In this study, supervised classification with the Maximum Likelihood Classifier is used to classify the images into the various land cover categories. The basic steps for supervised classification using ArcGIS tools are i) to create or use a multiband satellite image which is free from geometric, radiometric and terrain errors (Level 1G standard product from Landsat is used here); ii) to produce a set of training samples from known locations of desired classes; iii) to develop a signature file based on the collected training sample for each identified class; iv) to run the MLC (Maximum Likelihood Classifier) tool after specifying the required parameters using the created signature file (ESRI, 2007). A signature is a subset of cells that are representative of a class or cluster. It contains the statistical description of the classes derived from the samples identified on the input raster or feature sample data. The statistics of signatures are stored in a signature file that will be used to classify all cells in the raster. A signature file is required when we use the Maximum Likelihood Classification to classify an image. The whole process can be re-run and the signature file can be modified, edited and viewed until a satisfactory result is achieved. It is important to mention that selection of '*right band combinations*' where the separability of signature classes is optimal is required for the creation of a good signature file and subsequent for the classification process.

The Maximum Likelihood Classifier (MLC) is a parametric classifier that quantitatively evaluates both the variance and covariance of the category spectral response patterns when classifying an unknown pixel. In other words, it calculates for each class the probability of the cell or the pixel belonging to the class of the given attribute values. The unknown pixel or cell is assigned to the class with the highest probability (Lilesand et al., 2004; ESRI, 2007). The basic assumptions behind the MLC are:

1. The cloud of points forming the category training data, should form a normal (Gaussian) distribution.

2. In the absence of any weighting factor of attribute values, all classes are considered equally likely. This means that apriori probabilities of the classes must be equal.

Once the classifier is selected, the next important step for the classification is the identification of land cover present in the region and the collection of training samples from the satellite image. In addition, it is required to obtain reference data from various sources for the final accuracy assessment of the classified map. The model diagram and its workflow are shown in *Appendix 3*. Moreover, descriptions about the class identification, training and reference data collection along with background fundamentals of the accuracy assessment procedure is provided in *Appendix 4A and 4B*.

5.4 LULC Change Analysis

Change analysis or change detection of the earth's surface play an important role in order to understand and quantify the dynamics of a landscape whose pattern changes over time. There are various methods to carry out the change analysis of land cover between two or more different time periods. Widely used techniques are image differencing, principal component analysis and post-classification comparison of land cover statistics. Each technique has its own merits and no single approach is optimal and applicable to all cases. Extensive reviews on different change detection techniques and their applicability are available (Lu et al., 2004; Coppin et al., 2004). In this study, post-classification change analysis also known as "delta classification" is adopted to assess the changes in different land cover and land use classes from bi-temporal images, i.e. the classified images of 1973 and 2000. The main advantage of post-classification change analysis lies in the fact that the two dates of imagery are separately classified, thereby the problem of sensor calibration differences – such as radiometric differences – between the two dates is minimized (Coppin et al., 2004).

A comparison of the 1973 classified land use map with that of 2000 is done to determine "change from" and "change to" for a target class. The nature of the cover change between the two periods is provided spatially. The areal statistics of each change class are also determined.

5.5 Results and Analysis

5.5.1 Classified Image of 1973 and 2000

The classified LULC maps of the Upper Awash Basin corresponding to 1973 and 2000 are shown in Figure 5-1. Six broad classes are indicated in the image: forest, settlement, water bodies, grassland, agricultural land, shrubland or barrenland. It can be observed from the spatial distribution of different classes that the study area is dominated by agricultural land in both time-periods; the expansion of settlement zones plays also a dominant role. A detailed assessment will follow in the later part of this chapter.

5.5.2 Accuracy Assessment of the Classified LULC Maps

Accuracy assessment is done by setting up an error matrix or confusion matrix; this serves to summarize the relationship between the classified and the reference data. A total of 215 and 344 pixels for the classified LULC map of 1973 and 2000, respectively, are generated using the random sampling method corresponding. Then, the classified maps are evaluated or cross-referenced by comparing with the known geographical locations as obtained or referenced from high resolution imagery, existing LULC map and from Google Earth. The error matrix tables and the classification accuracies of the LULC map, meaning the "producer", "user" and "overall" accuracy, and kappa statistics are summarized in Tables 5-2, 5-3 and 5-4. The classified 1973 map from Landsat-MSS and 2000 map from Landsat-ETM+ have an overall accuracy of 60 % and 83.4 %, respectively. Their corresponding kappa coefficients are 0.50 and 0.80, respectively. This represents a moderate and strong agreement
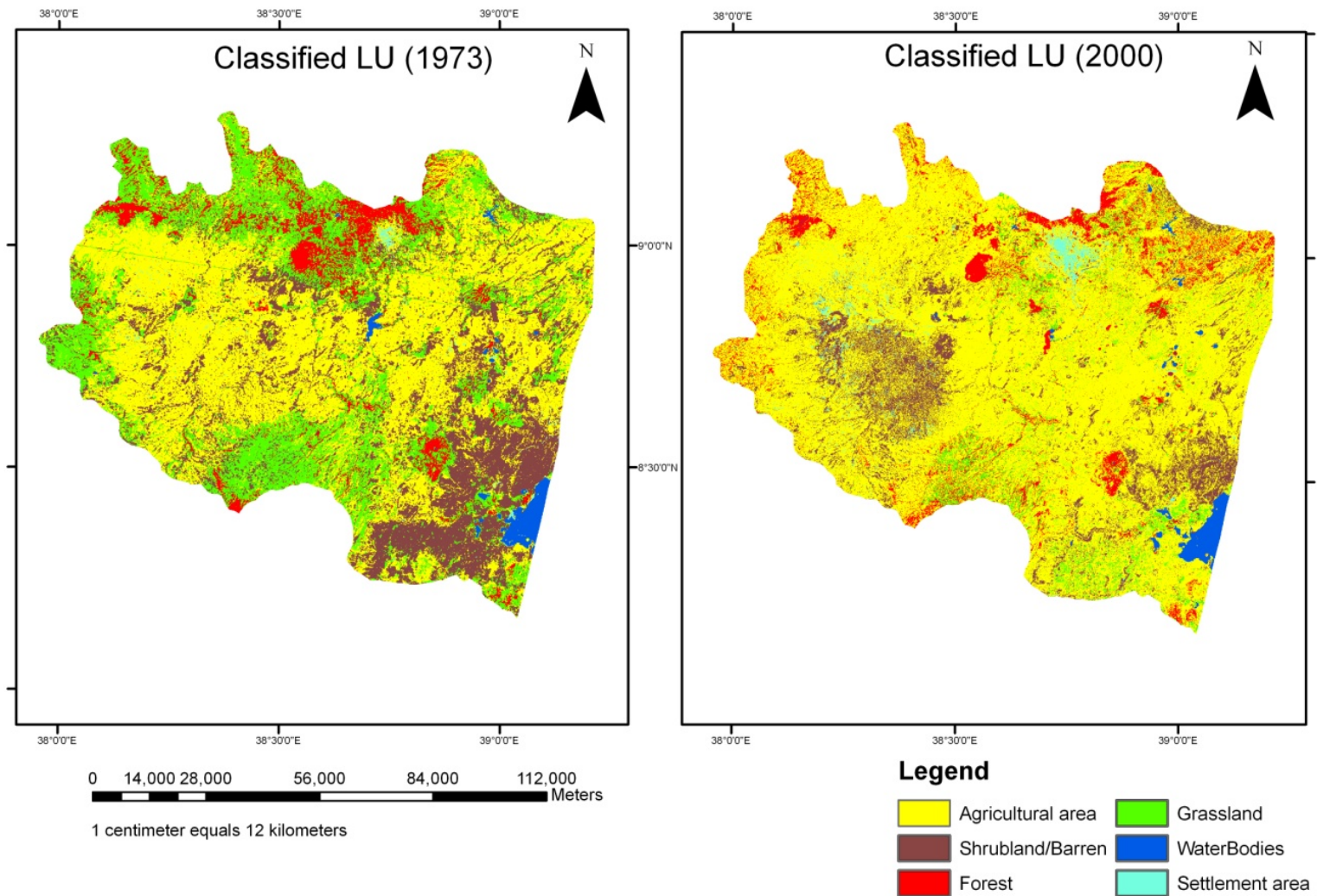
Figure 5-1: Classified land use maps of the Upper Awash Basin for two different time periods

between the classified land use with their corresponding reference points. A kappa value of 0.50 and 0.80 represents a probable 50 % and 80 % higher level of accuracy than if the classification had resulted from a random, unsupervised assignment instead of the maximum likelihood classification adopted in this study.

Table 5-2: Error matrix corresponding to land use classification of 1973

Classified land cover class	Reference (known land cover type location)						
	Settlement	Agriculture	Grassland	Water	Forest	Shrub/ Barren	**Row total**
Settlement	5	1	0	0	0	0	6
Agriculture	2	36	2	1	1	18	60
Grassland	2	1	17	1	10	11	42
Water	0	0	0	15	1	0	16
Forest	1	0	20	0	28	0	49
Shrub/Barren	0	6	5	0	3	28	42
Column total	10	44	44	17	43	57	215

In the LULC map of 1973 can be seen that out of 60 random sample locations of the agriculture class, 36 locations are correctly classified while the remaining locations are misclassified. Therefore, a user accuracy of 60 % and producer accuracy of 82 % results for this class. Similarly, for the same class corresponding to the 2000 map, from 107 random sample locations, 66 of these are correctly classified as agriculture with the remaining sample locations being misclassified. The corresponding user and producer accuracies are 62 % and 97 %, respectively. A similar case is found for the other LULC classes for both time periods. The results can be interpreted using the error matrix to calculate the overall accuracy.

Table 5-3: Error matrix corresponding to land use classification of 2000

Classified land cover class	Reference (known land cover type location)						
	Agriculture	Shrub/ Barren	Forest	Grassland	Water	Settlement	**Row Total**
Agriculture	66	16	3	17	0	5	107
Shrub/Barren	1	61	0	3	0	2	67
Forest	0	0	54	4	1	0	59
Grassland	1	0	2	31	0	0	34
Water	0	0	2	0	38	0	40
Settlement	0	0	0	0	0	37	37
Column total	68	77	61	55	39	44	344

Table 5-4: Classification accuracies for 1973 and 2000

LULC class	1973		2000	
	Producer accuracy (%)	User accuracy (%)	Producer accuracy (%)	User accuracy (%)
Agriculture	82	60	97	62
Shrubland/Barren	49	67	79	91
Forest	65	57	89	92
Grassland	39	40	56	91
Water	88	94	97	95
Settlement	50	83	84	100
Overall accuracy	**60**		**83.4**	
Kappa statistics	**0.50**		**0.80**	

5.5.3   Change Detection Analysis

The transformation of one land use class to another class for the period from 1973 to 2000 is analyzed. General LULC classification statistics along with their overall temporal trend for 1973 and 2000 are shown in Table 5-5. Post-classification change detection indicates that in both time-periods, the agricultural area remains the dominant land use class. This covers an area of 479783 and 766463 ha, which corresponds to 45.84 % and 73.24 % of the total study area, for 1973 and 2000 respectively.

Table 5-5: Land use and cover classification statistics of 1973 and 2000

LULC class	1973		2000		Change (1973-2000)	
	Area (hectare)	Area (%)	Area (hectare)	Area (%)	Area change	Percent change*(%)
Agricultural area	479783	45.84	766463	73.24	286680	+**59.75**
Shrubland/Barren	226730	21.66	121741	11.63	104989	-46.31
Forest	73832	7.05	74730	7.14	898	+1.22
Grassland	248012	23.70	54158	5.18	193854	**-78.16**
Water Bodies	13263	1.27	13143	1.26	121	-0.91
Settlements	5045	0.48	16258	1.55	11213	+**222.25**

* (+)-sign indicates the magnitude of the increase, in particular land cover and land use class from 1973 to 2000. (-)-sign indicates a decrease, in a particular class from 1973 to 2000.

A significant increase in agricultural area by 60 % from 1973 to 2000 is observed (Figure 5-2). On the other hand, there is a dramatic decrease of grassland by about 78 % from 1973 to 2000 (i.e. 23 % to 5 % reduction from 1973 to 2000). A similar pattern is observed for the shrubland/barren class (46 % reduction). The analysis shows that settlement area increased by about 222 % in 2000 compared to 1973. There is a slight increase in forest area by 1.22 % which shows an indication of reforestation from shrubland and grassland to forest. Nevertheless, the spatial pattern analysis also shows a clear

indication of deforestation along the northern part of the Upper Awash Basin (near to Addis Ababa and Debre Zeyit). This transformation can be linked to increasing human population growth and the subsequent increase in settlement areas and clearing of forest zones for agricultural practices.
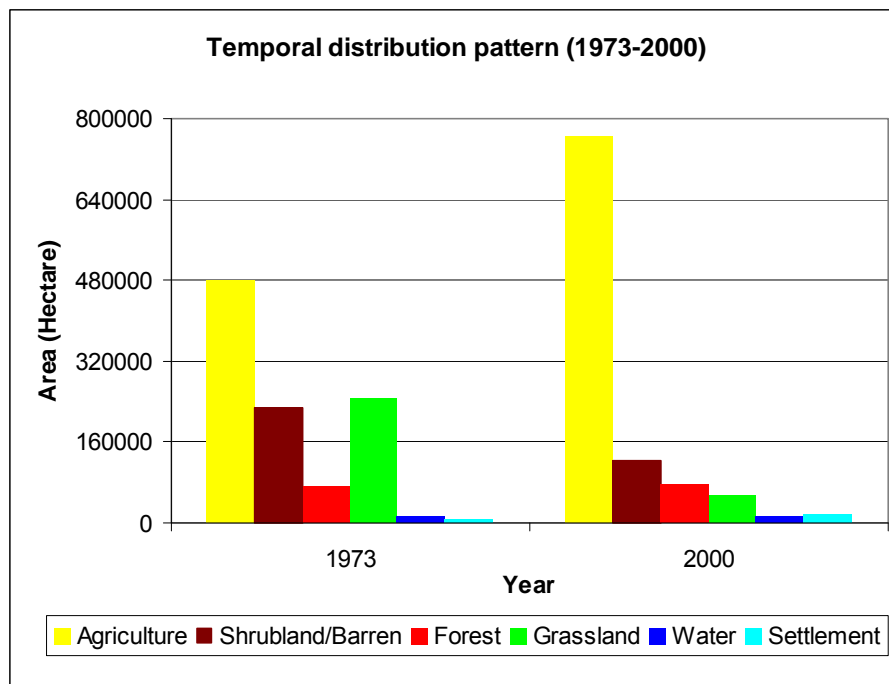
Figure 5-2: Temporal pattern of LULC change from 1973 to 2000

This finding is in accordance to the special report on "Population and Development in Ethiopia" by Haile (2004). Especially in the highlands region of Ethiopia, Haile (2004) observes that deforestation is accelerated by highly concentrated population coupled with archaic farming techniques. This leads to imbalances in the ecosystem. It is interesting to note that population growth in Ethiopia increased from 1.5 percent in the 1940's to 3.1 percent in the 1980's. The Demographic and Health Survey report estimates 2.7 percent growth rate for the year 2000 (CSA and ORC Macro, 2001).

These classified LULC maps provide a way to look into the spatial dynamic and the changing pattern of different LULC classes so that areas of significant change can be located and their probable causes might be understood.

5.5.4   Spatial Dynamic between Various Cover Types

An increase in human and livestock population has an anthropogenic effect on different LULC in semi-arid highland regions. This puts additional pressure on the natural resources. A rapid expansion of settlement area and agricultural land, reduction in grassland and water bodies from 1973 to 2000 is observed from the change detection analysis. It is found that 183073 ha of grassland are converted into agricultural land. Around 14538 ha of grassland are degraded into shrubland or barrenland, which is probably due to overgrazing through the increased livestock population. Patches of agricultural zones near the vicinity of human settlements are converted into settlement areas (approximately 10710 ha). Spatially, it is also observed that regions that were agricultural land in 1973 are reduced into barrenland or shrubland in 2000, corresponding to about 45203 ha of the study area. The probable

cause behind it is that land degradation, accompanied with a high degree of soil erosion and continuous removal of nutrients without replacement, make such region unsuitable and unfit for further cultivation. Hailemariam (2003) reports that most of the farmlands and grazing lands in the highlands are exposed to soil erosion follow by massive land degradation. The reduction of fertile agricultural land to barrenland or shrubland as observed in this study within 27 years strongly affirms the findings and comments by different researchers (Haile, 2004; Hailemariam, 2003; Taddese, 2001). It is reported that annually 20000 to 30000 ha of cropland in the highlands are being abandoned due to land degradation. The problem of soil erosion in the Upper Awash Basin is mainly due to the clearing of natural vegetation and increase in agriculture. There is a reduction in aerial extent of water bodies by 0.91 % from 1973 to 2000. One of the probable cause behind the reduction in water bodies could be due to sediment deposition over the years in water bodies.

5.5.4.1 An Insight into the Dynamic of Forest Cover of Upper Awash Basin

This section provides an approach on how a comprehensive assessment of a particular land cover class of a region can be carried out using the classified LULC map. For instance, the dynamics of forest cover in Upper Awash Basin is attributed to the possibility that a part of the region is being cleared, while other parts previously abandoned and other classes, are found to be regenerating into forest and therefore counterbalancing each other. Both deforestation and reforestation occurs spatially throughout the region. When examining the total forest cover present during the two different time periods, minor significant change in the total forest cover area is observed (i.e. 73832 ha in 1973 compared to 74730 ha in 2000). However, when we consider their spatial distribution pattern, location and structure, it is found that there are appreciable and significant changes over the 27 years period.

From the spatial analysis, it is found that a large part of dense forest, primarily composed of woodland and savannas, changed to agricultural land, grassland, shrubland or barrenland and settlement areas. About 38084 ha of forest area is converted to agricultural land in 2000, which accounts about 52 % of the total forest area in 1973. Similarly, 5.78 %, 1.49 % and 0.97 % of the total forest area is transformed into grassland, shrubland or barrenland and settlement region, respectively. It is interesting to note that conversion of other land cover classes to forest is also found at other parts of study area which indicates reforestation of the region. For instance, 10 % of grassland, 3.63 % of agriculture and 0.87 % of shrubland area are found to be regenerated into forest cover area within the 27 years period. About 40 % of the total forest area is unchanged between the two time periods both in their spatial location and distribution pattern. This areas can be identified and categorised as protective densely forest area which remains undisturbed and has witnessed only a low level of anthropogenic activity over the past 27 years. It can be concluded from the distribution pattern of forest that most of the forested riparian zone along the streams network during 1973 is cleared completely and turned into cultivated agricultural land by the year 2000.

5.6 LULC Change Dynamic on Land Degradation Problem in the Upper Awash Basin

From the change detection analysis of LULC of the Upper Awash Basin, it is seen clearly that forest cover and grassland are transformed into other classes in the study area. The conversion of forest area

and grassland into agricultural land (crops) and settlements have direct consequences on the hydrological cycle of the watershed. The increase in agricultural land has a direct effect on the soil erosion risk and hence the problem of reservoir siltation in the region. A large part of the study area identified by Elias (2003) as region of high erosion risk (i.e. the areas around Addis Ababa, its western escarpment, the major gorges of headwaters and the plain of the Modjo catchment) are found to be a region dominated by forest and grassland in 1973. In 2000, these regions are found to be converted into agriculture and shrubland or barrenland. The high risk of erosion and high erosion rates in these regions can be attributed to the poor system of land use, conventional agricultural practices, in addition to the prevailing climatic and soil factors.

From the hydrological standpoint, changes in LULC classes have an adverse effect due to a reduction of evapotranspiration (ET) and increase of surface flow or discharge (Costa et al., 2003). Since land use is an important factor that governs the climatic regime of a region, a slight variation in land use patterns can result in a large deviation in the overall hydrological function of the region. Hence, changes in land use over time have an indirect potential consequence in the alteration of rainfall regime and runoff response of the region. Changes in land use practice over time may lead to an increase in erratic nature of rainfall pattern. It is confirmed from the past annual rainfall pattern (1961-2002) analysis of the Eastern Highlands and Midlands of Ethiopia by USAID and USGS/EDC that there is a rapid increase in drought years. This is an indication of an alteration of the rainfall regime and climate change.

Population growth is reflected by an increase of settlement area; deforestation is reflected by reduction of vegetation cover across the temporal scale. When these effects are coupled with an increasing pressure on agricultural land we are able to identify the main indicators which affect the land resource system of the Upper Awash Basin. In general, a complex inter-conversion of multiple land use classes between specific time periods in addition to variability in climate, topography and soil nature are crucial factors contributing to the dynamic nature of erosion processes in a landscape.

5.7   Discussion

Multi-temporal LULC classification using public domain Landsat satellite data, ancillary data and aerial photographs from Google Earth are described here. Using the post-classification method of change detection, the dynamics of LULC pattern are analyzed. The result reveals that there is an appreciable increase of agricultural and settlement area by 60 % and 222 % from 1973 to 2000. In addition, a large reduction of 78 % in grassland from 1973 to 2000 is observed. In the case of forest area, a specific stable trend can be observed. This can be explain by the fact that a part of the forest area is being cleared between 1973 and 2000, other parts, previously abandoned and in other classes during this time, are regenerated into forest areas by the year 2000, therefore counterbalancing each other.

While the recent availability of Landsat satellite datasets in public domain enables LULC dynamic assessment studies, still the problem of cloud cover for the optical remote sensing data prevents many users from maximum utilization of the available data in the archive. The selection of cloud free data for a specific period of time or for multi-temporal based assessment as per the user requirement always pose a problem and tends to be a complex task.

The dynamics of LULC cover change over time can be controlled by setting up various regional and local land use management policies. These can consider the potential effects of LULC dynamics on a proper functioning of the ecosystem and toward a sustainable environment that can help to balance with the natural resources of the region. In addition, problems pertaining to population growth, deforestation, and pressure on agricultural land, which have significant negative onsite and offsite effects, should be taken into account when formulating any land use management strategy. For such investigations, the analysis of LULC can provide first hand information on the underlying driving factors that catalyse land degradation in the region.

In conclusion, by taking the remote sensing data, simple modelling and using limited ground data on a regional scale this study is able to provide a vehicle to understand the dynamics of LULC change and land degradation processes. In addition, this type of assessment can provide first hand information to the policy makers and the architects of land use to identify the potential regions where prioritization for land use management, soil conservative measures and closer overall monitoring is needed. One of the main advantages of this study is that the integration of classified LULC map as a reliable input source for the further assessment of spatial and temporal risks of soil erosion in the region.

6 Assessment of Satellite Based Rainfall Estimates (SBRE)

"Climate is what we expect; weather is what we get."

- Mark Twain

6.1 Introduction

In most of the hydrological and environmental models, long term rainfall data is an indispensible input parameter that reflects the intensities and its spatial distribution over a long time period. In reality, mostly in developing countries, there is limitation on rainfall data availability for long time periods and also on the number of gauging stations present over the region. This is a hindrance to obtaining the variation of spatial rainfall distribution over a region of interest. Traditionally, rainfall data are obtained from the gauging stations on hourly and daily basis and are aggregated depending on the desired time-step. Then, they are interpolated by statistical techniques to obtain a spatially distributed rainfall map over a region. Radar data is another source of data and it provides good spatial and temporal coverage. However, the problems of inter-radar calibration and mountain blockage limit its capability (Teschl, 2006). Moreover, radar networks are only present in a few countries in the world. With the advent of advanced satellite technology, remote sensing techniques using space borne sensors provide a means to monitor and measure rain events continuously over a large part of the globe. Geostationary satellites provide coverage between 60°S and 60°N while the polar orbiting satellites provide less frequent observations from South to North Pole but more direct estimation than the VIS/IR observations from geostationary satellites (Ba, 2008). Few reports exist in the literature about the feasibility of using indirect satellite rainfall estimates as a complementary dataset.

Therefore the aim of this part of the research work is to provide an insight to the scientific and user community about the potential and possibility of utilizing the right kind of satellite based indirect rainfall estimates for environmental and hydrological process monitoring. This is especially attractive for data-scarce regions of the world. For instance, there is only a small known number of rainfall stations present in and around the Upper Awash Basin study area in the Ethiopian Highlands. Due to the sparse number of rainfall stations in the study area, an indirect estimate of rainfall from various satellite based algorithms (Xie and Arkin, 1997; Huffman et al., 2007) is analyzed and compared to the data available from ground measured rainfall.

6.2 Literature Review of SBRE Studies

There are a small number of studies that compare and validate satellite rainfall estimates with other rainfall measurements in the field of environmental monitoring, water resource management, weather forecasting and climate prediction. Workshops and scientific projects on the calibration of satellite instruments and reviews of satellite based rainfall estimation methods are reported by different sections of the scientific community recently (Ohring, 2007; Levizzani et al., 2002). The use of Satellite Based Rainfall Estimates (SBRE) in environmental monitoring, especially in flood forecasting and hydrologic stream flow modelling, is limited in the past because of the perceived

uncertainty associated with such data (Artan et al., 2007). On the contrary, some researchers suggest that in tropical regions the SBRE are more reliable because precipitation is usually associated with deep convection (McCollum et al., 2000).

Research studies are reported in many different parts of Africa, South America and South Asia from data sparse regions. These studies report the use of indirect estimates of precipitation from satellites for stream flow modelling and the generation of information about water resource availability. Dinku et al. (2007) evaluates 10 different satellite rainfall products using station networks over the complex topography of Eastern Africa, where elevation varies from below sea level to 4620 m a. s. l. Funk and Verdin (2003) compares the RFE 2.0 product (NOAA-CPC) and the re-analysis precipitation product from the National Centre for Atmospheric Research (NCAR) with the ground station data for western Kenya. Their study concludes that substantially better agreement with station data is observed with the satellite rainfall estimates than it is the case with atmospheric model re-analysis fields. Artan et al. (2007) demonstrates the usefulness of remotely sensed precipitation data for hydrologic modelling; a need for recalibration of the model when such data products are used is highlighted. Similar work is carried out by Shrestha et al. (2008) for stream flow modelling using the rainfall estimates produced by NOAA-CPC (National Oceanic and Atmospheric Administration -Climate Prediction Centre) and observed at ground rain gauge stations. Their results show that SBRE are capable of detecting a particular rainfall event within their test site. Shrestha et al. (2008) observes that the magnitude of the rainfall is much lower in the RFE compared with the gauge observed rainfall. This then results in the underestimation of simulated flows when the RFE dataset is used to run the hydrological model. In a report from Hughes (2006), emphasis is mainly on the direct use of available satellite derived information products in water resource estimation procedures, i.e. satellite precipitation data and their potential use for input to monthly time-step, rainfall-runoff simulation models applied to relatively large basins. The author concludes that the satellite data does not reflect the strong influences of topography on precipitation in some of the basins. However, the prospects of applying relatively straightforward adjustments are promising and further assessments appear to be justified.

Recently, the use of different TRMM (Tropical Rainfall Measuring Mission) rainfall estimates to study the climatology and its validation is reported. Islam and Uyeda (2006) shows the merit of using TRMM products for climatological studies over Bangladesh and the better performance of the TRMM 3B43 V6 product as compared to other TRMM products. The better performance is accounted for by the fact that TRMM 3B43 V6 is based on fused products of multi-satellite and gauge analysis, (Huffman et al., 1997). This, in turn, yields a satellite estimate monthly rainfall in post real time. In general, various developing countries like Bangladesh or Thailand which have poor ground measuring stations could benefit from such indirect rainfall products for continuously monitoring the climatology of the region. Toward short term hydrological applications such as flood forecasting, such rainfall products still pose certain limitations and there is need for further research. Chokngamwong and Chiu (2006) highlight the need of continuous evaluation and further studies to quantify the use of satellite measurement. In general, the potential of satellite derived precipitation in different parts of the world still needs to be evaluated.

Three basic criteria are provided to quantify the usefulness of SBRE for different environmental applications, such as flood forecasting (Artan et al., 2007). The criteria are: i) the data should have historical depth i.e. long time series; ii) the data should be readily available to the wider public for use and iii) the data should have a high temporal resolution (daily, dekadal, or monthly time-steps). Additional criteria on the spatial resolution of the data can be incorporated depending on the scale of

the study. For instance, finer spatial resolution datasets e.g. 0.1º ~ 11 km or 8 km from NOAA-CPC RFE 2.0 estimates are preferred. Ba (2008) discusses the advantages of combined rainfall estimates from different methods and systems over the estimates from single methods. It is reported that combined estimates provided the best representation and reduced uncertainties of precipitation. This complies with the findings of many recent studies carried out in different regions of the world, as discussed earlier. To summarize, it can be said that the measurement of rainfall from satellites provides a cost effective and viable means to achieve an estimate that complements the ground measured rainfall gauging method. With the advancement in technology, new satellites are being implemented for the improvement in accuracy of global and continental scale rainfall estimates. One of the most significant examples is the GPM (Global Precipitation Measurement) of NASA and NASDA, which focuses on more accurate spatial information and temporal sampling of less than or equal to 3 hours. Details on GPM can be obtained from: http://gpm.gsfc.nasa.gov/.

6.3 Comparative Assessment of SBRE with Ground Measured Rainfall Data

In this study, satellite rainfall products from two different sources, having different spatial and temporal resolution are used to compare with ground measured rainfall over the Upper Awash Basin, Ethiopia. The two satellite rainfall estimates are the RFE 2.0 obtained from NOAA-Climate Prediction Centre and that of TRMM 3B43 V6 rainfall estimate from the TRMM satellite. Details about the database sources are discussed earlier in Chapter 4.

6.3.1 Data Processing and Methods

A) RFE 2.0 rainfall estimates

RFE 2.0 rainfall estimates (Xie and Arkin, 1997), having a spatial resolution of 8 km (original resolution of 0.1 degree) and a 10 days (dekadal) time-step for a period from 2001-2003, are downloaded from FEWS NET and processed to extract the grid cell value for the study area. Each grid value represents the rainfall depth over 10 days of accumulation. Originally, the data is projected using ALBERS Conical Equal-Area Projection and with the datum Clarke 1866 spheroid. The data is re-projected to Adindan UTM_Zone_37N; Datum: D_Adindan to match and overlay with the existing topographic and other datasets. After this, the study area is extracted for each corresponding dekadal resulting into 36 dekadal grids for the year. Since the 2001 to 2003 time-period is considered for the comparison with the gauge measured rainfall, a total of 36 x 3 = 108 grid layers are processed. Additional monthly accumulated grids are generated by summing the dekadal grid for a monthly based comparison with the ground measured rainfall.

Comparison of RFE 2.0 estimates and gauge rainfall data seems more feasible and reasonable if the latter is interpolated before comparison for their degree of statistical agreement. It is important to understand and remember that the RFE has a spatial resolution of 100 km^2 and the rain gauge opening is 100 cm^2, e.g. it is a point measurement, in reality. So, in light of these aspects, even when both datasets are perfect they will never be the same. Therefore, the need of interpolation of gauge data before the assessment is justified. Following on from the above discussion, daily accumulations from a network of the 8 available gauging stations are summed up to get dekadal (10 days accumulation) station data. The station data are interpolated by using the IDW (Inverse Distance Weighting) method,

which is a simple and efficient method implemented in ArcGIS. The IDW determines the rainfall in a respective grid cell by weighting the rainfall at the other gauges using their distances to the respective pixel. The comparison is done for the dekadal time series, seasonally and monthly accumulated average rainfall over the study region. The comparisons are made over a defined ROI (Region of Interest) which covers the study area and has a horizontal resolution of 8 km. (same as the spatial resolution of RFE 2.0 estimates over the Greater Horn of Africa). For the defined ROI, the corresponding grid cells are extracted from RFE 2.0 by using the masking procedure.

B) TRMM 3B43 V6

To assess a different satellite estimate having a different algorithm, TRMM 3B43 V6 data are also investigated and compared on monthly time-step (Huffman et al., 2007). This satellite estimate is coarser in spatial and temporal resolution than the NOAA-CPC RFE 2.0 data. In the case of the TRMM 3B43 V6 data, and because it is a monthly product, comparisons are made on a monthly basis during the time period (2001-2003), considered for this investigation. It can be seen that each ground station falls within the TRMM grid box of 0.25 x 0.25 degree ~ 27 km grids. As a comparative, the gauge observed rainfall stations are also interpolated using the IDW method to assign values to a 0.25 degree grid and subsequently compared with corresponding satellite estimates over the region of interest.

In general, the basic method of assessing model performance or two different types of estimates from different sources or algorithms is done by statistical comparison of model estimates or predictions. The predictions taken for comparison (where Si: i = 1,2,...,N) are assumed to be reliable and involve pair-wise matched observations (Gi: i = 1, 2,...,N). Individual model prediction errors usually are defined as $e_i = Si - Gi$ (S_i = satellite measured; G_i= gauge measured). The measurement of the average error or model performance is then based on statistical summaries of model-prediction errors. In this study, the below explained different measurements are used to describe the significance of satellite derived rainfall estimates compared to gauge measured rainfall. Willmott and Matsuura (2005) suggest that RMSE and its related measures should not be used alone for assessing the degree of agreement and model comparison since it is a function of three characteristics of a set of errors, rather than of one (i.e. the average error). It varies with variability within the distribution of error and average error magnitudes as with the square root of the number of errors ($n^{1/2}$). More focus is placed on the measurement of the mean error and the coefficient of determination, even though other measurements are computed for their significance. The following defined statistics are used to compare and evaluate the SBRE estimate with respect to the gauge measured rainfall data:

$$\text{M.E.} = \frac{1}{N}\sum(S - G) \tag{6.3a}$$

$$\text{Bias} = \frac{\sum S}{\sum G} \tag{6.3b}$$

$$\text{Eff.} = 1 - \frac{\sum(S - G)^2}{\sum(G - G')^2} \tag{6.3c}$$

$$\text{RMSE} = \sqrt{\frac{1}{N}\sum_{i=1}^{N}(S - G)^2} \tag{6.3d}$$

$$\text{Correlation (R)} = \frac{\sum_{i=1}^{N} SG - \dfrac{\sum_{i=1}^{N} S \sum_{i=1}^{N} G}{N}}{\sqrt{\left(\sum_{i=1}^{N} S^2 - \dfrac{\left(\sum_{i=1}^{N} S\right)^2}{N}\right)\left(\sum_{i=1}^{N} G^2 - \dfrac{\left(\sum_{i=1}^{N} G\right)^2}{N}\right)}} \qquad (6.3e)$$

$$\text{Coefficient of Determination (R}^2) = \frac{\left[\sum_{i=1}^{N}(S-S')(G-G')\right]^2}{\sum_{i=1}^{N}(S-S')^2 \sum_{i=1}^{N}(G-G')^2} \qquad (6.3f)$$

Where S = satellite estimate, G = gauge measured, G' = average of gauges, S' = average of satellite estimates and N = number of data pairs or observations. M.E. is the Mean Error in mm; Bias indicates the average deviation of the satellite estimates from the ground gauging observation. RMSE is the Root Mean Square Error in mm. Eff. is the Coefficient of Efficiency or NSCE (Nash-Sutcliffe Coefficient of Efficiency) (Nash and Sutcliffe, 1970). It can range from -∞ to 1. An efficiency of 1 (Eff. =1) corresponds to a perfect match of satellite estimate to gauge rainfall data. An efficiency of 0 (Eff. =0) indicates that the satellite based rainfall estimates are as accurate as the mean of the gauge rainfall data, whereas an efficiency less than zero (-∞< Eff. <0) occurs when the mean of the gauge measured rainfall is a better predictor than the satellite estimates rainfall.

6.3.2   Mean Monthly Rainfall Distribution Pattern of Upper Awash

The mean monthly accumulation of rainfall for the period 2001 to 2003 for each gauging station is plotted and the rainfall pattern trend within the region can be visualized through the time-trace plot in Figure 6-1. Large seasonal amplitudes (i.e. rainy and dry periods) can be inferred from the time-series plot. It is seen from Figure 6-1 that precipitation occurs throughout the year and is an indication that a bi-modal trend of climatology exists within the area under investigation.

Topography is the main factor that creates diverse microclimates within Ethiopia, ranging from hot deserts over the lowlands to cool highlands (Dinku et al., 2007). The major rain-producing feature during summer is the Inter-Tropical Convergence Zone (ITCZ), but topography of the region complicates the influence of ITCZ on rainfall distribution. In our study area, the climatic regimes fall within three seasons as categorized by USDA, Foreign Agriculture Service and Alemayehu et al., (2003). As can be seen from the time series plot, (Figure 6-1) during October-January there is less or no rain which is termed as "dry Bega season"; during February-May there is some rain which is termed locally as "Belg rains". The main rainy season is locally termed as "Kiremt rains" and occurs from June-September.
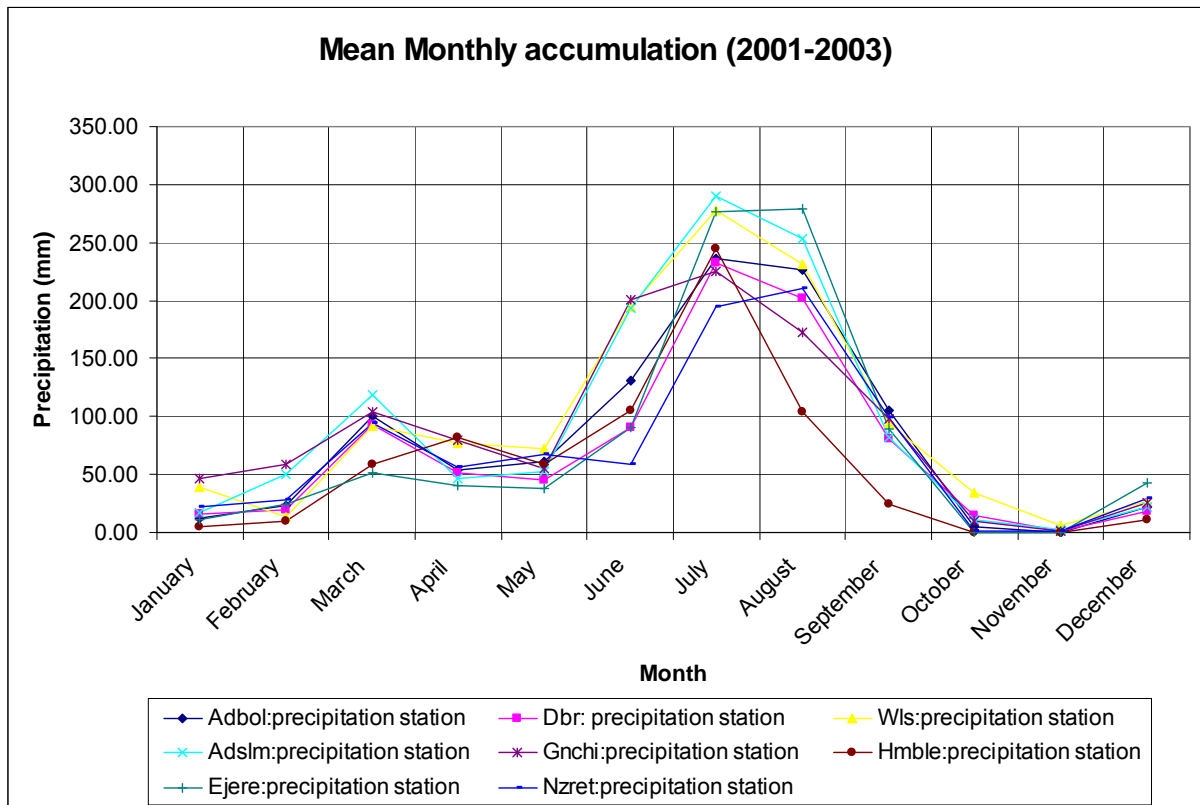
Figure 6-1: Mean monthly accumulated rainfall (2001-2003) at each gauging station

For each of the stations in our study site, pronounced rainfall is recorded during the period from June-September, peaking at 250-280 mm for the monthly mean for this period. For the "Belg rains" the average monthly rainfall at all stations ranged from 100-120 mm. There is more pronounced variation in rainfall records at different stations during the dry period; the magnitude of rainfall received during this period is scanty, though varied from 0-50 mm. At all stations, the heaviest amounts of rainfall occurred in July-August for all years under consideration.

6.3.3 Dekadal and Monthly Comparison: RFE 2.0 Estimates with Gauging Rainfall

Referring to Figure 6-2, it can be seen clearly that there is an underestimation of rainfall accumulation from the RFE 2.0 estimates, mainly during the rainy season compared to the measured gauge. It can be inferred that the temporal pattern of rainfall distribution from RFE 2.0 estimates follows very closely that of the measured gauge. The statistical significance between the two datasets is analyzed and discussed below and illustrated in Figure 6-3.

The dekadal data for each corresponding dekads is represented in this study by a notation: "**Rainfall Estimates_Year_Month_Corresponding Dekads**". For example, in Figure 6-2, the notation "REA01011" in X-axis represents the rainfall estimates for the first dekads of January i.e. 10 days accumulation of rainfall, for the year 2001.
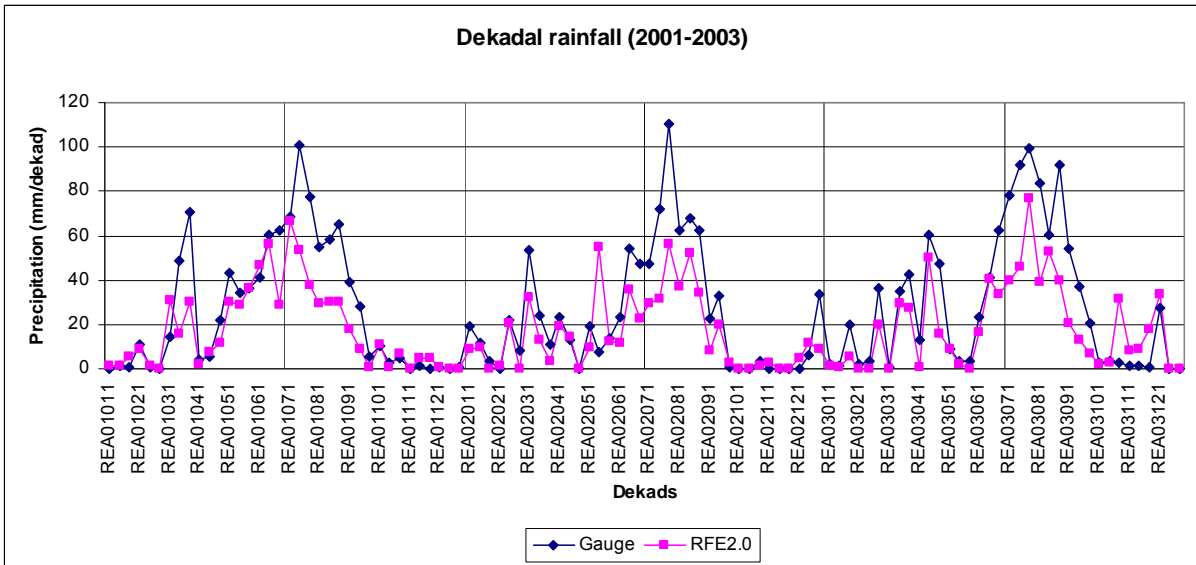
Figure 6-2: Time series dekadal mean rainfall (2001-2003) of the study area
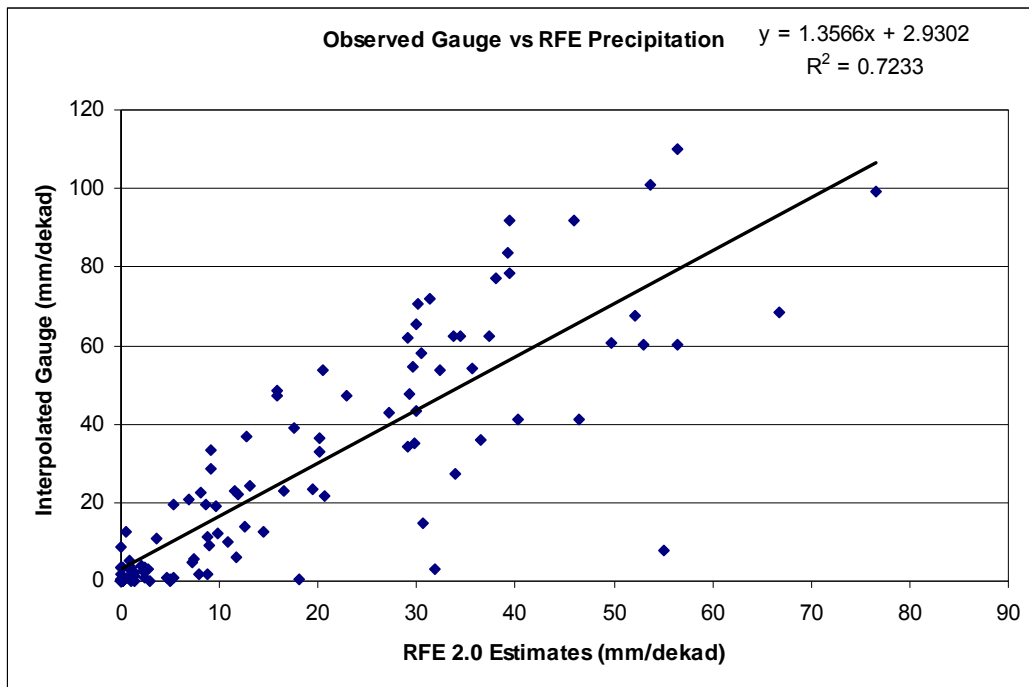
Figure 6-3: Scatter plot of the observed and RFE 2.0 estimates

The coefficient of determination (R^2) between the observed and RFE 2.0 estimates is found to be 0.72 and they exhibit a strong correlation of 0.87. The mean error is found to be 9.25 mm, which is the magnitude of underestimation by RFE 2.0 estimates when compared to the gauge measurements. This finding and the degree of agreement for RFE 2.0 estimates is quite consistent with an earlier study carried out by Funk and Verdin (2003) on dekadal basis over a region of Western Kenya.

A summary on the measurements of statistical significance for the dekadal rainfall is provided in Table 6-1. It is seen that RMSE tends to be higher than the mean error, i.e. RMSE of 18.86 mm compared to a mean error of 9.25 mm. From the statistical point of view, it can be pointed out that there is a concentration of large errors. Large errors have relatively greater influence on the total square error than the small errors when computing the MSE and RMSE. This clearly indicates that the total square

error grows as the total error is concentrated within a decreasing number of increasingly large individual errors. This significant observation may be due to a large underestimation of the rainfall estimates by RFE 2.0 during the heaviest rainfall period of June to September, which can be seen from the time-series plot on dekadal basis from 2001 to 2003.

Table 6-1: Mean dekadal RFE estimates comparison with interpolated gauge (2001-2003)

N= 108	RFE2.0 Estimates (CPC-NOAA)
Correlation coefficient (R)	0.85
RSQ (R^2)	0.723
Eff.	0.57
Mean Error (mm)	-9.25
Bias	0.65
RMSE (mm)	18.86

The degree of agreement, i.e. the amount of underestimation, between the two data sources varies quite significantly between each year. Time series and scatter plot are plotted and the variations in average rainfall for each year are also observed. The average dekadal rainfall (mm) for the year 2001 to 2003, obtained from RFE 2.0/Ground gauge, are 18/27, 16/24 and 20/30, respectively. In addition, the coefficients of determination (R^2) that correspond to the years 2001, 2002 and 2003 are found to be 0.75, 0.67 and 0.74, respectively.

When comparing at the monthly time-step, it is found that the degree of agreement with the gauge data is quite high with a correlation of 0.94, a positive coefficient of efficiency of 0.63 and a R^2 of 0.88. The monthly accumulated satellite RFE 2.0 estimates tend to perform well and provide a better agreement over the dekadal time-step comparison. These findings are quite consistent with some of the previous results reported by Artan et al. (2007), Xie and Arkin (1997) and Chokngamwong and Chiu (2006). Hence, the degree of agreement for the RFE 2.0 estimated rainfall with that of observed gauge estimates varies differently for the dekadal and monthly time-step. The agreement tends to fit better for the larger time-step than a smaller one.

6.3.4   Seasonal Comparison: RFE 2.0 with Gauging Rainfall

A comparison on the seasonal time frame is carried out to see any seasonal variation and agreement between the two data sources. The rainy (June-September) and dry (October-December) period for the years 2001-2003 are taken for the comparison of the rainfall estimates from RFE.2.0 (CPC-NOAA) with the gauged rainfall. For the rainy period of each year, there are 12 dekadal grids; for the three years a total of 36 grids are processed. Similarly, for the dry period a total of 27 grids are processed. From the pervious dekadal analysis, it is found that large differences in magnitude of the rainfall between the two datasets are found in main rainy and dry period of the year. Therefore, only the two extreme periods of the season in Upper Awash are accounted i.e. main rainy season and dry period, for the seasonal comparison purpose without taking into account the little rainy period from February to May of the corresponding years. For the dry season, only assessment are made corresponding to the months of October to December due to absence of ground measured rainfall data for the year 2004.

It is observed that there is an underestimation during the rainy period. The maximum mean rainfall during the rainy period of 2001, 2002 and 2003, as estimated by RFE 2.0, is found to be 69 mm, 58 mm and 79 mm, respectively. In comparison, the gauge record is found to be 102 mm, 118 mm and 108 mm, respectively (see Figure 6-4). A difference [i.e. (RFE2.0- Gauge)] of -33 mm, -60 mm and -29 mm can be observed which shows the variation of the underestimation. The mean Kiremt rainfall accumulation from the gauge estimate is 659 mm, 605 mm and 757 mm for 2001 to 2003 respectively. The corresponding estimates from the RFE 2.0 satellite are 353 mm, 341 mm and 435 mm, respectively. It can be observed that there is a large underestimation during the 2001 and 2002 rainy periods as compared with 2003. Considering the gauge as the standard reference, the percentage error is found to be in the order of magnitude of ~40 %.
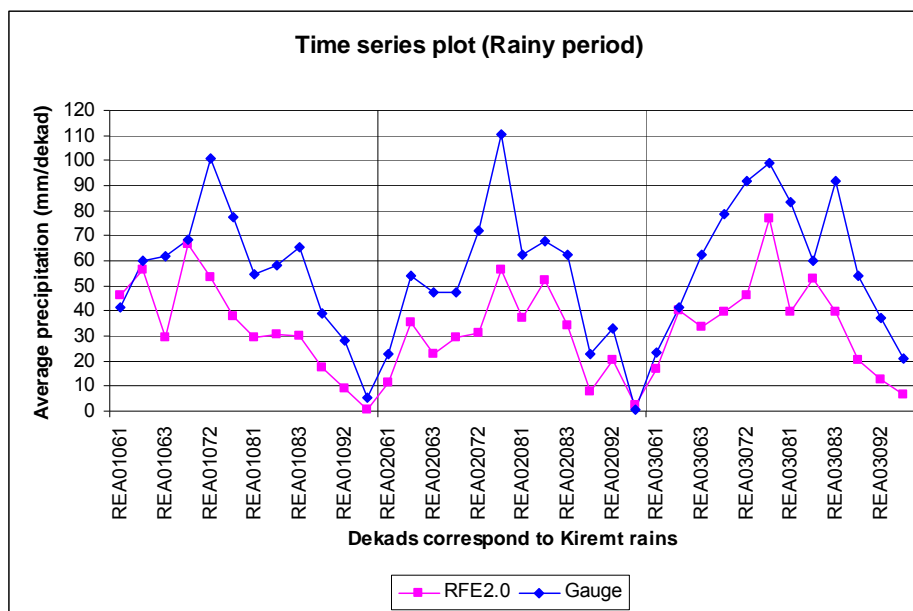
Figure 6-4: Time series dekadal mean precipitation for interpolated gauge and RFE 2.0 estimate (rainy season)

For the rainy season, the coefficient of determination decreased to 0.66. This indicates a large variation of the amount of rainfall between the measured ground gauge and RFE estimates (Figure 6-5). The large variation is quantified by the increase in mean error during the rainy period (i.e. 23 mm *versus* 10 mm), regardless of seasonality during the year. In general, the RFE 2.0 algorithm tends to underestimation especially during rainy months. This maybe due to inability of RFE 2.0 to incorporate the orographic precipitation which normally occurs during favourable low-level wind conditions when moist air condenses. This is in contrast to the previous RFE 1.0 algorithm of NOAA-CPC (Herman et al., 1997) which *does* take into account the precipitation due to orographic lifting. On the contrary, the improvements in RFE 2.0 lie within its ability to reduce random error and systematic bias. This is due to the ability of RFE 2.0 to process and merge all satellite data, and, subsequently, of the GTS (Global Telecommunication System) rain gauge.

Analysis also is carried out for the amount of accumulated rainfall during the dry season from 2001 to 2003. Figure 6-6 illustrates the time series trace. During the dry season of 2001, there is an evident pattern regarding the rainfall estimates between the satellite and gauge where the RFE 2.0 slightly overestimates. However, the trend seems to be opposite during the dry season of 2002 where there is large underestimation at a later stage, i.e. for December 2002. A similar trend can be observed during the dry season of 2003, where there is overestimation of RFE 2.0 during the initial stage in October.

From these results, it is clear that the amount of accumulated rainfall observed from the two different sources has large a variability during the dry season for the different time periods.
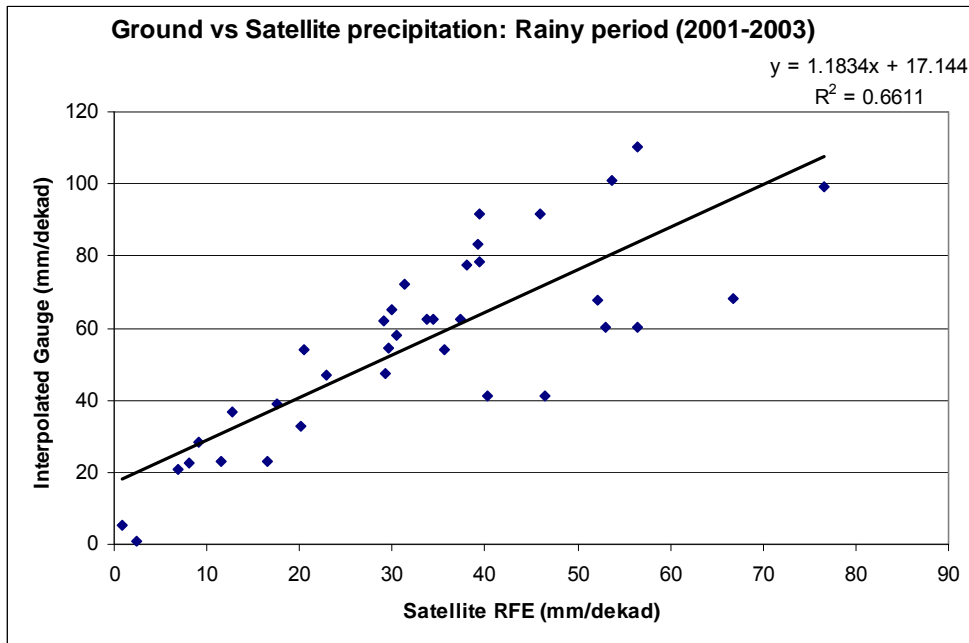
Figure 6-5: Scatter plot of observed and RFE 2.0 estimates, (rainy season)

The mean dry season accumulations for 2001 to 2003, as estimated from the gauge, are 20.25 mm, 44.50 mm and 44.10 mm, respectively. The corresponding estimates from the RFE 2.0 satellite are 27.13 mm, 30.00 mm and 85.75 mm, respectively. It can be observed that there is an overestimation by RFE 2.0 during 2001 and 2003 and a slight underestimation for 2002. Considering the gauge as the standard reference, the percentage error of RFE 2.0 is found to be in the order of magnitude of ~30% in 2001 and 2002. In terms of percentage difference between the gauge and RFE 2.0, this amounts to about 29-40 %. A major deviation can be seen in accumulated rainfall during the dry season of 2003 having percentage error of in the region of 90 % and percentage difference of 65 %.

When examining the statistical significance, the two datasets are found to have a low coefficient of determination (i.e. 0.26) and a correlation of 0.68. The mean error is 1.26 mm, which indicates an overestimation of RFE 2.0 compared to the measured one. The observed variation between the gauge rainfall and RFE 2.0 does not follow a specific trend during the dry season. This can be attributed due to nature of observed rainfall and climatology of the region. In this respect, we are referring to the influence of the ITCZ (Inter-Tropical Convergence Zone) during the dry season in the Upper Awash Basin. It is important to note that the variability in the degree of agreement between the two rainfall data obtained from different sources is not very surprising, since the approaches used for the estimation of rainfall are designed and based on different concepts.
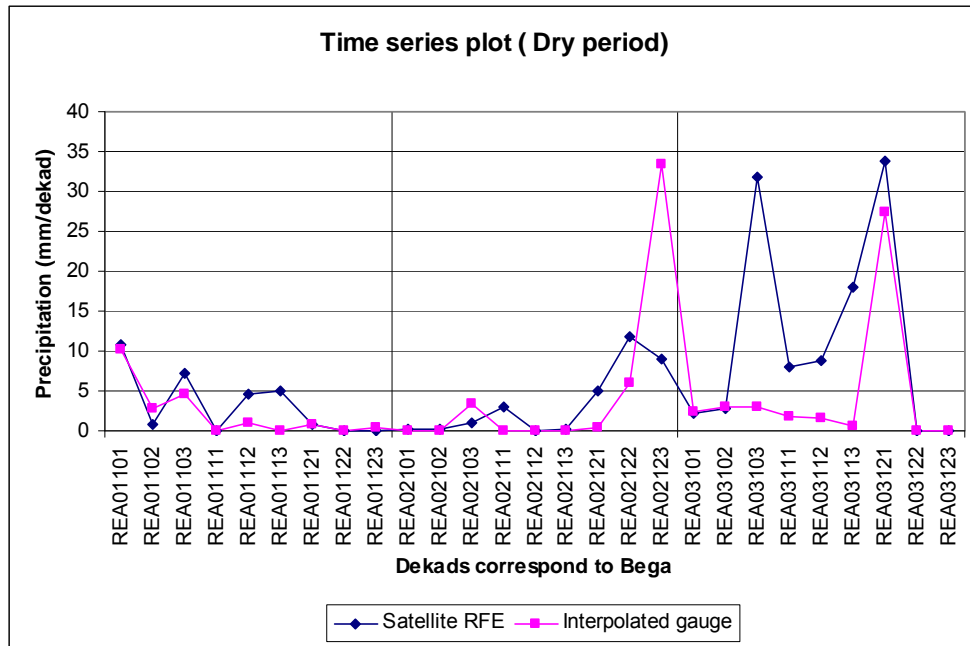
Figure 6-6: Time series dekadal mean precipitation for interpolated gauge and RFE 2.0 estimate (dry season)

6.3.5 Comparing the TRMM 3B43 V6 Estimates with Gauging Rainfall

a) Monthly comparison

Separate time series traces of mean precipitation of the study area (mm/month) are plotted for each year to observe the bias and difference in trend between the TRMM 3B43 V6 estimates and the ground reference standard (Figure 6-7). It can be clearly seen that 3B43 estimates follow the trend consistently with a minimum bias and mean error when compared with the ground measurements in all the years. Unlike the RFE 2.0 estimates, known to underestimate, there is a tendency for overestimation by the TRMM data during the rainy periods. In 2001, the degree of agreement is quite high for all months, except March, where there is a significant overestimation of 70 mm. On the contrary, during 2002 and 2003 monthly time series, the TRMM data seems to underestimate in comparison to the reference ground data during the rainy period; the magnitude of this underestimation ranges from 50 mm to 70 mm.

Referring to the statistical measures from Table 6-2, it is evident that the 3B43 V6 estimate performs well ground reference data, despite its coarser spatial resolution of 0.25 degree, when compared with the RFE 2.0. This strong degree of agreement can be attributed to the fact that the TRMM 3B43 V6 data is a merged gauge and satellite (3B42) estimate. Regression analysis yields a coefficient of determination of 0.90 with a correlation of 0.95; this is quite consistent with the previous findings on the monthly time-step and from current literature on this type of rainfall estimates. A coefficient of efficiency of 0.90 which is closer to 1 indicates that there is a strong agreement between the two datasets.
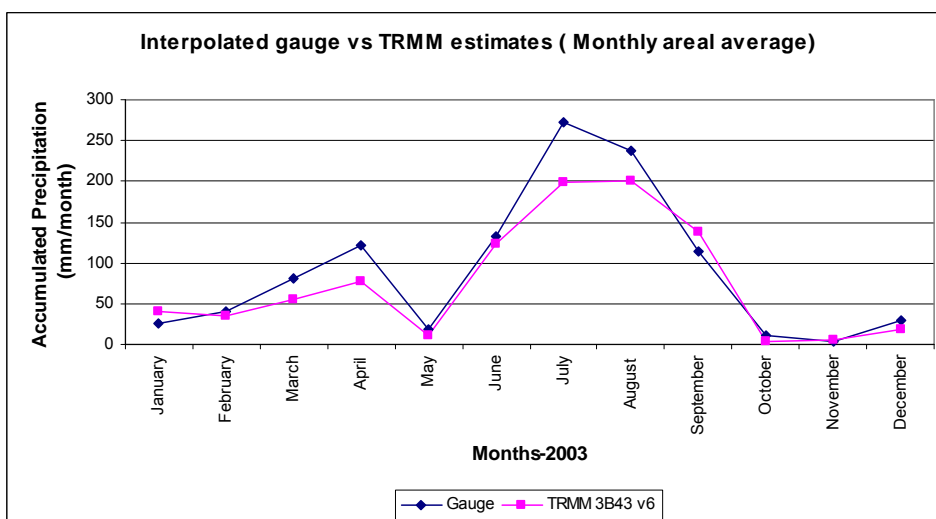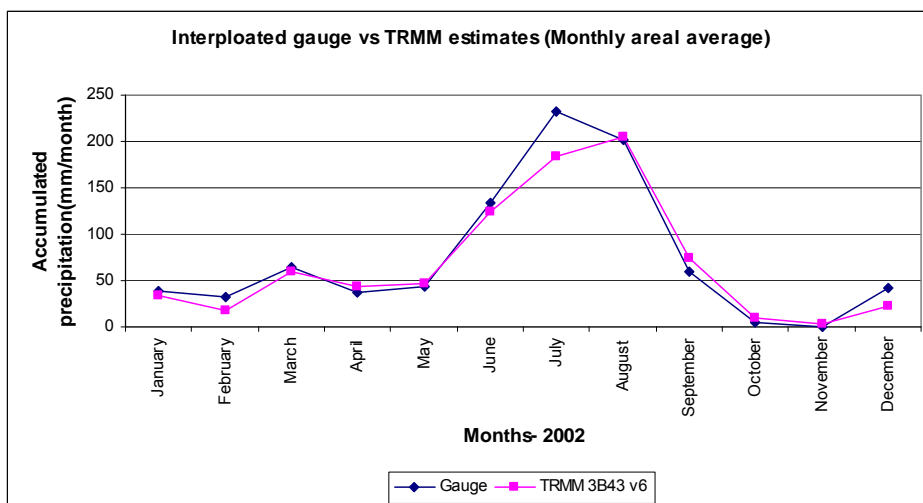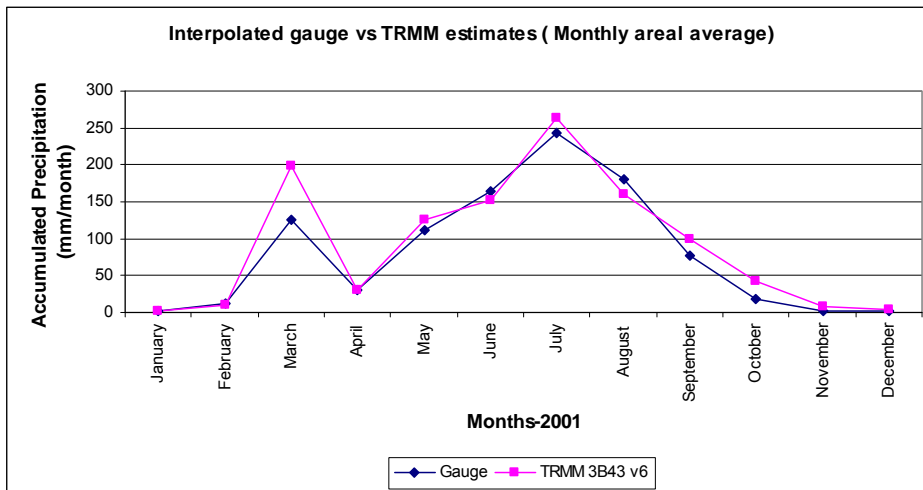
Figure 6-7: Time series of monthly mean precipitation for interpolated gauge and 3B43 V6 satellite estimate for 2001 to 2003

Table 6-2: Mean monthly TRMM 3B43 V6 estimates comparison w.r.t. interpolated gauge for 2001-2003

N = 36	3B43 V6 Estimates (TRMM), 0.25 x 0.25 degree spatial resolution
Correlation coefficient (R)	0.95
RSQ (R^2)	0.90
Eff.	0.90
Mean error (mm)	-3.5
Bias	0.95
RMSE (mm)	24.58

b) Seasonal comparison

During the rainy period the degree of agreement is quite high with a low overestimation in 2001 and an underestimation during 2002 and 2003. Hence, it can be seen that 3B43 estimates, in general for the satellite based rainfall estimation, are not fairly consistent and their significance, as a reliable data source for any environmental and hydrological application, depends on the temporal scale under investigation. During the rainy period of the year, an underestimation of the average accumulated rainfall by 10.36 mm is observed. A negative value of Eff. (coefficient of efficiency) here (i.e. -0.13) indicates that the rainfall estimates by TRMM during the rainy period produce more variation than it could be observed from the gauge data.

Table 6-3: Mean monthly 3B43 V6 estimates comparison with interpolated gauge during rainy season, for 2001-2003

N= 12	3B43 V6 Estimates (TRMM), 0.25 x 0.25 degree spatial resolution
Correlation coefficient	0.90
RSQ (R^2)	0.82
Eff.	-0.13
Mean Error (mm)	-10.36
Bias	0.939
RMSE (mm)	31.17

For the dry period within the year, no specific pattern or trend can be identified. This result is quite similar to the RFE 2.0 data. There is a large overestimation during the dry season of 2001 and an underestimation during the dry seasons of 2002 and 2003 with a magnitude of 25 mm and 20 mm, respectively. The mean error and average bias is found to be 0.29 mm and 1.02, with an RMSE of 11.51 mm. The coefficient of determination and correlation is less significant between the reference data and 3B43 during the dry season, yielding 0.37 and 0.60, respectively.

6.3.6   Comparison of RFE 2.0 and TRMM 3B43 V6 with Gauging Rainfall

The analysis is done by comparing the two satellite estimates of rainfall data with the gauge measured rainfall, interpolated at two different spatial resolutions that correspond to the spatial resolution of the two satellite datasets. The comparison is carried out with consideration of the accumulated average monthly rainfall over the region provided by RFE 2.0 and the TRMM 3B43 V6.
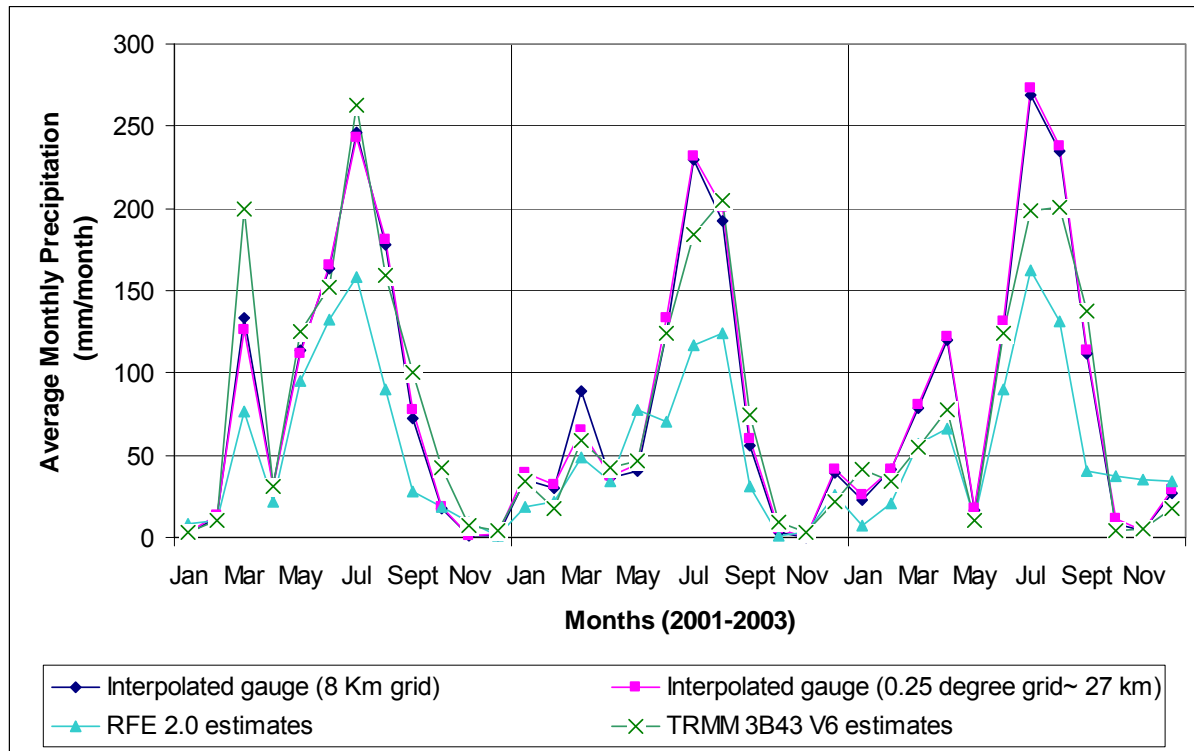
Figure 6-8: Comparison of rainfall distribution estimated from RFE 2.0, 3B43 V6 and interpolated gauge

It is seen that the RFE 2.0 underestimates relatively high during the rainy season when compared with the reference gauge data. The trend seems to be present in the TRMM 3B43 V6 also, though with a lesser extent of underestimation (Figure 6-8). Overall, the TRMM data performs better than the RFE 2.0 estimates. There is a better correspondence between 3B43 and gauge data in terms of their bias and mean error. The regression analysis yields a coefficient of determination (RSQ) of 0.90 with a correlation of 0.95 for 3B43 dataset; for the RFE 2.0, a RSQ of 0.88 and a correlation of 0.94 are found. Both datasets seem to perform well with the ground measured gauge reference data for the monthly time-step. It is found earlier that in the case of RFE 2.0 estimates, the monthly time-step correlates more accurately and has a higher agreement than the dekadal time-step.

Analyzing the two data sources separately, both estimates perform reasonably well with the ground gauge data. In general, since the two rainfall estimate algorithms use different methodological approaches and have a different spatial and temporal scale, a specific conclusion on their agreement with ground gauge data is not feasible. Nonetheless, the consistency of such indirect rainfall estimates with the ground data in terms of statistical significance and their agreement can be analyzed on individual specific datasets before such data are employed for any environmental application.

6.4   Summary

This study investigates the potential of indirect satellite based precipitation estimates. A comparison of these estimates with the reference gauging data is carried out. Dekadal time-steps of rainfall estimates from CPC-NOAA RFE 2.0 algorithm and that of TRMM 3B43 V6 monthly precipitation from 2001-2003 are used for the assessment purpose. In general, the degree of agreement between the reference data and the satellite estimates, i.e. RFE 2.0 and TRMM 3B43 V6 estimates, varies with temporal scale, that is, dekadal, monthly and seasonally. A better degree of agreement and statistical significance are found in the larger time-step than in the smaller time-step (i.e. *monthly* better than *dekadal*). The important conclusions to be drawn from this study are highlighted below.

The analysis of the reference gauge data shows three major distinct seasons: Little rainy period (Belg) from February-March; main rainy season (Kiremt) from June-September and dry period (Bega) from October-January. The histogram of monthly rainfall shows a bimodal distribution. This distribution of climatology within the Upper Awash Basin is quite consistent to previous reports by USDA and Alemayehu et al. (2003).

The analysis of the RFE 2.0 estimates from the Climate Prediction Centre (CPC) seems to be in favorable agreement with the reference ground data, measured with a correlation of 0.85 and R^2 of 0.72 on the dekadal time-step. The RFE 2.0 estimates significantly capture the pattern of rainfall although a trend of underestimation during the rainy period throughout the series can be observed. The statistical significance seems rather poor during the dry period. Better agreement is achieved when it is analyzed on a monthly time scale which gives a correlation of 0.94 and R^2 of 0.88. In general, as it is well documented by Funk and Verdin (2003), the performance of the RFE 2.0 rainfall estimates perform better in tropical areas than in other regions. The main reason behind this could be due to improvement of its algorithm by incorporating daily stations GTS (Global Telecommunication System) observations to correct the potential bias, thereby leveraging the utility of sparse gauge networks. In addition, the observations are based on cloud top temperature. These are related to vertical motion and convection and the estimates have a consistent spatial resolution of 0.1 degree, or 10 km. The analysis of 3B43 V6 monthly estimates yields very low bias, ME and RMSE, despite its coarser resolution of 0.25 degree, in comparison to the finer resolution of the RFE 2.0 results. A significant R^2 of 0.90 and coefficient of efficiency of 0.90 on the monthly basis from the 3B43 data is observed.

Overall, it is apparent that the TRMM product performs relatively better than RFE 2.0 on the basis of statistical measures that are taken here for comparison. Since the two rainfall estimates data are based on different algorithms and have different resolutions, it is further recommended to test the feasibility of such datasets as an input parameter for an environmental modelling purpose, and to analyze the sensitivity of the model that uses such kind of data. The most important aspect on choosing the right kind of Satellite Based Rainfall Estimates (SBRE) depends on the intended application or purpose, the climatic zone, the resolution of the data (temporal and spatial) and the accessibility of such data to the end user. For instance, in this research, the SBRE data is used for computing the rainfall erosivity of the region, which then serves as one of the input parameter for mapping the potential soil erosion risk of the Upper Awash basin by F-WERCAM model. A detailed procedure of rainfall erosivity estimation using the SBRE data will be discussed in the coming chapters.

7 Fuzzy Sets and Rule Base Development for Erosion Risk Assessment in Upper Awash Basin

"As the complexity of a system increases, our ability to make precise yet significant statements about its behaviour diminishes until a threshold is reached beyond which precision and significance (or relevance) become almost mutually exclusive characteristics." - Lotfi Zadeh

7.1 Developing the Knowledge Base of the Parameters Influencing Soil Erosion Risk

Understanding the phenomenon of soil erosion processes and identification of the primary influential variables is one of the necessary steps for developing the knowledge base on soil erosion risk as discussed earlier in Chapter 3. Here, a detailed assessment on some of the identified parameters along with an expert based questionnaire survey conducted for this research is presented.

7.1.1 Assessment of the Soil Erosion Risk Indicators or Parameters

i) Rainfall erosivity (R) assessment

Precipitation is considered as one of the important climatic variables that influences the complex hydrological processes on the surface of the earth. The ability of producing kinetic energy, thereby detaching the soil particles from the earth's surface causes degradation of the land which is termed as 'erosion'. The greater the intensities and duration of storms, the higher is the potential of 'erosivity'. 'Erosivity' is defined as the potential ability of precipitation to cause erosion and is a function of the physical characteristics of rainfall (Wischmeier and Smith, 1978). The higher the rainfall, the higher will be the surface runoff thereby increasing the susceptibility of soil particles to detachment and transportability. Hence, the 'rainfall erosivity index' or so called R-factor is considered as one of the input parameters for the F-WERCAM model.

Various experimental and statistical based rainfall erosivity determination equations exist for different regions of the world (Wischmeier and Smith, 1978; Renard and Freimund, 1994; Van Leeuwen and Sammons, 2003; Diodato, 2004; Hussein, 1986; Ferro et al., 1999; Hellden, 1987; Roose, 1977). Furthermore, a vast body of literature exists about the details and computation of the rainfall erosivity index (R) (Atesmachew et al., 2006; De Santos Loureiro and de Azevedo Couthino, 2001; Panigrahi et al., 1996; Richardson et al., 1983). Some of the work done in tropical zones for the estimation of the R-factor is extensively reviewed by Deore (2005). It can be concluded that there is no acceptable standard formulation for the determination of R. The rainfall erosivity component in the case of the widely used USLE and RUSLE soil erosion models is directly obtained from an existing iso-erodent map or can be computed using the equation given by Wischmeier and Smith (1978). In various regions of the world, the rainfall intensity is not recorded at the meteorological stations and there is an even

more sporadic availability of long term continuous rainfall data which is a prerequisite to compute the R-factor. Therefore, the direct calculation of rainfall erosivity poses a problem to data scarce areas. To cope with this problem, researchers have developed various indirect estimative models. The advantage of using such models for computation of erosivity is that they require less data and are easier to calculate. The drawbacks of such equations for estimation of the erosivity index is that they are generally site-specific, i.e. only applicable in the areas where they were developed.

From the various existing rainfall erosivity computation equations, the erosion index or R-factor by Wischmeier et al., (1978) appears to quantify the effect of raindrop impact. The erosion index also reflects the amount and rate of runoff likely to be associated with the rain better than any of the many other rainfall parameters and groups of parameters tested against the field plot data (Renard et al., 1997). However, the lack of long-term rainfall intensity data for the computation of R limits the wider applicability of this calculation method especially in data-poor regions of the world.

Considering the drawback of data requirements in the computation of the R-factor according to Wischmeier et al. (1978), Renard and Freimund (1994) provides an equation to estimate the R-factor using the monthly mean and annual precipitation data. The derived relationship between R and the modified Fournier index (F) is given as:

$$R = 0.7397 * F^{1.847}, \text{ for } F < 55mm \tag{7.1a}$$

$$R = 95.77 - 6.081 * F + 0.4770 * F^2, \text{ for } F > 55mm \tag{7.1b}$$

$$F = \frac{\sum_{i=1}^{12} p_i^2}{P} \tag{7.1c}$$

Where F (mm) is the modified Fournier index (Renard and Freimund, 1994), p_i (mm) is the average monthly precipitation, P is the average annual precipitation and R is the rainfall erosivity in MJ mm ha^{-1}h^{-1}yr^{-1}. This equation by Renard and Freimund (1994) on the modified Fournier Index (F) has found wide application in different parts of the world.

In addition, erosivity equations after Hellden (1987) and Roose (1977) based on average annual precipitation (mm) of a region are found to be applicable to African climate conditions. According to Hellden (1987), monthly precipitation records of Ethiopia are used to establish a linear regression ($r^2 = 1.00$) to describe the R-factor as a function of mean annual precipitation. This can be given as:

$$R_{ann, Hellden} = -8.12 + (0.562 * P) \tag{7.1d}$$

Where, P = mean annual precipitation (mm).
$R_{ann, Hellden}$ = annual erosivity factor, Hellden

For the tropical climate, while working in West Africa, Roose (1977) reported a simple relationship between the average annual erosivity (R) and the average annual rainfall (P) in mm, as follows:

$$R_{ann, Roose} = 0.5 * P * 17.02 \tag{7.1e}$$

Where, P = mean annual precipitation (mm).
$R_{ann, Roose}$ = annual erosivity factor, Roose

This erosivity equation is applied to different parts of the African continent with success. For instance, it is applied to the Awash Basin for the assessment of annual soil erosion owing to its simplicity and possibility of using only precipitation data (Atesmachew et al., 2006; ILRI report on soil erosion of Awash Basin).

Here, the annual erosivity index (R) for the Upper Awash Basin is computed using the three different types of erosivity equations. Then, the computed erosivity maps of the Upper Awash Basin are compared and analyzed. It is found that the range of erosivity of the region changes significantly depending on the type of computation method adopted and the type of source datasets (see Table 7-1). Different precipitation sources of the region provide different ranges of average annual precipitation and thereby affecting the computation of R. For instance, indirect satellite based estimates from CPC-NOAA are found to have a lower range of average precipitation when compared with ground interpolated rainfall, indicating an underestimation. Subsequently, the computed R from the CPC data is found to be in a lower range for all the adopted methods. On the other hand, the R computed using the TRMM data is found to be quite reasonable when compared with the R estimates using the ground rainfall data. In relation to the different types of computation methods, it is found that the R computed using the Hellden (1987) method yields a lower range when compared with the other two methods, irrespective of the source data used. Considering the two types of indirect satellite rainfall estimates, it is found that the computed R using TRMM corresponds well with that of computed R using ground interpolated data, despite its coarser resolution (0.25 degree). The CPC- NOAA gridded data which have a moderate resolution of 8 km show a trend of underestimation in both the annual precipitation and the magnitude of R.

Table 7-1: Rainfall erosivity (R) estimation of the Upper Awash Basin with three different erosivity estimation methods using rainfall data (2001-2003) from different sources

Upper Awash Basin			Annual erosivity computation methods (R) [SI units]					
Data source	Average annual precipitation (mm)		Renard and Freimund method (1994)**		Roose method (1977)*		Hellden method (1987)*	
	Min	Max	Min	Max	Min	Max	Min	Max
Ground interpolated data	703	1140	8004	15936	6084	9864	3944	6400
TRMM estimates	738	1265	4867	16675	6288	10768	4144	7103
CPC-NOAA estimates	489	811	1552	7017	4161	6901	2740	4549

*Applicable in African conditions; ** Applied in different climatic zones of the world*

The R value of the Awash Basin computed with the Roose (1977) method in an earlier study from Bizuwerk, et al. (2003) from ILRI, Addis Ababa is found to be in the range of 1167.75-11867.8 MJ mm ha^{-1} h^{-1} yr^{-1}. In this study, the estimated R value of the Upper Awash by Roose (1977) using a different data source falls within the range as reported in earlier works. On the other hand, Hellden's

method tends to underestimate while the method of Renard and Freimund (1994) tends to overestimate the erosivity value of the region.

Further assessments regarding the observation of the distribution pattern of R are carried out by comparing the extracted erosivity value corresponding to each of the gauging stations present within the study area. From the plot for each erosivity equation using a different input source, it is found that the magnitude of R computed using Renard and Freimund (1994) has a large difference for each dataset used at each station (see Figure 7-1); in case of Hellden (1987) and Roose (1977), the magnitude of R at each station is comparable especially for the ground-based and TRMM-based source.
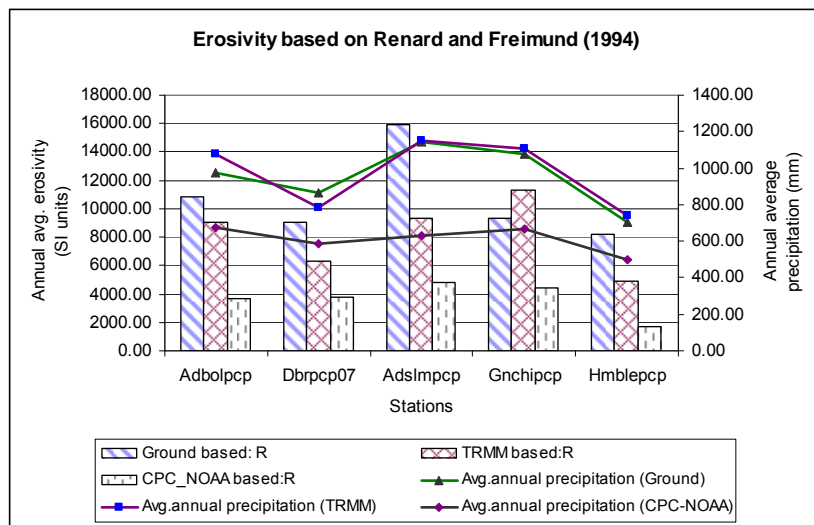
Figure 7-1: Average annual precipitation and erosivity at each station after Renard and Freimund (1994)
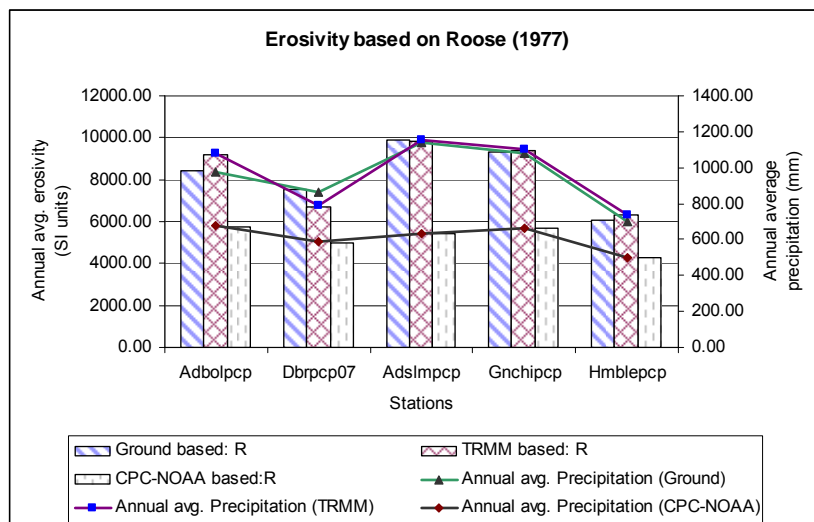
Figure 7-2: Average annual precipitation and erosivity at each station after Roose (1977)
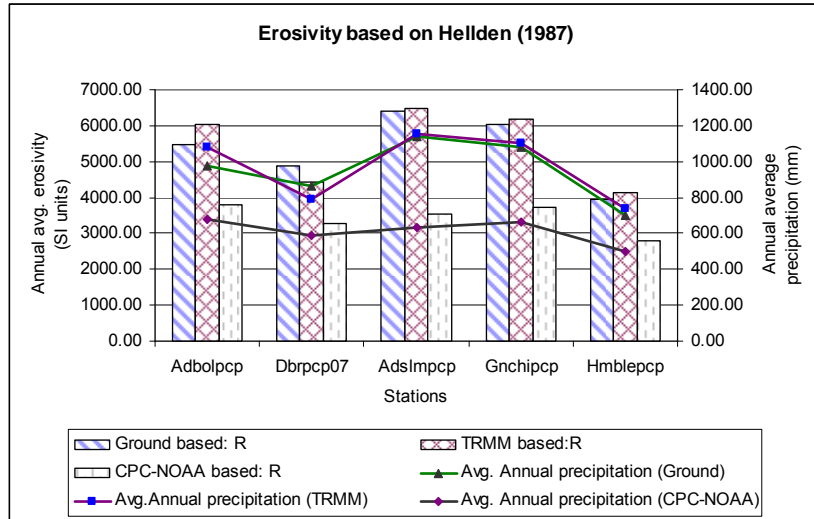
Figure 7-3: Average annual precipitation and erosivity at each station after Hellden (1987)
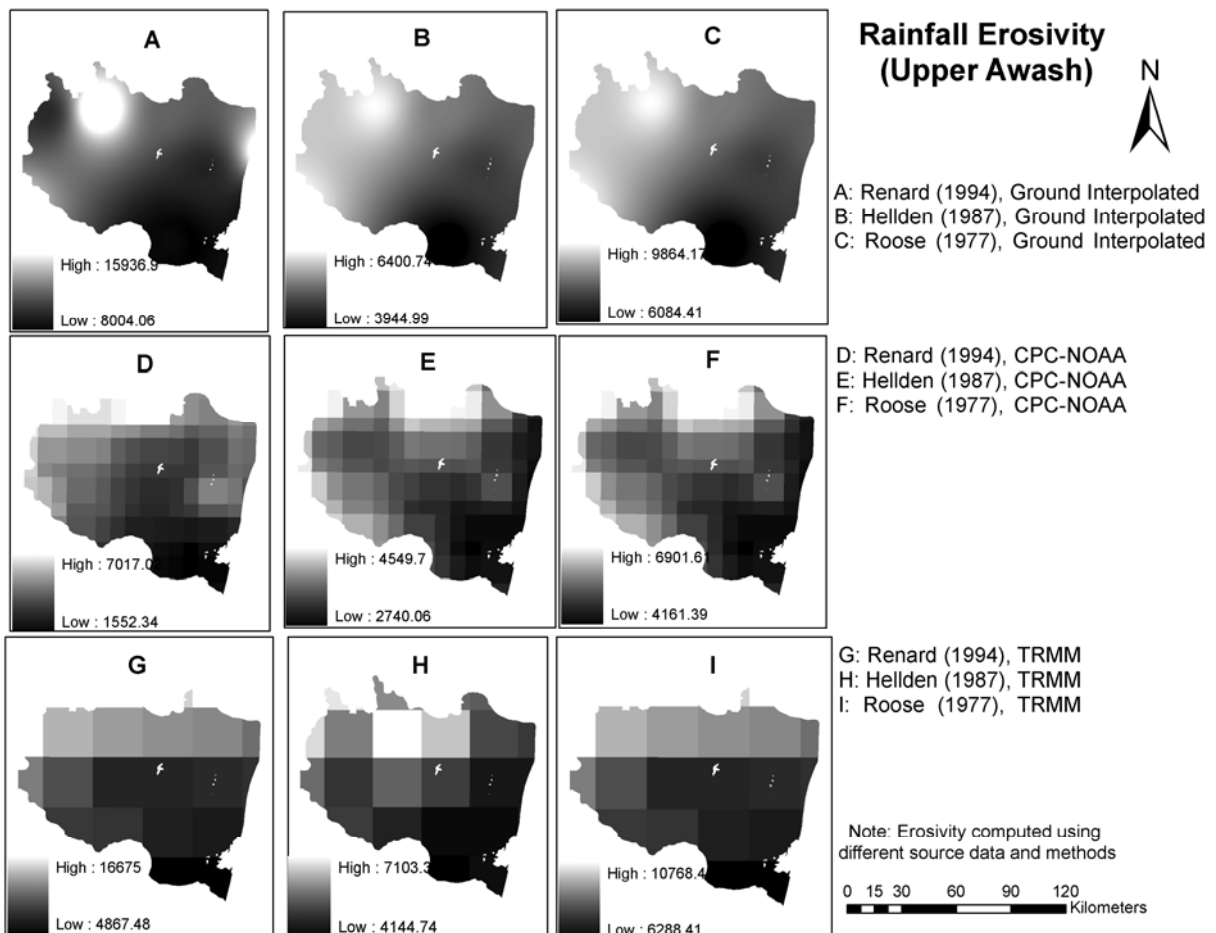
Figure 7-4: Rainfall erosivity map of the Upper Awash Basin

The large differences that are observed in the Renard and Freimund (1994) method can be an indication of the higher sensitivity of Fournier index (F) as compared to using the average annual precipitation (P), in case of Hellden (1987) and Roose (1977). The similarity in the distribution

patterns (Figures 7-2 and 7-3) of erosivity for different input sources in case of Roose (1977) and Hellden (1987) can be attributed to the fact that both methods were developed for African conditions and are based on the relationship between average annual precipitation and R.

It is shown here that depending on the type of rainfall datasets and methods used, the variability of R within a region changes significantly which in turn can have a potential effect on computing the overall erosion risk of a region. The spatial erosivity map of the region computed using different methods and data sources can be seen in Figure 7-4. From this figure, it is evident that the spatial pattern of the erosivity distribution within the study area follows a similar trend irrespective of the data source, having a lower erosivity in the south eastern part of the region and higher erosivity toward the northern and north-western part of Upper Awash. A variation in the magnitude of the erosivity can be observed depending on the type of method used for computing the erosivity of the region. After considering all the methods and the range of the erosivity as documented in earlier studies in Awash Basin, the erosivity map of the Upper Awash Basin by the Roose method is considered for further assessment of the soil erosion risk in this study.

In general, this type of assessment gives an overview for estimating rainfall erosivity. Depending on the type of source data used and method employed, one would certainly expect to have a different degree or range of the erosivity in the region. Hence, this approach can be considered as an appropriate strategy to test the applicability of such estimators using the range of available datasets prior to the overall assessment of soil erosion risk of a region. Unavailability of rainfall intensity and long term rainfall data for most regions in the tropics, these equations show an alternate reasonable way for estimating R since it is based on the relationships between monthly or annual average rainfall and R values. Rainfall erosivity parameters (R) generated using such equations should be interpreted with care and the selection of estimators should be based on available source dataset of the region under investigation.

ii) Soil Erodibility assessment (K)

The soil erodibility factor (K) is computed as a function of soil properties such as texture, organic matter content, permeability and bulk density. Lal (1981) described soil erodibility as the composite factor which comprises "detachability" and "transportability". Detachability of soil particles depends on soil and rainfall characteristics while overland flow with or without rill systems and their characteristics, governs transportability.

USLE and RUSLE use a restrictive and applied definition of soil erodibility and it is considered as the change in the soil per unit of applied external force or energy, when viewed from a fundamental standpoint (Renard et al., 1997). Research on soil erodibility is important toward understanding the mechanism of soil erosion. This factor is taken into account in most of the empirical, conceptual as well as in some physical based erosion models. But in most of the models, the erodibility factor has a different physical meaning and employs different equations for its computation. For example, in USLE and RUSLE, the K factor is considered to be a lumped parameter that represents an integrated average annual value of the total soil and soil profile reaction to a large number of erosion and hydrologic processes (Wischmeier and Smith, 1978; Renard et al., 1997). On the other hand, physically based models like WEPP (Water Erosion Prediction Project) have separate values of erodibility (K) for rill and inter-rill processes under steady state conditions of rainfall and runoff (Alberts et al., 1995). Hence, the physical meaning of erodibility varies with the equations in which they are used. Detailed

reviews and analysis on the methods to measure and compute the soil erodibility factor are reported by Yang et al. (2005) and Zhang et al. (2008).

Direct measurement of the soil erodibility factor is both, costly and time consuming and is feasible only for a few major soil types (Wischmeier and Smith, 1978). Since the 1950's, research on soil erodibility by many researchers on the basis of experimental-quantitative studies provides various formulae to calculate soil erodibility. Many of the formulae are region specific (temperate and tropical zone) and for a specific type of soil (Kaolinite dominate soil; Vertisols dominate soils). A list of equations to calculate the soil erodibility related to the soil type is given in Yang et al. (2005). Selecting the most appropriate one always poses a problem if the equation is not developed specifically for the considered region. In this study, certain criteria are applied for the selection: These are based on their simplicity, principal component involved in the equations, availability of data for computation and its wider applicability in soil erosion research.

In general, data on soil erodibility are not avaliable and it is difficult and impractical to setup runoff plots for each and every type of soil. Therefore, a need of estimators of soil erodibility using soil data that are more readily available is desirable. Estimation of the soil erodibility factor based on Wischmeier's nomograph is considered inappropriate when used on soils significantly different to the ones from which the nomograph was developed. Wischmeier's nomograph is based on the soil information and data from temperate zones. Roose (1977) found out that the nomograph is less applicable for tropical soils where vertisols soil dominates. Other methods for K computation by Shirazi and Boersma (1984) or Zhang et al. (2008) are also deemed inappropriate for this study due to the parameters involved that are not readily available without the need of a field experimental and laboratory testing. On the other hand, William's erodibility equation (William and Arnold, 1997) and other methods like the representative value of soil erodibility factor table (Stewart et al., 1975) or texture based triangle used for estimation of K values (Monchareon, 1982; Bahadur, 2009), based on readily available soil textural information and organic matter content, can be considered as an alternate and more feasible way to derive the K factor of a region. This is particularly useful when there is no natural runoff plot available to measure the erodibility of the soil.

In this study, K factors are computed separately using the William's erodibility equation, Stewart's erodibility table and Monchareon's K value triangle. A comparison is made between the ranges of computed K values for different type of soils present in the Upper Awash Basin. The computed range of K values for the different soil units of the region using three different approaches are provided in *Appendix 5*. A comparison of computed K values for different soil units present in the study area by the three different methods are presented in Figure 7-5. The mean K of the study area computed using the three methods are 0.222, 0.162 and 0.219, respectively. The computed mean K using Monchareon's equation is relatively low for each soil unit as compared to that of William's and Stewart's method. Lawal et al. (2007) reports that estimation of the erodibility factor by William's equation is strongly influenced by texture related soil characteristics. The components of the equation correct the soil erodibility values for factors like high coarse-sand content, high clay, silt ratios and high organic carbon content. Eventually, the value of K obtained from William's equation, which was originally used in EPIC (Erosion Productivity Impact Calculator), (Williams, 1990) is selected for preparing the input K factor grid for F-WERCAM.
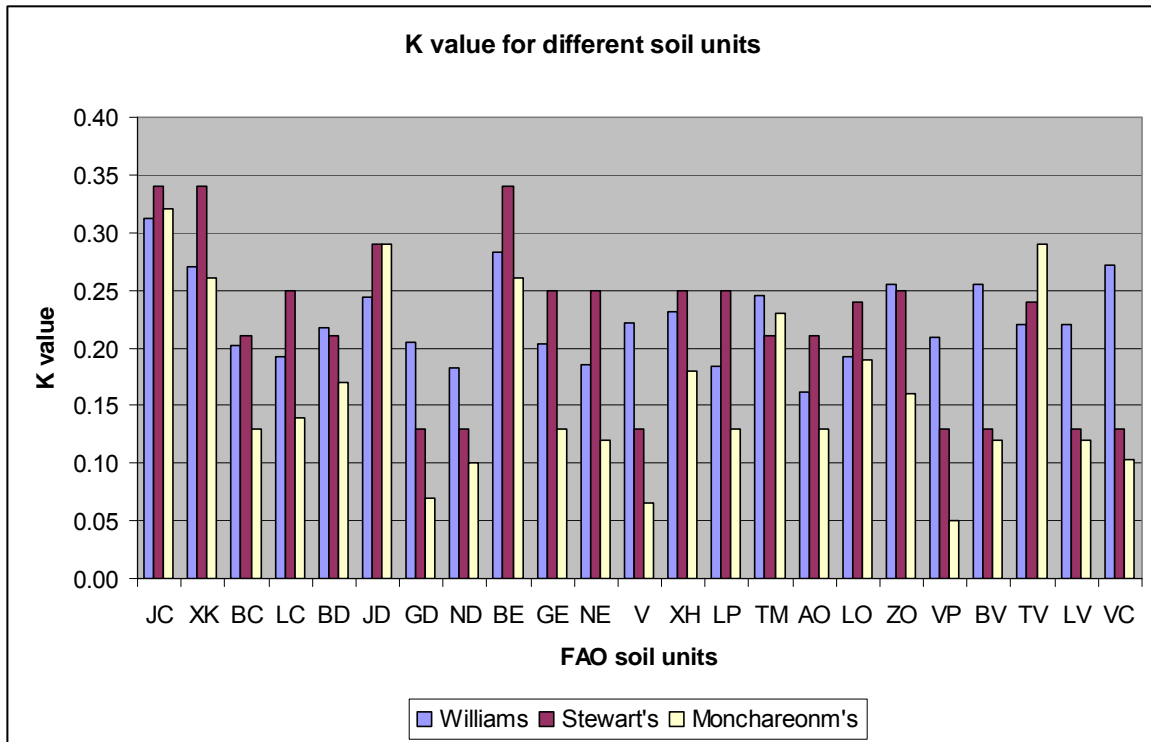
Figure 7-5: Comparison of computed soil erodibility value (K) for different soil units
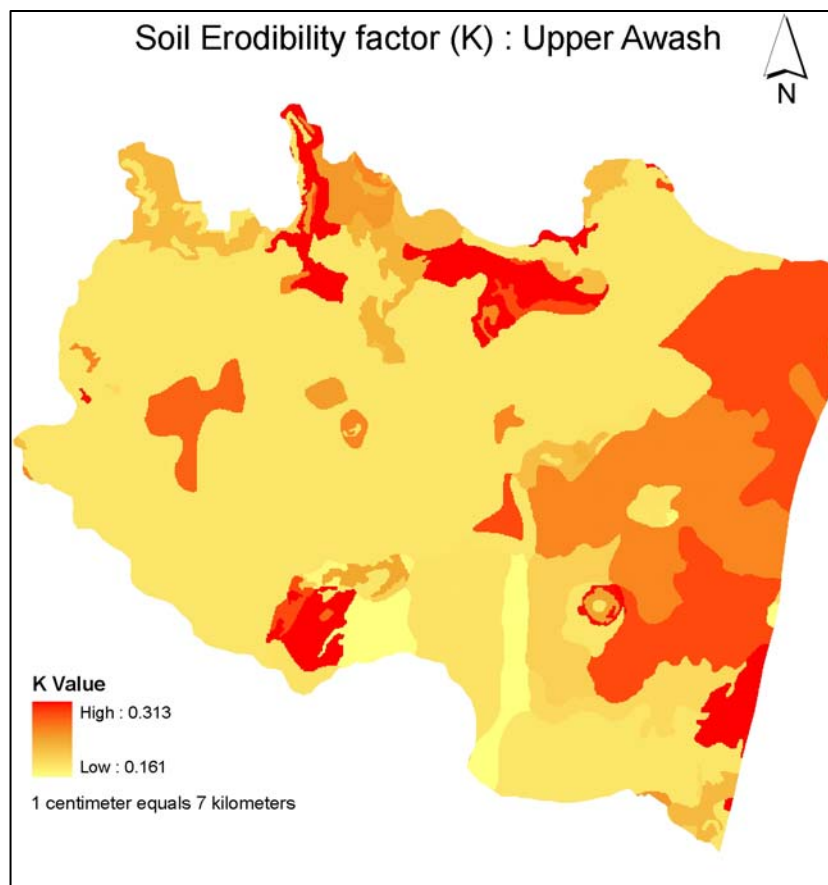
Figure 7-6: Soil erodibility map of the Upper Awash Basin after William's erodibility method

Using the Geo-coded soil map obtained from the Federal Ministry of Water Resource (FMWR), Ethiopia and the computed K factor for each soil type, an erodibility factor (K) grid map of the region is prepared in ArcGIS (Figure 7-6).

iii) Slope Gradient (%)

Slope steepness is critical to the erosion intensity and is proved that there is an exponential relation between average slope, soil loss and sediment yield (Schumm, 1977). Generally, the steeper the slope gradient, the greater the potential of soil erosion risk. Ghadiri and Paynet (1988) examined in their laboratory study the formation and characteristics of splash following raindrop impact on soil. One of their studies on the effect of slope and wind speed on splash indicates that intense erosion tends to occur when slope steepness is greater than 25 degrees, due to soil detachment; more specifically, the kinetic energy of the rebounding splash droplets increases from 11 % on horizontal surfaces to 33 % on a 30 degree slope. Another study by Wan, et al. (1996) concludes that wash dominated inter-rill sediment transport occurs at low slopes (< 9 %) and is linearly related with slope while down slope splash transport was dominant at high slopes (> 9 %) and was best described by a power function model. Study based on semi-arid rangeland by Wilcox and Wood (1989) indicates that slope gradient has a large positive impact on inter-rill erosion because sediment concentration (not runoff) is greater from steep slopes. It is also found that the effect of slope can be greatly muted by vegetation cover. Inter-rill erosion is also affected by slope with increasing soil moisture. The effect of slope as one of the driving parameters in the soil erosion risk assessment is summarized below in Table 7-2.

Table 7-2: Effect of slope steepness or gradient in soil erosion processes according to some selected reports

Descriptions and Explanations	Source
Slope less than 11 % (5°) is reported to be depositional and slope > 45 % (20°) as erosional.	MacGillivray and Donovan (2007)
Examined soil loss from slope between 8 to 30 % in Burundi test site and reported loss of soil increase with significant increase in slope gradient.	El-Hassanin et al. (1993)
Soil loss to be linearly related to the sine of slope angle and shows an increase in soil loss for slope from 9 to 55 % (Loess plateau, China).	Liu et al. (1994)
Soil loss increases logarithmically with increasing slope gradient and length; a convex steep slope over 57 % or 30° is found to be highly susceptible to erosion (Kenya).	Gachene (1995)

Table 7-3: Some of the slope classification range for erosion risk studies carried out in Ethiopian Highland region as reported in literature

Sl. No.	Test site	Class range (%)	Source
1	Ethiopia Highland, Dir-Dira	0-2,2.1-7,7.1-13,13.1-21, >21	Reusing (2000)
2	Awash basin, Ethiopia	0-2,2-8,8-30,30-50, >50	Griffiths and Richards (1989)
3	Awash basin, Ethiopia	0-2,2-8,8-30,30-50, >30	Elias (2003)

Such ranges of slope class or threshold provide the necessary information and background prior to the fuzzification of slope as one of the primary terrain parameter considered in F-WERCAM.

iv) LULC and NDVI

LULC and NDVI are considered to be the most dynamic factors that can be readily manipulated to produce wide variations in rates of erosion and its corresponding risk. Different types of LULC classes have different degrees of erosion risk associated with them. For instance, natural forest and densely forested region are considered to have a very low erosion risk as compared to regions which are dominated by agricultural practices, barren land and degraded forested area, which tend to have a higher potential of soil erosion risk. On the other hand, the presence or absence of vegetation cover greatly affects the top soil layer from being protected against external agents irrespective of the type of LULC. Hence, NDVI which is basically a remote sensing based vegetation index is used here to reflect the vegetation cover characteristic of the region. Incorporation of these two factors as input parameters in F-WERCAM will provide an understanding of the influence of vegetation parameters in assessing the degree of soil erosion risk.

Measuring the percentage of vegetation cover for a large region is time consuming and sometimes becomes difficult due to the terrain configuration. To cope with such difficulties, a remote sensing based vegetation index such as NDVI is used extensively to measure vegetation health and cover characteristics on a broad-scale worldwide (Rouse et al., 1973, Tucker, 2006). A recent study by Glenn et al. (2008) provides a theoretical basis of the remotely sensed vegetation indices and their use and application in many aspects of environmental monitoring.

The values are computed as the ratio of the measured intensities in the red (R) and the near-infrared (NIR) spectral bands of the electromagnetic spectrum using the formula:

$$NDVI = \frac{(NIR - R)}{(NIR + R)} \qquad\qquad (7.1f)$$

The resulting index value is sensitive to the presence of vegetation on the earth's land surface and can be used to address issues of vegetation type, amount, and condition. Its value varies between -1 and 1, where low values indicate water bodies, bare soil and built-up areas. A detailed interpretation on the range of NDVI and its physical meaning is provided in *Appendix 6*.

Overall, these assessments of the identified parameters provide the primary information and knowledge for the fuzzification and setup of fuzzy rules for F-WERCAM.

7.1.2   Expert Knowledge and Questionnaire Survey on Erosion Risk Assessment

An additional expert knowledge is obtained by conducting a questionnaire survey. The questionnaires are sent to various experts on soil erosion, water resource management that comprised professors and scientists. The development of the questionnaire is based on the selected parameters that are found to influence the soil erosion as discussed in Section 7.1.1. Experts are asked to rank the parameters and provide a corresponding weight on a scale which is solely based on their experience and judgments.

Ranking of the primary parameters considered in F-WERCAM and that of the LULC class present in the study area, considering their potential risk on soil erosion, is obtained through this survey. A sample of the questionnaire feedback provided by an expert can be found in *Appendix 7*. According to the expert feedback and analysis, it is found that LULC parameter with a varying degree of vegetation cover (NDVI) is the most influential parameter to reflect the degree of soil erosion risk. This is then followed by soil erodibility (K), slope (%), and the rainfall erosivity (R) of the region. With respect to the type of LULC type, forest area is indicated to have the lowest potential for erosion risk intensity, whereas agricultural zone has the highest.

In addition, a multi-criteria decision making technique known as AHP (Analytical Hierarchy Process) developed by Satty (1980) is used to quantify the influence of each parameter on the soil erosion risk. It tries to quantify relative priorities for the given set of identified parameters, based on the expert judgments. It also stresses the importance of intuitive judgments of the experts in the decision making process. Based on AHP, it is found that the SPI, which is a function of LULC and NDVI, has more influence or dominant role in the assessment of erosion risk when compared to other parameters like the soil erodibility (K), rainfall erosivity (R) and slope (%) of the region.

7.2 Fuzzification and Fuzzy Rule Base for Each Stage

This section deals with the fuzzification for each parameter and the fuzzy rule used for modelling at each stage of F-WERCAM. In addition, a discussion on the output scale adopted is provided along with their fuzzy sets. A general discussion on the selection of the right membership functions for the fuzzified input-output parameters is also described here.

The rule base is a set of rules in IF-THEN form. The development of the fuzzy rules is based on the expert knowledge and the inductive reasoning method (Giere, 1984; Heit, 2000). When setting up the fuzzy rules for each stage, contextual and semantic knowledge of the soil erosion process obtained through experts and literature are taken into account. Generally, the information contained in the premises of the rules provides support for the corresponding conclusion or the consequences. For instance, '*IF Soil Erodibility = High, and Rainfall Erosivity = High, and Slope = Very High, THEN PERI = Very High*', i.e. the consequence of a specific rule reflects the information which the premises of the rule are based on.

Choosing the right membership functions

In past fuzzy logic-based environmental assessment studies, functions like trapezoid or bell-shaped curves with two parameters and Gaussian function are found to give reasonable and satisfactory results (Metternicht and Gonzales, 2005; Mitra et al., 1998; Salski, 1999). Fuzzy membership functions may take on many forms, but in practical applications simple linear functions such as triangular ones are preferred (Tayfur et al., 2003). So, there is not a "defined membership function" set that can be fitted to each parameter involved in the model. However, the main important fact – according to experts in Google's Fuzzy Logic group[*] – is to see that "the chosen membership function satisfies the requirement of being semantically representative of the relationship existing between the crisp values

---

[*] *This is a group setup in google and the purpose of this group is to allow people who work with fuzzy logic to exchange knowledge and information; link: http://groups.google.com/group/fuzzy/about*

of the input space and the linguistic terms identifying each subset of the input space". Through personal correspondence with members of Google's Fuzzy Logic Newsgroup and own experience, it can be concluded that "the best input membership" function is problem dependent and the choice remains arbitrary.

As discussed earlier, the fuzzification process requires defining the type of membership function to be used and the fuzzy boundaries (value of each class range) to be assigned to the selected function (Metternicht and Gonzales, 2005). In this study, selection of the membership functions for the input parameters, for instance, LULC and NDVI (for Stage 1) is done based on knowledge found in literature about the corresponding parameter and by consulting expert opinion on the soil protection level and associated erosion risk factor. When converting the possible value range of input parameters to linguistic fuzzy sets, criteria of "overlapping and completeness" of the membership functions are taken into account (Mizumoto, 1998). Kainz (2002) suggests that when setting up the initial membership function, it is required to see that the crossover points (i.e. membership value of 0.5) are at the boundary of the crisp set. In addition, the natural local distribution pattern of the continuous input data (such as slope, NDVI) is taken into account for natural grouping of the class using the Jenkin optimization technique in ArcGIS (Baz et al., 2009; Xiaodan et al., 2004). This step helps to decide upon the dividing and break point, which makes the summation of each class inner variance the least and to find grouping and patterns inherent in the data itself. This accounts for the local distribution patterns of the parameter when defining the class range and linguistic classes.

It is one of the main tasks of the user to select a function that best represents the fuzzy concept to be modelled. By choosing proper values for A, B, C and D, one can define simple membership functions like triangle or trapezoid functions (Figure7-7).

Triangular Membership function

$\mu= 0$ For $X< A$
$\mu= (X-A)/(B-A)$ For $A < X \leq B$
$\mu= (C-X)/(C-B)$ For $B< X \leq C$
$\mu= 0$ For $C < X$

Trapezoidal Membership function

$\mu= 0$ For $X \leq A$
$\mu= (X-A)/(B-A)$ For $A < X \leq B$
$\mu= 1$ For $B < X \leq C$
$\mu= (D-X)/(D-C)$ For $C < X \leq D$
$\mu= 0$ For $D < X$
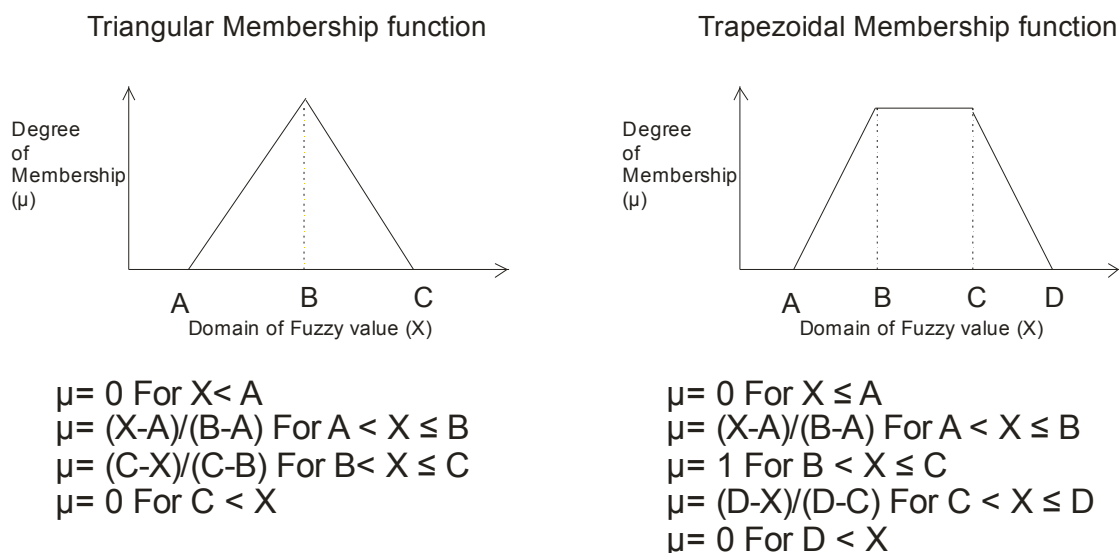
Figure 7-7: Linear membership functions (triangular and trapezoidal)

Above all, experience, expert judgment and knowledge about the process under investigation play an important role in determination of fuzzy sets (Murtha, 1995). The user of the system must define the linguistic classes such that reasonable system output will be achieved. This can be termed as the critical process of tuning the fuzzy system.

7.2.1　Stage 1: Soil Protection Index (SPI)

The SPI is defined as a function of land use practices and intensity of vegetation cover. Basically, this index provides the relative degree of protection of top soil from being eroded by action of external agents like rainfall and overland flow.

$$SPI = f\left(LULC; NDVI\right) \tag{7.2a}$$

Where LULC = Land Use and Land Cover classes and NDVI = Normalized Difference Vegetation Index (used as proxy of vegetation cover).

A similar concept is adopted successfully in past studies, e.g. CORINE (Coordination of Information on the Environment) and the ICONA model. These are used by the countries of the European Union to determine erosion risks and qualities of the land (PAP/RAC, 1997; CORINE, 1992; cf. overview by Yuksel et al., 2008). Most of the existing simulation models develops for soil erosion modelling (empirical, conceptual and process-based) are seen to incorporate the concept of soil protection and the cover factor in various forms that are applied to account for the influence of land use practices and vegetation cover distribution on erosion risk.

Up to now, there is no set standard classification index or scale that can be adopted for mapping the protection level of soil based on spatial vegetation distribution and corresponding land use practices. In general, it can be considered as site specific depending on the nature of the parameters considered and their local distribution pattern. Hence, in this study a relative scale from 0-1 (0 being "very low" protection and 1 being "very high" protection) for the lower and upper threshold, has been used to map the spatial distribution of the Soil Protection Index (Table 7-4). Five categories of soil protection levels of the region are defined at the outset and then the defined classes are transformed into 5 linguistic fuzzy sets. This forms the desired output fuzzy sets to map the spatial variability of SPI in the region (Figure 7-8).

Table 7-4: Class definition of SPI

Class	Description	Class range (0-1)	Details and definition (based on vegetation cover (VC) and land use class)
1	Very High	0.8-1	Region having high density of VC, mainly high densely forested region.
2	High	0.6-0.8	Region having good VC, mainly of grassland, forest, protected areas, etc.
3	Medium	0.4-0.6	Region having VC but fragmented due to anthropogenic factors; especially areas like settlements and urban fringes, fragmented forest areas, etc.
4	Low	0.2-0.4	Topsoil is exposed due to scanty VC; barren land, desert areas, degraded lands due to human activities, like high population density, livestock populations.
5	Very Low	0-0.2	Highly modified region due to agricultural practices and improper management practices; region of very low or no VC especially barren and wasteland region.
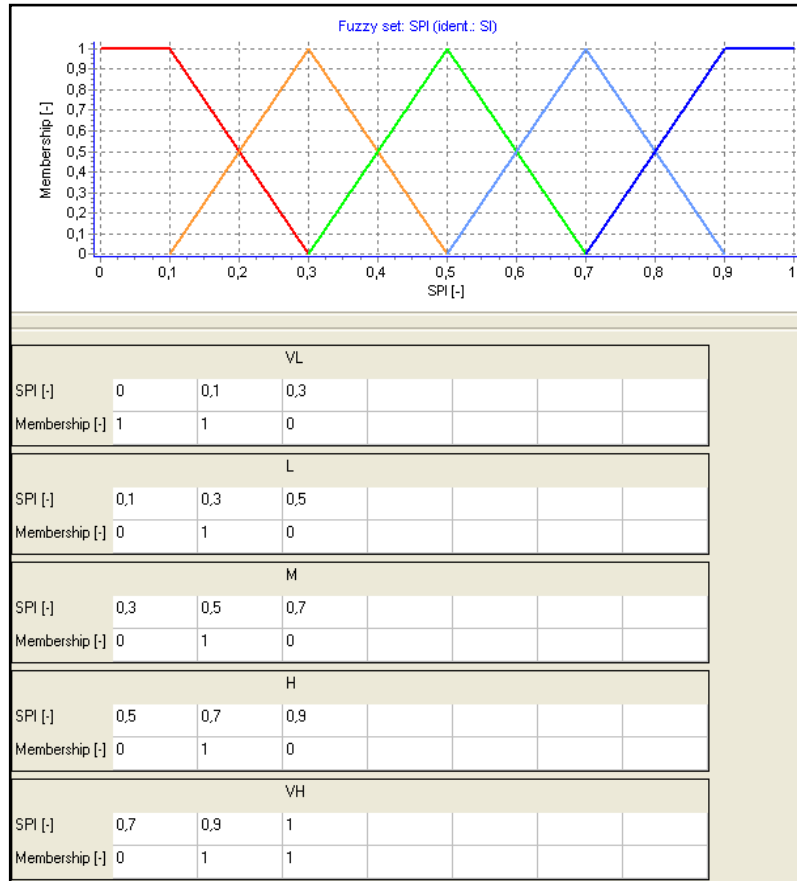
Figure 7-8: **Membership functions associated with SPI (system output)**

For mapping SPI, LULC and NDVI are needed as input parameters. LULC classes are categorical variables and do not manifest numerically. Each land use class category is represented as a fuzzy singleton, resulting into 5 linguistic sets from VL (Very Low) to VH (Very High). These linguistic sets correspond to the LULC class present in the study area. They represent the potential degree of influence of different LULC class on SPI of the region. Membership functions associated with the LULC classes are shown in Figure 7-9(a). Similarly, the membership functions or linguistic sets associated with NDVI take the same descriptors, i.e. VL (Very Low), L (Low), M (Medium) and H (High) (4 fuzzy sets). This is shown in Figure 7-9 (b).

Fuzzy rules for the SPI (Soil Protection Index) are developed using expert knowledge and literature reviews. When setting up the rules, the variability of NDVI class (Vegetation cover) is considered to have greater influence on the desired output SPI. The rules represent the varying degree of SPI due to the influence of NDVI distribution on different LULC classes. Since the total number of rules equals all possible permutations of model inputs, there are 5 sets x 4 sets = 20 rules that define the model output. The associated rules used to map SPI are shown in Table 7-5. The Stage 1 of F-WERCAM is executed once the membership functions for the two input parameters are defined and the set of associated fuzzy rules are developed. If we update the rule base by introducing additional expert knowledge, the SPI map tends to update accordingly. The rule base forms the overall knowledge of influence of vegetation cover and land use cover practices on SPI, i.e. it is the representation of knowledge and experience about the process under investigation. The effect of the modified fuzzy rule base, which takes into account the influence of surface sealing, impervious surface over the region, especially in urban or settlement regions, is also discussed in later chapters.
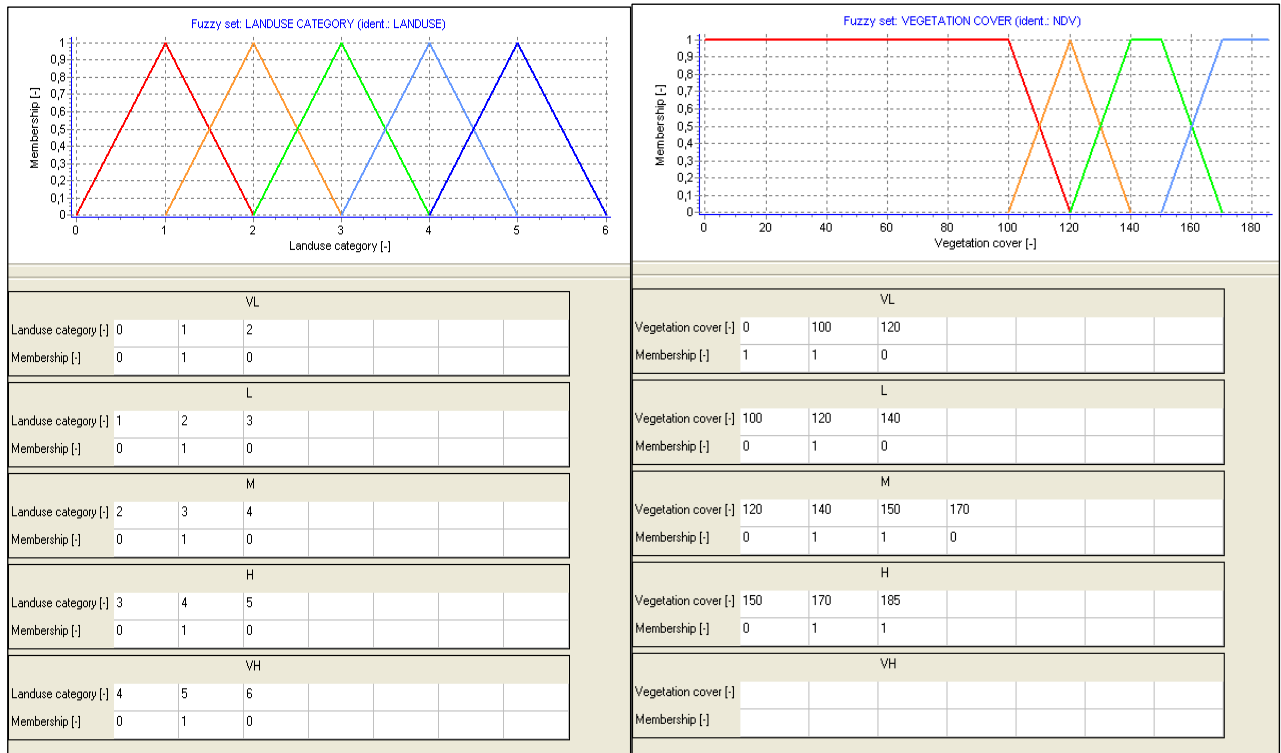
Figure: 7-9 Input membership functions for a) LULC and b) NDVI parameters

Table 7-5: Rule base for mapping the SPI (IF NDVI = '…' AND LULC = '…' THEN SPI = '…')

SPI (Soil Protection index) [20 rules]	NDVI (Vegetation cover) [4 classes]			
LULC classes [5 classes]	*VL*	*L*	*M*	*H*
VH (Forest)	L	M	H	VH
H (Grassland)	VL	L	L	H
M (Settlement)	VL	VL	L	M
L (Shrubland/Barren)	VL	VL	L	M
VL (Agriculture)	VL	L	M	H

Stage 1 of F-WERCAM provides the spatial variability of Soil Protection Index (SPI) over the region. The assessment of output SPI maps and their temporal based analysis over the Upper Awash Basin are discussed in subsequent chapters.

7.2.2 Stage 2: Potential Erosion Risk Index (PERI)

Potential erosion risk is defined as the inherent susceptibility of land to erosion without considering the influence of different land use practices. It is the worst possible scenario of soil erosion in the region without any protection factor like vegetation cover. In this study, potential erosion risk of Upper Awash Basin is mapped using soil erodibility factor (K), rainfall erosivity index (R) and slope gradient (%) as the system input fuzzy parameters.

The desired output at this stage of the F-WERCAM is the Potential Erosion Risk Index (PERI) and it can be represented as:

$$PERI = f(K, R, \%) \hspace{4cm} (7.2b)$$

For any type of processes, there is an associated "physical range" and "interest range". For instance, the physical range of temperature can be from 0-100°C, but for a certain application under assessment the temperature range from 25-45°C can be considered as the interest range. The concept of physical and interest range is used here to identify the range of acceptable soil loss for a region under consideration. We also want to develop an appropriate index scale and to map the degree of potential and actual erosion risk by using the F-WERCAM framework.

In the context of soil erosion risk mapping, "physical range" of soil loss can be defined as the range that corresponds to the possible amount of soil loss that is likely to occur in any part of the world under various topographical and environmental settings (Figure 7-10). On the other hand, "interest range" can be seen as the amount of soil loss that is region specific and provides the range of soil loss that can be expected under certain geographical and environmental settings. The main difference between physical and interest range with respect to soil loss, in particular, is in the upper limit range of soil loss that is to be expected.
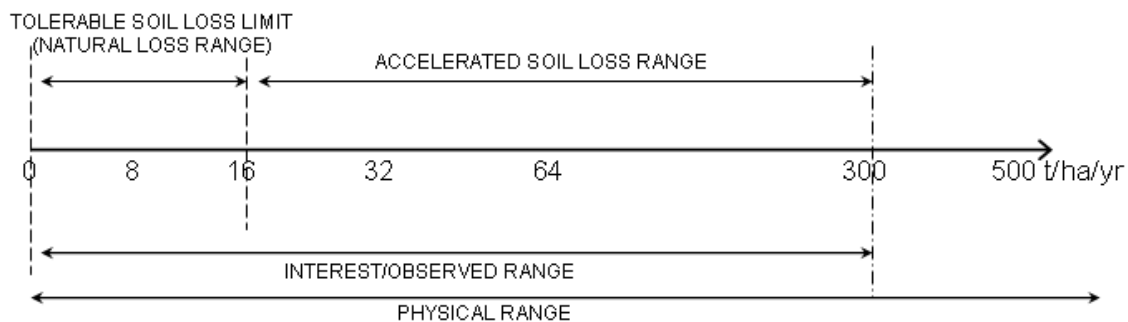
Figure 7-10: Schematic description of soil loss range and concept of "interest range" and "physical range". The observed range corresponds to Ethiopian condition (i.e. 0-300 t/ha/yr), which equates to having a tolerable soil loss limit of 16 t/ha/yr.

For Ethiopian conditions, particularly in the Ethiopian Highlands, the recorded annual soil erosion ranges from 16 t/ha/yr to 300 t/ha/yr depending mainly on the slope, land cover and rainfall intensities (Hawando 1995, 1997; Hurni, 1988). The observed range of soil erosion that is reported to occur in the Upper Awash Basin is divided into 5 classes to consider the concept of permissible or tolerable soil loss limit. The tolerable soil loss limit is defined as the maximum soil loss that allows an acceptable level of crop productivity to be sustained economically and indefinitely. A classification based on soil loss tolerance is adopted in several soil erosion risk assessment studies (Ahamed et al., 2000). According to Hurni (1983a, b), the tolerable soil loss of the region is estimated to be within the range from 1-16 t/ha/yr. The lowest two classes, Very Low (VL) and Low (L), are within the range of soil loss tolerance values (i.e. 1-16 t/ha/yr). The medium class (M) is aimed to cover the range of soil loss that is high but usually has to be accepted. The highest two classes, High (H) and Very High (VH), have soil losses that are destructive to the land with serious onsite and potential offsite effect. The range of soil loss within High (H) and Very High (VH) classes are considered here to be unacceptable

for any land use practices that have the aim of sustainable productivity. Broadly speaking, the lower two classes can be categorized under the *"natural erosion processes"* and the classes above tolerable soil loss can be categorized under the "*accelerated form of erosion with higher risk*". A similar concept on the classification of soil loss range is provided by Bergsma (ITC, The Netherlands) on the aspect of mapping units in a rain erosion hazard catchment survey.

Using the observed range of soil loss of the region, a qualitative scale of 0-100 (unit-less index) is adopted as the system output to map the potential erosion risk of the region. Based on the concept of tolerable soil loss as discussed above, the whole range from 0-100 has been classified into 5 erosion risk classes [VL: 0-2.67; L: 2.67-5.33; M: 5.33-10.67; H: 10.67-20 and VH: >20] and later fuzzified, i.e. the crisp ranges of erosion risk is converted to linguistic variables by assigning an appropriate membership function. These output fuzzy sets have trapezoidal membership functions corresponding to "Very Low", "Medium" and "High" erosion risk classes, shown in Figure 7-11.
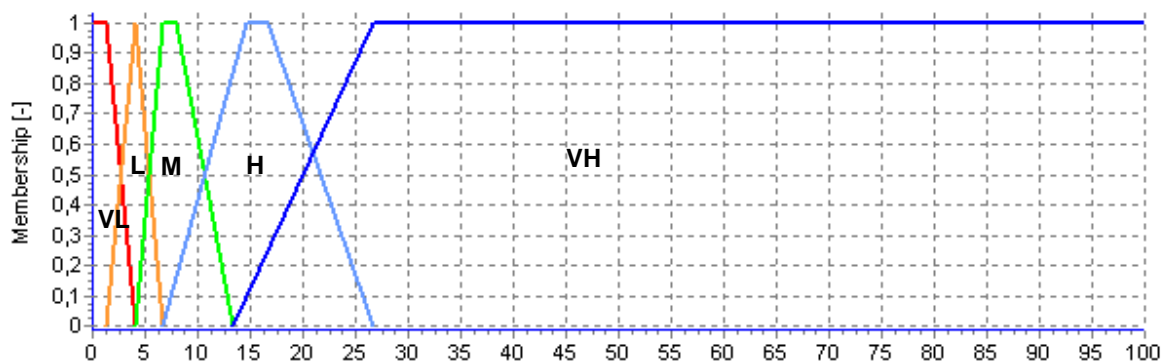
Figure 7-11: Membership functions associated with PERI using the defined qualitative scale

In addition, another output fuzzy set has been set up for PERI using the same defined range with 3 triangular membership functions corresponding to "Very Low", "Medium" and "High" erosion risk classes. For the identification purpose, this output fuzzy set is designated as "PERI_FS1". The output fuzzy set having trapezoidal membership functions (as in Figure 7-11) corresponding to very low, medium and high erosion risk classes is designated as "PERI_FS2". This allows studying the sensitivity of the shape of membership function on the output erosion risk map of the region.

From the initial parameter estimation and analysis in Chapter 7 the corresponding values for slope, rainfall erosivity (R) and soil erodibility (K) are obtained for the Upper Awash Basin. Then, the three input variables are treated as fuzzy variables by assigning corresponding membership functions.

The range of slope (%) of the Upper Awash Basin is initially classified into 5 categories and then fuzzified into 5 linguistic sets. It is to be noted here that the entire physical domain or range of the slope is described by fuzzy sets. Membership functions associated with the slope (%) are referred to as VL, L, M, H and VH (see Figure 7-12).

The second input variable is the soil erodibility factor (K). The sensitivity of different soil types to erosion is largely influenced by soil texture and other properties like particle size distribution, structural stability, organic matter content and nature of clay minerals etc. Wischmeier and Smith (1978) found that the differences in the natural susceptibilities of soils to erosion are difficult to quantify from field observations. Soils with low erodibility values may show signs of high risk when

they occur on steep slopes. On the other hand, soils with high erodibility may show little or no evidence of erosion risk under gentle rainfall when they are situated on a gentle slope.

VL		
Slope [%]	0	4
Membership [-]	1	0

L		
Slope [%]	0	4	12
Membership [-]	0	1	0

M			
Slope [%]	4	12	20	40
Membership [-]	0	1	1	0

H		
Slope [%]	20	40	60
Membership [-]	0	1	0

VH		
Slope [%]	40	60	130
Membership [-]	0	1	1
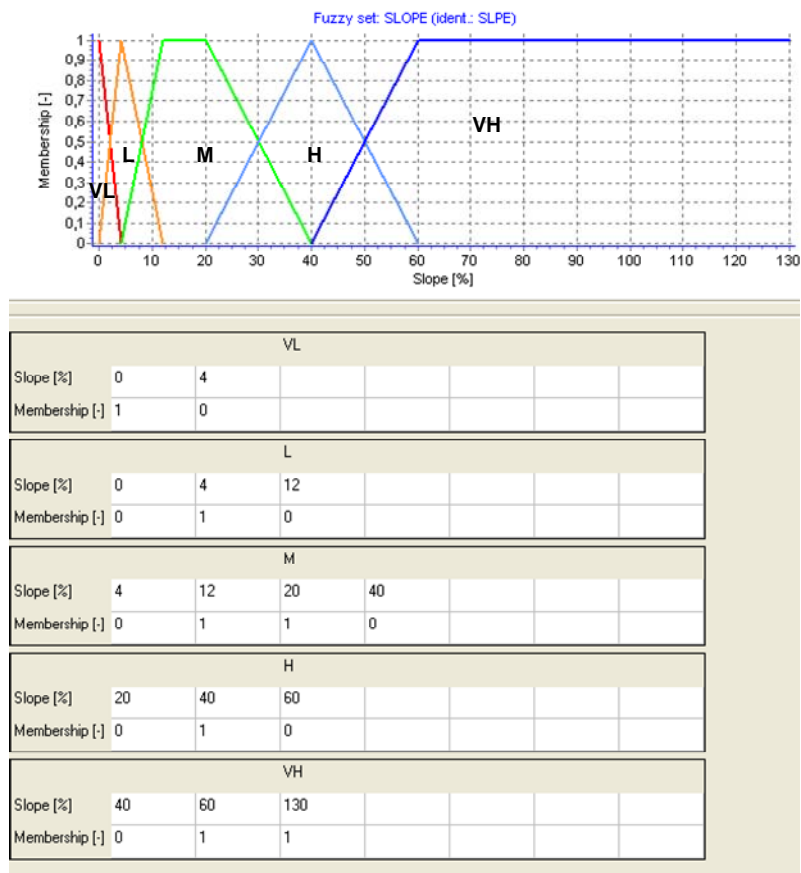
Figure 7-12: Membership functions associated with slope (%) for Upper Awash Basin

Table 7-6: Classification of erodibility factor (K) based on soil type and its composition

Soil Type	K (in US unit)*	K (SI unit)^	Erodibility class	Description
Fine textured soils High in clay content	0.05-0.15	0.006-0.0197	Low	Resistant to detachment
Coarse textured soils e.g. sandy soils	0.05-0.20	0.006-0.0263	Low	Resistant to detachment due to low runoff
Medium textured soils e.g. silt loam soils	0.25-0.45	0.0329-0.0592	Medium	Susceptible to detachment and produce moderate runoff
Soils with high silt content	> 0.45	> 0.0592	High	Highly susceptible to erosion, easily detached, tend to crust, produce large amount of runoff, tend to produce fine sediment that is easily transported

^ Conversion from US to SI units: multiply by factor of 0.1317. SI unit of K: t ha h (ha MJ mm)$^{-1}$; * US unit: 0.01 ton acre h (acre ft-ton in)$^{-1}$

Based on the soil texture (composition of sand, silt and clay fraction, etc.), Foster et al. (2003) provide a general classification and range of the soil erodibility factor, K. This provides the necessary background information on the general classification of the range of erodibility present in the Upper Awash Basin. The range of K within the study area is computed and compared within the context of possible range of K values and classification as shown in Table 7-6. The range of the erodibility (K) factor is 0.161-0.313 in US units (0.01 ton acre h (acre ft-ton in)$^{-1}$) and 0.021-0.041 in SI units (t ha h (ha MJ mm)$^{-1}$) for the study area and falls within the "Low" and "Medium" erodibility class.

VL						
Soil erodibility [SI]						
Membership [-]						

L						
Soil erodibility [SI]	0	0,01	0,03			
Membership [-]	1	1	0			

M						
Soil erodibility [SI]	0,01	0,03	0,04	0,07		
Membership [-]	0	1	1	0		

H						
Soil erodibility [SI]	0,04	0,07	0,09			
Membership [-]	0	1	1			

VH						
Soil erodibility [SI]						
Membership [-]						
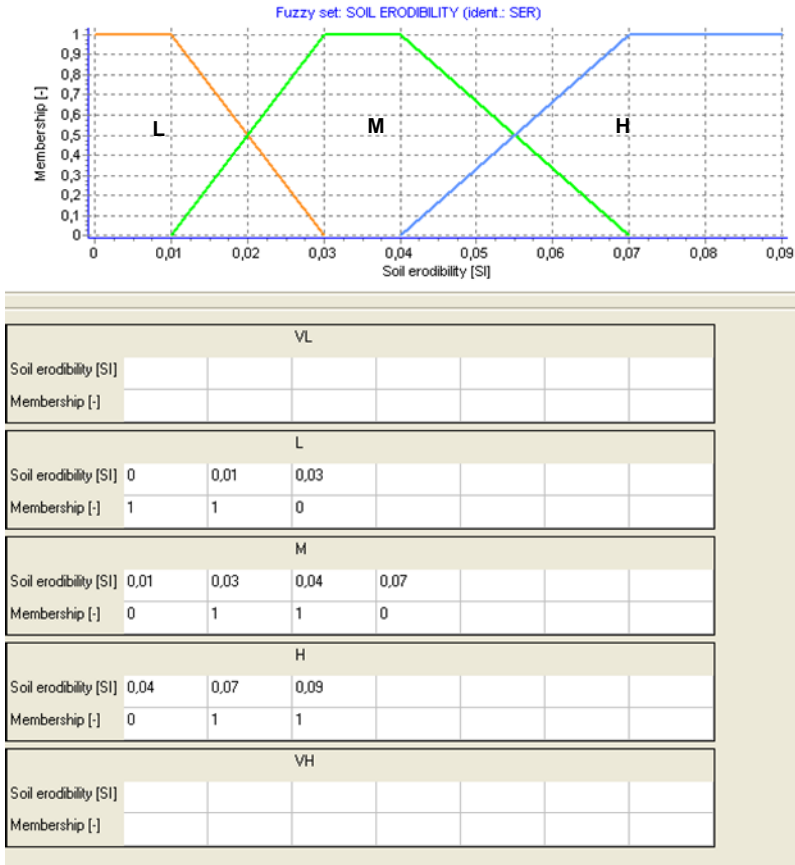
Figure 7-13: Membership functions associated with soil erodibility factor (K) for Upper Awash Basin

The K factor is treated as a fuzzy variable and is fuzzified into 3 fuzzy sets: Low (L), Medium (M) and High (H) and assigned a membership function to each corresponding set. Since a sub-division of the erodibility factor is made by taking into consideration the whole possible range of K (0-0.085), it can be considered to be valid for most cases encountered in practice. The fuzzy sets for the erodibility factor (K) along with its support value are shown in Figure 7-13.

Similarly, for the rainfall erosivity index (R), the range of erosivity is described by fuzzy sets. The whole range of rainfall erosivity is categorized into three linguistic sets, namely, Low (L), Medium (M) and High (H). The support values for each fuzzy set are based on expert knowledge and the general concept is: the higher the erosivity value, the higher the risk of soil erosion of the region and *vice versa*. For this example, which took the rainfall erosivity value computed by Roose's method and ground measured rainfall data, the whole range is fuzzified again into L, M, H(Figure 7-14).

Figure 7-14: Membership functions associated with rainfall erosivity index (R) for Upper Awash Basin

The total number of rules is the product of the fuzzy sets that represent the system. For this stage of modelling, the total number of rules that defined the system is 5*3*3 = 45 rules, i.e. 5 sets associated with slope (SLPE), 3 with rainfall erosivity (RESV) and another 3 with soil erodibility (SER). It is to be noted here that by increasing the number of parameters, the formulation of rules becomes quite complex and less transparent. It is seen that there is always a trade-off between the increasing complexity of fuzzy rules and the resolution of the model output. The fuzzy rules (FR) defined for mapping the potential erosion risk of the region is provided in Table 7-7. The rules and consequences are properly assessed after consideration of the interactions and influences of the three input parameters on the potential erosion risk in the region. The final output PERI map reflects the rule system that is employed.

Table 7-7: Expert Fuzzy Rule base for mapping the PERI

	Rule Antecedents			Rule Consequent
Sl.No.	IF 'SER' = …	'RESV' = …	'SLPE' = …	Then 'PERI' = …
1	L	L	L	L
2	L	L	M	M
3	L	L	VH	H
4	L	L	H	M
5	L	L	VL	VL
6	L	M	L	L
7	L	M	M	M
8	L	M	VH	H
9	L	M	H	H
10	L	M	VL	VL
11	L	H	L	L
12	L	H	M	M
13	L	H	VH	VH
14	L	H	H	VH
15	L	H	VL	L
16	M	L	L	L
17	M	L	M	H
18	M	L	VH	VH
19	M	L	H	H
20	M	L	VL	VL
21	M	M	L	L
22	M	M	M	H
23	M	M	VH	VH
24	M	M	H	VH
25	M	M	VL	L
26	M	H	L	M
27	M	H	M	H
28	M	H	VH	VH
29	M	H	H	VH
30	M	H	VL	L
31	H	L	L	M
32	H	L	M	H
33	H	L	VH	VH
34	H	L	H	VH
35	H	L	VL	L
36	H	M	L	M
37	H	M	M	H
38	H	M	VH	VH
39	H	M	H	VH
40	H	M	VL	M
41	H	H	L	M
42	H	H	M	VH
43	H	H	VH	VH
44	H	H	H	VH
45	H	H	VL	L

7.2.3   Stage 3: Actual Erosion Risk Index (AERI)

For the actual erosion risk index, the defined scale of (0-100) is used with the same crisp class definition of VL to VH. Basically, the actual erosion risk tends to quantify the effect of vegetation cover and land use practices on potential erosion. In F-WERCAM, the vegetation cover and land use practices factor are accounted by an index termed as the Soil Protection Index (SPI). Hence, the final output from this modelling approach is the actual erosion risk map of the region, i.e. AERI. The output from Stage 1 (SPI map) and Stage 2 (PERI map) are used as the input fuzzy parameters for Stage 3. Here, the output fuzzy sets of AERI are taken as to be the same as those of Stage 2, since this stage of F-WERCAM is used to quantify the effects of SPI on PERI.

The implementation of the fuzzy rule base of this stage takes into account the influence of SPI on PERI. When integrating the two parameters, SPI is considered to have higher influence on the AERI of the region. To test the sensitivity of the rules, another fuzzy rule base is set up considering a situation when both parameters have a similar influence. For the identification purpose, RB1 denotes the fuzzy rule base which determines the SPI parameter to be more influential than PERI for assessing the degree of actual erosion risk. For RB2, this denotes a fuzzy rule base where SPI and PERI are given equal importance. The fuzzy rule base that produces the actual erosion risk value and the map of the Upper Awash Basin are shown in Tables 7-8 and 7-9.

Table 7-8: Expert fuzzy rule base 1 (RB1) for mapping AERI (If SPI = '…' And PERI = '…' Then AERI = '…') [SPI considered being more influential than PERI]

RB1	PERI (5 classes)				
SPI (5 classes)	VL	L	M	H	VH
VL	VL	VL	M	H	VH
L	VL	L	L	M	VH
M	VL	VL	L	M	H
H	VL	VL	VL	VL	L
VH	VL	VL	VL	VL	VL

Table 7-9: Expert fuzzy rule base 2 (RB2) for mapping AERI (If SPI = '…' And PERI = '…' Then AERI = '…') [SPI and PERI are equally important]

RB2	PERI (5 classes)				
SPI (5 classes)	VL	L	M	H	VH
VL	VL	L	M	H	VH
L	VL	VL	L	M	H
M	VL	VL	VL	L	H
H	VL	VL	VL	L	L
VH	VL	VL	VL	VL	L

To test the influence of output membership functions with different membership functions and fuzzy rule base, i.e.RB1 and RB2, four different scenarios are set up. Detailed descriptions of the scenarios can be seen in Table 7-10.

Table 7-10: Description of the different scenarios for assessing the influence of output membership functions and different rules on AERI

	Combination of fuzzy sets and fuzzy rules		
Scenarios	**Output fuzzy sets for AERI**	**Fuzzy rules adopted**	**Designations**
Scenario 1	trapezoidal MF's for VL, M and H classes	RB1	AERI1_RB1
Scenario 2	triangular MF's for VL, M and H classes	RB1	AERI2_RB1
Scenario 3	trapezoidal MF's for VL, M and H classes	RB2	AERI1_RB2
Scenario 4	triangular MF's for VL, M and H classes	RB2	AERI2_RB2

Assessment and analysis of different combinations of fuzzy sets and rules on the predicted AERI map by F-WERCAM, discussed in Chapter 8.

7.3   Summary

From the questionnaire and empirical knowledge, fuzzy sets are formulated for all identified input parameters and the defined system output. The detailed assessment of the identified parameters provides the necessary information for the setup of fuzzy rules for each stage of F-WERCAM. The fuzzy rule base forms the overall knowledge. It represents the knowledge and experience of the soil erosion risk process in a region. The output erosion risk map of the region is mapped using the defined qualitative scale and it provides the degree of sensitivity of spatial erosion risk. The analysis and interpretation of the output SPI, PERI and AERI of the Upper Awash Basin is discussed in Chapter 8.

As an attempt to quantify the output erosion risk index, the documented soil loss range of 0-300 t/ha/yr is considered as the lower and upper limits for the setup of the output fuzzy sets. Such a classification scheme of soil erosion risk is tested in this study, since it may provide a possible way to quantify the erosion risk within the documented soil loss range for the region. A detailed assessment on the quantification of soil erosion risk by different methods is discussed in Chapter 9 and 10.

8 Implementation of F-WERCAM in Upper Awash Basin

8.1 Mapping the Soil Protection Index (SPI): Stage 1

Stage 1 of F-WERCAM is tested using the LULC map of 2001 and NDVI map of January 2001. Here, the rule base system for SPI described in Section 7.2.1 is used. The SPI map along with the input parameters (i.e. defuzzified output) is given in Figure 8.1.The output map represents the spatial distribution of SPI; its protection level ranges from VL to VH.
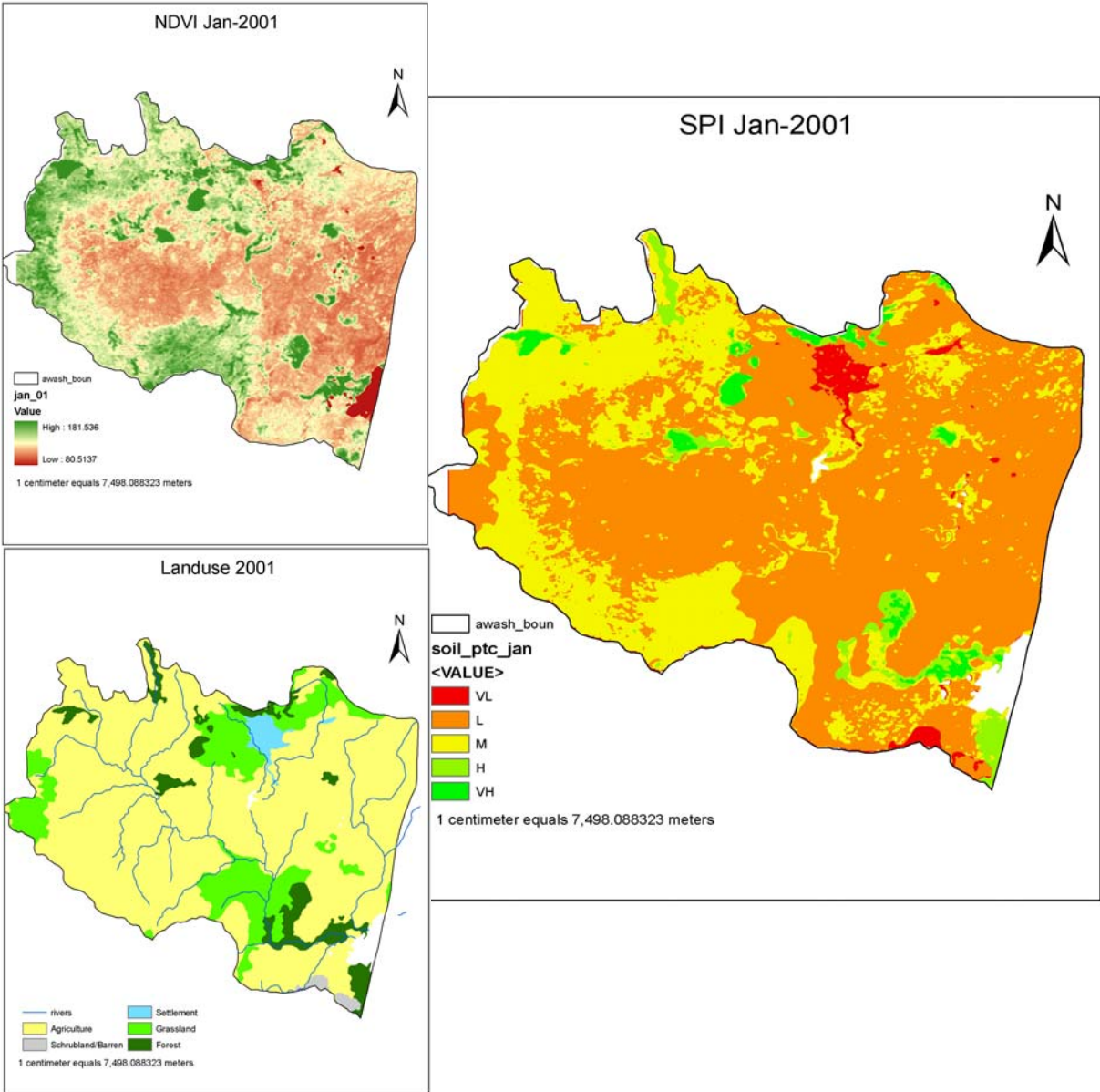
Figure 8-1: Input grid parameters (LULC, NDVI) and output SPI map

Figure 8-1 shows that 63.4 % of the whole study area falls within the low SPI class. Most of the regions which have a low SPI are found to be associated with agricultural land. This is mainly attributed to low vegetation cover in the agricultural fields during the month of January. In the Upper Awash Basin, the distribution pattern and amount of vegetation cover as reflected by NDVI is found to be very low during the dry season. The forest area within the study area is categorized in term of soil protection under "High to Very High" except for the area adjoining of grassland which falls within the "medium" class. This may be due to fragmented forest area with a lower density of vegetation cover. This kind of qualitative information can help to categorize the influence of vegetation cover and land use practice on the soil erosion risk distribution.

8.1.1 Spatial and Temporal Assessment of SPI

Using the LULC map and average monthly NDVI map, the monitoring of the spatial and temporal pattern of SPI is carried out. This analysis allows us to understand the dynamics of landscape and the variability of vegetation cover distribution over a short temporal interval. In this study, a monthly time period corresponding to three climatic seasons of the Awash Basin is considered. The SPI is derived for January, April and July. These months represent the Bega season (dry period), Belg season (little rain) and Kiremt season (main rain), respectively. Spatial distributed SPI maps of the three time periods and their associated temporal change maps and spatial statistics are determined using the "spatial analyst" in ArcGIS.

The qualitative SPI maps of the three time periods show that during the dry season (Bega), most of the regions are dominated by low SPI (Figure 8-2). The trend in increased vegetation growth from January to April (Figure 8-3) is reflected in the SPI map of April, with an increase in medium SPI class distribution. The changes in the spatial pattern between each season differ most for the agricultural land followed by grassland and settlement areas. It is interesting to note that during the main rainy season period most of the region is dominated by medium and high SPI (Figure 8-3). This can be attributed to increased vegetation growth over the region after the short rain period from February to May. It shows also that the rainfall has a two-fold effect on erosion: first, it can increase the erosion intensity of a region and, second, it can subsequently decrease the erosion intensity by increasing the vegetation biomass to its natural state (Xu, 2005). The influence of the rainfall pattern on vegetation growth (rainfall-NDVI monthly temporal distribution) can also be considered to understand the effect of rainfall on vegetation distribution (Figure 8-4). The temporal change pattern of SPI can be explained by the response of vegetation growth to the rainfall pattern of the region.

From the rainfall-NDVI monthly temporal distribution, it is observed that with an increase of rainfall in April the trend of NDVI increases positively. There is also a time lag between peak rainfall (in July) and peak vegetation cover (NDVI in September) over the year. When the distribution pattern of monthly SPI (% areal coverage) of each class is compared to average rainfall, it is found that the rainfall patterns has a significant influence to the change of SPI class temporally (Figure 8-5). When there is a decrease in percentage areal coverage of the "Low" SPI class from February to March, it is seen that there is a corresponding increase in "Medium" SPI class. This dynamic variability within a short interval can be attributed to a growth in vegetation cover which is indirectly reflected by increase in average rainfall from February to March.
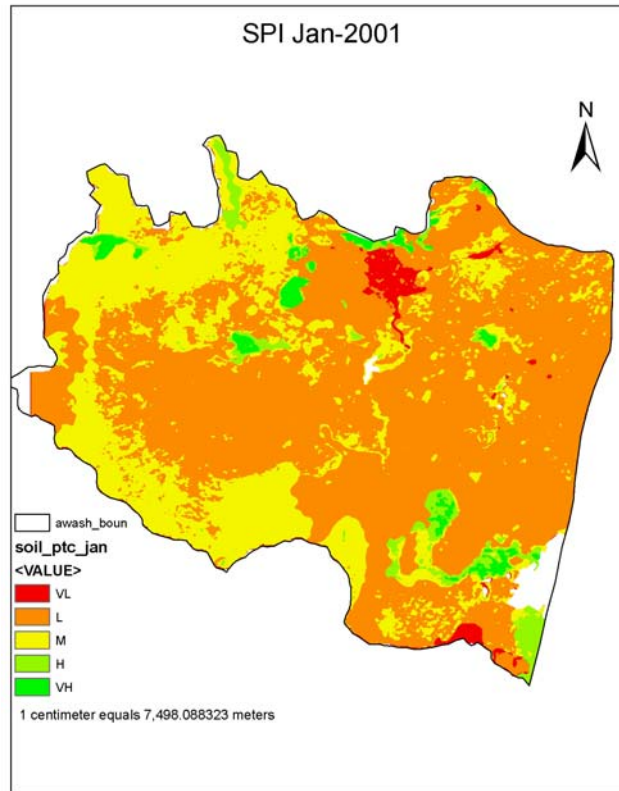
Figure 8-2: **SPI map for month of January 2001 (dry season)**
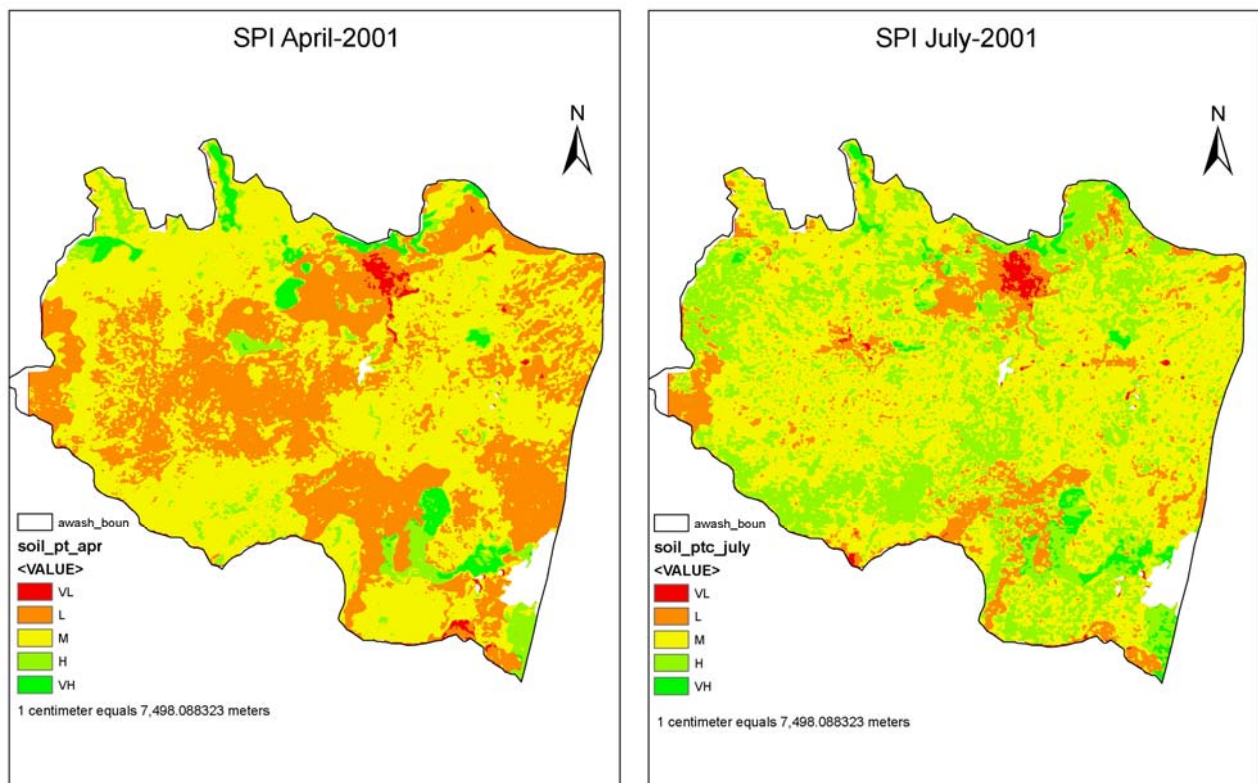
Figure 8-3: SPI map for month of April (moderate rainy season) and July (main rainy season) 2001
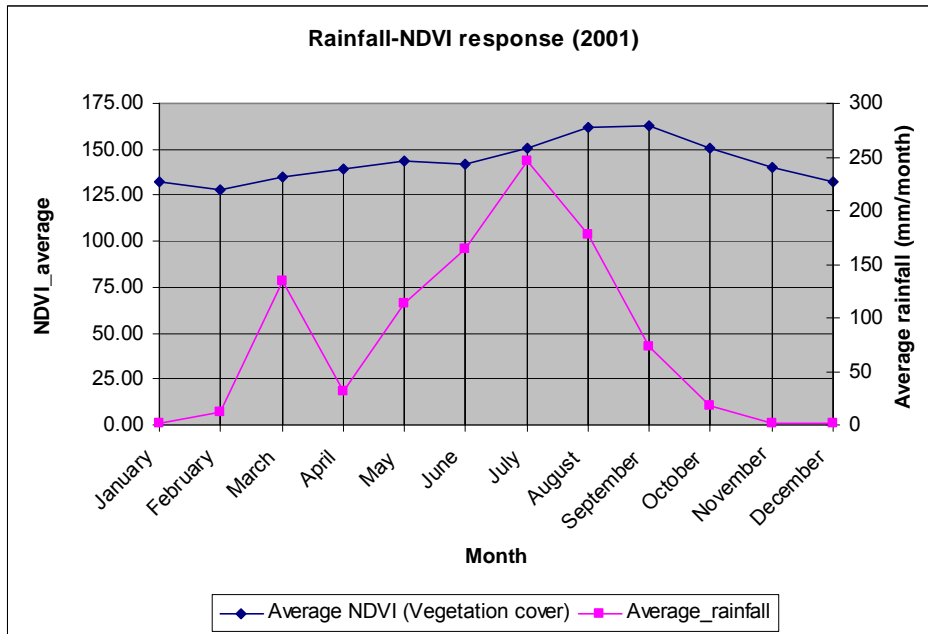
Figure 8-4: Response of vegetation growth pattern on monthly precipitation
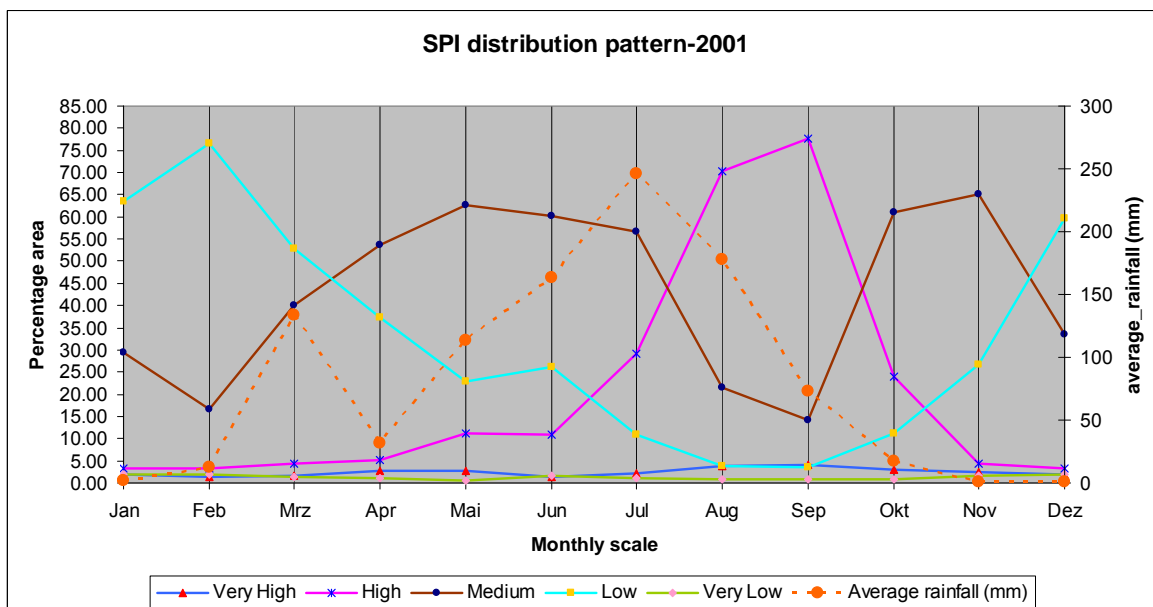
Figure 8-5: SPI class distribution (percentage areal coverage) temporally over the year

An example for the spatial distribution of SPI within each LULC class is provided for the month of July 2001 in Table 8-1. Different soil protection levels within agriculture zones are mapped where 0.44 % and 4.14 % of the agriculture area correspond to "Very Low" and "Low" SPI. This provides a clear discrimination of higher potential risk zones within a particular LULC class. From a general perspective, LULC corresponding to forest zone is considered to have a lower potential of soil erosion risk. The spatial distribution of SPI provides a discrimination of different soil protection levels within a forest cover area. It is clearly seen from this example that even within the forest area, there are regions which correspond to 'low' SPI. This region corresponds to the deforested or degraded forest

lands which are heavily affected by anthropogenic activities. Specifically, such regions are not under the protected forest zones like the Managesha National Forest and Chilimo Forest which are located within the Upper Awash. This indicates a higher potential erosion risk.

Table 8-1: Area of SPI distribution (hectare) for the month of July 2001 within each land use class

SPI	Agriculture	Shrubland/Wasteland	Settlement	Grassland	Forest
Very High	0	0	0	0	20899
High	229812	0	0	36865	30608
Medium	532334	1083	964	40087	5355
Low	33030	4826	7608	65424	*1746*
Very Low	3535	337	5781	838	0

Hence, the analysis done here allows us to identify and focus on specific regions within each LULC class which are susceptible to soil erosion. This subtle spatial variability of SPI that is mapped within each land use class can be effectively used as a secondary input parameter for further assessment of the region in the context of erosion risk and land degradation.

8.1.2   Evaluation of Output SPI Map

a) Evaluation using random field observation and survey data

The current status of potential land degradation of the observed field locations in the study area is evaluated according to 3 qualitative classes: Low, Medium and High. Field photographs which comprises of ground pictures, satellite images and local knowledge are used for qualitative assessment of the mapped SPI of the region.

Table 8-2: Assessment of the SPI map with field based observations on potential land degradation

Observation (X, Y)			F-WERCAM mapped SPI class for 3 different time periods (2001)			Field based potential risk (2009)
Location ID	X	Y	JAN_ BEGA	APR_ BELG	JULY_KIREMT	*Bega season* (Dry period)
1	441000.12	977422.35	3	3	2	Low
2	441652.38	976422.35	4	4	3	Low
3	464916.44	955767.55	4	3	2	High
4	478179.12	930111.86	4	4	4	High
5	477092.02	929894.44	4	4	3	High
6	485354.02	937727.60	3	3	2	Medium
7	449834.41	989133.10	1	1	2	Low
8	471568.77	995506.51	5	5	5	High
9	475212.51	942975.50	4	4	2	High
10	474156.09	989235.86	5	5	4	High

Note: SPI class range according to definitions (1: Very High, 2: High, 3: Medium, 4: Low, 5: Very Low)

The evaluation of the fuzzy model output at these random field locations forms the initial step of evaluating a model at a large regional scale. Details about each field location and attributes is given in *Appendix 2*. It is found that locations which are mapped with "Low" and "Very Low" SPI classes at different time periods of the year have a high potential for land degradation, as can be gathered from the field assessment (Table 8-2). On the other hand, regions of low potential land degradation are mapped under "High" and "Medium" SPI classes by the fuzzy model. It should be added, however, that the quantification of the relationship between SPI and the observed land degradation status is tested and found to be inappropriate. This is because the number of ground observation locations is too limited to establish any statistical relationship. Nevertheless, this qualitative comparison gives an indication that the SPI distribution classes of the Upper Awash Basin reflect the current land degradation potential risk of the region.

b) Evaluating SPI using the socio-economic and environmental data

The increase in human population, excessive livestock, deforestation and limited areas of fertile soils for crops are considered to be the major causes for soil erosion and land degradation in Ethiopia (Taddese, 2001; Hurni, 1988). Therefore, we can take human population density and livestock density data of the region as an independent socio-economic factor that has an indirect influence on soil erosion and land degradation in the region.

Human population density (census: 2000) and livestock density data of the study area at the wereda (district) level are obtained from ILRI (International Livestock Research Institute), Addis Ababa, Ethiopia. To examine whether the population and livestock density distribution of the Upper Awash has an influence on the spatial pattern of the predicted SPI, a regression analysis is performed. Population and livestock density are considered to be the explanatory variables and the predicted SPI to be the dependent variable. From the spatial regression analysis, it is found that population and livestock density explained 68% of the spatial distribution pattern of predicted SPI, here an adjusted R-squared value of 0.681 is obtained. It is further observed that both population density and livestock density has a negative spatial correlation with SPI ($r_{population}$= -0.095; $r_{livestock}$ = -0.037). This reflects the trend that regions with a higher population or livestock density has a lower Soil Protection Index (SPI) and *vice versa*. Relatively very low spatial correlation may be due to the averaging of the SPI value corresponding to each district level. This significance of the correlation may reflect the degree of correspondence over the entire map or it may be due to a large deviation in a small region of the map. The low spatial correlation may be improved if finer or more detailed data on population and livestock density is used, i.e. at a sub-administrative level. Even though the spatial significance is found to be low, these findings agree well with the common perception that increasing livestock density in a region tends to increase the overgrazing problem and reduce the soil protection level, thereby contributing to the overall land degradation. Furthermore, increasing human population levels tend to raise the pressure on the limited land resources of the region, thereby magnifying the potential regional risk of erosion and degradation.

Further assessment is made by comparing the SPI with the population density and livestock distribution for each district in the region (Figures 8-6 and 8-7). The magnitude of population density for each district corresponded relatively well with the SPI class categories. The district associated with high population density (> 20,000 people/km^2) is found to have either a low or very low SPI. It is quite

interesting to note that regions with low livestock density and consequently lower SPI are found to be those districts which have a relatively high human population density.

On the other hand, one can see that with a decrease in livestock density range, the soil protection level class tends to shift toward a higher protection class except in some districts or administrative units (Wereda 08, 21, 23, 3, 5, 7). The influence of livestock density on SPI cannot be clearly linked and found to be insignificant especially in districts which have a very high population density. From the analysis, a trend can be observed that areas with high population density correspond to lower livestock density and *vice versa*. For instance, Wereda 5 with a low livestock density is found to be classified within the 'very low' SPI. This can be explained by the influence of higher population density. Hence, it can be deduce that for a particular region or district, both the livestock and population density has an influence on the SPI distribution.
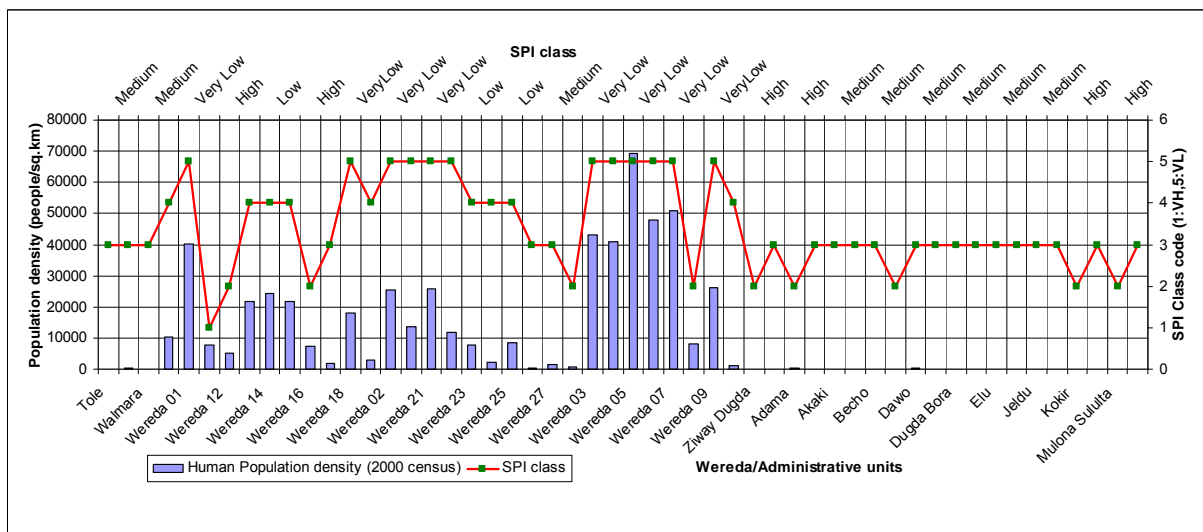
Figure 8-6: Human population density and SPI class distribution in each Wereda
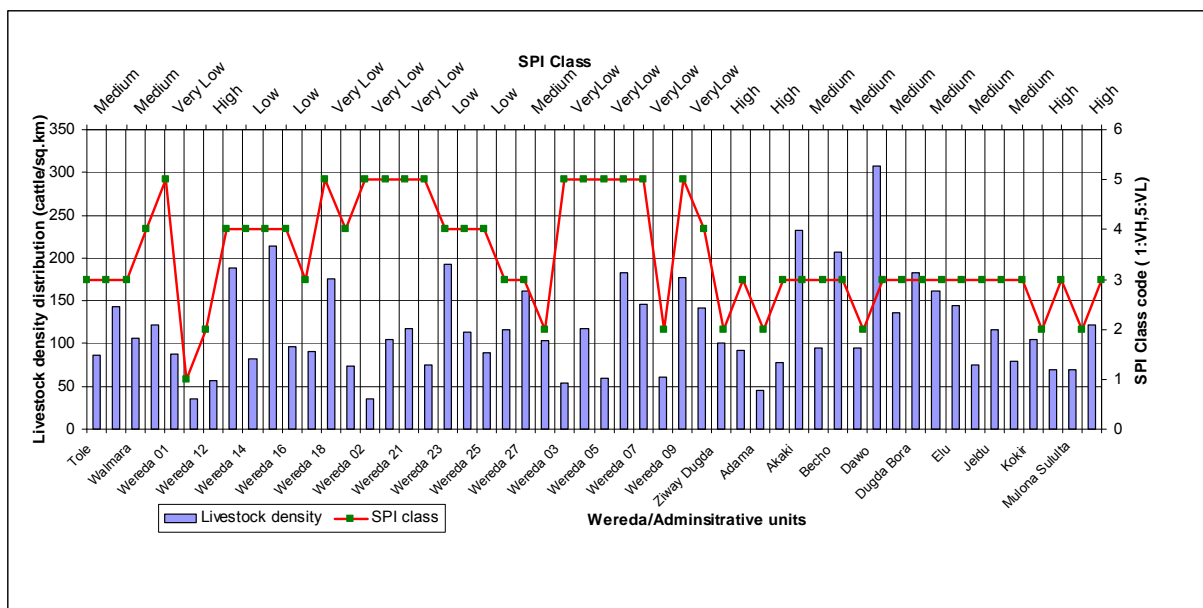
Figure 8-7: Livestock density and SPI class distribution in each of the Wereda

However, it is clear from the analysis that the distribution of the SPI in the Upper Awash basin cannot be explained simply by livestock or the population density. This becomes obvious when the SPI is correlated spatially with each of the independent parameters to yield a very low spatial correlation.

The elevation of the Upper Awash Basin and the soil erodibility factor (Williams et al., 1984) are used to correlate with the SPI of the region. The soil erodibility factor (K) is a function of several soil properties such as texture, organic matter content, permeability and bulk density. Yang et al. (2005) considered soil erodibility as the most significant soil property that describes the link between soil sensitivity and erosion. Here, the focus is to see whether the SPI pattern reflects the soil sensitivity and, therefore, soil erosion of the region.

$R^{2jan} = 0.4082$ $R^{2july} = 0.502$

SPI (average)

Soil erodibility (average)

- ◆ SPI_july and avg. soil erodibility
- ■ SPI_jan and avg. soil erodibility
- —— Linear (SPI_july and avg. soil erodibility)
- —— Linear (SPI_jan and avg. soil erodibility)
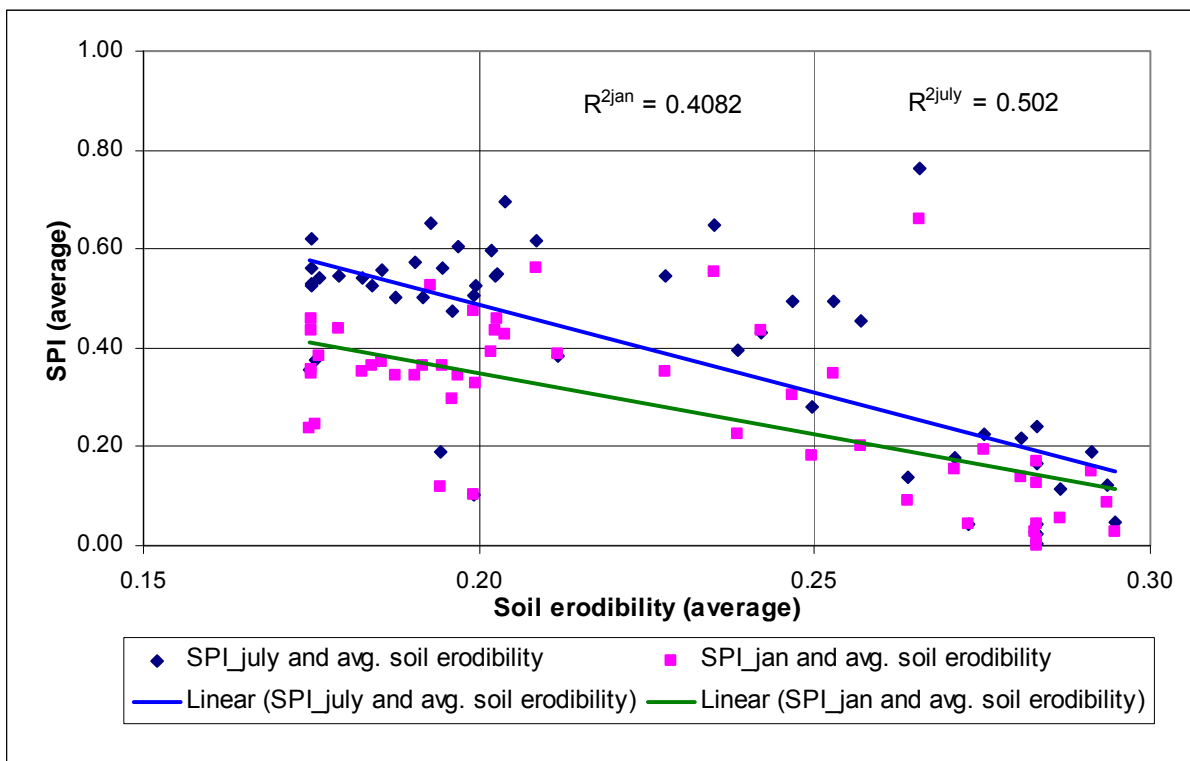
Figure 8-8: Relationship between SPI distribution and soil erodibility of the Upper Awash Basin

It is found that the SPI distribution over the region correlated positively with the soil erodibility of the region (Figure 8-8). From this established relationship, we can conclude that the SPI captured quite well the most potential areas associated with varying degrees of erosion risk. On the other hand, the elevation of the Upper Awash Basin is found to have a low negative correlation with SPI. This maybe due to the complex interplay between elevation, slope and vegetation cover distribution of the region. For instance, at higher elevation the slope gradient tends to increase. This leads to a reduction in the soil protection level (or conversely, a greater potential erosion risk); at the same time, an increase in the vegetation biomass and cover at higher altitudes increase the soil protection level (or reduces the potential erosion risk).

8.1.3 Influence of the Modified Rule Base on SPI distribution

The fuzzy rules used to map the SPI distribution over the Upper Awash Basin are modified to reflect the effect of surface sealing and imperviousness layers in urban and settlement zones. In these zones, it is assumed that soil protection remains moderately high, irrespective of the amount and intensity of the vegetation cover. This additional knowledge is supported by the fact that upper layers of the soil, specifically in a highly urbanized area are normally protected by surface sealing and impervious layers. An exception to this assumption applies to fragmented regions within the urban areas where the soil surface is exposed. Such regions have a higher risk of soil erosion or lower SPI due to higher runoff potential. In context of this modelling framework at a regional scale, such regions are considered to be small and insignificant. For instance, the influence of features associated with regions which are smaller than the mapping units are considered to be negligible.

Using the same input parameters with the modified fuzzy rules for settlement zone (see Table 8-3) the SPI of the region is mapped again. The effect of the modified rules is reflected by the percentage of VL and VH distribution in the SPI class. A shift in the SPI classes from "Low" to "High" is found in the urbanized zones of the Upper Awash Basin, especially in and around Addis Ababa. It is found that the addition of new knowledge to the fuzzy rule base does not affect the whole modelling output; this tends only to update the SPI distribution pattern of the corresponding regions where the new knowledge base is applicable.

Table 8-3: Modified Rule base for mapping the SPI (IF NDVI = '…' AND LULC = '…' THEN SPI = '…')

SPI (Soil Protection Index) [20 rules]	NDVI (Vegetation cover) [4 classes]			
LULC classes [5 classes]	*VL*	*L*	*M*	*H*
VH (Forest)	L	M	H	VH
H (Grassland)	VL	L	L	H
M (**Settlement**)	*M*	*M*	*H*	*VH*
L (Shrubland/Barren)	VL	VL	L	M
VL (Agriculture)	VL	L	M	H

A dynamic spatial variability of the SPI is found within the range of "Low" to "High" SPI. The variability is more dominant within agriculture and the grassland classes of the Upper Awash Basin. "Very High" SPI corresponds to areas which have permanent vegetation cover, located in areas within dense forest regions. Settlement zones or urbanized areas are found to be associated with a higher SPI class. "Very Low" SPI is associated with shrubland and barrenland regions.

Regarding the temporal context using the modified rule base, the "Very High" SPI class has a significant distribution of about 5% for the period from August to October (Figure 8-9). The amount of rainfall is quite high in the preceding months: May (113.6 mm), June (163.5 mm), July (246.4 mm) and August (177.9 mm). High rainfall events tend to increase the vegetation cover and, consequently, the soil layer protection level. During August to September, most of the region that fall under "Medium" SPI class is shifted to the "High" SPI class. In the other direction, for October to December, regions with a "High" SPI class are shifted to the "Medium" and "Low" SPI class.

The influence of SPI on the soil erodibility factor of the Upper Awash is examined here. The spatial distribution of the SPI using the modified fuzzy rules is found to have higher correlation with the soil erodibility of the region. For instance, a negative correlation of -0.79 and $R^2 = 0.64$ is found between the average SPI (rainy season) and the soil erodibility factor of the region. Similarly, a negative correlation of -0.85 and $R^2 = 0.71$ was found between SPI (dry season) and the soil erodibility factor of the region. It is seen from this assessment that regions with a low SPI have a higher soil erodibility factor and *vice versa*. This relationship can be due to the fact that SPI is an index that relates to density of vegetation growth while increasing of growth of vegetation depends on the nature of the underlying soil type, its organic carbon content in addition to the amount and distribution of rainfall of the region.
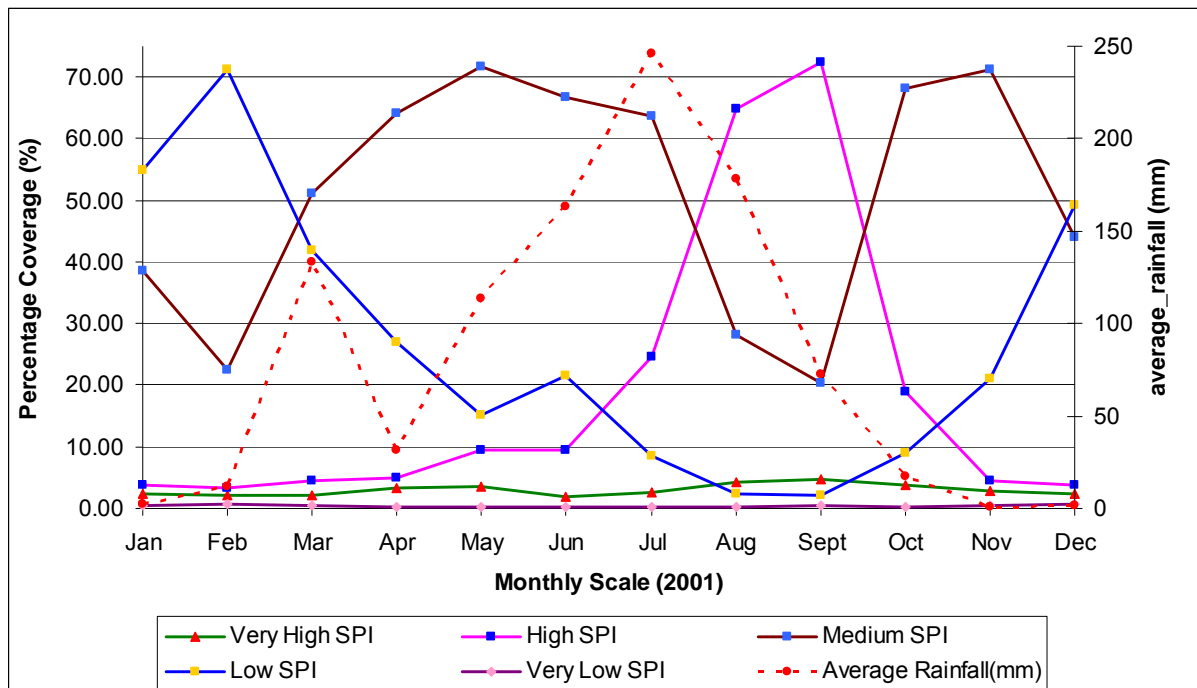
Figure 8-9: **SPI class temporal distribution over the year (using modified fuzzy rules)**

The initial fuzzy rules consider the degree of the soil protection level in settlement zones regardless of the impervious covers. In contrast, the modified fuzzy rule base takes into account the effect of soil layer protection layer by impervious surfaces and sealing. The choice of an appropriate fuzzy rule base depends on the background of the test site. For instance, if the settlement zone present within the test site is considered to be in a rural setting (i.e. no surface sealing or impervious surfaces), then the application of the initial fuzzy rules may provide a reasonable system output, Whereas if the test site is considered to be in a highly urbanized zone, then the modified rules may provide a reasonable system output. From the regional scale perspective, this effect is found to be insignificant, however, since it is difficult to identify and classify a settlement zone as being either urban or rural. This assessment shows that for fuzzy based modelling, with additional expert knowledge about the processes or the region, fuzzy rules can be updated and tested easily to reflect the actual ground situation.

8.1.4   Discussion

The importance of vegetation cover and land use practices as a resisting factor to soil erosion risk is shown using the SPI. It can be seen from the analysis that the use of SPI can lead to a better capture of the changes to the spatial variability of vegetation cover and discriminate subtle changes within a

LULC class. Model evaluation is carried out using socio-economic data such as human population and livestock density, or other environmental parameters, and field data. It is interesting to observe that SPI is able to capture quite well the variability and the associated degree of soil sensitivity to erosion, in terms of the soil erodibility factor (K) of the region. The influence of the modified rule base on the output SPI is also presented and discussed. At a later stage in the modelling process, the SPI map will serve as an input for assessing the actual soil erosion risk by being integrated with other factors like rainfall erosivity, soil erodibility and slope. These are additional criteria which can influence the potential erosion risk of the region.

Land use management practices and conservation measures are motivated by the effective utilization of resources on limited identified hotspot regions. The SPI derived from this model can be utilized by decision makers to locate and point out the zones of extreme need for a special treatment. Such series of maps will help policy makers to initiate steps toward the prioritization of the landscape for proper land management practices, land use and soil conservation measures. For example, maps which have 29 administrative zones within the study area are used here for illustration. It is found from the model results, that three units, namely Wenchi, Sodo and Addis Abeba need immediate attention for a proper land management in order to prevent the loss of valuable soil. On the other hand, Dodata (West) and Sululta region are found to have relatively high SPIs, which indicates highly vegetated cover and forest zone with low potential land erosion.This simple example shows how the SPI map can effectively be used as a tool for prioritization and decision making purposes.

8.2 Mapping the Potential Erosion Risk Index (PERI): Stage 2

As discussed in Chapter 7, the PERI of the Upper Awash Basin is mapped using slope, soil erodibility and rainfall erosivity parameters. The output PERI map indicates the degree of potential risk of erosion by classifying the region into 5 risk classes ranging from VL to VH.

The potential erosion risk map of the Upper Awash Basin is obtained by applying the sets of fuzzy rules (Table 7-7) to all input variables (Figure 8-10). Using the standard fuzzy system parameters now, Stage 2 of the model can be executed. Considering a region within the Upper Awash having a soil erodibility value = 0.02, slope = 12.36 % and rainfall erosivity index = 9232.32, two fuzzy rules are fired having degrees of membership (DOFs) of 0.39 and 0.61, respectively. We arrive at:

(i) If Soil erodibility (SER) = Low, Rainfall erosivity (RESV) = Medium and Slope (SLPE) = Medium Then PERI = Medium,

ii) If Soil erodibility (SER) = Low, Rainfall erosivity (RESV) = High and Slope (SLPE) = Medium Then PERI = Medium.

The corresponding computed defuzzified potential erosion risk index (PERI) equals 8.17, which falls within the "Medium" erosion risk class.

In the absence of vegetation cover, the potential erosion risk map of the region indicates a varying degree of erosion risk: higher erosion risk is located in regions of steeper slopes and corresponds to soil units having sandy clay loam, clay, sandy loam and clay loam. On the other hand, low erosion potential risk is concentrated in plain areas in the central part of the Upper Awash and most of the

region is dominated by leptosols type of soil. Some dispersed spots on the central eastern part of the Upper Awash Basin are attributed with "High" to "Very High" erosion risk. These areas correspond to mountainous regions that have steep slopes and therefore a higher potential for erosion risk. The low lying area of the Upper Awash located in the south eastern part is found to be associated with a "Very Low" potential risk.
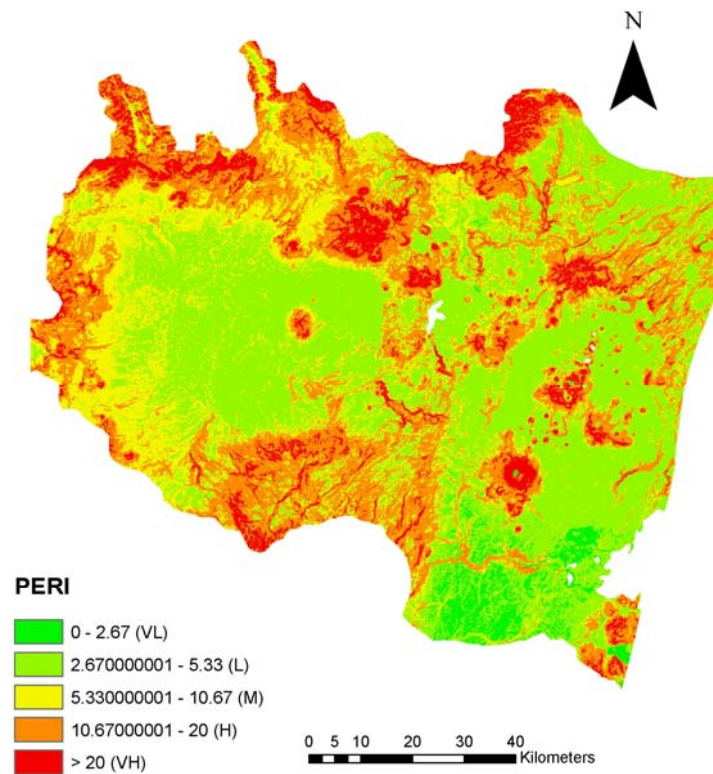
Figure 8-10: PERI map of the Upper Awash Basin using F-WERCAM

8.2.1   Effect of the Output Fuzzy Membership Functions on PERI Distribution Pattern

The sensitivity of the output fuzzy sets corresponding to PERI is tested by applying two scenarios with different output membership functions with the standard pre-defined fuzzy parameters. The output fuzzy sets corresponding to PERI_FS1 have a triangular membership function assigned to VL, M and H linguistic sets; PERI_FS2 with trapezoidal membership functions are assigned to VL, M and H linguistic sets.

The two outputs of the PERI map of the region are compared to assess the influence of shape of the membership functions. A difference map (Figure 8-11) of the PERI showed that 51 % of the region has no influence on the degree of erosion risk class due to shape of the output fuzzy sets. A distinct shift in the spatial distribution of the potential risk class from "Low" to "Very Low" is found in the eastern part of the Upper Awash Basin, which covered 21 % of the total study area. This can be directly attributed to the change in the membership function of VL and M linguistic sets from trapezoidal to triangular functions. This change in the membership functions has an influence on the

overlapping areas between the two adjacent fuzzy sets. Indeed, their influence is observed in the defuzzfied output maps. Also noteworthy is that the fuzzy rule base remains the same for both scenarios. It can be concluded that the influence of the membership functions is more prominent in the lower erosion risk categories than in the higher erosion risk regions. One of the probable reasons behind this behavior may be due to the setup of the fuzzy sets, i.e. the domain of the PERI is fuzzified in a way to have more subsets in lower ranges of risk classes.
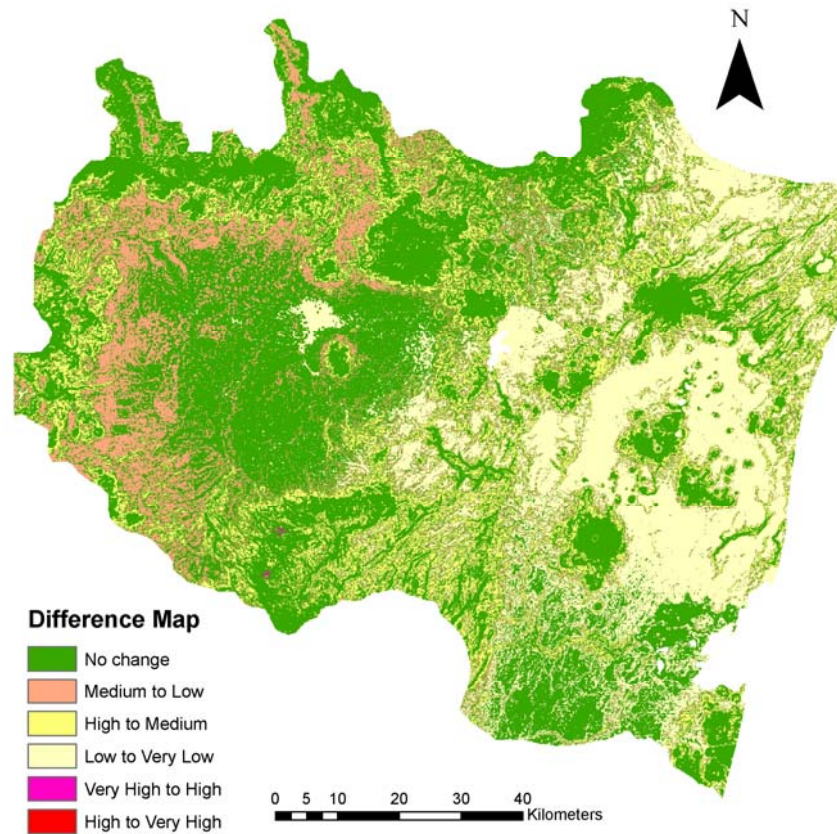
Figure 8-11: Difference map of PERI mapped using PERI_FS1 and PERI_FS2 output fuzzy sets

Irrespective of the spatial distribution pattern, the classified percentage area corresponding to each risk class is compared (Figure 8-12). It is found that for all the erosion risk classes except VL and H, the percentage distribution remained almost the same. A change in the risk class category from one class to its immediate next lower or higher class is observed. Overall, this analysis provides a basic overview on the perception of the results which are obtained using two different output fuzzy sets. This F-WERCAM-based PERI map highlights the general soil erosion susceptibility trends of the region. Further comparative assessment of the output PERI map with a RUSLE based erosion model is discussed later on in this chapter.

This PERI output map will serve as one of the input fuzzy parameters to assess the actual erosion risk of the region. The influence of SPI from Stage 1 of F-WERCAM on the PERI will provide the actual erosion risk of the region.
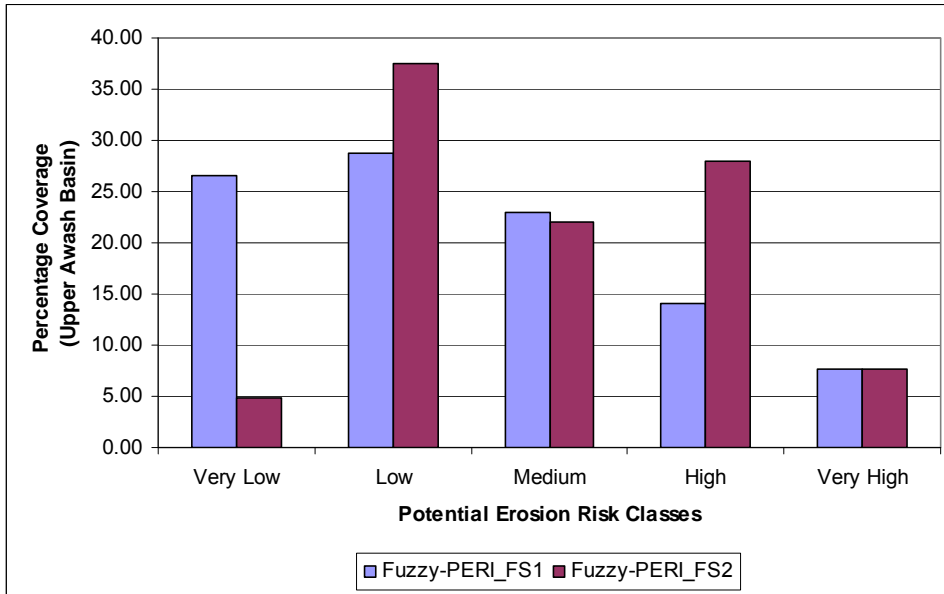
Figure 8-12: Comparison between the two output PERI erosion risk class distributions

8.3   Mapping the Actual Erosion Risk Index (AERI): Stage 3

The final stage of the F-WERCAM provides the actual erosion risk distribution pattern of the region. The output AERI map of the Upper Awash Basin used fuzzy rules dataset RB1 which is given in Table 7-8. This relates SPI and PERI to the actual erosion risk.
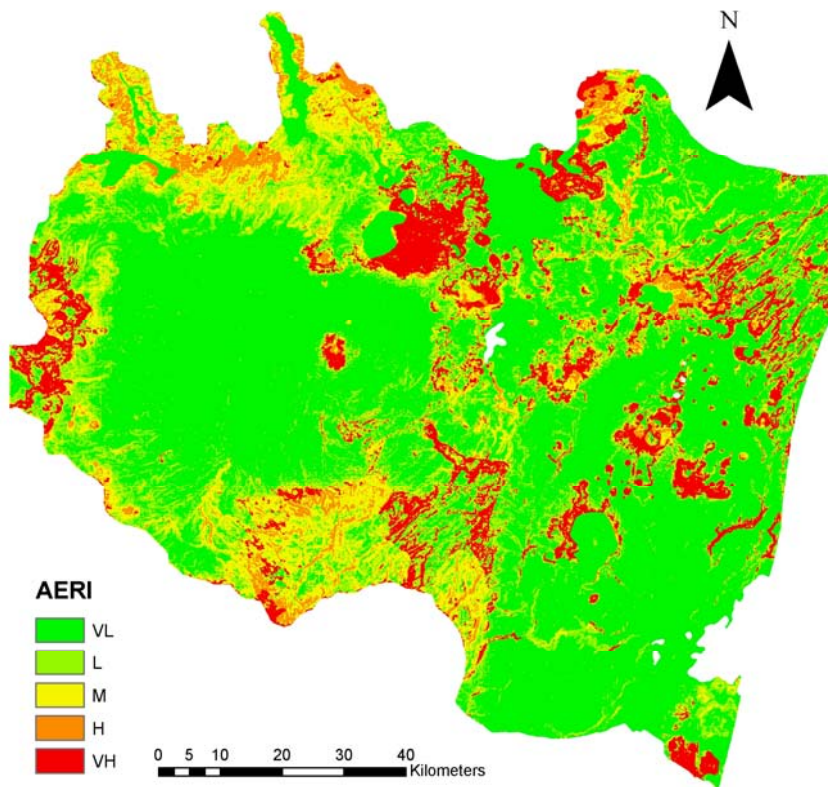
Figure 8-13: AERI map of the Upper Awash Basin showing different degrees of erosion risk

From the AERI spatial distribution map (Figure 8-13), it can be seen that about 50 % and 16 % of the total study area is found to be within the VL and L soil erosion risk, respectively. These regions correspond to the "tolerable soil loss" limit of Upper Awash Basin which is below 16 t/ha/yr. The areas of high slope gradient and less vegetation cover correspond to "High" and "Very High" erosion risk zones. These comprise about 14 % of the Upper Awash Basin. The areas with "Medium" risk of erosion (i.e. 14 % of the region) are found in north-western and the southern part of the study area. Overall, the actual erosion risk map of the Upper Awash Basin indicates higher erosion risk in regions of higher PERI and lower SPI and these areas need immediate prioritization measures. Such qualitative maps provide a way to compare the degree of erosion risk associated to different regions within the study area.

8.3.1 Influence of Membership Functions and Fuzzy Rule Base on Predicted AERI Map

An assessment on the influence of the output membership functions is carried out with different fuzzy rule bases for mapping the actual erosion risk of the Upper Awash. Four different scenarios with two different combinations of rule bases and fuzzy membership functions are setup for the model and executed.

Table 8-4: Comparison of erosion risk distribution obtained by different scenarios

	Percentage erosion risk class distribution (%)			
	Scenario 1	**Scenario 2**	**Scenario 3**	**Scenario 4**
Erosion risk class	AERI1_RB1	AERI2_RB1	AERI1_RB2	AERI2_RB2
Very Low	39.743	55.137	59.336	67.608
Low	21.552	16.450	15.438	17.229
Medium	23.865	14.259	18.499	9.006
High	5.083	4.065	6.589	6.018
Very High	9.757	10.089	*0.138*	*0.134*

Note: Refer Table 7-10 for the description of each scenarios provided here

An assessment is made by comparing results of the erosion risk distribution pattern corresponding to the different scenarios as shown in Table 8-4. It is observed that the influence of different membership functions on the output erosion risk distribution is quite low and insensitive. Comparing Scenario 1 and 2 or Scenario 3 and 4, which have the same fuzzy rule base (RB1 or RB2) but different fuzzy sets, the distribution of output erosion risk classes after considering the spatial dependency, is found to have a similar trend. Nevertheless, it should be kept in mind that changing the shape of the membership functions has some influence on the overlapping region of the adjacent fuzzy sets. This is reflected in the output erosion risk class distribution. The effect of the fuzzy rules on the output risk distribution is found to be quite significant and high. For example, by comparing Scenario 1 and 3, which have the same fuzzy set but different rule bases, it is found that there is a large percentage difference of predicted risk area corresponding to "Very High" and "Very Low" in addition to the difference in their spatial distribution pattern. Similarly, when comparing Scenario 2 and 4, it is found that there is a large difference in predicted erosion risk for the "Very High" class, even though there is an overall spatial

agreement of 65 % between the two output erosion maps. Both the fuzzy rule bases RB1 and RB2 are found to be quite sensitive when classifying the extreme erosion risk classes. From this analysis it is evident that the combination of the different rule bases with different fuzzy sets produces a number of dissimilar erosion risk distribution maps of the region. Hence, in a fuzzy based modelling approach, it is imperative to choose the right fuzzy rule base that reflects the process under investigation as the modelling output is very sensitive to the fuzzy rule system. In order to determine which output AERI map can be considered as representative of the actual erosion risk map of the Upper Awash Basin, there is a need for further assessment of the results. One of the approaches used in this study is to compare the output from F-WERCAM with the RULSE model output of the region. A detailed assessment and comparison of this approach is discussed in the following section.

8.4   RUSLE Model and its Predicted Erosion Risk Map

For comparing the F-WERCAM predictive erosion risk map with the results of other existing erosion prediction models, the RUSLE model is adopted in this study as an alternate model. A brief description of the RUSLE model is given in Chapter 2.

The RUSLE model is selected here because of its wide applicability throughout the world and the advantage of limited amounts of data required for the assessments. In addition, some of the input parameters adopted in F-WERCAM framework are the same as in RUSLE, such as soil erodibility (K) and rainfall erosivity (R) factors. This provides a good platform for comparing the two models, even though the resultant erosion risk maps are based on different conceptual ideas.

Each of the input factors and parameters used in RUSLE is computed using the available datasets of the region. The computation of the soil erodibility factor (K) and the rainfall erosivity index (R) are described earlier in Chapter 7. Below, a brief account on computing the LS factor (Engel, 1999; Moore and Bruch, 1986; Mitasova et al., 1996) and the C and P factor of the Upper Awash Basin for soil erosion estimation is discussed.

a) Computing the LS factor

The LS factor reflects the effect of topography on soil erosion of the region. There are various methods available to compute the LS factor and the accuracy of this factor is largely governed by the resolution of the surface elevation or DEM of the region. In this study, the LS factor is computed using equations developed by Moore and Bruch (1986a, b) and Mitasova et al. (1996). For both there are modified LS equations that replace the slope length with the upslope contributing area; this is represented by multiplying the flow accumulation by the cell resolution of the source data, and gives the upslope contributing area per cell width. These equations are considered to be applicable when modelling erosion in a large landscape of complex topography.

In general, replacing the slope length by an upslope area based factor reflects the impact of concentrated flow on increased erosion. For both equations, the LS factor map of the Upper Awash Basin is computed. Both maps are used for a final computation of soil loss by the RUSLE method.

LS factor (Moore and Bruch, 1986a, b):

$$LS = \left(\frac{A}{22.13}\right)^{0.4} \times \left(\frac{\sin\theta}{0.0896}\right)^{1.3}$$ (8.4a)

Where A = (flow accumulation * grid size) and θ is the slope in degrees. Both are obtained from DEM of the region.

The LS factor by Mitasova et al. (1996) is given by:

$$LS\ (r) = \left((m+1)[A(r)/a_o]^m [\sin b(r)/b_o]^n\right)$$ (8.4b)

Where $A\ (r)$ is upslope contributing area per unit contour width
$b(deg)$ is the slope; m and n are parameters; a_o = 22.1 m; b_o = 0.09 = 9 %= 5.16 degrees.

For instance, m = 0.4 and n = 0.1 is taken for a region of natural vegetation; m = 0.6 and n = 1.3 for regions which are disturbed, e.g. deforested region, barrenland etc.

b) C and P factor

The crop management factor (C) represents the ratio of soil loss under a given crop and the base soil. It is evaluated using the existing LULC map of the region. The C value from Hurni (1985) for the Ethiopian condition (see also: Nyssen et al, 2004) and the C value rating database from the FAO method for soil loss estimation for the Awash Basin (Griffiths and Richards, 1989) is taken. The C factor map of the region is prepared in GIS for the use in this study. Similarly, the management practice map (P value) of the region is prepared according to Wischmeier and Smith (1978). The P value ranges from 0-1 and depends on the soil management activities and the slope of the region. According to Wischmeier and Smith (1978), agricultural areas with varying slope gradients are provided with P values ranging from 0.1 to 0.33; other land use areas have a P value of 1.

Once all the input parameters or factors are derived, the potential and actual soil loss map of the Upper Awash Basin is computed using the RUSLE equation $E = R * K * L * S * C * P$; where E is the actual predicted soil loss of the region. The product of ($R * K * L * S$) corresponds to the potential soil loss of the region. Since two LS factor maps are computed and used in this study, two different soil loss maps of the region are obtained: RUSLE (Moore & Bruch: LS) and RUSLE (Mitasova: LS).

Using the Moore & Bruch computed LS factor, RUSLE soil loss map of the Upper Awash Basin has an average soil loss of 17.90 t/ha/yr (Figure 8-14, left). For the Mitasova computed LS, RUSLE average soil loss is 23.99 t/ha/yr (Figure 8-14, right). The computed ranges of soil loss are classified into 5 ordinal erosion risk categories. This along with area and soil loss proportion of each category is compared and shown in Table 8-5.

The Upper Awash Basin can be characterized mostly by VL to L erosion risk classes, covering about 70 % of the total study area in both cases. Most of the regions having a higher erosion risk are located on steeper slopes where agricultural land and grassland are present. For both the soil loss maps, erosion risk class distribution is more diverse at higher elevations, ranging from "Medium" to "Very

High". From the soil loss spatial distribution pattern both RUSLE-based erosion maps indicates a similar distribution pattern with respect to the erosion risk class.
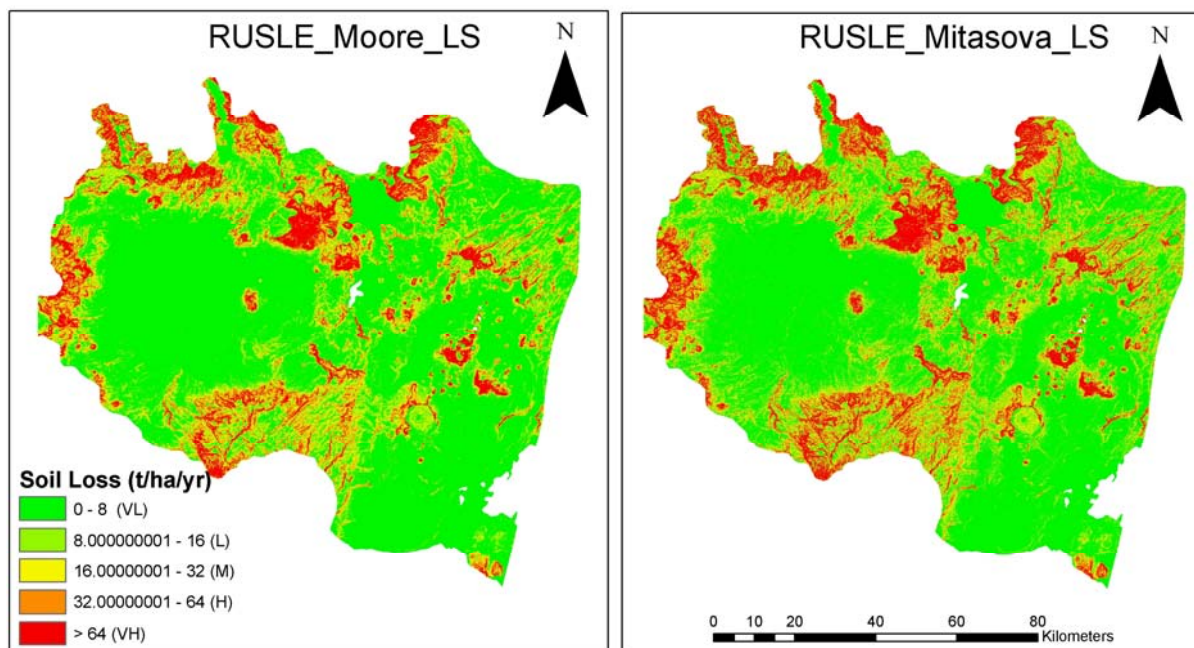
Figure 8-14: Soil loss map of the Upper Awash Basin obtained using different LS factor equations

Table 8-5: Comparison of the two different RUSLE-based soil loss map of the Upper Awash Basin

Soil erosion risk classes	Range of soil loss (t/ha/yr)	Proportion of area (%)	
		RUSLE (Moore & Bruch: LS)	RUSLE (Mitasova: LS)
Very Low	0-8	59.93	52.40
Low	8-16	13.54	15.04
Medium	16-32	10.85	12.69
High	32-64	7.84	9.17
Very High	>64	7.83	10.68

8.4.1 Qualitative Comparison of F-WERCAM Erosion Risk Map with RUSLE Erosion Map

The erosion risk map of the Upper Awash Basin using the RUSLE model is taken as the reference image for comparison with the classified soil erosion risk map by F-WERCAM. The assessment is made by constructing the *error matrix* or *confusion matrix*, which provides the degree of agreement between the two different model outputs (Lilesand et al., 2004).

To obtain a quantitative measure of accuracy between the two modelling outputs, *overall accuracy* and the corresponding *kappa statistics* are determined for each possible combination or comparison scenario. In addition, another measure of accuracy is used here which is considered to be more flexible which assumes that a one–class difference is acceptable (Vrieling et. al, 2006). This is justifiable as the risk classification is based on an ordinal class. With the help of Kappa statistics the total number of cells taken by the individual risk classes or categories can explain the cell-by-cell agreement between

two maps. The range of Kappa lies between 0-1, where 0 indicates "poor" agreement and 1 indicates "almost perfect" agreement between the two maps (Cohen, 1960). More details on the definition of the performance parameters and the significance of *Kappa* values can be referred in *Appendix 4-B*.

a) Comparison of PERI with RUSLE based potential erosion risk map

The histogram of the Upper Awash Basin obtains from F-WERCAM and RUSLE model is shown in Figure 8-15. It can be seen that there is an underestimation of the "Very High" risk class by F-WERCAM compared to the RUSLE outputs. Major differences are found to occur between the classes "Very Low" and "Very High" while least difference is found in the "Medium" erosion risk classes.
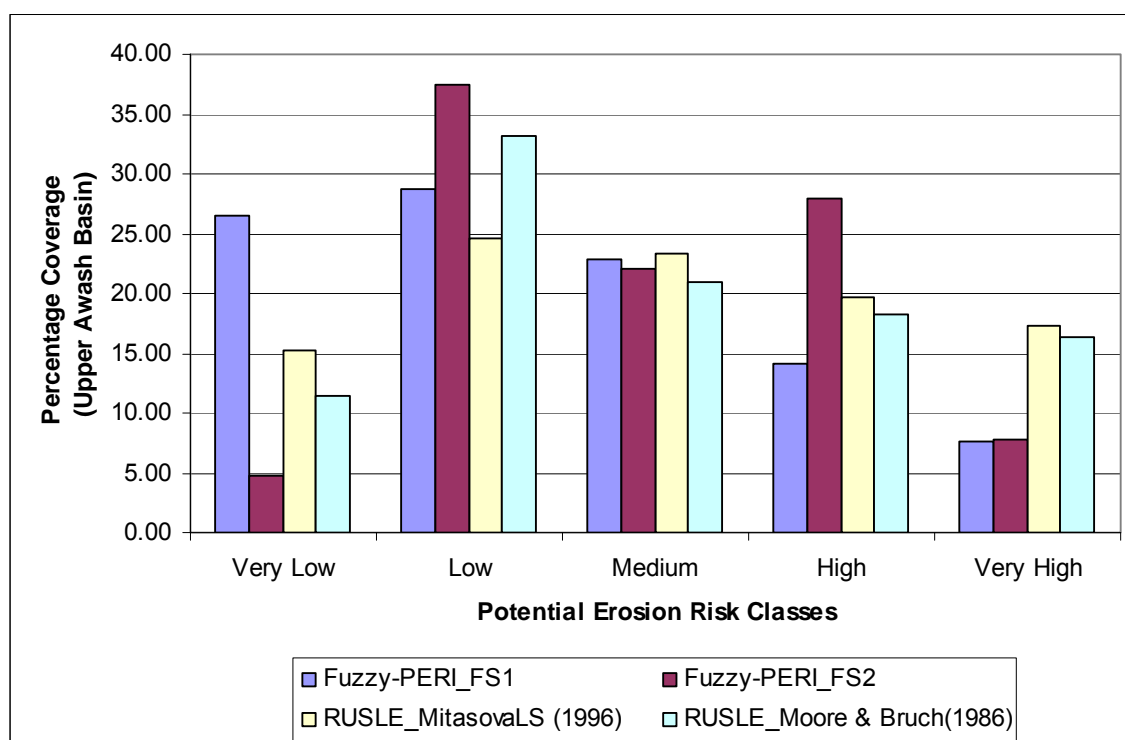
Figure 8-15: Qualitative comparison of soil erosion risk classes when computed using F-WERCAM and RULSE

To evaluate in detail, the spatial erosion risk distribution, the classified PERI map is compared with the RUSLE-based potential erosion risk map. The "error matrix" corresponding to the comparison between PERI_FS2 and RUSLE (Moore & Bruch: LS) is given in Table 8-6. From the error matrix analysis, it is found that 29 % of the VL risk class from the RUSLE model is correctly classified in the F-WERCAM based model while 69 % of the VL risk class in the F-WERCAM model correctly depicts the VL class in the reference map, i.e. the RUSLE model. Similarly, 83 % and 47 % of H and VH risk classes from the RUSLE output are correctly classified in the F-WERCAM model, while 54 % and 100 % of H and VH risk classes in F-WERCAM correctly depicts the corresponding classes in the reference map. The sum of the diagonal values (in italics) gives a value of 62.4 % for the overall accuracy between the two maps.

For all other possible combinations, similar analysis is performed. The results are given in Table 8-7. The results from the comparison and analysis show that PERI_FS2 has the highest level of agreement

with the RUSLE-based output which used the Moore & Bruch LS factor. An overall accuracy of 62.4 % and a corresponding *kappa* of 0.50 (i.e. a moderate agreement) are obtained after comparing the two maps. When one risk class difference is allowed between the F-WERCAM and RUSLE, the overall accuracy increased to 99.95 %. This indicates that a certain region classified as "Low" risk by F-WERCAM is found to be classified as "Very Low" or "Medium" by the RUSLE model.

Table 8-6: Error matrix of PERI_FS2 and RUSLE (Moore & Bruch LS)

	Risk classes	RUSLE: (Moore & Bruch: LS)					
		VL	**L**	**M**	**H**	**VH**	Total
PERI_FS2	**VL**	*3.31*	1.48	0	0	0	4.79
	L	8.05	*24.44*	4.99	0.033	0	37.51
	M	0.01	7.22	*11.73*	3.008	0.001	21.96
	H	0	0	4.17	*15.23*	8.58	27.98
	VH	0	0	0	0.02	*7.68*	7.70
	Total	11.37	33.14	20.90	18.29	16.261	100

* Values here indicate the percentage area contribution to each soil erosion risk class

Table 8-7: Results showing the level of agreement between the classified potential erosion risk by F-WERCAM and RUSLE models

Model comparison	Statistical measures		
	Kappa Statistics	Overall accuracy*	Accuracy**
PERI_FS2: RUSLE (Moore & Bruch: LS)	**0.50 (Moderate)**	**62.39%**	**99.95%**
PERI_FS2: RUSLE (Mitasova: LS)	0.40 (Fair)	52.69 %	97.86 %
PERI_FS1: RUSLE (Moore & Bruch: LS)	0.33 (Fair)	47.12 %	96.1 %
PERI_FS1: RUSLE (Mitasova: LS)	0.25 (Fair)	41%	90.5%

* When the predicted potential erosion risk classes of F-WERCAM correctly matched with RUSLE prediction of erosion risk classes.
** When one erosion risk class difference is allowed between the two model predictions

b) Comparison of AERI with RUSLE-based actual erosion risk map

The basis for this comparison of the relative occurrence of the actual erosion risk classes is the data plotted in the histogram shown in Figure 8-16. The histogram of the RUSLE-based output maps is quite similar to that the histogram of F-WERCAM. A large difference in the percentage area of "VH" class is observed between the AERI map (adopting the RB2) and the RUSLE-based output. From the results, it is clear that only a small part of the study area is classified under "VH" erosion risk class when output FS2 with RB2 (AERI2_RB2) is adopted. On the other hand, when RB1 is used, the degree of agreement between the RUSLE and F-WERCAM became quite significant as can be seen from their respective histograms. This is due to the setup of the RB1, which considers SPI to have a greater influence or importance in determining the actual erosion risk of the region.
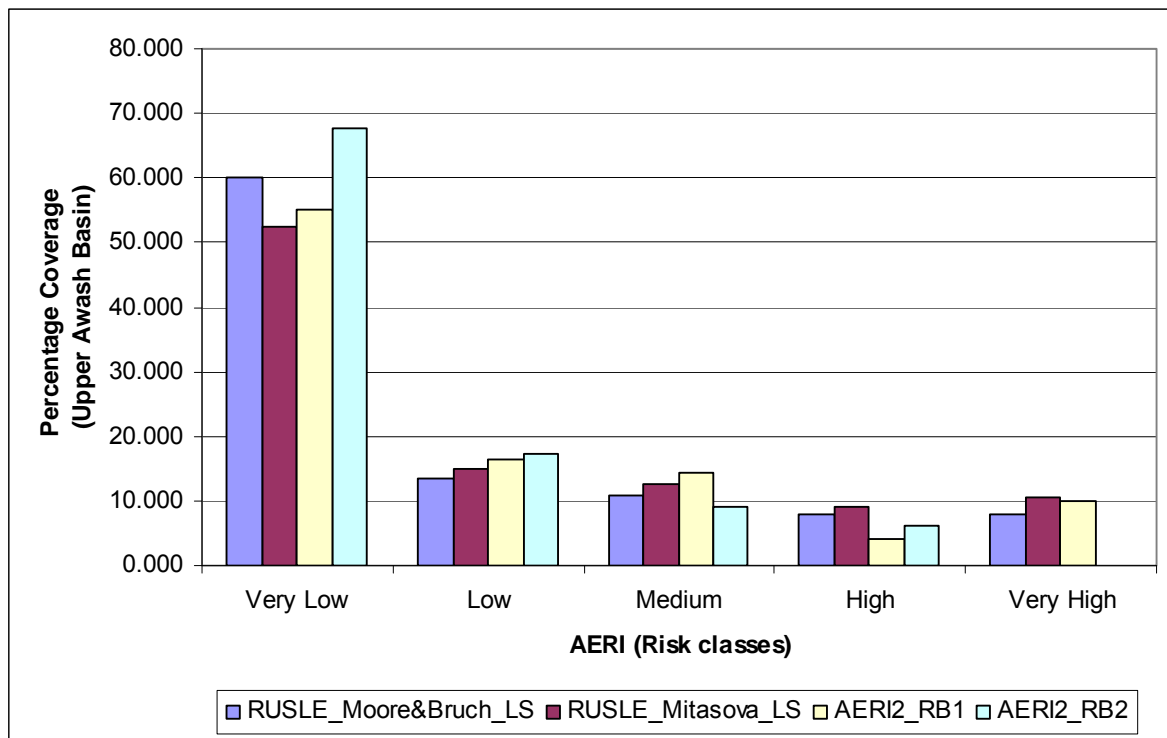
Figure 8-16: Histogram of actual soil erosion risk classes as computed using different scenarios of F-WERCAM and RULSE

Table 8-8: Summary of the results of the assessment between the classified actual erosion risk index by F-WERCAM and RUSLE model

Model comparison	Statistical measures		
	Kappa Statistics	Overall accuracy*	Accuracy**
AERI1_RB1: RUSLE***	0.34 (Fair)	54.64 %	92.27 %
AERI2_RB1: RUSLE***	0.51 (Moderate)	70.45 %	94.85 %
AERI1_RB2: RUSLE***	0.52 (Moderate)	71.30 %	96.96 %
AERI2_RB2: RUSLE ***	0.41 (Moderate)	66.89 %	92.65 %

* When the predicted erosion risk classes of F-WERCAM correctly matched the RUSLE predictions.

** When one erosion risk class difference is allowed between the two model predictions.

*** RUSLE based on Moore & Bruch's LS equation.

From the accuracy assessment of the maps, significant agreement between the AERI2_RB1 and AERI1_RB2 with RUSLE (Moore & Bruch: LS) are found (Table 8-8). From the various combinations of rules and output fuzzy sets, the range of overall accuracy varied from 54.64 % to 71.30 %, with corresponding kappa values of 0.34 to 0.52. Hence, it is seen that depending on the type of defined output membership functions and the adopted fuzzy rule system, the output erosion risk maps differ in their spatial distribution pattern as reflected by the difference in their accuracy. For

further analysis, the output erosion risk map which corresponds to AERI2_RB1 is considered. The output risk map which corresponds to AERI1_RB2 which is also statistically significant when compared with RUSLE output is not used for further analysis. Despite having a higher overall accuracy, this scenario is found to underestimate the spatial erosion risk which corresponds to "Very High" class. This type of comparative assessment provides us with the capability to pass proper judgement on the rule base systems which reflect and capture the erosion risk of the region.

The computed spatial distribution maps of the soil erosion risk from RUSLE and F-WERCAM are given in Figure 8-17. From the map on the right, the north western region of Upper Awash Basin is seen to be classified under "Medium" to "High" erosion risk classes by F-WERCAM; correspondingly, the same region in the map on the left has "High" to "Very High" risk classes for the RUSLE map. Similar distribution patterns are also observed in the southern part of the basin. The central and south eastern parts of Upper Awash Basin are classified under same erosion risk classes ("Very Low" to "Low") by both model outputs.
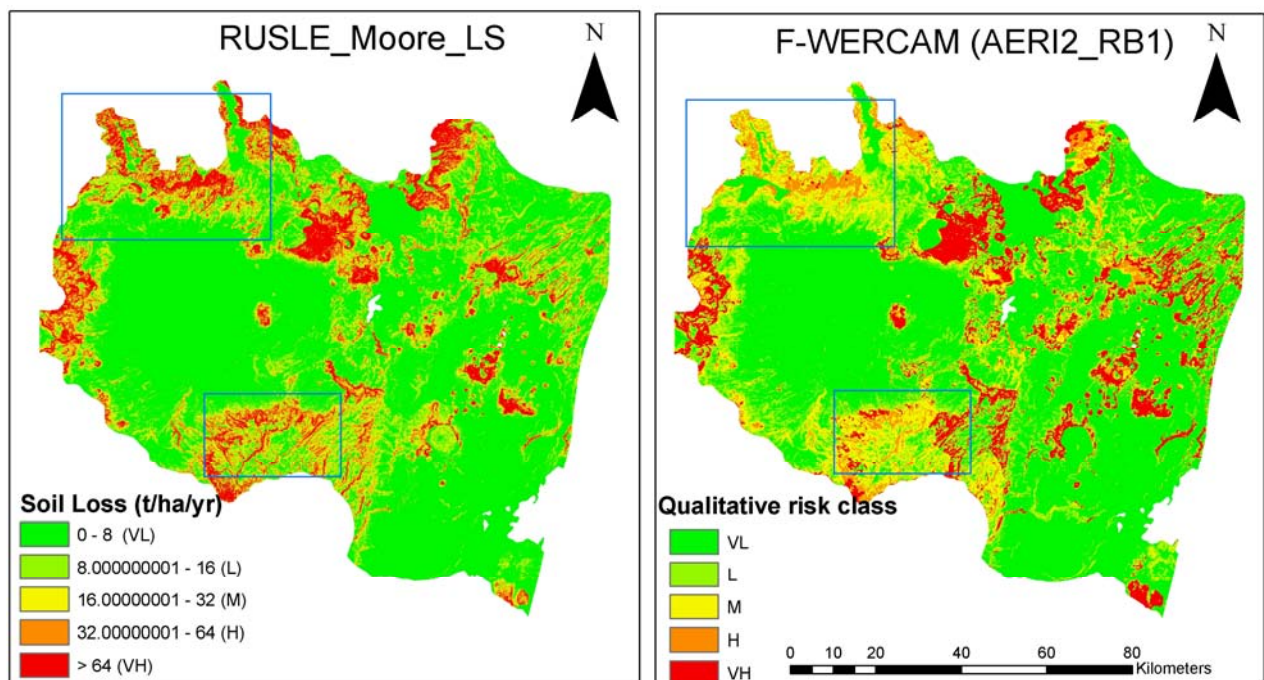
Figure 8-17: Spatial distribution of the soil erosion risk classified map according to F-WERCAM (right) and RUSLE (left)

In F-WERCAM, the slope is considered to be the only parameter influencing the effect of topography on soil erosion, whereas for RUSLE, slope length *and* slope gradient are taken into account in the form of LS factor. This explains the differences in risk classes from the model outputs. It is evident that the difference in risk classes is found to be concentrated in areas of higher elevation having a higher slope length and gradient. In case of plain areas which are subject to a lower slope gradient and slope length, the influence of LS is minimized, resulting in a more similar distribution of risk classes, i.e. VL to L. Moreover, the inherent differences between fuzzy-based and empirical-based modelling concepts may also be a contributing factor for the differences in the output of soil erosion risk. For example, the accuracy of the predicted erosion risk is largely influenced by the adopted fuzzy rule base for F-WERCAM, whereas it is the multiplication of the input parameters that produce the erosion risk distribution for RUSLE. Overall, it is difficult to make a straight forward conclusion whether the F-

WERCAM-based modelling approach represents the soil erosion risk distribution pattern of Upper Awash Basin more accurately than the RUSLE based erosion risk map. Nevertheless, considering the input parameters, i.e. slope gradient compared to LS factor, the representation of vegetation cover dynamic in form of SPI and the flexibility of fuzzy logic to incorporate additional expert knowledge in the form of fuzzy rules, made F-WERCAM an innovative approach for the assessment of soil erosion risk on a regional scale.

Discussion on the possible approaches toward the quantification of the F-WERCAM-based soil erosion risk map is provided in the next chapter, where also the transferability of the rule base for mapping the erosion risk of the Upper Awash Basin to other geographical regions is discussed.

8.5   Temporal Effects of SPI and LULC on the F-WERCAM-based AERI map

Modelling soil erosion risk very often incorporates static maps of vegetations classes, climate, soils and terrain parameters, but rarely the seasonal patterns of vegetation cover and land use practice are taken into account (Van Leeuwen and Sammons, 2003). Incorporation of vegetation growth and its cover dynamics in the form of NDVI and LULC map of different time periods allow us a greater understanding of the feedback mechanisms, temporal variability of erosion risk intensity and the interaction between different erosion risk governing parameters that are dynamic in temporal scale.

Computing the PERI of the region before integrating SPI in order to obtain the AERI map, annual rainfall erosivity index, R is only taken into account, i.e. the effect of temporal rainfall is not considered. One of the probable reasons is that computation of monthly rainfall erosivities requires rainfall intensity (I), duration of rain segments (T) to compute the EI30 (kinetic energy times the maximum sustained intensity lasting for 30 minutes) index (Hoyos et al., 2005; Svetlana et al., 2006). Absence of rainfall intensity data from pluviographic stations in Upper Awash Basin limits the study to compute the seasonal rainfall erosivities. Nevertheless, Stocking et al., (1988) points out that for a wider geographical coverage, with simpler and more available variables the quality of the resultant assessment of erosivity increases. Hence, using the available monthly and annual rainfall data from limited gauging stations and satellite based rainfall estimates the long term annual rainfall erosivity of the Upper Awash Basin is computed and used in this analysis.

8.5.1   Effect of Monthly SPI on the Actual Erosion Risk Distribution (AERI)

To understand the temporal effect of SPI on the soil erosion risk class distribution for the Upper Awash Basin, Stage 3 of the F-WERCAM is executed on a monthly basis using the RB1. The corresponding SPI map from January-December 2001 is combined with the PERI map to generate the monthly AERI map. It is seen that SPI of different time periods have a varying degree of influence on the actual soil erosion risk class distribution over the region. In the Upper Awash Basin, it is found that with increasing monthly rainfall there is an increasing tendency of regions with "low" erosion risk. This is due to the increase of vegetation biomass and causes the SPI to increase and the AERI to decrease. For instance, considering the distribution of the VL and VH erosion risk classes over the region (see Figure 8-18), the pattern of the VL erosion risk class is quite consistent throughout the year except for a slight increase in the percentage coverage in August-September (mainly during the rainy period). On the other hand, during the December-February dry period, the distribution pattern of the

VH erosion risk class peaked. This is maybe related to the reduction in vegetation cover during the dry period to lead to exposure of the soil surface. This, in turn, reduces the SPI of the region.
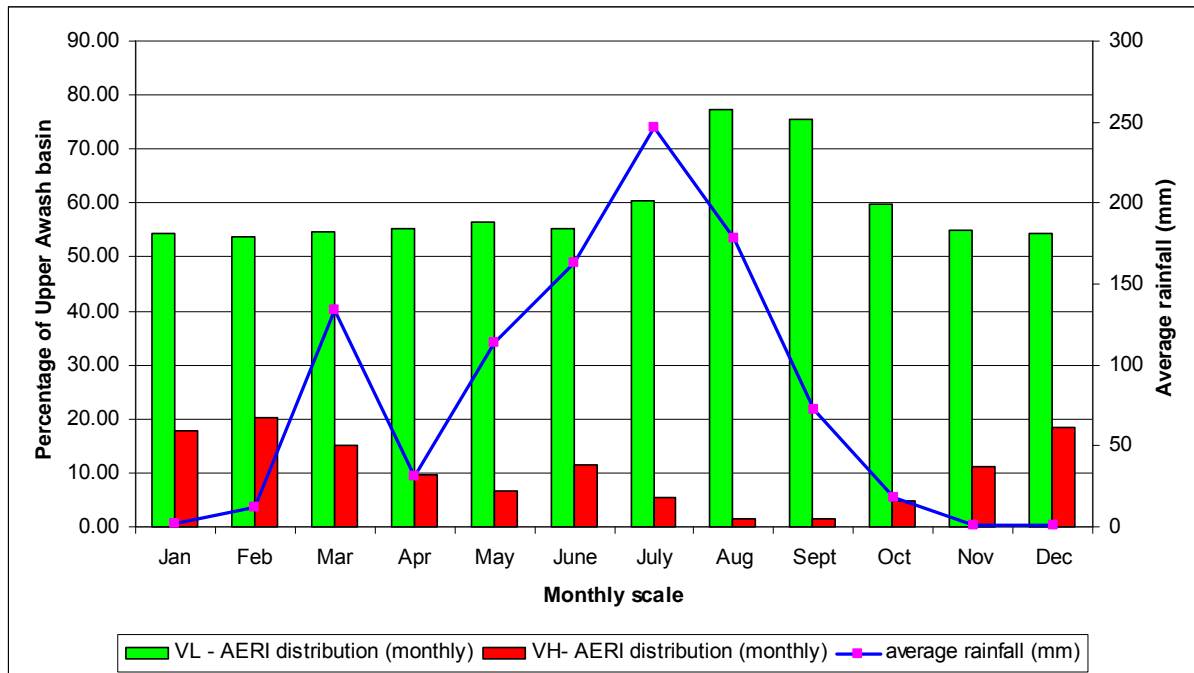
Figure: 8-18 Temporal distribution pattern of VL and VH erosion risk class

It is to be pointed out that this assessment does not take into account the variability of temporal rainfall since annual rainfall erosivity is used as an input fuzzy parameter for the computation of the PERI map. The temporal pattern of soil erosion risk distribution account only for the variability of vegetation cover in the form of SPI. From this analysis, it is found that during the dry period of the year, there is an increase in the percentage coverage of higher soil erosion risk classes. This trend of increasing erosion risk may be possibly due to extreme rainfall events with higher intensity during the little rainy period and dry period in Upper Awash Basin. It is also found from the rainfall-NDVI analysis that with a decrease of monthly rainfall there is a decrease in vegetation cover within the study area. Hence, low vegetation cover coupled with few extreme rainfall events during these periods may be the potential cause for increasing the risk of soil erosion in the region.

Overall, in the Upper Awash Basin, the effect of rainfall is greatly muted by the vegetation cover distribution. This can be clearly deduced from the fact that with an increasing monthly rainfall during the year, there is a tendency of increasing vegetation cover which is reflected in the distribution of NDVI within the region. Even though there is a high amount of precipitation during the main rainy period, the increase in vegetation cover provides the protection layer of soil from being eroded. This comparatively decreases the percentage coverage of higher soil erosion risk class of the region during this period compared to other periods of the year. Hence, the influence of the vegetation cover on the soil erosion risk of the Upper Awash Basin is arguably found to be the most important temporal parameter. Further temporal based assessment is necessary by taking into account the monthly rainfall erosivity in addition to the temporal vegetation cover as it may provide additional results concerning the additive or synergetic influence of both parameters on the temporal soil erosion risk distribution of Upper Awash Basin.

Nevertheless, this assessment indicates that for temporal-based prioritization over the Upper Awash Basin, the focus should be given to those months that correspond to the dry period or season of the year. The F-WERCAM output erosion risk distribution map clearly indicates that the rainfall distribution pattern of the region has an influence on the temporal dynamics of vegetation cover. This has a direct influence on the SPI of the region and, in turn, affects the degree of the actual erosion risk of the region.

8.5.2   Effect of Temporal LULC Map on the Actual Erosion Risk

To study the effect of LULC map on the actual erosion risk of the region, LULC and NDVI maps for the year 2000 is used to map the SPI of the region. This is then combined with the PERI map to generate the AERI map of 2000 using the Stage 3 of F-WERCAM. The actual erosion risk map corresponding to the year 2000 is then compared against the actual erosion risk map of 2001. The LULC map use to generate the SPI of 2001 is extracted from the land cover map of Awash Basin provided by the Ministry of Water Resource, Ethiopia.

The actual erosion risk index maps, i.e., the AERI corresponding to the years 2000 and 2001, are shown in Figure 8-19. The spatial distribution of AERI over the study area clearly indicates that LULC distribution of different time periods influence the degree of soil erosion risk and hence the potential rate of land degradation of the region.
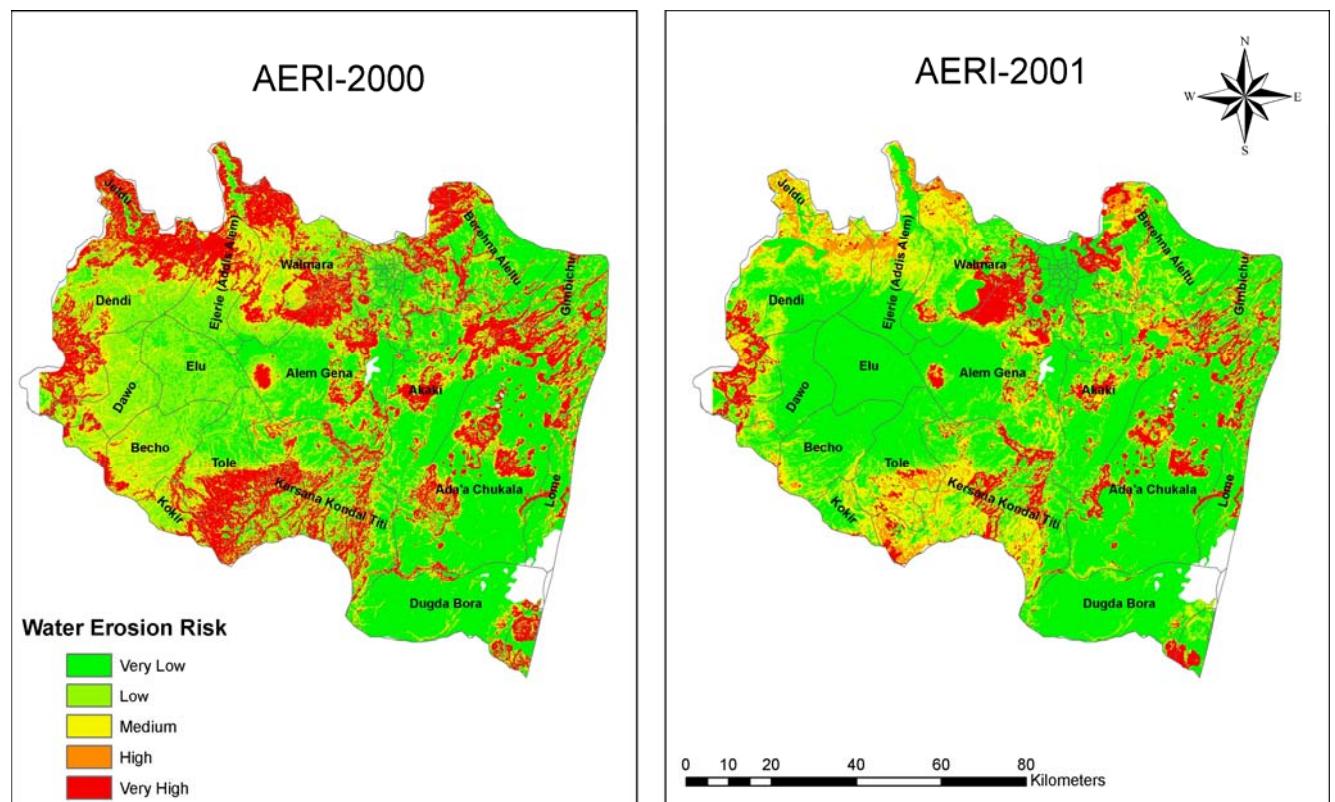
Figure 8-19: AERI map showing the water erosion risk class distribution of the Upper Awash Basin for the year 2000 and 2001

Low lying and flat terrain area having an average slope of 2-6 % are within the "Very Low" and "Low" erosion risk classes for both time periods cover approximately 40 % of the total study area. Most of these low lying areas are agricultural land. A shift in the pattern of risk distribution from "Low" to "Very Low" is found in the central part of Upper Awash Basin in the Elu, Dawo, Bacho and Dendi administrative units. This is attributed to the difference in the adopted agricultural practices which is reflected in the differences shown in the NDVI maps for the vegetation cover intensities for the two time periods. Most of the regions in the north-western part and the southern hilly regions of Upper Awash Basin (about 11% of the total area), categorize as "Very High" erosion risk in 2000, has change to "High" and "Medium" erosion risk classes by 2001. Indeed, 44 % of the whole study areas show a decrease in their soil erosion risk class; the remaining 53 % of the total area show, however, only insignificant changes to their erosion risk distribution. Elevated areas, which comprise barrenland and grassland and amount to about 3% of the total area, shows an increase in the erosion risk class distribution. When comparing the erosion risk distribution of 2000 to 2001 (Figure 8-20), it is found that the "Very Low" risk class increases in area by 20 %; at the same time, the "Very High" risk class decreases by 11 %. In the other risk classes, only slight variations are observed.
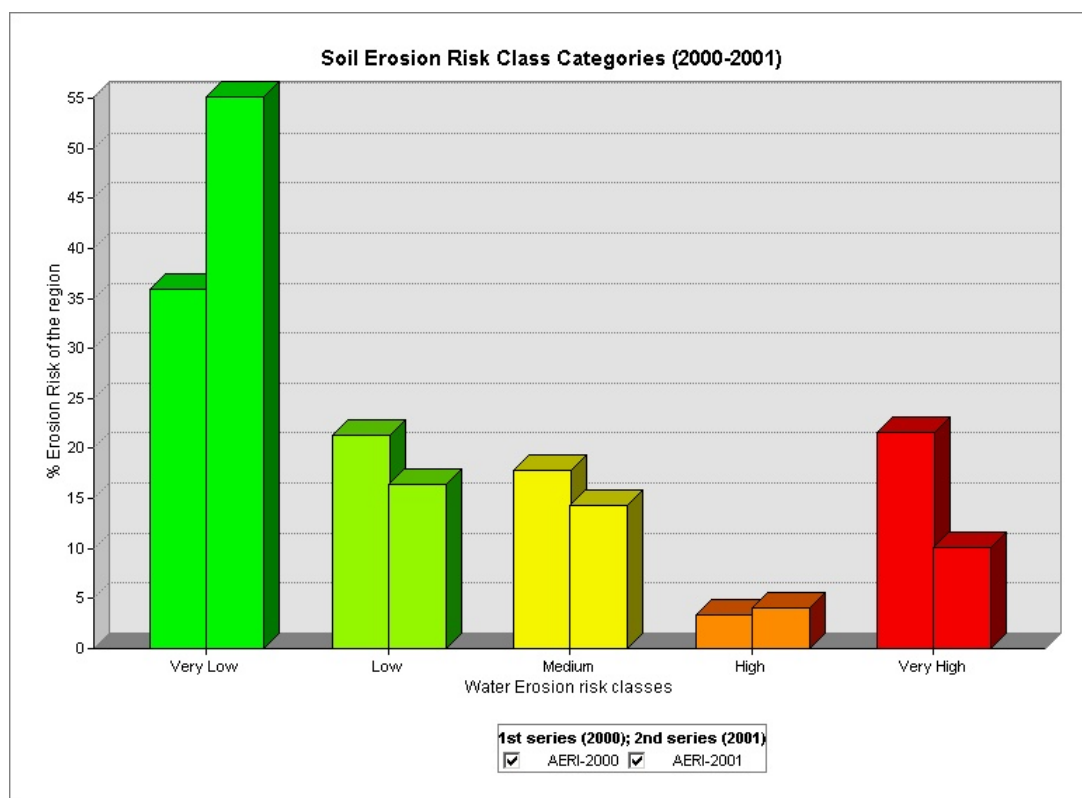
Figure 8-20: Distribution of actual soil erosion risk class (% coverage) of the Upper Awash Basin for the year 2000 and 2001

Another important aspect to be pointed out from this temporal analysis is the source of data used from each different time period. For instance, in this study the LULC map of 2000 is obtained using the maximum likelihood classification method using the Landsat satellite data. The LULC map of 2001, on the other hand, is obtained from the Ministry of Water Resource, Ethiopia. Hence, there is a possibility that some variations in the actual erosion risk distribution may be linked to the nature of source data. To minimize the influence of the source data, the NDVI data from the same source

(MODIS NDVI), which acts as a proxy for vegetation cover density over the region, is also used in the analysis.

This temporal analysis provides a framework to understand the distribution of erosion risk pattern. It serves as a basis for the development of future options for more sustainable land use over a large landscape. Focusing on the implementation of sustainable land use, the control of the soil erosion problem in the region is possible. With respect to the study area, of the Upper Awash Basin, a focus of soil erosion measures in the Tole, Ada Chukala, Addis Alem and Walmara regions is recommended, since these areas have a "Very High" erosion risk, irrespective of the effect of temporal LULC and vegetation cover.

8.6 Applicability of the Satellite-Based Indirect Rainfall Estimates for Assessment of Erosion Risk

This part of the study focuses on the utilization of satellite estimated rainfall as input data for mapping the soil erosion risk of the region. Initial assessments of SBRE with ground rainfall data are discussed in Chapter 6. The actual erosion risk map produced by using the TRMM data and CPC data are compared with the actual erosion risk map of the region, which is obtained by using the ground rainfall data. This analysis aims to test the applicability of rainfall data obtained from satellites for monitoring the soil erosion risk over a large landscape. The need of such an assessment is underpinned by the fact that there is often a lack of ground monitoring rainfall stations, associated with data-holes in various parts of the world, especially in developing countries. This study is an attempt for bridging the gap of data scarcity in the developing world for a timely monitoring of environmental problems like soil erosion.

The spatial erosion risk distribution (percentage of potential and actual risk classes) of the Upper Awash Basin which is computed by using the ground rainfall, TRMM and the CPC based rainfall erosivities is as shown in Table 8-9 and Table 8-10.

Table 8-9: Comparison of the potential erosion risk distribution in the Upper Awash Basin

Potential erosion risk index classes (PERI)	Percentage distribution of potential erosion risk class		
	PERI_G (using ground based rainfall data)	PERI_TRMM (using TRMM based rainfall data)	PERI_CPC (using CPC based rainfall data)
Very Low	4.79	6.19	4.47
Low	37.51	40.80	43.46
Medium	21.99	17.41	16.44
High	27.98	28.00	27.46
Very High	7.71	7.58	8.16

From the analysis, it can be seen that there is strong agreement in the erosion risk class prediction and the distribution pattern between the computed potential erosion risk maps using the different source data. The percentage of the erosion risk class corresponding to "Very Low", "High" and "Very High" are found to be same in all cases with only slight variations. For the erosion risk class "Low", the

classified percentage of risk area for both, PERI_TRMM and PERI_CPC, tend to overestimate by 6 %, and the risk class corresponding to "Medium" tends to underestimate by 5.6 % when compared with PERI_G.

The actual erosion risk map of the region is generated using the different PERI maps (i.e. PERI_G, PERI_TRMM and PERI_CPC) and the SPI maps of the region. It is found that in all cases, more than 50 % of the study area is classified under the "Very Low" erosion risk class, while 10 % of the study area is classified under "Very High". The spatial erosion risk distribution patterns for the three different cases can be seen in Figure 8-21. A detailed spatial analysis shows that 1.7 % of the region has erosion risk class differences when comparing the AERI_TRMM to AERI_CPC. Similarly, when comparing the AERI_CPC and AERI_TRMM to AERI_G, it is found that there is a difference in erosion risk class distribution which comprises about 2.1 % and 1.7 % of the total study area, respectively. It can be concluded from the analysis that irrespective of the input rainfall source data, the actual erosion risk map by F-WERCAM is found to give low variations and differences for the predicted erosion risk classes.

The trend of the erosion risk distribution can be explained by the use of the same input fuzzy sets of rainfall erosivity, even though differences in the computed range of erosivity are observed when using the different source data. In another words, the representation of the input rainfall erosivity parameter using the fuzzy linguistic sets reduces the difference in the range of the erosivity when computed by using different rainfall data sources.

Table 8-10: Comparison of actual erosion risk distribution maps using different rainfall data sources

Actual erosion risk index classes (AERI)	Percentage distribution of actual erosion risk class		
	AERI_G (using ground based rainfall data)	AERI_TRMM (using TRMM based rainfall data)	AERI_CPC (using CPC based rainfall data)
Very Low	55.13	55.87	56.02
Low	16.45	15.75	15.46
Medium	14.25	14.27	14.03
High	4.06	4.02	4.36
Very High	10.08	10.06	10.10

Satellite-based rainfall datasets can be used effectively as an alternate source of rainfall data, which in turn can be used to compute the rainfall erosivity of the region for an assessment of soil erosion risk. The high temporal and spatial coverage of such satellite based rainfall estimates will help toward the timely and regular monitoring of soil erosion risk in a landscape. It is important to understand that the comparative assessment provided here is qualitative in nature and is intended to provide an overview on the varying degree of soil erosion risk over the Upper Awash Basin for prioritization purposes. More assessment and comparison of any SBRE with ground observed data is required before it can be utilized as a fully reliable data source.
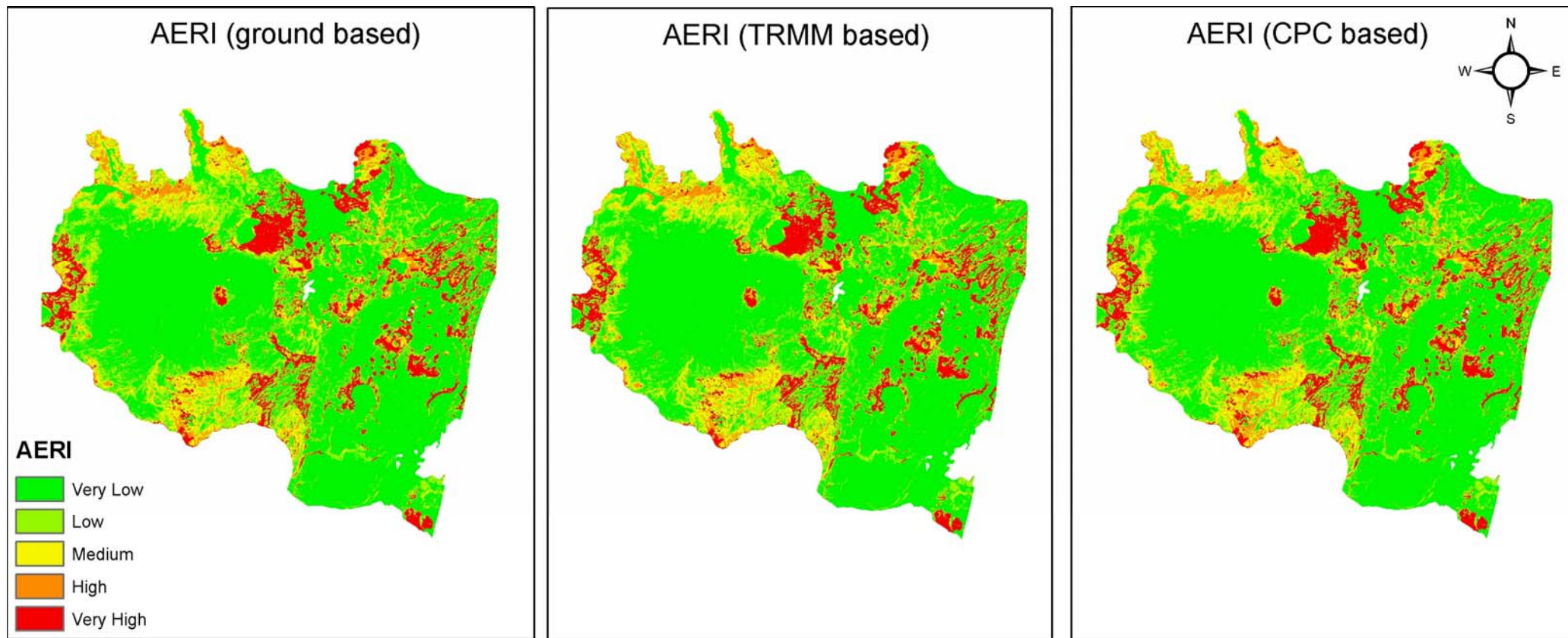
Figure 8-21: Spatially distributed Actual Erosion Risk Index (AERI) maps of the region using 3 different rainfall data sources

8.7 Summary

This chapter describes the analysis of the three different stages of the F-WERCAM applied to Upper Awash Basin. The implemented fuzzy sets and the fuzzy rules for each stage of the model are tested and produced satisfactory results. The first stage of F-WERCAM produces SPI which is considered to be a function of LULC and NDVI. Stage 2 of F-WERCAM maps the potential erosion risk which is a function of soil erodibility, annual rainfall erosivity and slope of the region. Finally, the integration of SPI and PERI yield to the final output erosion risk index map.

A qualitative assessment is carried out to observe the influence of the shape of membership functions associated with the output fuzzy sets and with different fuzzy rules for mapping the PERI and AERI. The combination of a simple triangular and trapezoidal membership function for the output fuzzy sets is deemed satisfactory when mapping the actual erosion risk of the region. From the different combinations of output fuzzy sets and fuzzy rules, it is observed that shapes of the membership functions are less sensitive to the output of erosion risk. In contrast, the fuzzy rules are found to be very sensitive to the erosion risk distribution of the region. The results of the F-WERCAM outputs of soil erosion risk classes compared to the RUSLE based predicted erosion risk maps indicates a satisfactory performance of F-WERCAM.Different scenarios are tested using different combinations of fuzzy rules and output fuzzy sets. The accuracy assessments of the results are performed by constructing an error matrix using the RUSLE-based output maps as reference map. The AERI map produce using RB1, corresponding to Stage 3 of F-WERCAM, is found to map the erosion risk distribution in a similar degree as the RUSLE-based output.

Furthermore, the F-WERCAM-based assessment is carried out in order to understand the effect of temporal parameters like vegetation cover (NDVI) in the form of SPI, on erosion risk distribution pattern of the region. The influence of the temporal LULC and SPI on the spatial soil erosion risk distribution provides a means to understand the distribution of erosion risk classes on a temporal scale and form a basis for the development of options for a more sustainable land use. The effectiveness of utilizing SBRE in this fuzzy based modelling approach is also studied. The results from the analysis have shown that satellite-based rainfall datasets can be effectively used as an alternate source of rainfall data.

Overall, it is shown that the F-WERCAM-based modelling can act as the first step toward monitoring a large landscape for soil or land degradation, using an expert-based fuzzy rule system with a limited amount of input datasets. This modelling approach should not be considered as a replacement for other existing erosion models. Nevertheless, the F-WERCAM can be considered as an exploratory erosion risk assessment model for large regional landscapes where the amount of data is limited. This type of modelling approach will help to produce synergetic effects when used together with other existing models. Additionally, this kind of modelling approach with a fuzzy expert system addresses the problem of uncertainty associated to input parameters in the form of fuzzy linguistic sets, and it allows updating the output easily by incorporating additional expert knowledge in the rule base system.

9 Quantification of F-WERCAM-Based Erosion Risk Index

This chapter focuses on the possibility of quantifying the output erosion risk index of the F-WERCAM model. Two different approaches are tested in this study. The initial approach considers the domain of the output fuzzy sets, i.e. the defuzzified output range of the model which is set as the actual observed soil loss range within the study area. The latter of the approaches then quantifies the soil erosion risk by establishing a relationship between the F-WERCAM output risk indexes with the actual soil loss range as predicted by RUSLE. The main focus in this approach is to see whether the qualitative erosion index (0-100) by F-WERCAM can be quantified with actual soil loss as observed from ground or predicted from other models by setting up a relationship between them. Due to the absence of ground measured spatially referenced soil loss data, the predicted soil loss values of the study area by RUSLE at different locations is considered as the proxy or test data to establish a relationship with the F-WERCAM index scale.

9.1 Setting Up the Range of Output Fuzzy Sets Using Observed Annual Soil Losses

As an initial approach to test a possible estimation or quantitative mapping, the actual documented range of soil loss (0-300 t/ha/yr) occurring in the study area serves as the output range when setting up the output fuzzy sets for the soil erosion risk. Using the standard fuzzy parameters, the soil erosion risk of the Upper Awash Basin is mapped within the actual soil loss range as represented by the defuzzified output values. Next, the average soil loss within each of the LULC classes is compared to that of corresponding predicted soil loss by RUSLE. This assessment uses the RB1, which corresponds to Stage 3 of F-WERCAM. The results of the comparison of F-WERCAM (using the expert definition of annual soil loss range [0-300 t/ha/yr] for Upper Awash Basin as the valid fuzzy output domain) with annual soil loss predicted by RUSLE is shown in Table 9-1.

The analysis clearly shows that the average soil loss of the region by F-WERCAM tends to be overestimated when compared to the RUSLE approach. Specifically, there is a large overestimation of soil loss in scrubland or wasteland (110.38 t/ha/yr) and grassland regions (91.79 t/ha/yr) when compared to the RUSLE-based average soil loss within the LULC classes (Table 9-1). From this assessment, it is difficult to make a straight forward conclusion about the accuracy of the quantitative soil loss value derived from the fuzzy model, which is basically a by-product of the functional mapping between the input and the output using defined linguistic variables. This is mainly because of the absence of real ground observed erosion data for the purpose of comparison. This assessment is intended to examine how well the fuzzy model performs compared to other existing erosion models.

In F-WERCAM using the fuzzy inference process, it is evident that the fuzzy mapping rules are attempting to establish a relationship between input and output. The F-WERCAM based soil loss value is found to be limited within the user defined range which is based on the established relationship between the input and output parameters; and the range of actual soil loss observed on the ground.

Table 9-1: Comparison of the quantified soil loss for each LULC by F-WERCAM with RUSLE

Average soil loss of the Upper Awash Basin (t/ha/yr)		
	F-WERCAM	RUSLE model
LULC Classes (2001)	AERI2_RB1	LS : Moore and Bruch (1986)
Agriculture	17.47	15.54
Scrubland/Wasteland	**110.38**	**22.83**
Settlement zone	2.67	0.02
Grassland	**91.79**	**47.61**
Forest	4.98	4.73
Average annual soil loss (t/ha/yr)	27.11	17.90

More precisely, the input-output ranges are set prior to the implementation of the model specific to the particular type of soil erosion. Hence, the results are dependent and influenced by the fuzzy sets and the fuzzy rule base adopted for consideration of the erosion processes in the region. The results may be improved if the models are trained and tested using the real observed ground soil loss data of the region. However, the lack of the sufficient observed field data for a large region like the Upper Awash Basin limits the study to use the fuzzy rule system based on expert knowledge and literature. Consequently, a system must be developed where both the input and output membership functions can be developed during the real-time processing of the actual application. With such applications, higher accuracy and control of the output can be maintained.

Nevertheless, this assessment provides a comparison of soil loss values predicted by using two different types of models. A proper evaluation of such quantification methods may be reasonable when the output from expert-based models is compared directly to the observed ground data. The straight forward analysis using F-WERCAM shows the possibility of using the fuzzy inference mechanism for an approximate quantitative assessment in addition to a purely qualitative analysis.

9.2 Quantification of Results by Establishing a Relationship between F-WERCAM-Based Erosion Index and Predicted Soil Loss of RUSLE Model

Another approach is attempted in order to quantify the F-WERCAM-based actual soil erosion risk index map. This approach sets out a statistical relationship between the output PERI and AERI index and the soil loss of the region predicted by RUSLE. In the absence of actual ground observed soil loss data, the established relationship can be based on the predicted values from the RUSLE model only. However, in regions where real observed ground data is available, this method can be applied effectively for the translation of the index scale to a real quantitative value. This provides the possibility of extending the qualitative-based fuzzy output to a quantitative scale. A similar approach is applied successfully for the translation of the index scale into a quantitative value for an expert-based erosion modelling tool like PSIAC or FSM (Vente and Poesen, 2005).

In this research, the quantification of the fuzzy based qualitative output index map is carried out in order to evaluate the prediction capability of the F-WERCAM output. The translated soil loss value represents the relationship between the index scales and the predicted soil loss by RUSLE. For this part of the assessment, 600 random pair-wise values of soil loss estimated by RUSLE across the study area are extracted along with the corresponding PERI and AERI index values from the related output maps. These random values are considered to represent the variability of the soil erosion risk in the region. These extracted data points are used to see whether there is a strong correlation or relationship between them. Finally, appropriate relationships are established and analyzed by taking regression plots of the data (Table 9-2).

Table 9-2: Relationship between the PERI, AERI and the predicted soil loss values by RUSLE

Predicted Annual Soil Loss	F-WERCAM based Erosion risk index (1-100)	Statistical measures		Established relationships with RUSLE
		Pearson's correlation (R)	Explained Variance (R^2)	
RUSLE	PERI <20	0.83	0.78	$Y_P = 4.0929*PERI^{1.8566}$
	PERI >20	0.50	0.33	$Y_P = 22.424*PERI^{0.9968}$
	AERI <12	0.78	0.72	$Y_A = 0.7418*AERI^{1.961}$
	AERI >12	0.56	0.37	$Y_A = 15.685*e^{0.0225*AERI}$

a) Translation of PERI index

Two equations are established for translation of the whole range of PERI into a RUSLE-based quantitative soil loss estimate (Figure 9-1).

It is found that for PERI < 20, the relationship is quite significant: PERI < 20 explains 78 % of the variation in soil loss estimated by the RUSLE model. On the other hand, for PERI > 20, only 33 % of the variance can be explained, showing poor agreement on estimating or mapping the higher erosion risk areas between the F-WERCAM and RUSLE. One of the main reasons behind this trend could be due to the initial setup of the fuzzy sets: finer sub-sets are concentrated within the lower ranges of the output domain while large portions of the higher domains are covered by fewer fuzzy sets. However, such a setup of fuzzy sets is considered desirable so that the output reflects best the non-linear soil erosion processes as documented in literature.

These equations are used to translate the qualitative fuzzy based map into a relative quantitative map. The quantified soil loss values for each LULC class present in the region are then compared to the original soil loss predicted by RUSLE (Table 9-3). The quantified soil loss values match quite well with the predicted values by RUSLE. For example, the quantified average potential soil loss of the Upper Awash Basin is found to be 344.45 t/ha/yr as compared to 360.72 t/ha/yr predicted by RUSLE.
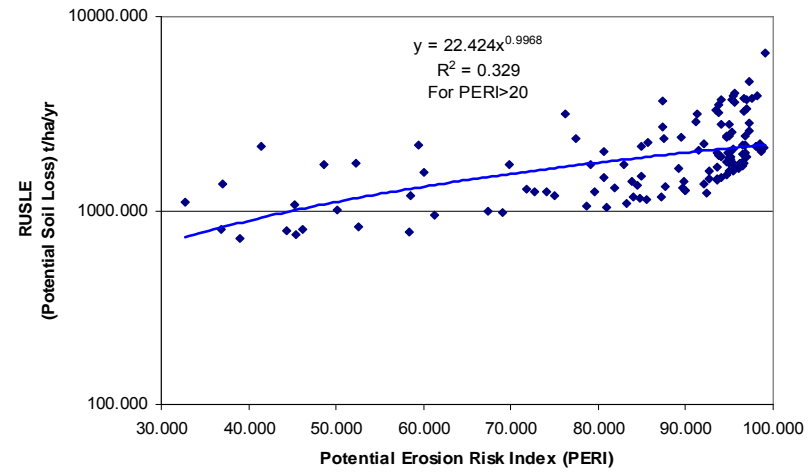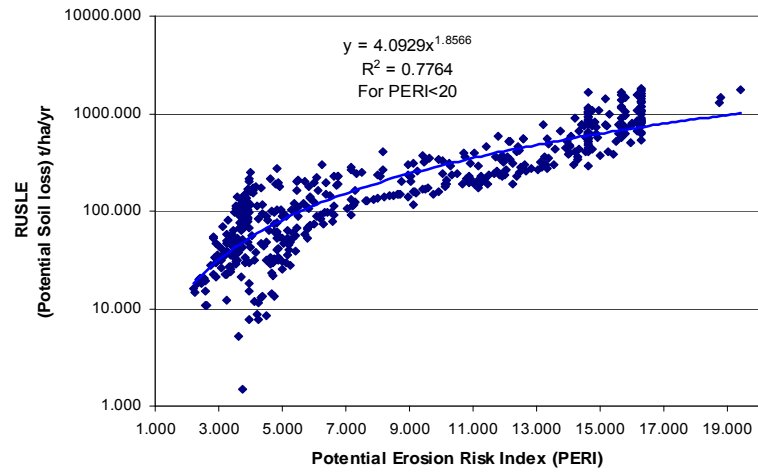
**Figure 9-1: Scatter plot between the PERI and RUSLE based potential soil loss (t/ha/yr)**
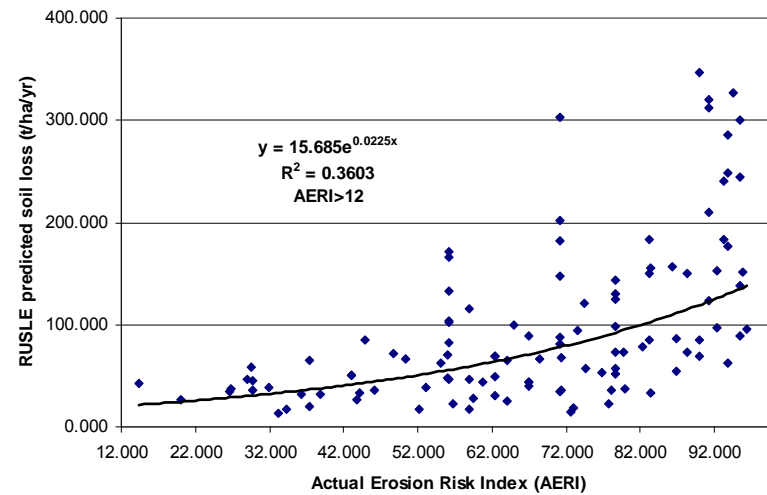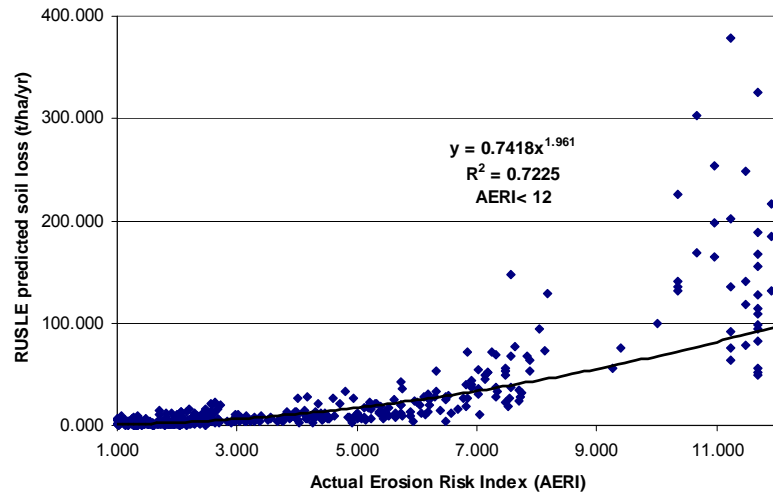

Figure 9-2: Scatter plots between AERI and the predicted actual soil loss (t/ha/yr) by RUSLE of the Upper Awash Basin

Table 9-3: Comparative assessment between PERI and RUSLE predicted potential soil loss (t/ha/yr)

LULC classes	Quantified F-WERCAM average potential soil loss (t/ha/yr)	RUSLE predicted average potential soil loss (t/ha/yr)
Agricultural area	298.07	323.49
Forest	617.59	675.75
Grassland	527.09	553.65
Settlement	163.70	162.00
Scrubland/Wasteland	449.70	456.73

b) Translation of AERI index

Similarly, for the AERI two distinct relationships are compared to the predicted actual soil loss by RUSLE as shown in Figure 9-2. For AERI < 12, a correlation of 0.78 and R^2 of 0.72 is observed. For AERI > 12, a correlation of 0.56 and R^2 of 0.37 is found. This indicates that the capability of AERI to capture the variability of the actual predicted soil loss at the lower soil loss is better than in the upper ranges. A similar trend also exists for the PERI case. This tendency is found earlier when comparing the AERI map with the RUSLE map in qualitative terms. This analysis proves that the soil erosion risk index or risk classes on a regional scale can be quantified relatively in terms of actual soil loss. This is only possible however, if sufficient ground data are available for quantification and thus a statistical assessment can be carried out prior to a fuzzy analysis. The absence of ground data for the Upper Awash Basin makes it difficult to validate the F-WERCAM model results. Hence, the results from other models like RUSLE are used here as proxy data to compare and test whether the predicted erosion risk map by F-WERCAM reflects the soil erosion risk distribution pattern of the region in a similar way as other independent models.

After quantifying the AERI soil erosion risk map using the established relationships, the annual average soil loss from each of the LULC is estimated and compared to the actual soil loss predicted by RUSLE. The average soil loss of the Upper Awash Basin is found to be 15.66 and 17.90 t/ha/yr when quantified by F-WERCAM and RUSLE, respectively. This is however, only an approximate translation that can be utilized for comparison purposes for the evaluation of the F-WERCAM model with RUSLE. This comparison indicates the degree of agreement between the mapped soil erosion risk classes by the F-WERCAM approach with that of RUSLE in a quantitative way (see Table 9-4).

Table 9-4: Comparative assessment between AERI and RUSLE predicted actual soil loss (t/ha/yr)

LULC classes	Quantified F-WERCAM average actual soil loss (t/ha/yr)	RUSLE predicted average soil loss (t/ha/yr)
Agricultural area	12.19	15.54
Forest	2.90	4.73
Grassland	40.25	47.61
Settlement	0.59	0.02
Scrubland/Wasteland	48.73	22.83

9.3   Discussion

Two different approaches for the translation of the fuzzy based qualitative soil erosion risk classes into a quantitative soil loss (t/ha/yr) are presented here. The quantification is first carried out by using the predicted soil loss data from the RUSLE model due to the absence of real ground observed soil loss data. The quantified soil loss using the developed relationships between the F-WERCAM-based index and RUSLE predicted soil loss is in good agreement and satisfactory. The first approach of quantification tries to consider the output range of the final fuzzy sets as the actual soil losses range from 0-300 t/ha/yr as documented in literature. In both approaches, the quantified average soil losses for each of the LULC classes are compared to the soil losses as predicted by RUSLE. The assessment and analysis indicate that this is a reliable approach for cases where a qualitative-based erosion risk index can be quantified relatively in terms of actual soil loss on a regional scale. These approaches serve as an indirect method to evaluate the F-WERCAM-based soil erosion risk map. Additionally, the assessments show the promising performance of the fuzzy sets and rule based system when adopted to erosion risk modelling on a regional scale.

10 Application of F-WERCAM to Produce a Soil Erosion Risk Map of Italy

10.1 Introduction

Soil erosion is one of the major environmental problems throughout Europe. To identify areas with risk of soil erosion, the European Soil Bureau (ESB) has initiated and carried out various national level projects for different parts of Europe using standardized and harmonized datasets (van der Knijff et al., 2002a, b; Grimm et al., 2003). For instance, erosion risk by water is assessed using the USLE model by the European Soil Bureau and a soil erosion risk map of Italy is elaborated. The map provides a way to identify areas that are likely to be vulnerable to long-term rill and inter-rill erosion.

Figure 10-1: Map of Italy showing the different elevation zones

In this research, the geospatial datasets having grid cells of 6.25 ha (250 m x 250 m) used by the European Soil Bureau (ESB) to estimate and produce the soil erosion risk map of Italy, is obtained from JRC, ISPRA, and the European Commission. These datasets are used here to produce a soil erosion risk map of Italy based on the F-WERCAM approach. Here, the existing soil erosion risk map of Italy is taken to compare to the fuzzy-based output and is validated using sedimentation records from lakes and reservoirs by Van Rompaey et al., 2003. They find the R^2 between observed and predicted values to be 62 % and 0.41 for the optimal model efficiency.

This part of research will help evaluating the F-WERCAM model and, in addition, to assess the employed fuzzy rules for mapping the soil erosion risk in different regions of the world.

10.2 Implementing and Mapping the Soil Erosion Risk of Italy

Using the datasets of Italy the F-WERCAM model is executed. Initially, the Soil Protection Index (SPI) map of Italy is produced using Stage 1 of the F-WERCAM model. Here, the NDVI and LULC maps (CORINE land cover 2000 data) of Italy are used as input parameters. The same fuzzification procedure of the parameters and fuzzy rules for mapping SPI is applied as for the Upper Awash Basin in Ethiopia.

Stage 2 and 3 of F-WERCAM produces the Potential and Actual Erosion Risk Index (PERI and AERI) map of Italy. Modifications of the fuzzy sets for all the parameters are carried out to reflect the range of parameter values concerning the environmental conditions of Italy. The number of fuzzy sets adopted for each input parameter remains the same as for the Upper Awash Basin setting, i.e. 5 sets associated with slope, 3 with rainfall erosivity and another 3 with soil erodibility. For instance, the rainfall erosivity map, slope map and soil erodibility map, obtained from ESB, are used as input parameters for the fuzzification. The slope map is derived using the SRTM elevation (0-4560 m a.s.l.) data of the region. The annual rainfall erosivity index ranges from 340-1656 MJ mm (ha h y)$^{-1}$ and the soil erodibility factor ranges from 0.0155-0.08 t ha h (ha MJ mm)$^{-1}$.

The soil erosion risk classes estimated for Italian conditions in t/ha/yr, i.e. range from 0 to > 40 (after van der Knijff et al., 2002a,b) and are used to define the linguistic terms of the output fuzzy sets ("Very Low", "Low", "Medium", etc.). The output soil erosion risk is mapped within the range of 0-300 t/ha/yr, where 0-1 (VL); 1-5 (L), 5-20 (M), 20-40 (H) and > 40 (VH). The upper threshold of output soil loss range of 300 t/ha/yr is adopted here, since a soil loss value greater than 40 t/ha/yr is considered to be within a "Very High" soil erosion risk class for Italian conditions (van der Knijff et al., 2002). The range of the output linguistic sets is redefined in order to capture the tolerable soil loss limit of Italy which ranges from 0- 5 t/ha/yr (Rusco et al., 2009; Alexander, 1988). The fuzzy rules used to produce PERI of Upper Awash Basin are adopted here also. Finally, the actual soil erosion risk map is obtained using the SPI and PERI map of Italy as input fuzzy parameters. The fuzzy rules base (RB1) defined for assessing the actual soil erosion risk of the Upper Awash Basin is used to map the soil erosion risk of Italy.

Once the SPI and AERI maps of Italy are obtained from F-WERCAM, they are compared to the existing soil erosion risk map of Italy provided by the European Soil Bureau (ESB). This allows us to compare the degree of agreement between the two soil erosion risk maps as obtained from two different modelling approaches. Such an assessment can show how well the fuzzy rule system developed for a specific region can be transferred for the use in another region provided that the parameters influencing soil erosion risk in both regions are considered to be similar.

10.2.1 Establishment of a Relationship between the SPI and the Erosion Risk Map of Italy

For this purpose, the SPI distribution map is compared to the soil erosion risk map of Italy. It is found that the distribution pattern of the SPI over the region explains quite well the variability of the soil erosion risk distribution pattern provided by the ESB. In general, regions of higher SPI are found to have a lower soil erosion risk and *vice versa*. For example, low lying areas in and around Milan, Bologna, Turin is categorized under High SPI and its corresponding soil loss is found to be within the range of 0-3 t/ha/yr; this is within VL to L erosion risk classes. It can be clearly seen that the Alps and the central part of Sicily has a higher soil erosion risk potential; consequently, their corresponding SPI is found to be within the VL class (Figure 10-2). Hence, the SPI distribution map from the F-WERCAM model is able to capture quite well the spatial distribution pattern of soil erosion risk.
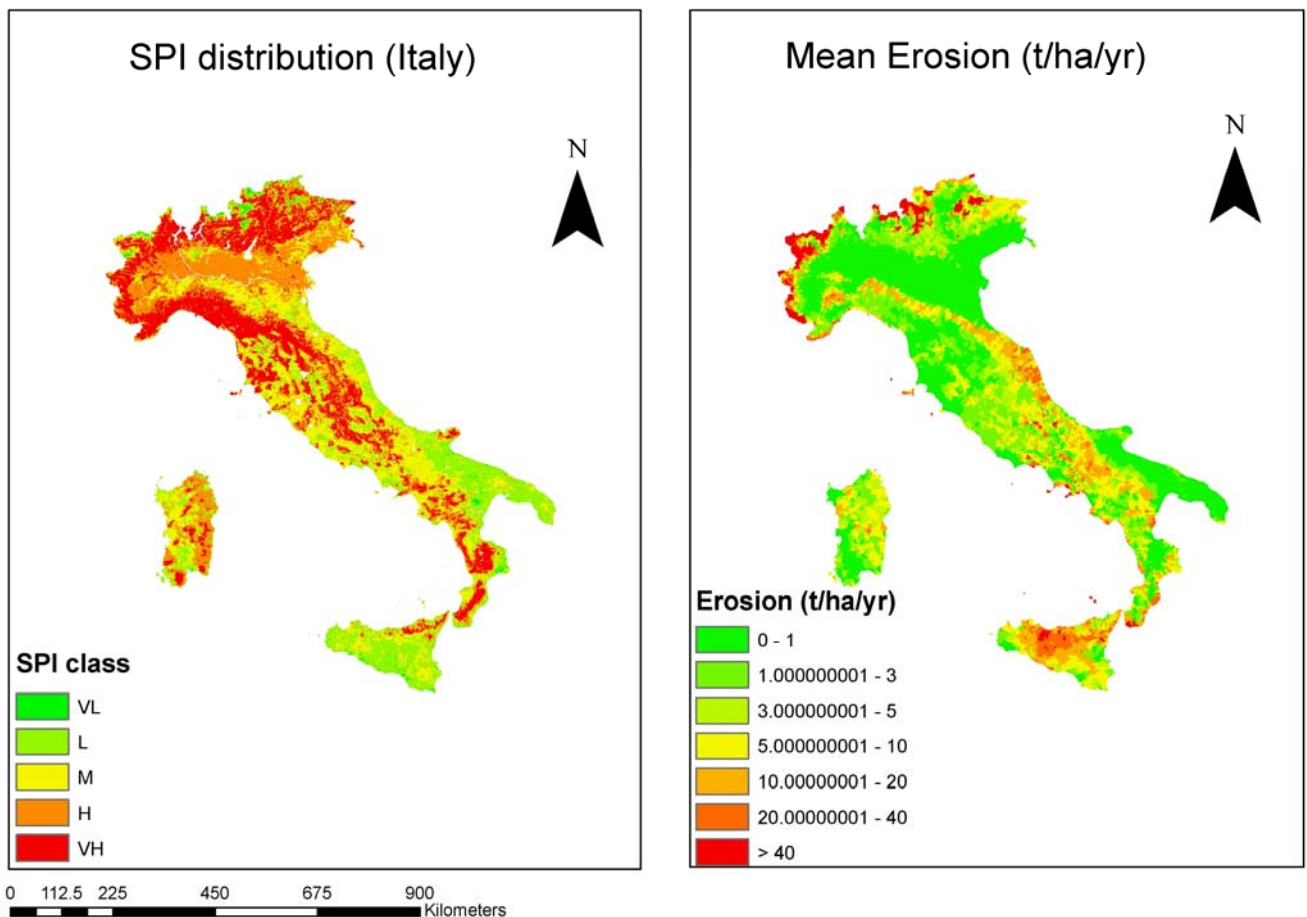

Figure 10-2: SPI distribution map of Italy mapped using F-WERCAM and the mean soil erosion risk map of the region (adopted from van der Knijff et al., 2002a, b)

A detailed assessment is carried out by comparing the distribution pattern of SPI and soil erosion risk in and around Sicily (Figure 10-3). It is found that the SPI distribution clearly explains the variability of soil loss distribution, covering around 83 % of Sicily. On the other hand, the SPI cannot explain the variability in the distribution of the soil erosion risk that covers the remaining app. 17 % of the region. It is found that the SPI response is insignificant, in areas with higher elevation and, accordingly, higher slope gradients. This demonstrates clearly the influence of topography on the assessment of soil

loss. It is reported that the soil erosion risk map of Italy from the ESB seems to overestimate in regions with a higher slope gradient. The overestimation of soil loss in these regions may be due to the coarse resolution of ~250 m for the elevation data used to compute the slope map. This may be one of the reasons behind the insignificant response of SPI on soil loss in these regions.

In general, the SPI distribution map captures and provides an overview on the potential soil loss of the region irrespective of the topography, soil type and climatic factors. The mean SPI and soil losses for each province of Italy are computed and relationships are established by scatter plots. The two parameters are found to be correlated with a correlation coefficient of -0.30 and P values below 0.05. This indicates that as one variable tends to decrease the other increases. It is found that with an increase in the mean SPI of each province the mean soil loss values tend to decrease as illustrated in Figure 10-4.
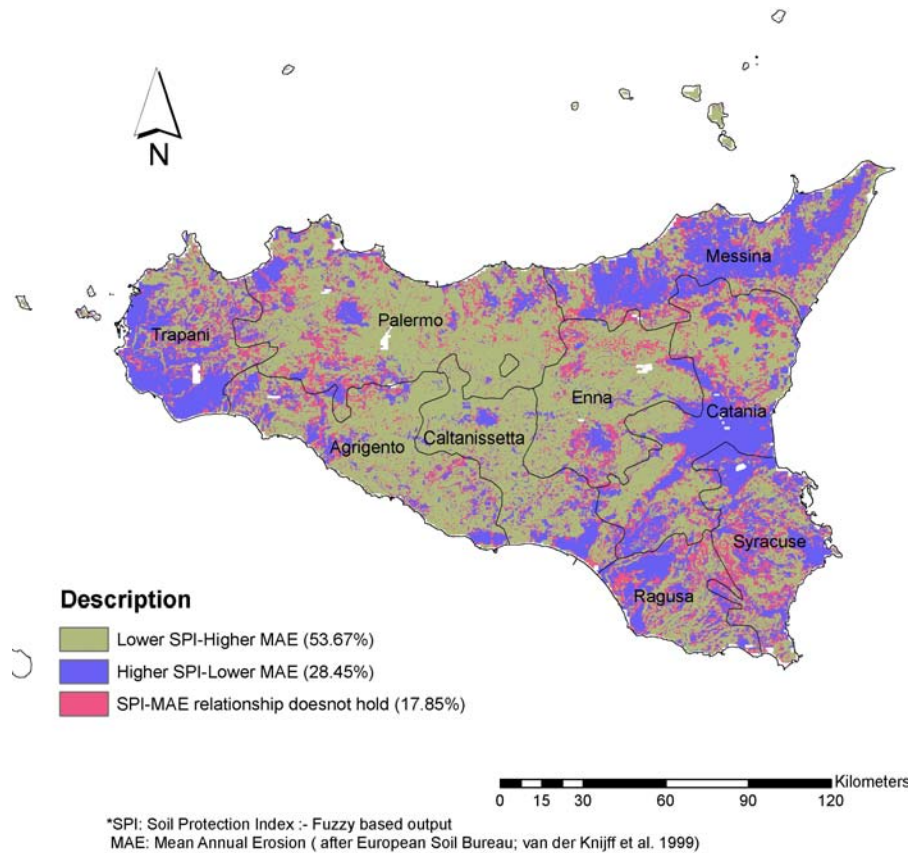

Figure 10-3: Response of spatial distribution of SPI on the mean annual erosion as predicted by European Soil Bureau for Sicily (Italy)

From this analysis, it can be seen that the fuzzy rules developed for the Upper Awash Basin for mapping SPI are able to map satisfactory also the SPI of Italy. This indicates that the fuzzy rules can be transferred provided the ranges of the input fuzzy parameters and sets are redefined to capture the local variation and distribution of the parameters considered. For example, when defining the fuzzy sets for NDVI, the possible value-ranges of NDVI are taken into account, thereby allowing it to be implemented into the rules and sets in different environmental setups. A similar case can be found for the LULC parameters, where the existing land cover and land use classes are simplified to major LULC classes present in any part of the globe.
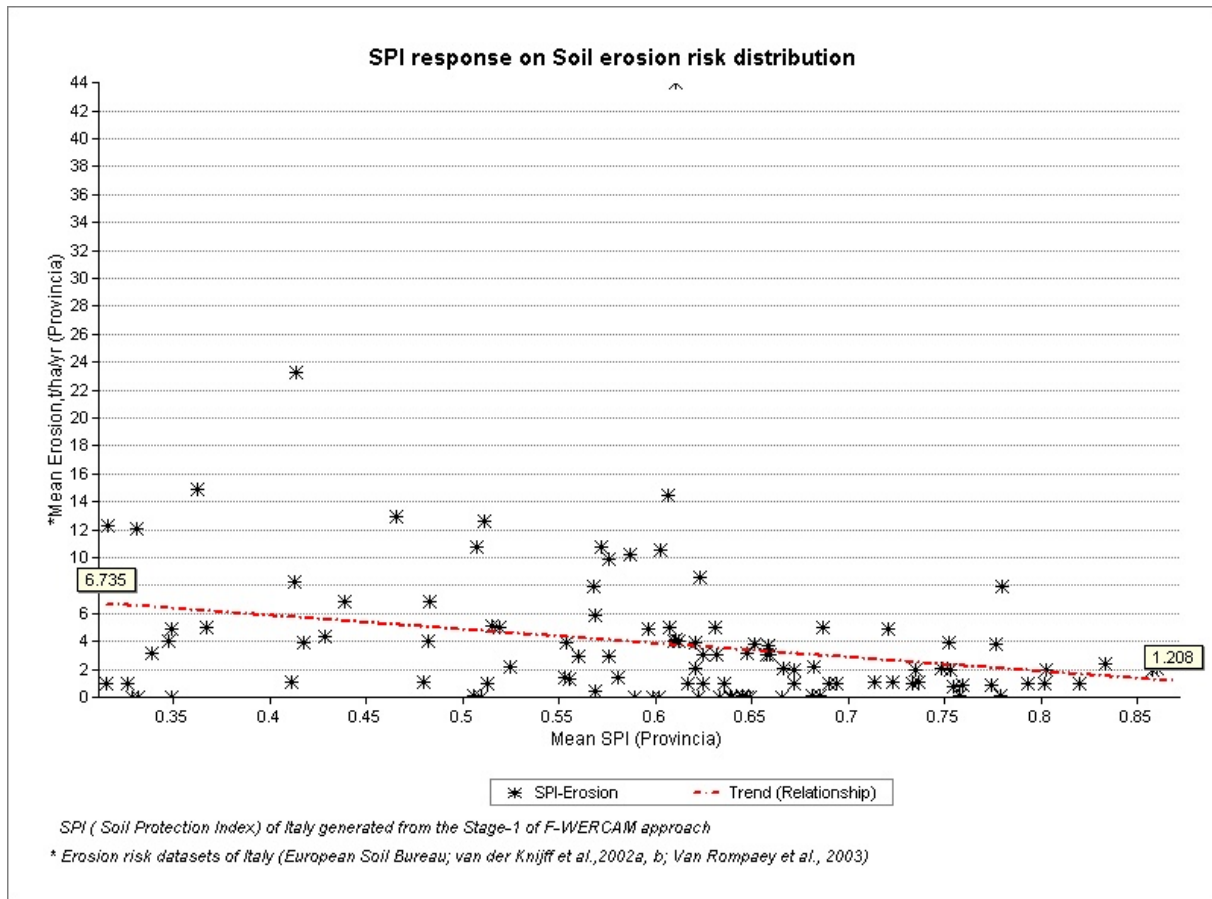
Figure 10-4: Response of SPI distribution on the spatial soil erosion risk distribution of Italy

10.2.2 Evaluation of Fuzzy-based Erosion Risk Map with Existing Erosion Risk Map of Italy

The spatial distribution of the erosion risk maps of Italy from two different approaches are shown in Figure 10-5. The fuzzy based erosion risk map is able to explain about 41 % of the variability of the erosion risk distribution classes as classified in the existing erosion risk map provided by ESB. The comparison is done by taking into account the spatial dependency of the risk distribution classes. If one class difference in the erosion risk between the two erosion risk maps is considered as sufficient, the overall accuracy of the map is found to increase to 71 %. It is observed that the fuzzy-based erosion risk distribution map captures the general pattern of erosion risk as predicted by USLE method of ESB.

For instance, the predicted soil erosion risk map by F-WERCAM indicates that the central region of Sicily and some localized regions in the northern Alps near Aosta, Bolzano are under a "Very High" (VH) erosion risk. This prediction by F-WERCAM agrees quite well with the soil loss map of Italy provided by ESB. Moreover, Costantini et al. (2004) also report that most parts of Sicily are found to have areas with high soil erodibility. This, combined with the high energy of the relief and Mediterranean type of climate, lead the authors to classify the risk of soil erosion in these regions to be "Very High" (VH). Some isolated regions with higher soil erosion risk in the northern Alps are found

to correspond to areas with abandoned agricultural fields and degraded forests with steep slope gradients. From this point of view, the performance of the F-WERCAM prediction can be considered to be quite satisfactory.
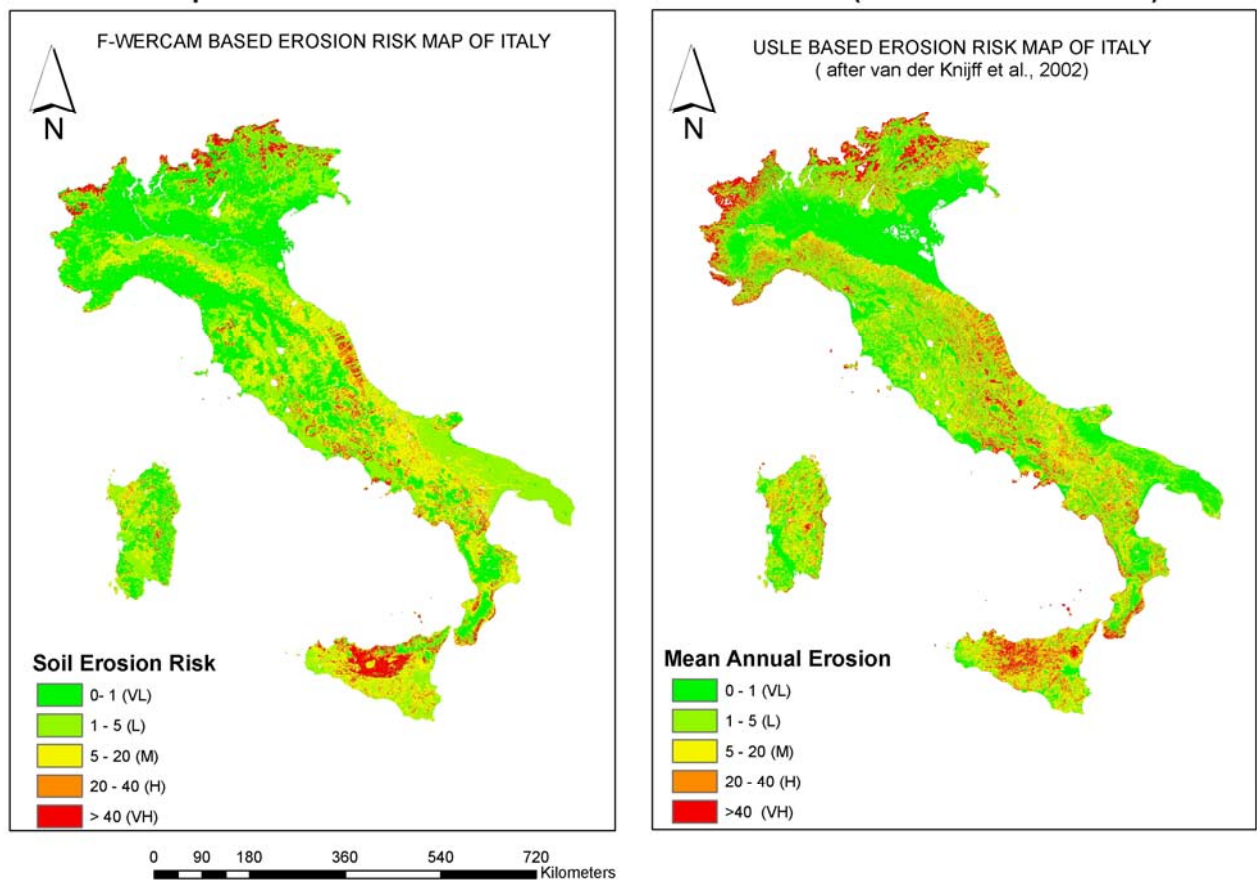

Figure 10-5: Comparison of F-WERCAM-based actual erosion risk map with the USLE-based existing mean annual soil loss map of Italy

Furthermore, the occurrence of soil erosion risk classes is assessed by plotting the histogram of the two risk maps (Figure 10-6). It is seen that there is an underestimation of the percentage coverage in H and VH erosion risk classes by F-WERCAM, whereas overestimation is observed in the distribution of the lower risk classes. One of the probable reasons behind the differences is due to the difference in the modelling approaches.

Even though the existing soil erosion risk map used for reference and comparison purpose is based on the most accurate data available for the whole of Italy, van der Knijff et al. (2002a, b) warn about possible errors involved in model simplifications and input errors. Moreover, the fuzzy rules used to produce the erosion risk map of Italy are transferred from the Upper Awash Basin – a substantially different study area. However, at least modifications to the fuzzy sets to reflect the local environmental conditions of Italy are carried out here. In all certainty, these factors may influence the output soil erosion risk distribution of the two approaches. It is necessary to remind that the comparison between the two maps is only intended to draw conclusions on the *general* pattern of the erosion risk distribution over a large regional scale and the possibility of transferring a fuzzy rules system.
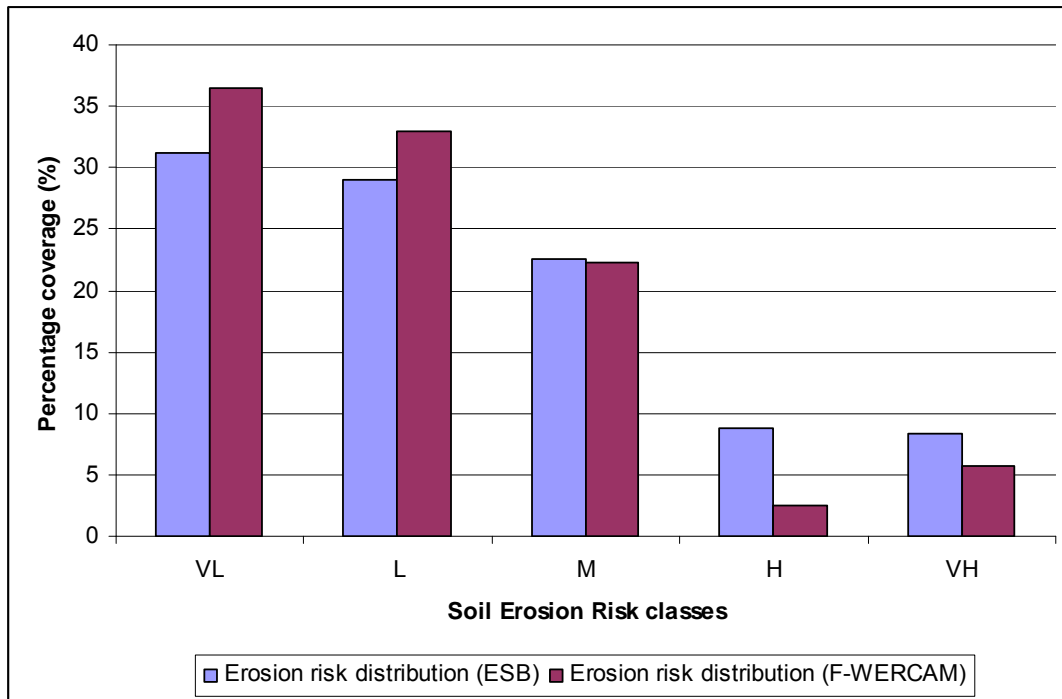
Figure 10-6: Histogram of erosion risk classes of Italy as obtained using F-WERCAM and ESB

10.2.3   Soil Loss Quantification for Italy Using F-WERCAM

Considering the output defuzzified value by F-WERCAM to be the actual soil loss in t/ha/yr, the mean soil loss for each of province of Italy is extracted and compared to the predicted mean soil loss for each province based on the existing soil erosion risk map of Italy. The average annual soil loss obtained from F-WERCAM is 18.90 t/ha/yr and that of the existing map is 18.19 t/ha/yr. A positive correlation coefficient of 0.62 is found when comparing the mean soil loss for each province. This indicates that the variation compared to the existing soil loss map is about 62 %. A table showing the mean annual soil loss by extraction from the two different erosion risk maps for each Italian province can be found in *Appendix 8*. Here, discussions on the typical cases for some provinces which have a good and very poor agreement on the soil loss values are provided in Table 10-1. It is found that provinces which have a low average slope gradient (< 11 %) are found to have a good agreement on the predicted soil loss values. For example, Cagliari, Gorizia and Bologna are some of the selected provinces that are found to have similar soil loss values as predicted by the two approaches. On the other hand, poor agreement on the soil loss values or higher mean error between the two maps are found in areas of higher slope gradients, (i.e. greater than 35 %). For instance, an underestimation of soil loss values by F-WERCAM can be seen in Trento, Aosta, Sondrio etc., compared to the predicted soil loss values by ESB.

The difference in input parameters when computing the soil erosion risk of the region by the two methods in addition to the difference in the modelling approach may be the main reason behind the difference in predicted soil loss values.

Table 10-1: Comparison of mean average soil loss values of some selected provinces of Italy

ID	Province	Mean average soil loss (t/ha/yr)	
		Soil erosion risk map (van der Knijff et al., 2002a, b)	Erosion risk map (F-WERCAM)
1	Milan	0.342	0.907
2	Gorizia	2.416	2.598
3	Bologna	4.999	4.638
4	Cagliari	6.513	7.340
5	Udine	37.657	23.480
6	Verbano Cusio Ossola	35.913	21.605
7	Trento	52.538	19.748
8	Aosta	151.095	72.356
9	Sondrio	124.354	78.268
10	Enna	21.175	110.564
11	Caltanissetta	19.993	79.290
12	Agrigento	18.900	50.211

More precisely, the difference in incorporation of effects of the vegetation cover factor, i.e. usage of the C factor in USLE and SPI in F-WERCAM and the topographic factor, i.e. incorporation of the slope gradient in F-WERCAM as compared to the LS factor of USLE, seems to be the main reason behind the difference in the predicted soil loss by these two approaches. Nevertheless, the overall predicted values by F-WERCAM are found to be reasonable, given that, the F-WERCAM approach uses expert knowledge in the form of fuzzy rules to map the soil erosion risk while USLE based soil erosion map of ESB uses empirical equations for the computation of soil loss values.

From the above discussion, it can be seen that the fuzzy rules developed for the Upper Awash Basin are able to satisfactorily map the soil erosion risk of Italy. It can be pointed out that the transferability of the fuzzy rules from one place to another depends on the variability of the influencing parameters considered to develop the fuzzy sets. The use of more generalized and standardized parameters tends to cover a large domain of application. This allows the fuzzy rules and sets to be applied to other locations with none or little modifications depending on the scale and the type of data availability.

10.3 Summary

The implementation of the F-WERCAM model is carried out for Italy using geospatial datasets obtained from JRC, European commission. Fuzzy rules developed for the Upper Awash Basin are tested to produce an erosion risk map of Italy. For the fuzzy rules to be applied effectively, it is required that similar input parameters adopted for the Upper Awash Basin are considered for Italy, too. The SPI and AERI maps of Italy are evaluated by comparing them to the existing soil erosion risk map of Italy. The response of the SPI to the erosion risk distribution of the region is assessed and it is found that SPI is negatively correlated with the annual soil loss of the region. This assessment shows that the produced SPI map of Italy, using the fuzzy rules of Upper Awash Basin, is able to capture quite well the variability of the soil erosion risk distribution predicted by the European Soil Bureau.

The erosion risk map produced by the F-WERCAM model is found to represent the general trend of the erosion risk distribution as predicted in the existing erosion risk map. When comparative analysis is performed, it is found that there are areas with similar and dissimilar erosion risk classes but a good overall agreement between the two maps is shown.

It is also seen that there is an underestimation of the percentage coverage in the H and VH erosion risk classes by F-WERCAM, while a slight overestimation is observed in the distribution of lower risk classes. Even though the existing soil erosion risk map used here for comparison is ground validated, possible errors involved in the model application resulting from both, model simplification and input errors, need to be taken into consideration when evaluating the two erosion risk maps. This assessment provides an understanding of the erosion risk distribution as predicted by different modelling approaches. In addition, it shows the potential and capability of implementing the F-WERCAM model under different environmental conditions. There is a possibility to carry out a more detailed assessment and mapping by adding other input parameters (depending on data availability) and implementing new expert-based fuzzy rules that reflect the local conditions.

11 Conclusions and Recommendations

11.1 Overview of Research Objectives and Results

A simple and efficient fuzzy logic-based soil erosion risk model for monitoring the erosion risk distribution over a regional landscape is developed. The F-WERCAM model is designed in such a way that it has fewer input data requirements, provided that the considered parameters are the main governing parameters influencing the soil erosion risk of a region. The identification of the influential parameters is based on literature and expert based knowledge. Detailed literature reviews of the erosion processes over a regional landscape and expert-based questionnaires provide the background for the formulation of fuzzy sets and fuzzy rules. The multi-stage modelling framework of F-WERCAM allows the simplification of the fuzzy rule bases by reducing the number of input parameters at each stage of the modelling. This approach allows a step-by-step evaluation of the intermediate results. For instance, Stage 1 of the modelling approach stands for the evaluation of the Soil Protection Index (SPI) of a region, before integrating the Potential Erosion Risk Index (PERI) of Stage 2 obtaining the final Actual Erosion Risk Index (AERI) of a region. The final soil erosion risk map provides qualitative based information on the distribution pattern of the soil erosion risk classes over a region. In addition, a possibility of quantifying the output soil erosion risk index into a relative soil loss value (in t/ha/yr) is given. The quantified soil loss using the relationships between the F-WERCAM-based index and RUSLE predicted soil loss is in good agreement and satisfactory.

The assessment of LULC classes of the Upper Awash Basin and the influence of temporal changes in LULC patterns on the soil erosion risk distribution of the region is also addressed in this research. A LULC model is set up within ArcGIS for this purpose. The actual erosion risk map corresponding to the year 2000 is evaluated against the actual erosion risk map of 2001. The spatial distribution of AERI at different time periods clearly indicates that changes in LULC affect the degree of soil erosion risk and hence the potential rate of land degradation of the region. From this assessment study, it is found that soil erosion prioritization measures in the Upper Awash Basin should focus on the areas in Tole, Ada Chukala, Addis Alem and near to the Walmara region. These areas are classified within "High" and "Very High" erosion risk; irrespective of the effect of temporal land use and vegetation cover over the region.

The potential of utilizing indirect satellite-based rainfall estimates as input parameters for the modelling purpose by deriving the rainfall erosivity of the region is also investigated and discussed in this research. Different soil erosion risk maps are computed using different rainfall erosivity maps of Upper Awash Basin to assess the applicability of other rainfall source data.

The absence of ground observed spatial distributed soil loss data over the Upper Awash Basin limits the study in terms of a validation of the fuzzy based erosion risk map. In addition, since the F-WERCAM framework is developed specifically for mapping the qualitative soil erosion risk distribution on a large regional scale using limited available data, a proper validation becomes one of the major issues. Hence, to evaluate the F-WERCAM output, a comparative assessment of F-WERCAM and RUSLE soil erosion risk map is carried out. Similar predictions of erosion risk classes

are found mostly in low-lying plain and valley areas while major differences in risk classes are seen in higher elevated regions of the Upper Awash Basin.

Additionally, the developed model is tested by producing the erosion risk map of Italy using the same fuzzy rules developed for the Upper Awash Basin. The resulting erosion risk map is compared to the existing ground validated erosion risk map of Italy. The average annual soil loss of Italy obtained from the F-WERCAM model is found to be around 18.90 t/ha/yr and that of the existing map to be 18.19 t/ha/yr. A positive correlation coefficient of 0.62 is found when comparing the mean soil loss for each province. This indicates that the variation between the results obtained from the F-WERCAM model compared to the existing soil loss map of Italy is about 62 %. This assessment provides a preliminary insight for the possible applicability of the developed model in other environmental conditions.

Most of the past soil erosion prediction studies using a fuzzy logic approach seem to lack the incorporation of important indicators or surrogate parameters that influence the soil erosion risk. For instance, most of the fuzzy erosion prediction models reported in literature are found to incorporate only parameters pertaining to topography, geomorphology and soil type without considering the influence of vegetation cover, type of LULC and rainfall. These approaches make the models simpler (i.e. development of fuzzy rules), although the soil erosion processes are not captured adequately. In this research, in order to reflect the erosion processes over the catchment more accurately, the F-WERCAM model is set up by incorporating the standard soil erosion governing parameters like soil erodibility, rainfall erosivity, slope gradient in addition to LULC and NDVI. Utilization of these standard parameters as inputs for the modelling allows the experts and users to provide consistent and less subjective judgements when setting up the fuzzy sets and fuzzy rules. On the other hand, in most of the GIS based soil erosion models classifying the input source data results in information loss. The results of the analysis are more or less dependent on the class limits and the number of classes used for the input parameters. This limitation of GIS based modelling is addressed in F-WERCAM by fuzzifying the input parameters to account for the uncertainty of the threshold of the classes adopted. The developed F-WERCAM model tries to represent the soil erosion process adequately over the catchment and the inherent problem related with a crisp logic approach in GIS. Nevertheless, F-WERCAM is intended to provide a general pattern of the relative difference of soil erosion risk over the test site rather than providing accurate absolute erosion risks.

Furthermore, modelling within GIS allows a regional scale soil erosion risk assessment, thereby addressing the problem of large scale field-based erosion studies which is considered to be an unviable option by many researchers and policy makers. This kind of model is intended for a quick appraisal or monitoring of erosion risk over a large landscape and should help in identifying the hotspot zones for mitigation measures and further detailed assessments. To conclude, the integration of fuzzy logic within GIS using remotely sensed data in this research provides a new direction toward soil erosion risk assessment which tries to address the problems of data scarcity, uncertainty in input model parameters and handling of large spatial data effectively.

11.1.1 Addressing Research Questions

Specific conclusions of this PhD study are given here with respect to each of the research questions framed in the beginning of this thesis.

- **Can simple linguistic fuzzy rules which are based on literature and expert knowledge capture the soil erosion risk distribution patterns as efficiently as other existing erosion models in a regional landscape?**

Fuzzy rules provide functional mapping between an input and a predicted output in a fuzzy logic model. It is observed that using the developed F-WERCAM model, once the fuzzy sets and rules are set up the fuzzy inference system allows mapping and predicting the soil erosion risk. It is found that expert-based fuzzy rules are capable of displaying the variability of the erosion risk distribution over the Upper Awash Basin. For instance, when mapping the actual erosion risk (AERI), utilization of the Rule Base 1 (RB1) with output fuzzy sets having a combination of triangular and trapezoidal membership functions provides a better degree of agreement, having an overall accuracy of 70 % and a kappa value of 0.51 compared to the RUSLE-based erosion risk map. Nevertheless, differences in predicted erosion risk classes between the two modelling approaches are also found. Furthermore, the fuzzy rules are tested on Italian conditions and the mapped SPI and erosion risk map of Italy is found to be in good agreement with the existing erosion risk map of the region provided by the European Soil Bureau (ESB). Hence, the role of linguistic fuzzy rules based on literature and expert knowledge are able to capture quite well and to represent the information on soil erosion risk distribution patterns over a large landscape. Representation of the water erosion processes by fuzzy rules results in an easily understandable and simplified erosion risk model. But the absence of ground training dataset limits the development of fuzzy rules that are based on literature and expert knowledge only.

- **Which factors can explicitly represent the variability of vegetation cover distribution and their significance on erosion risk classification or assessment over the basin?**

The combined effect of the LULC and NDVI map of the Upper Awash Basin can be combined into a 'Soil Protection Index' to evaluate the influence of vegetation cover distribution on the soil erosion risk intensity of the region. The variability of vegetation cover within a specific land use class is taken into account by the NDVI distribution pattern. From the analysis, the SPI is found to capture the spatial variability and the associated degree of soil sensitivity to erosion as represented by the soil erodibility of the region. The SPI is negatively correlated with the soil erodibility of the region. The effect of the monthly averaged SPI on the actual erosion risk of the Upper Awash Basin is also estimated. With increasing monthly rainfall there is an increasing tendency of lower erosion risk in the region. This can be linked to the fact that with increasing rainfall, there is an increase in vegetation biomass, thereby increasing the SPI and lowering the soil erosion risk of the region. In general, susceptibility of the Upper Awash Basin to higher erosion risk is found during the little rainy and dry periods (January-March and November-December) than in the main rainy period of the year, thereby reflecting the influence of vegetation cover dynamics on the erosion risk distribution pattern. For the computation of the potential erosion risk (PERI) of the region, only the annual rainfall erosivity is taken into account. The influence of monthly rainfall erosivity is not considered in the assessment due to the lack of rainfall intensity data. Nevertheless, the effect of rainfall on the erosion risk in Upper Awash Basin is found to be greatly muted by the presence of dense vegetation cover during the main rainy period. Similarly, the SPI is mapped for Italy and it is found to capture well the variability of the erosion risk distribution pattern of Italy as well. To

conclude, the importance of the temporal distributed NDVI and LULC as influential parameters in the assessment of erosion risk using a fuzzy rule-based approach is discussed and verified in this research.

- **Is there a way toward quantitative assessment in addition to qualitative assessment of the erosion risk using the F-WERCAM model framework?**

The F-WERCAM model results in soil erosion risk index classes, which are qualitative in nature. With respect to the qualitative based assessment, it is found that from the various combinations of rules and output fuzzy sets, the range of the overall accuracy compared to the RUSLE model output, varies from 54.64 % to 71.30 %, having corresponding kappa values of 0.34 to 0.52. Hence, it can been seen that depending on the type of defined output membership functions and adopted fuzzy rules, the output erosion risk maps differ in their spatial distribution pattern as reflected by the difference in their accuracy. On the other hand, two different possible approaches for the quantitative assessment are carried out in this research. The initial approach considers a fuzzy output range of 0-300 t/ha/yr to be the actual soil loss range within the Upper Awash Basin by applying the concept of tolerable soil loss of the region. With this approach, the average soil loss of the Upper Awash Basin can be estimated to 27.11 t/ha/yr. The approach tends to overestimate when compared to the RUSLE predicted soil loss value of 17.90 t/ha/yr. Another approach is exerted to quantify soil erosion risk by establishing a relationship between the F-WERCAM model output risk index and the actual soil loss range as predicted by RUSLE. The main focus is to see whether the qualitative based index (0-100) by F-WERCAM can be translated to the actual soil loss as observed from the ground or predicted from other models by setting up a relationship between them. In the absence of ground soil loss measured data, the predicted soil loss value of the region by RUSLE at different locations is considered as the proxy data to establish a relationship of the F-WERCAM index scale for quantification purposes. The average soil loss of the Upper Awash Basin is found to be 15.66 and 17.90 t/ha/yr quantified by F-WERCAM and RUSLE, respectively. This is, however, only an approximate translation used for comparison purposes for the evaluation of the F-WERCAM model with RUSLE. Hence, the possibility of approximate quantitative reasoning of the soil erosion risk in addition to qualitative based analysis is investigated and discussed in this research.

- **What is the accuracy of mapped erosion risk when satellite-based rainfall estimates are used as a climatic parameter, instead of gauged measured rainfall?**

The need of using satellite-based rainfall data for erosion risk assessment is underpinned by the fact that there is lack of sufficient ground monitoring rainfall stations and associated data in various parts of the world, especially in developing countries. The actual erosion risk map produced by using the TRMM data and CPC data are compared to the actual erosion risk map computed using ground rainfall data (AERI_G). From the visual interpretation and histogram analysis, it is observed that when comparing the AERI_CPC and AERI_TRMM to AERI_G, there is a slight difference in the erosion risk class distribution which comprises about 2.1 % and 1.7 % of the total study area, respectively. It can be concluded from the analysis that, irrespective of the input rainfall source data, the classified erosion risk map by F-WERCAM has a very good agreement with the ground rainfall-based erosion risk map and only a slight variation and difference in erosion risk classes' distribution is noticeable. Hence, the use of

satellite-based rainfall estimates as an alternate source of data looks promising and may be able to bridge the gap of data scarcity in developing countries and help in monitoring the soil erosion risk of a region.

11.2 Strengths and Weaknesses of the Developed F-WERCAM Model Framework

The strengths and weakness of a model can be assessed by examining whether the model serves its intended purpose and goal. The F-WERCAM framework is unique as it adopts the underlying principle of fuzzy logic for erosion risk classification and analysis in a multi-stage approach. From this research, the main strengths and weaknesses of the F-WERCAM modeling framework can be discussed as below.

Strengths of the F-WERCAM framework

o F-WERCAM effectively handles the problem of uncertainty and imprecision by representing each of the identified model parameters as fuzzy parameters. This modeling approach handles both the qualitative and quantitative variables effectively in the form of linguistic sets, defined by using the membership functions.

o The multi-stage modelling framework allows handling the problem of dimensionality when formulating the fuzzy rule bases. Fewer input fuzzy parameters at each stage mean simpler rules and the evaluation of the model at each intermediate stage is possible. For instance, for mapping the SPI, the fuzzy rule base consists of only 20 rules and for PERI the rule base consists of only 45 rules. The final stage that combines SPI and PERI consists of only 25 logical rules.

o Smaller input data requirements and capabilities to incorporate additional expert knowledge in the form of fuzzy rules allow this modelling framework to be tested and applied to other parts of the world. Here, F-WERCAM is tested satisfactory for producing the erosion risk map of Italy.

o Implementation of the framework within GIS allows the handling of both spatial and non-spatial data with ease and it allows for an efficient decision making through spatial analysis. In addition, fuzzy modeling within GIS provides a spatial dimension to the nature of the predictive soil erosion risk results, thereby providing the spatial variability of the outcomes visually and statistically. This research shows the spatial and temporal-based analysis of the F-WERCAM output in GIS to understand the dynamic of erosion processes in the Upper Awash Basin.

o Overall, the F-WERCAM methodology is easy to use and interpret since it adopts the standard governing parameters of soil erosion that are widely accepted all over the globe. This approach allows rapid scenario analysis for large regions and has the potential to be used as a practical tool for the assessment of soil erosion risk by policy makers and scientists.

Weaknesses of the F-WERCAM framework

   o F-WERCAM based soil erosion risk mapping provides only qualitative information about the varying degree of surface water erosion risk in a region. A possible quantification or translation of the qualitative erosion risk classes to a quantitative soil loss range is discussed in this research even though the outcome is not fully satisfactorily. From the quantification approach tested and assessment carried out, it can be concluded that there is a potential of quantification of soil loss value by the fuzzy based model. With ground observed soil loss data, more detailed assessment on the quantification procedure can be developed, implemented and tested.

   o The model results are more or less dependent on the design of the fuzzy sets and the fuzzy rule base adopted. In another words, the predicted erosion risk distribution pattern over the region is influenced by the expert knowledge base and the experience of the user. Hence, the question of subjectivity is still a concern in such expert based modelling approach.

   o Proper validation of F-WERCAM is still another issue due to lack of ground measured soil loss data on a large regional scale. To evaluate the effectiveness of the F-WERCAM model, an indirect approach of assessment with RUSLE based soil loss data and a comparison with the existing soil erosion risk data of Italy is worked out in this research. The model is still open for further assessment and improvement with regard to validation.

   o The F-WERCAM does not account for mapping the deposition of the eroded soil and concentrated flow erosion in the landscape.

   o The selection of the input parameters that govern the soil erosion risk processes is specific and limited due to the fact that an increasing amount of input parameters results into a complex fuzzy rule base.

11.3 Outlook and Recommendations

Some of the future prospects and recommendations to enhance and improve the F-WERCAM modelling capabilities are listed below:

a) Further quantification of the model output in addition to the approach tested in this research should be examined. The possibility of generating fuzzy rules from numerical data should be investigated as an extension of this research. Specifically, the possibility of applying the data driven fuzzy rules optimization techniques is recommended. One of the pre-conditions for applying such algorithms is that prospective test regions need to have sufficient ground data for training the rules. Only then a comparison of the soil erosion risk maps obtained from expert and data driven approaches can be performed to assess the overall model performance. For example, the HILK algorithm (Highly Interpretable Linguistics Knowledge bases using Fuzzy Logic Formalism) after Alonso et al. (2008) can be used to generate the fuzzy sets and rules, then finally employed in the F-WERCAM model to map the soil erosion risk of a region.

b) Further temporal based assessment can be done by taking into account the monthly rainfall erosivity in addition to temporal vegetation cover as it may provide additional results or findings on the synergetic influence of both parameters on the temporal soil erosion risk distribution of Upper Awash Basin. For this assessment, computation of the monthly or seasonal rainfall erosivities is required. This can be done when long term data on rainfall intensity (I) or duration of rain segments (T) of the region is made available.

c) Additional stages of fuzzy modelling can be implemented in the developed framework by introducing relevant input parameters that focus on identifying the large gullies and mapping the depositional area within the region. Factors such as drainage density, lithology, surface runoff, and Topographic Wetness Index (TWI) can be considered as potential fuzzy parameters which account for topogpahic influence on soil erosion risk. In addition, various satellite based vegetation indices for example FVC (Fractional Vegetation Cover), EVI (Enhanced Vegetation Index), LAI (Leaf Area Index), etc. can be considered as potential fuzzy parameters which can reflect the vegetation cover distribution. Especially, FVC (Fractional Vegetation Cover) can be used to represent the amount of vegetation distributed in a horizontal perspective.

12 References

Adinarayana J., Rao K.G., Krishna N.R., Venkatachalam P. and Suri J.K., (1999) *A rule-based soil erosion model for a hilly catchment*; Catena, 37, pp. 309-318.

Ahamed T.R.N., Rao K.G. and Murthy J.S.R., (2000) *Fuzzy class membership approach to soil erosion modelling*; Agricultural Systems, 63, (2), pp. 97-110.

Alberts E.E., Nearing M.A., Weltz M.A., Risse L.M., Pierson F.B., Zhang X.C., Laflen J.M. and Simanton J.R., (1995) *Soil Component, Chapter 7 of WEPP User Manual*; (URL: http://www.ars.usda.gov/SP2UserFiles/ad_hoc/36021500WEPP/chap7.pdf).

Alemayehu T., Ayenew T., Legesse D., Tadesse Y., Waltenigus S. and Mohammed N., (2003) *Scientific Report on the Groundwater Vulnerability Mapping of the Addis Ababa Water Supply Aquifers, Ethiopia*; UNEP/UNESCO/UNHABITAT/ECA. Accessed on 15-02-2009 from the URL: (http://www.unep.org/dewa/water/GroundWater/English/GWhmEng/Country%20Profiles/Ethiopia/AddisAbaba-Report.pdf).

Alexander E.B., (1988) *Strategies for Determining Soil Loss Tolerance*; Environmental Management, 12, (6), pp. 791-796.

Al-Harbi K.M.A., (2001) *Application of the AHP in project management*; International Journal of Project Management, 19, (4), pp. 19-27.

Anderson R., Hardy E.E., Roach J.T. and Witmer R.E., (1976) *A land use and land cover classification system for use with remote sensor data*; Sioux Falls, USA: USGS Professional Paper 964.

Artan G., Gadain H., Smith J.L., Asante K., Bandaragoda C.J. and Verdin J.P., (2007) *Adequacy of satellite derived rainfall data for stream flow modelling*; Natural Hazards, 43(2), pp. 167-185.

Atesmachew B.H., Taddesse G., Peden D. and Yasin G., (2006) *Application of GIS for classification of production system and determination of grazing pressure in Upland of the Awash River Basin*; Ethiopian Veterinary Journal, 10, (1). ISSN: 1683-6324.

Aynekulu, E., Wubneh W., Birhane E. and Begashaw N., (2006) *Monitoring and Evaluating Land Use/ Land Cover Change Using Participatory Geographic Information System (PGIS) Tools: A Case Study of Begasheka Watershed, Tigray, Ethiopia*; The Electronic Journal of Information Systems in Developing Countries, (EJISDC), 25, (3), pp. 1-10.

Ba M., (2008) *An overview of Satellite based Rainfall Techniques*; Sixth NOAA-CREST Symposium, Mayaguez, Puerto Rico, February 20-22, 2008.

Bahadur K.C.K., (2009) *Mapping soil erosion susceptibility using remote sensing and GIS: a case of the Upper Nam Wa Watershed, Nan Province, Thailand*; Environmental Geology, 57, pp. 695–705.

Bahrami H.A., Vaghei H.G., Vaghei B.G., Tahmasbipour N and Taliey-Tabari F., (2005) *New Method for Determining the Soil Erodibility Factor Based on Fuzzy Systems*; Journal of Agricultural Science and Technology (JAST), 7, pp.115-123.

Banko G., (1998) *A Review of Assessing the Accuracy of Classifications of Remotely Sensed Data and of Methods Including Remote Sensing Data in Forest Inventory;* Interim Report IR-98-081 /November 1998, IIASA.

Bardossy A. and Duckstein L., (1994) *Fuzzy Rule-Based Modeling with Applications to Geo-physical, Biological and Engineering Systems*; CRC Press, Boca Raton, FL.

Baz I., Geymen A. and Nogay S., (2009) *Development and application of GIS-based analysis/synthesis modelling techniques for urban planning of Istanbul Metropolitan Area*; Advances in Engineering Software, 40, pp.128–140.

Beasley D.B., Huggins L.F. and Monke E.J., (1980) *ANSWERS: a model for watershed planning*; Transactions of American Society of Agricultural and Biological Engineers,(ASABE), 23, (4), pp. 0938–0944.

Berry L., (2003) *Land degradation in Ethiopia: its extent and impact*; Global-Mechanism/World Bank (URL: http://lada.virtualcentre.org/eims/download.asp? pub_id=92120; retrieved 15 July 2009).

Bhattarai R. and Dutta D., (2007) *Estimation of Soil Erosion and Sediment Yield Using GIS at Catchment Scale*; Water Resource Management, 21, pp.1635-1647.

Bizuwerk A., Taddese G. and Getahun Y., (2003) *Application of GIS for modelling soil loss rate in Awash River Basin, Ethiopia*; Project of ILRI, Addis Ababa, Ethiopia; (URL: http://www.iwmi.cgiar.org/Assessment/files/pdf/publications/WorkingPapers/GIS%20for%20modeling%20soil.pdf).

Blinkov I. and Kostadinov S., (2010) *Applicability of Various Erosion Risk Assessment Methods for Engineering Purposes*; Fourth International Scientific Conference, BALWOIS (Balkan Water Observation and Information System for Balkan countries), Ohrid, Republic of Macedonia,25-29 May 2010.

Boakye E., Odai S.N., Adjei K.A. and Annor F.O., (2008) *Landsat Images for Assessment of the Impact of Landuse and Landcover changes on the Barekese Catchment in Ghana*; European Journal of Scientific Research, 22,(2), pp.269-278, ISSN 1450-216X.

Borah D.K. and Bera M., (2003) *Watershed-Scale Hydrologic and NonPoint-Source Pollution Models: Review of Mathematical Bases*; Transactions of the American Society of Agricultural Engineers (ASAE), 46 (6), pp. 1553-1566.

Brule J.F., (1985) *Fuzzy systems-A Tutorial*; (URL: http://www.austinlinks.com/Fuzzy/tutorial.html).

Chokngamwong R. and Chiu L., (2006) *TRMM and Thailand daily gauge rainfall comparison*; The 86th AMS annual meeting, 28 Jan.–2 Feb, Atlanta, GA. H23A-10 (URL: http://ams.confex.com/ams/pdfpapers/103039.pdf).

Cihlar J., (2000) *Land cover mapping of large areas from satellites: status and research priorities*; International Journal of Remote Sensing, 21, (6&7), pp. 1093–1114.

Cohen S., Svoray T., Laronne J.B. and Alexandrov Y., (2008) *Fuzzy-based dynamic soil erosion model (FuDSEM): Modelling approach and preliminary evaluation;* Journal of Hydrology, 356, pp. 185– 198.

Congalton R.G., (1996) *Accuracy assessment: A critical component of land cover mapping;* Gap Analysis. American Society for Photogrammetry and Remote Sensing, pp.119- 131; ISBN-1-57083-03603.

Congalton R.G., (1991) *A review of assessing the accuracy of classifications of remotely sensed data;* Remote Sensing of Environment, 37, pp. 35-46.

CORINE, (1992) *Soil Erosion Risk and Important Land Resources in the South eastern Regions of the European Community* ; EUR 13233, Luxembourg, BELGIUM 1992; pp. 32-48.

Costa M.H., Botta A. and Cardille J.A., (2003) *Effects of Large-Scale Changes in Land Cover on the Discharge of the Tocantins River, South-eastern Amazonia*; Journal of Hydrology, 283, pp. 206-217.

Costantini E.A.C., Urbano F. and L'Abate G., (2004) *Soil Regions of Italy*; Publication made from the project: "Pedological Methodologies: criteria and procedures for the creation and up-dating of the soil map of Italy (scale 1:250,000)" promoted by the Italian National Observatory for Pedology and Soil Quality and financed by Italian Ministry for Agricultural and Forestry Policies. (URL: http://www.soilmaps.it/download/csi-BrochureSR_a4.pdf).

CSA and ORC Macro, (2001) *Ethiopia demographic and health survey 2000*; Addis Ababa, Ethiopia, and Calverton, MD (CSA: Central Statistical Authority and ORC Macro). *Cross-reference* from Haile S., (2004).

De Santos L.N. and de Azevedo C.M., (2001) *A new procedure to estimate the RUSLE EI_{30} index, based on monthly rainfall data applied to the Algarve region, Portugal*; Journal of Hydrology, 250, pp. 12-18.

Deore S.J., (2005) *Prioritization of Micro-watersheds of Upper Bhama Basin on the Basis of Soil Erosion Risk Using Remote Sensing and GIS Technology*; PhD Thesis: University of Pune, India.

Dinku T., Ceccato P., Grover-Kopec E., Lemma M., Connor S.J. and Ropelewski C.F., (2007) *Validation of satellite rainfall products over East Africa's complex topography;* International Journal of Remote Sensing, 28,(7), pp. 1503 -1526.

Diodato N., (2004) *Estimating RUSLE's rainfall factor in the part of Italy with a Mediterranean rainfall regime*; Hydrology and Earth System Sciences, 8(1), pp. 103-107.

EHRS-FAO, (1986) *Highlands Reclamation Study Ethiopia;* Final Report, Vol. I & II. Rome, Italy.

El-Hassanin A.S., Labib T.M. and Gaber E.I., (1993) *Effect of vegetation cover and land slope on runoff and soil losses from the watersheds of Burundi;* Agriculture, Ecosystems and Environment, 43 pp. 301-308.

Elias E., (2003) *Case Studies - Genetic Diversity, Coffee and Soil Erosion in Ethiopia;* Paper prepared for the Roles of Agriculture International Conference, 20-22 October, 2003, Rome, Italy, ESA, FAO-UN.

Elias E., (2003) *Roles of Agriculture Project: Environment Module: Ethiopia;* International Conference, 20-22 October, 2003, Rome, Italy. Agricultural and Development Economics Division (ESA); Food and Agriculture Organization of the United Nations.

El-Swaify S.A., Dangler E.W. and Armstrong C.L., (1982) *Soil Erosion by Water in the Tropics*; Research Extension Series 024, Department of Agronomy and Soil Science, University of Hawaii.

Engel B., (1999) *Estimating Soil Erosion Using RUSLE (Revised Universal Soil Loss Equation) Using ArcView,* Purdue University, (http://pasture.ecn.purdue.edu/~abe526/resources1/gisrusle/gisrusle.htm).

ESRI, (2007) *An overview of the Multivariate tools;* Accessed from the website: (URL: http://webhelp.esri.com/arcgisdesktop/9.2/index.cfm?TopicName=An_overview_of_the_Multivariate_tools).

European Commission, (2007) *Environmental fact sheet: soil protection-a new policy for EU*; January 2007.

FAO, (2008) *Land degradation on the rise*; Retrieved on 10-08-2009 from the website (URL: http://www.fao.org/newsroom/en/news/2008/1000874/index.html).

FAO, (2003) *Data sets, Indicators and Methods to assess Land Degradation in Drylands;* Report of the Land Degradation Assessment in Drylands (LADA); ISBN 92-5-104925-4.

Favis-Mortlock D. (1998) *The GCTE validation of field-scale soil erosion models: In Experiences with Soil Erosion Models;* Klik A (ed.).Wiener Mitteilungen: Vienna; 151, pp. 91-109.

Ferro V., Porto P. and Yu B., (1999) *A comparative study of rainfall erosivity estimation for southern Italy and southeastern Australia;* Hydrological Science, Journal des Sciences Hydrologiques, 44, (1), pp. 3-24.

Funk C. and Verdin J., (2003) *Comparing Satellite Rainfall Estimates and Reanalysis Precipitation Fields with Station Data for Western Kenya;* JRC-FAO International Workshop on Crop Monitoring for Food Security in Africa, January 28-30, 2003, Nairobi, Kenya.

Gachene C.K.K., (1995) *Evaluation and mapping of soil erosion susceptibility: an example from Kenya;* Soil Use & Management, 11, pp. 1-4.

Ghadiri H. and Paynet D., (1988) *The formation and characteristics of splash following raindrop impact on soil;* Journal of Soil Science 39, pp. 563-575.

Giere R.N., (1984) *Logical Basis of Hypothesis Testing in Scientific Research*; Materials by Dan Herms, Ohio State University (URL: http://www.dartmouth.edu/~bio125/logic.Giere.pdf).

Glenn E., Huete A., Nagler P. and Nelson S.,(2008) *Relationship Between Remotely-sensed Vegetation Indices, Canopy Attributes and Plant Physiological Processes: What Vegetation Indices Can and Cannot Tell Us about the Landscape;* Sensors, 8(4), pp. 2136-2160.

Gobin A., Govers G., Jones R., Kirkby M. and Kosmas C., (2003) *Assessment and reporting on soil erosion. Background and workshop report;* EEA Technical Report No. 94, European Environment Agency, Copenhagen.(URL: http://www.environmental-center.com/articles/article1400/tech_94.pdf).

Gournellos T., Evelpidou N. and Vassilopoulos A., (2004) *Developing an Erosion Risk Map Using Soft Computing Methods (Case Study at Sifnos Island)*; Natural Hazards, 31, pp. 63–83.

Griffiths J.S. and Richards K.S., (1989) *Application of a Low-Cost Database to Soil Erosion and Soil Conservation Studies in the Awash Basin, Ethiopia;* Land Degradation and Rehabilitation,1, pp. 241-262.

Grimm M., Jones R.J.A., Rusco E. and Montanarella L., (2003) *Soil Erosion Risk in Italy: a revised USLE approach;* European Soil Bureau Research Report No.11, EUR 20677 EN, (2002), 28pp. Office for Official Publications of the European Communities, Luxembourg.

Haile S., (2004) *Population, Development and Environment in Eithiopia*; Special Report, Chapter 43, Environmental Change and Security Project (ECSP), Issue 10.

Hailemariam A., (2003) *Population growth, environment and agriculture in Ethiopia*; Paper presented at the National Symposium on the Occasion of the 10th Anniversary of the Launching of the National Population Policy of Ethiopia, Addis Ababa, Ethiopia.

Hakkeling R.T.A., (1989) *Global Assessment of Soil Degradation in Eastern and Southern Africa*; Vol.1 Main report Netherlands Soil Survey Institute; Wageningen, The Netherlands. *Cross-reference*: Berry, L. (2003)

Hawando T., (1995) *The survey of the soil and water resources of Ethiopia;* United Nation University, UNU/Tokyo.

Hawando T., (1997) *Desertification in Ethiopian Highlands;* RALA Report No. 200, International workshop on Rangeland Desertification, Iceland. (http://www.rala.is/rade/ralareport/Hawando.pdf).

Heit E., (2000) *Properties of inductive reasoning;* Psychonomic Bulletin & Review, 7 (4), pp. 569-592.

Hellden U., (1987) *An Assessment of Woody Biomass, Community Forests, Land Use and Soil Erosion in Ethiopia—A feasibility study on the use of remote sensing and GIS-analysis for planning purposes in developing countries* (Lund: Lund University Press).

Hoyos N., Waylen P.R. and Jaramillo A., (2005) *Seasonal and spatial patterns of erosivity in a tropical watershed of the Colombian Andes*; Journal of Hydrology, Volume 314, Issues 1-4, pp. 177-191.

Huffman G.J., Adler R.F., Arkin P., Chang A., Ferraro R., Gruber A., Janowiak J., McNab A., Rudolf B. and Schneider U., (1997) *The Global Precipitation Climatology Project (GPCP) combined precipitation dataset;* Bulletin of the American Meteorological Society, 78, pp. 5−20.

Hughes D.A., (2006) *Comparison of satellite rainfall data with observations from gauging station networks;* Journal of Hydrology, 327, (3&4), pp.399-410.

Hurni H., (1983a) *Ethiopian highland reclamation study design for Didessa State Farm, Wollega;* Field report: Soil conservation research project, Addis Ababa, Ethiopia.

Hurni H., (1983b) *Ethiopian highland reclamation study: Soil formation rates in Ethiopia*; Working paper No. 2, Addis Ababa, Ethiopia.

Hurni H., (1985) *Erosion-productivity-conservation systems in Ethiopia;* Proceedings 4th International Conference on Soil Conservation, Maracay, Venezuela, pp. 654-674.

Hurni H., (1988) *Degradation and conservation of soil resources in the Ethiopian highlands;* Mountain Research and Development, 8, pp. 123-130.

Hussein M.H., (1986) *Rainfall erosivity in Iraq*; Journal of Soil and Water Conservation, 41, pp. 336-338.

Islam M.N. and Uyeda H., (2006) *Use of TRMM in determining the climatic characteristics of rainfall over Bangladesh;* Remote Sensing of Environment, 108, pp. 264-276.

Kainz W., (2002) *Fuzzy Logic and GIS;* Retrieved on July 5, 2009, from (URL: http://homepage.univie.ac.at/Wolfgang.Kainz/Lehrveranstaltungen/ESRI_Fuzzy_Logic/File_2_Kainz_Text.pdf).

Kandel A., (1986) *Fuzzy Mathematical techniques with applications;* Addison-Wesley Publishing Company, ISBN 0-201-11752-5.

Kisi O., Karahan M.E. and Zekai S., (2006) *River suspended sediment modelling using a fuzzy logic approach;* Hydrological Processes, 20, pp. 4351- 4362.

Kopecki I., (2008) *Calculational Approach to FST-Hemispheres for Multiparametrical Benthos Habitat Modelling;* PhD Thesis, Mitteilungen des Institutes für Wasserbau, Universität Stuttgart, Heft 169.

Kothyari U.C., Jain M.K. and Raju K.G.R., (2002) *Estimation of temporal variation of sediment yield using GIS;* Hydrological Sciences, 47, pp. 693-706.

Lal R., (1981) *Analyzes of different processes governing soil erosion by water in the tropics;* Erosion and Sediment Transport Measurement (Proceedings of the Florence Symposium, June 1981); IAHS Publ. no. 133.

Landis R.J. and Koch G.G., (1977) *The measurement of observer agreement for categorical data;* Biometrics, 33, pp. 159-174.

Lawal O., Thomas G. and Babatunde N., (2007) *Estimation of Potential Soil Losses on a Regional Scale: A Case of Abomey- Bohicon Region Benin Republic;* Agricultural Journal, 2, pp.1-8, Medwell Journals.

Lee J. and Wong D.W.S., (2001) *Spatial Analysis with ArcView GIS.* Wiley & Sons.

Levizzani V., Amorati R., and Meneguzzo F., (2002) *A review of satellite-based rainfall estimation methods*; European Commission Project MUSIC Report (EVK1-CT-2000-00058), 66 pp. (URL: http://www.isac.cnr.it/~meteosat/papers/MUSIC-Rep-Sat-Precip-6.1.pdf).

Lilesand T., Kiefer R. and Chipman J., (2004) *Remote Sensing and Image Interpretation,* John Wiley & Sons, Inc.New York, Fifth edition.

Lim K.J., Sagong M., Engel B.A., Tang Z., Choi J. and Kim K.S., (2005) *GIS-based sediment assessment tool*; Catena, 64, pp. 61–80.

Liu B.Y., Nearing M.A. and Risse L.M., (1994) *Slope gradient effects on soil loss for steep slopes;* Transactions of the American Society of Agricultural Engineers (ASAE)*,* 37, pp. 1835-1840.

Lu D., Mausel P., Brondi´zio E. and Moran E., (2004) *Change detection techniques;* International Journal of Remote Sensing, 25,(12), pp. 2365-2407.

MacGillivray C.M.I. and Donovan S.K., (2007) *A Relative Potential Erosion Detection (PED) model for the upper Buff Bay catchment, parish of Portland, Jamaica: A Geographical Information System application*; Scripta Geologica, Special Issue*,* 6, pp.1-202.

McCollum J., Gruber A. and Ba M., (2000) *Discrepancy between gauges and satellite estimates of rainfall in Equatorial Africa;* Journal of Applied Meteorology, 39,(5), pp.666-679.

McNeill J.R. and Winiwarter V., (2004) *Breaking the Sod: Humankind, History, and Soil;* Science*,* 304, pp. 1627-1629.

Mendel J.M., (1995) *Fuzzy Logic Systems for Engineering: A Tutorial;* 0018-9219/95$04.00, IEEE.

Merritt W.S., Letcher R.A. and Jakeman A.J., (2003) *A review of erosion and sediment transport models;* Environmental Modelling & Software 18, pp.761-799.

Mesev V., (2007) *Integration of GIS and Remote Sensing;* Wiley: Chichester.

Metternicht G. and Gonzales S., (2005) *FUERO: foundations of a fuzzy exploratory model for soil erosion hazard prediction;* Environmental Modelling & Software, 20, pp.715-728.

Mitasova H., Hofierka J., Zlocha M. and Iverson R. L., (1996) *Modeling topographic potential for erosion and deposition using GIS;* International Journal of Geographical Information Science, 10(5), pp.629-641.

Mitra B., Scott H.D., Dixon J.C. and McKimmay J.M., (1998) *Applications of fuzzy logic to the prediction of soil erosion in large watershed;* Geoderma, 86, pp.183-309.

Mizumoto M., (1988) *Fuzzy controls under various fuzzy reasoning methods;* Information Sciences 45, pp.129-151.

Monchareon L., (1982) *Application of soil maps and report for soil and water conservation;* Department of land development, Bangkok.

Moore I. and Burch G., (1986a) *Physical basis of the length-slope factor in the universal soil loss equation;* Soil Science Society of America Journal, 50, pp. 1294-1298.

Moore I. and Burch G., (1986b) *Modeling erosion and deposition: topographic effects;* Transcations of the American Society of Agricultural Engineers (ASAE), 29(6), pp.1624-1630.

Morgan R.P.C., Quinton J.N., Smith R.E., Govers G., Poesen J.W.A., Auerswald K., Chisci G., Torri D. and Styczen M., (1998a) *The European Soil Erosion Model (EUROSEM): a dynamic approach for predicting sediment transport from fields and small catchments;* Earth Surface Processes, 23, pp.527-544.

Murtha J., (1995) *Applications of fuzzy logic in operational meteorology;* Scientific Services and Professional Development Newsletter, Canadian Forces Weather Service; pp.42-54.

NASA, (2006) *Landsat7 Science Data Users Handbook;* Accessed on 2/08/2009 from (URL: http://landsathandbook.gsfc.nasa.gov/handbook/handbook_toc.html).

Nash J.E. and Sutcliffe J.V., (1970) *River flow forecasting through conceptual models, Part I: a discussion of principles*; Journal of Hydrology, 10 (3), pp. 282-290.

Nearing M.A., Foster G.R., Lane L.J. and Finckner S.C., (1989) *A process-based soil erosion model for USDA-Water Erosion Prediction Project technology;* Transactions of the American Society of Agricultural Engineers (ASAE), 32, pp.1587-1593.

Nyssen J., Poesena J., Moeyersonsc J., Deckersd J., Haileb M. and Lange A., (2004) *Human impact on the environment in the Ethiopian and Eritrean highlands—a state of the art;* Earth-Science Reviews 64 , pp.273-320.

Ohring G., (2007) *Achieving Satellite Instrument Calibration for Climate Change (ASIC);* Report of Workshop at National Conference Centre, VA, US by NOAA, NASA, NIST, NPOESS and Space Dynamic Laboratory of Utah State University.

Oldeman L.R., Hakkeling R.T.A. and Sombroek W.G., (1990) *World Map of the Status of Human-Induced Soil Degradation: An Explanatory Note;* International Soil Reference and Information Centre, Wageningen, The Netherlands.

Panda S.S., Hoogenboom G. and Paz J., (2009) *Distinguishing blueberry bushes from mixed vegetation land use using high resolution satellite imagery and geospatial techniques.* Computers and Electronics in Agriculture, 67(1&2), pp. 51-58.

Panigrahi B., Senapati P.C. and Behera B.P., (1996) *Development of erosion index model from daily rainfall data;* Journal of Applied Hydrology, 9 (1&2), pp.17-22.

Panigrahi D.P. and Mujumdar P.P., (2000) *Reservoir Operation Modelling with Fuzzy Logic;* Water Resources Management, 14, pp.89-109.

PAP/RAC, (1997) *Guidelines for Mapping and Measurement of Rainfall-Induced Erosion Processes in the Mediterranean Coastal Areas;* PAP-8/PP/GL.1. Split, Priority Actions Programme Regional Activity Centre (MAP/UNEP), with the cooperation of FAO. pp xii+70.

Pham D.T. and Castellani M., (2002) *Action aggregation and defuzzification in Mamdani-type fuzzy systems;* Proceedings of the Institute of Mechanical Engineers, Vol. 216, Part C: Journal of Mechanical Engineering Science.

Prakash T.N., (2003) *Land Suitability Analysis for Agricultural Crops: A fuzzy Multi-criteria Decision Making Approach;* Master Thesis: ITC; Enschede, The Netherlands.

Raj A.P. and Kumar D.N., (1998) *Ranking multi-criterion river basin planning alternatives using fuzzy members;* Fuzzy Sets System, 100, pp.89-99.

Ramsewak D., (2006) *The integration of Remote Sensing and GIS technologies for the development of a Land Use/Cover map of the island of Tobago;* Fourth LACCEI International Latin American and Caribbean Conference for Engineering and Technology (LACCET'2006) *"Breaking Frontiers and Barriers in Engineering: Education, Research and Practice"* 21-23 June 2006, Mayagüez, Puerto Rico.

Renard K.G., Foster G.R., Weesies G.A., McCool D.A. and Yoder D.C., (1997) *Predicting soil erosion by water: A guide to conservation planning with Revised Universal Soil Loss Equation (RUSLE);* Agriculture Handbook; 703, U.S. Gov. Prin. Office, Washington, DC.

Renard K.G. and Freimund J.R., (1994) *Using monthly precipitation data to estimate the R-factor in the revised USLE;* Journal of Hydrology, 174, pp. 287-306.

Renard K.G., Foster G.R., Weesies G.A. and McCool D.K., (1991a) *Predicting Soil Erosion by Water: A Guide to Conservation Planning With the Revised Universal Soil Loss Equation (RUSLE);*Report ARS-703,US Dept Agriculture, ARS, Washington DC, USA.

Renschler C.S. and Harbor J., (2002) *Soil erosion assessment tools from point to regional scales—the role of geomorphologists in land management research and implementation;* Geomorphology, 47, pp. 189-209.

Reusing M., Schneider T. and Ammer U., (2000) *Modelling soil loss rates in the Ethiopian Highlands by integration of high resolution MOMS-02/D2-stereo-data in a GIS;* International Journal of Remote Sensing, 21, (9), pp.1885-1896.

Richardson C.W., Foster G.R. and Wright D.A., (1983) *Estimation of erosion index from daily rainfall amount;* Transactions of the American Society of Agricultural Engineers (ASAE), 26, pp.153-156.

Roose E.J., (1977) *Use of the Universal soil loss equation to predict erosion in West Africa;* Soil Erosion: Prediction and Control. Soil Conservation Society of America, Iowa.

Ross T.J., (2004) *Fuzzy Logic with Engineering Applications*; 2nd Edition. ISBN: 978-0-470-86075-5.

Rouse J.W., Haas R.H., Schell J.A. and Deering D.W., (1973) *Monitoring vegetation systems in the great plains with ERTS;* Third ERTS Symposium, NASA, SP-351 I, pp. 309-317.

Rusco E., Montanarella L. and Marechal B., (2009) *SoCo project Overview on soil degradation, practices and policies;* JRC-IES, Land Management and Natural Hazard Unit, Soil Action, EU.

Saaty T.L., (1980) *The Analytic Hierarchy Process;* New York: McGraw- Hill, 1980.

Sablani S.S., Datta A.K., Rehman M.S. and Mujumdar A.S., (2007) *Handbook of Food and Bioprocess Modeling Techniques;* CRC Press, ISBN: 978-0-8247-2671-3, e-Book ISBN: 978-1-4200-1507-2.

Salski A., (1999) *Fuzzy logic approach to data anaysis and ecological modelling;* Proceedings of European Symposium on Intelligent Techniques (ESIT'99), Orthodox Academy of Create, Greece: CD-ROM BC-01.

Salski A., Holsten B. and Trepel, M., (2008) *Fuzzy approach to ecological modelling and data analysis;* In: S.E. Jorgensen, T-S. Chon, F.A. Recknagel: The Handbook of Ecological Modelling and Informatics. WIT Press, Chapter 8, pp. 125-140.

Schneider M.,(2001) *Habitat- und Abflussmodellierung für Fließgewässer mit unscharfen Berechnungsansätzen;* PhD Thesis, Mitteilungen des Institutes für Wasserbau, Universität Stuttgart, Heft 108.

Schumm S.A., (1977) *The fluvial system;* John Wiley and Sons, N.Y.

Shirazi M.A. and Boersma L., (1984) *A unifying quantitative analysis of soil texture;* Soil Science Society of America Journal, 48, pp.142–147.

Shrestha M.S., Artan G.A., Bajracharya S.R. and Sharma R.R., (2008) *Using satellite-based rainfall estimates for streamflow modeling: Bagmati Basin;* Journal of Flood Risk Management, 1(2), pp.89-99.

Sonneveld B.G.J.S., (2003) *Formalizing Expert Judgements in Land Degradation Assessment: A case study of Ethiopia;* Land Degradation & Development, 14, pp.347-361.

Sousa S., Caeiro S. and Painho M., (2002) *Assessment of map similarity of categorical maps using Kappa Statistics: The Case of Sado Estuary;* Paper presented at the ESIG 2002, Tagus Park, Oeiras.

Stewart B.A., Woolhiser D.A., Wischmeier W.H., Caro J.H. and Frere M.H., (1975) *Control of water pollution from cropland. Volume I: A manual for guideline development;* EPA~0012-75-026a. U.S. Environmental Protection Agency, Washington DC.

Stocking M., Chakela Q. and Elwell H., (1988) *An Improved Methodology for Erosion Hazard Mapping Part I: The Technique;* Geografiska Annaler. Series A, Physical Geography, Vol. 70, No. 3, pp. 169-180.

Streile G.P., Shields K.D., Stroh J.L., Bagaasen L.M., Whelan G., McDonald J.P., Droppo J.G. and Buck J.W., (1996) *The Multimedia Environmental Pollutant Assessment System (MEPAS): Source-Term Release Formulations;* PNNL-11248/UC-602, 630, Pacific Northwest National Laboratory, Richland, Washington.

Svetlana B., Tomislav S. and Sonja B., (2006) *Definition of Rainfall Erosivity in the Area of the Experimental Station Snagovo;* Fourth International Scientific Conference, BALWOIS (Balkan Water Observation and Information System for Balkan countries), Ohrid, Republic of Macedonia, 23-26 May 2006.

Swets D.L., Reed B.C., Rowland J.D. and Marko S.E., (1999) *A weighted least-squares approach to temporal NDVI smoothing;* ASPRS Annual Conference: From Image to Information, Portland, Oregon, May 17-21. Proceedings: Bethesda, Maryland, American Society for Photogrammetry and Remote Sensing.

Taddese G., (2001) *Land Degradation: A Challenge to Ethiopia;* Environmental Management, 27, (6), pp. 815-824.

Tadesse W., Tsegaye T. D. and Coleman T. L., (2001) *Land Use/Cover Change Detection of the City of Addis Ababa, Ethiopia Using Remote Sensing and Geographic Information System Technology;* 0-7803-7031-7/01/$10.00 (C) IEEE.

Tayfur G., Ozdemir S. and Singh V.P., (2003) *Fuzzy logic algorithm for runoff-induced sediment transport from bare soil surfaces;* Advances in Water Resources, 26, pp.1249-1256.

Teschl R., (2006) *Weather Radar Estimates of Rainfall Adjusted to Rain Gauge Measurements Using Neural Networks;* International Joint Conference on Neural Networks, Sheraton Vancouver Wall Centre Hotel, Vancouver, BC, Canada.

Toy T.J., Foster G.R. and Renard K.G., (2002) *Soil erosion: processes, prediction, measurement, and control;* New York, NY: Wiley.

Tran L.T., Ridgley M.A., Duckstein L. and Sutherland R., (2002) *Application of fuzzy logic-based modeling to improve the performance of the Revised Universal Soil Loss Equation;* Catena, 47 (3) pp.203-226.

Tucker C., (2006) *Historic Perspective: History of the NDVI and Vegetation Indices.* Global Vegetation Workshop: Long term global monitoring of vegetation variables using moderate resolution satellites, August 8-10, 2006, University of Montana.

USDA, (2003) *Production Estimates and Crop Assessment Division;* Updated: September 5, 2003 URL: http://www.fas.usda.gov/pecad2/highlights/2002/10/ethiopia/baseline/Eth_Annual_Rainfall.htm.

Van der Knijff J.M., Jones R.J.A. and Montanarella L., (2002a) *Soil erosion risk assessment in Italy;* Proceedings of the third International Congress Man and Soil at the Third Millennium, J.L. Rubio, R.P.C.Morgan, S.Asins and V.Andreu, eds. Geoforma Ediciones, Logrono.

Van der Knijff J.M., Jones R.J.A. and Montanarella L., (2002b) *Soil erosion risk assessment in Italy;* European Soil Bureau, European Commission, Joint Research Centre, Space Applications Institute.

Van Leeuwen W.J.D. and Sammons G., (2003) *Seasonal Land Degradation Risk Assessment for Arizona;* Proceedings of the 30th International Symposium on Remote Sensing of Environment, Honolulu, Hawaii November 10-14, 2003 (Retrieved on March, 2009 from URL: http://wildfire.arid.arizona.edu/docs/Erosion_8-15-03_WvL.pdf).

Van Rompaey A.J.J., Bazzoffi P., Jones R.J.A., Montanarella L. and Govers G., (2003) *Validation of Soil Erosion Risk Assessments in Italy;* European Soil Bureau Research Report No.12, EUR 20676 EN, 25pp. Office for Official Publications of the European Communities, Luxembourg.

Vente J. and Poesen J., (2005) *Predicting soil erosion and sediment yield at the basin scale: Scale issues and semi-quantitative models;* Earth-Science Reviews, 71, (1&2), pp. 95-125.

Vrieling A., (2006) *Satellite remote sensing for water erosion assessment: A review;* Catena, 65, pp.2-18.

Vrieling A., Sterk G. and Vigak O., (2006) *Spatial evaluation of Soil erosion risk in the west Usambara mountains, Tanzania;* Land Degradation & Development, 17, pp.301-319.

Wan Y., El-Swaify S.A. and Sutherland R.A., (1996) *Partitioning interrill splash and wash dynamics: a novel laboratory approach;* Soil Technology, 9, pp.55-69.

Weier J. and Herring D., (2000) *Measuring Vegetation (NDVI& EVI);* Feature Article on Earth Observatory, NASA: Accessed on 02-05-2009.

Wilcox B.P. and Wood M.K., (1989) *Factors Influencing Interrill Erosion from Semiarid Slopes in New Mexico;* Journal of Range Management,42,(1), pp. 66-70.

Williams J.R. and Arnold J.G., (1997) *A system of erosion-sediment yield models*; Soil Technology, 11 pp.43-55.

Williams J.R., (1975) *Sediment routing for agricultural watersheds;* Water Resource Bulletin, 11, pp.965-974.

Williams J.R., (1990) *The Erosion-Productivity Impact Calculator (EPIC) Model: A Case History;* Philosophical Transactions: Biological Sciences, Vol. 329, No. 1255, pp. 421-428.

Willmott C.J. and Matsuura K., (2005) *Advantages of the mean absolute error (MAE) over the root mean square error (RMSE) in assessing average model performance;* Climate Research Published December 19, Vol. 30: pp.79-82.

Wischmeier W.H. and Smith D.D., (1978) *Predicting rainfall erosion losses. A guide to conservation planning;* The USDA Agricultural Handbook No. 537.

Wunderle S., (2003) *NOAA / AVHRR RSGB Normalized Difference Vegetation Index (NDVI) Data Set*; (URL: http://saturn.unibe.ch/rsbern/noaa/dw/realtime/RSGB_AVHRR_NDVI.pdf).

Xiaodan W., Xianghao Z. and Jianrong F., (2004) *Assessment and spatial distribution of sensitivity of soil erosion in Tibet;* Journal of Geographical Sciences, 14, (1), pp. 41-46.

Xie P. and Arkin P.A., (1997) *A 17-year monthly analysis based on gauge observations, satellite estimates, and numerical model outputs;* Bulletin of the American Meteorological Society, 78(11), pp. 2539-58.

Xiong L.H., Shamseldin A.Y. and O'Connor K.M., (2001) *A nonlinear combination of the forecasts of rainfall-runoff models by the first order Takagi-Sugeno fuzzy system;* Journal of Hydrology, 245, (1&4), pp. 196-217.

Yang L., Stehman S.V., Wickham J.D., Smith J.H. and Van Driel N.J., (2000) *Thematic Validation of Land Cover Data of the Eastern United States Using Aerial Photography: Feasibility and Challenges.* Proceedings of the 4th International Symposium on Spatial Accuracy Assessment in Natural Resources and Environmental Sciences, Delft University Press, The Netherlands, pp. 747-754.

Yang S., Lianyou L., Ping Y. and Tong C., (2005) *A review of soil erodibility in water and wind erosion research;* Journal of Geographical Sciences, 15, (2), pp.167-176.

Young R.A., Onstad C.A., Bosch D.D. and Anderson W.P., (1987) *AGNPS: an agricultural non point source pollution model;* Conservation research report 35, US Dept. Agric. Res. Services, Washington, DC, USA.

Yu P.S. and Yang T.C., (2000) *Fuzzy multi-objective function for rainfall runoff model calibration;* Journal of Hydrology, 238, (1–2), pp. 1-14.

Yuksel A., Gundogan R. and Akay A.E., (2008) *Using the Remote Sensing and GIS Technology for Erosion Risk Mapping of Kartalkaya Dam Watershed in Kahramanmaras, Turkey;* Sensors, (8), pp. 4851-4865.

Zadeh L.A., (1965a) *Fuzzy Sets;* Information and Control, 8, pp. 338-353.

Zhang K.L., Shu A.P., Xu X.L., Yang Q.K. and Yu B., (2008) *Soil erodibility and its estimation for agricultural soils in China;* Journal of Arid Environments, 72, pp. 1002-1011.

Zhang N., Luo Y. and Wang C., (2008) *Identification of Winter Wheat and its distribution using CBERS-02B images in an Irrigation district along the Lower Yellow River, China;* International Workshop on Earth Observation and Remote sensing Applications, 1-4244-2394-1/08 IEEE.

Zhang Y., Degroote J., Wolter C. and Sugumaran R., (2009) *Integration of Modified Universal Soil Loss Equation (MUSLE) into a GIS framework to assess soil erosion risk;* Land Degradation and Development, 20, pp.84-91.

Zhu A.X and Mackay D.S., (2001) *Effects of spatial detail of soil information on watershed modelling*; Journal of Hydrology, 248, pp. 54-77.

ZONUMS, (2009) *Digipoint3 tool;* Build 17.2.09 (http://www.zonums.com/zmaps/digipoint.html).

13 Appendices

Appendix 1: Flow diagram of the customized fuzzy tool for F-WERCAM using ArcGIS Model builder

A. Module 1:

This tool extracts the corresponding grid values from all the input parameters and stores them as a table in a Geo-database. The output table is used as an input parameter for the Module 2. The ArcGIS Model Builder flow diagram is shown here. This flow diagram employs the Database Management tools of Arc Toolbox in ArcGIS 9.2/9.3.
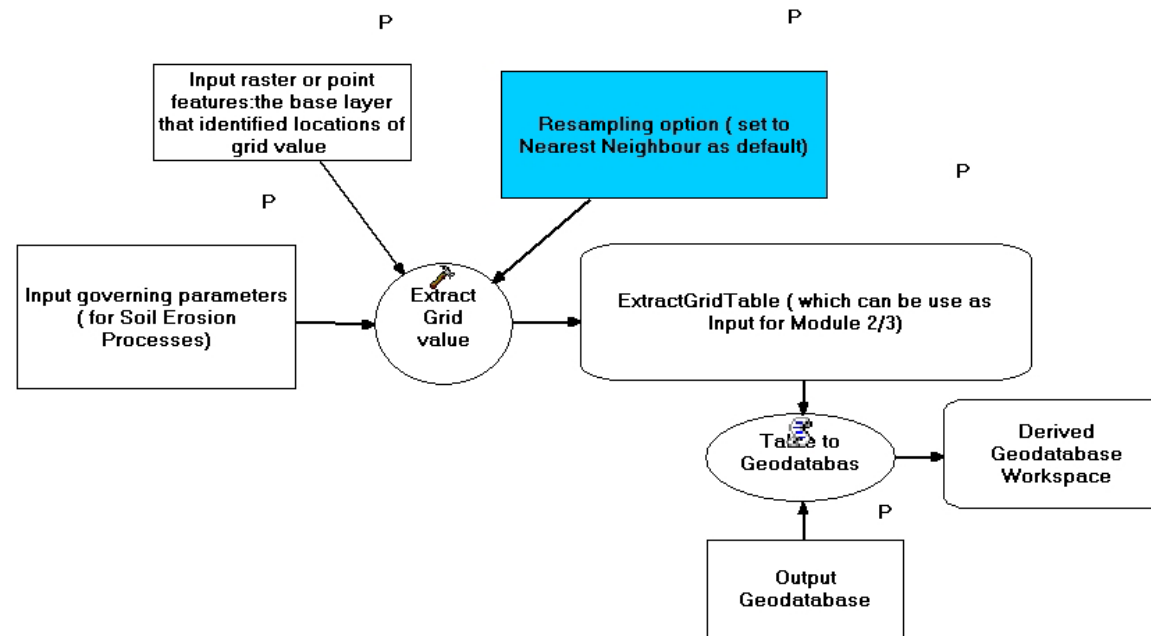
B. Module 2:

This interface or module customizes the extracted input grid table from Module 1. This is then fed into the Fuzzy Inference Calculator tool to compute the SPI or erosion risk index value, i.e. PERI or AERI. Here, the ArcGIS Model Builder flow diagram for computation of SPI or AERI (for an input table containing two input parameters) is shown below. This step employs the Database Management and Fuzzy Inference Calculator tools.
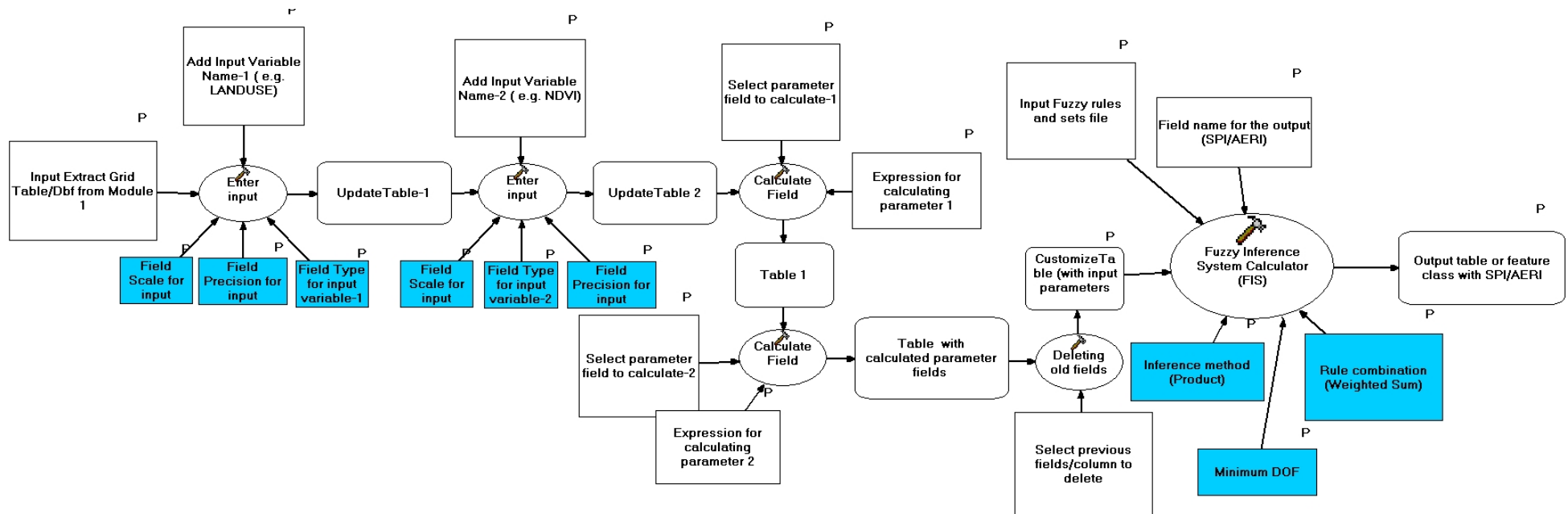
C. Module 3:

This step produces the spatial distribution soil erosion grid map corresponding to the output defuzzified value field as obtained from Module 2. This step employs the Database Management, Make Feature Layer and Feature to Raster tools of Arc Toolbox in ArcGIS 9.2/9.3.
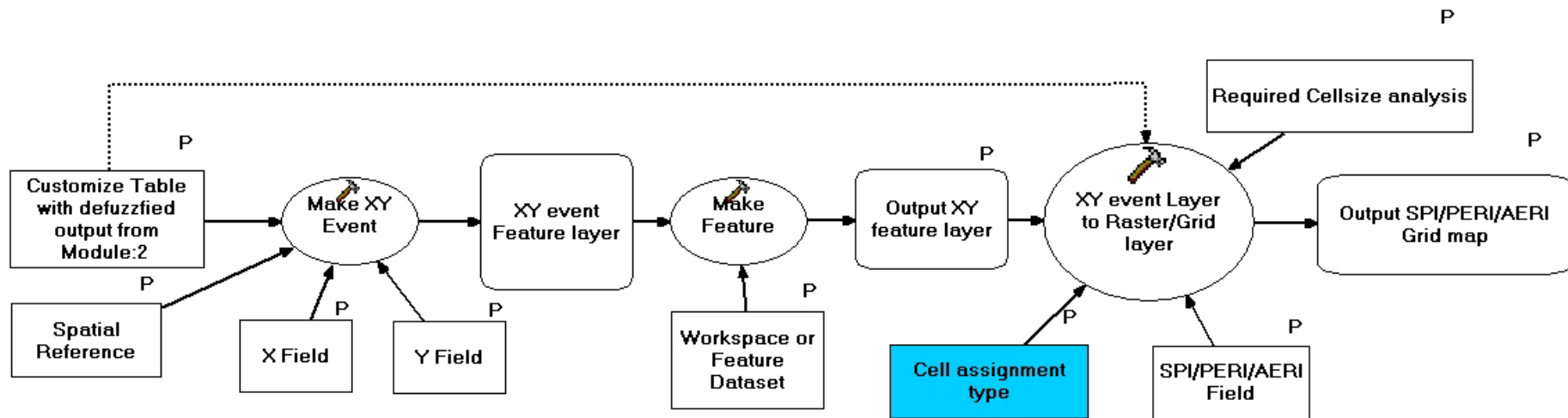
Note on symbols of the Model Builder: **P** indicates input and output model parameter; blue rectangular box indicates that a value has been pre-assigned and set before executing the model.

Appendix 2: Current land degradation potential in Upper Awash

A: Field observed locations with a brief description on current status of land degradation

Location	Coordinates (X,Y)		Land use type	Field observed land degradation risk status (as of 2009)
ID1	441000.12	977422.35	Agriculture	Vegetation cover and cropping present; low potential risk
ID2	441652.38	976422.35	Agriculture	Vegetation cover and cropping present; low potential risk
ID3	464916.44	955767.55	Schrubland/Barrenland	Presence of fragmented vegetation, bushes, gully formation and degraded soil layer, higher potential risk
ID4	478179.12	930111.86	Schrubland/Barrenland	Degraded landscape, absence of vegetation cover, undulating sloping area
ID5	477092.02	929894.44	Schrubland/Barrenland	Degraded land, outcropping of rock can be seen without any soil protecting layer, very less or no vegetation, high risk of degradation by external factors
ID6	485354.02	937727.60	Agriculture	Sparsely vegetated, mosaic of fragmented forest can be observed in nearby distant areas, higher potential risk
ID7	449834.40	989133.10	Forest	Densely vegetated zone and low potential risk
ID8	471568.70	995506.50	Settlement	Low fragmented vegetation can be seen; mosaic of sparse vegetation and built up areas
ID9	475212.50	942975.50	Agriculture	Abandoned agricultural field can be seen, protecting layer of soil is very low, experiencing degradation, high potential risk
ID10	474156.09	989235.86	Settlement	Area of urban-rural settlement zone, presence of fragmented vegetation growth, high risk potential due to human interaction and activities

B: Map showing the field observation locations and some of the photographs taken in 2009 (Dry season) highlighting the current potential of degradation in the region
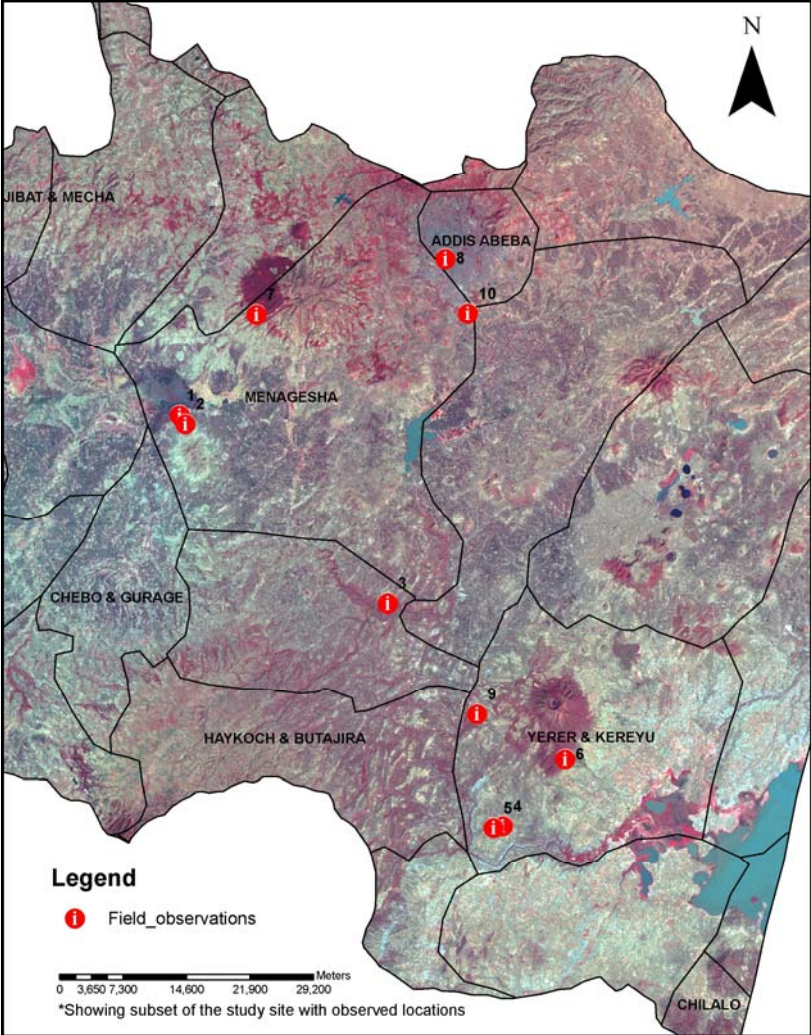
ID 1: Agricultural land   ID 3:   Schrubland/Barrenland

ID 4: Barren zone (undulating land)   **ID 6: Agricultural land patches**

Picture Source: *Habtamu Itefa, Institute of Hydraulic Engineering, Stuttgart*

Appendix 3: ArcGIS model flow diagram for generating the signature file and executing the Maximum Likelihood Classifier (MLC) for LULC classification

A: Signature generation using training and sample data or iso-data clustering process for classification
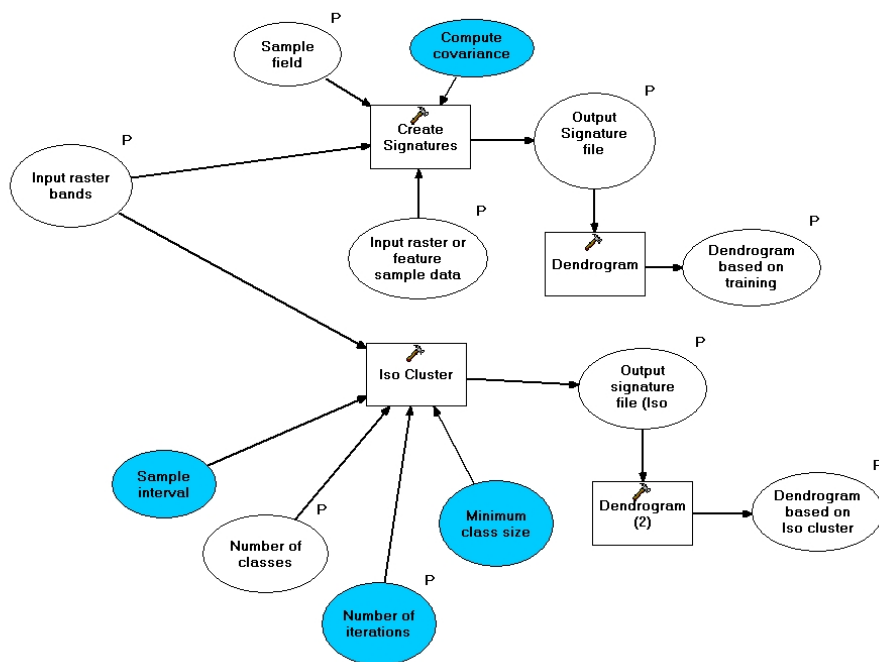
B: Generated signature file from above is fed into the MLC tool in ArcGIS
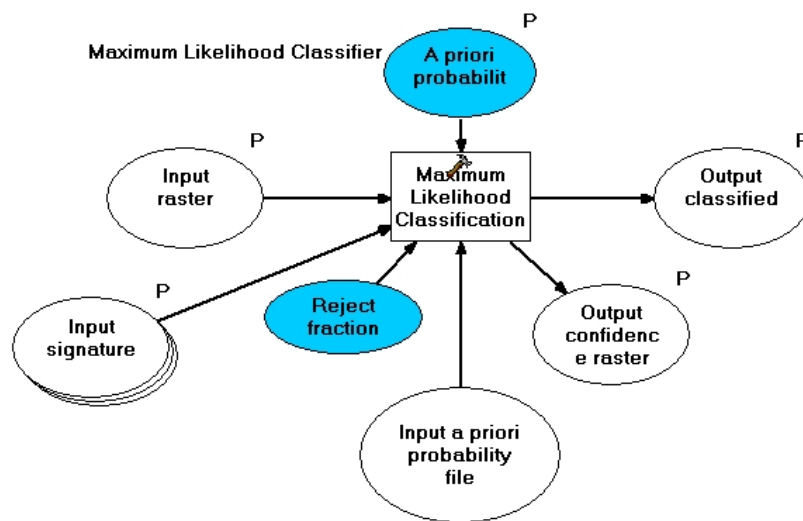
*Note***: P** indicates input and output model parameter; the blue oval indicates that a value has been pre-assigned and set as constant before executing the model. For example, a reject fraction of '0' and *a priori* probabilities of 'Equal' is set as pre-defined parameter value.

Appendix 4: Descriptions on LULC class identification, training and reference data collections for LULC classification and the fundamentals on accuracy assessment of maps

A: LULC class identification, training and reference data collections

Different LULC classes in the data are identified based on image interpretation keys like tone, shape, size, association, texture etc. and using ancillary data of the region like existing land use map and aerial photographs. The classification scheme of the existing land use map along with the USGS Level I classification scheme (Anderson et al. 1976) are referred to for the broad identification of land use and land cover categories in the study area. Six broad classes are identified: forest cover, settlement area, water bodies, grassland, agricultural land, schrubland or barrenland. The agricultural zone consists primarily of cropland, practiced on levelled or slightly undulating ground.

Training samples for each class are digitized from the image. About 50 training samples are collected in a uniform manner covering the whole study area for each class. The existing land use map, aerial photographs and background information of the study area are used for collecting the training samples. These digitized training polygons are used for generating the signature file for use in maximum likelihood classification.

Generally, assessing the accuracy of the map generated from remote sensing data is both time and money consuming. When mapping a large area, it is not possible to check the whole mapped areas in detail. Hence, sampling becomes the way by which accuracy of land cover map can be assessed (Conglaton, 1991; Banko, 1998; Boakye et al., 2008). In other words, it is necessary to collect a reference data or sample corresponding to each identified class of the study area for the purpose of

accuracy assessment. In general, ground truth or field data collections are done using GPS to obtain accurate location point data for the validation purpose. However, as in large scale area mapping and in inaccessible mountainous areas, with ground truth sampling it is not always possible to collect sufficient and accurate data. In such a case, an alterative way of collecting reference data from a high resolution aerial photograph and using ancillary data is suggested (Yang et al., 2000; Zhang et al., 2008). In this study, high resolution aerial photographs and satellite images of the region from Google Earth, which is a web-based location server, are used to collect reference points corresponding to each class. A random sampling is carried out throughout the study area to collect the reference XY co-ordinates using the '*Online Digipoint 3*' tool (Zonums, 2009). A total of 230 reference points for the identified classes are collected and each reference point is attributed by their XY co-ordinate (UTM) and the land cover class. These reference points are put into GIS for evaluating the accuracy of the derived land cover from 2000 data. Similarly, in the case of the 1973 classified image, 215 reference points are randomly collected with the help of the 1965 land use map created by Imperial Government of Ethiopia and United Nation Fund.

B: The fundamentals of the accuracy assessment between maps

Accuracy assessment is an important step as it quantifies the accuracy between thematic maps. Generally, accuracy assessment is done by setting up an "Error matrix or Confusion matrix" thereby it summarizes the relationship between the classified and the reference data (Lilesand et al., 2004). This is typically done in a tabular or array form. In the case of LULC classification assessment this step is important as it quantifies the accuracy of the classified images and their agreement with the different land cover class present on the ground.

Quantitatively, the performance of the classification process or between two maps is assessed by determining the producer's accuracy (*Omission error*), the user's accuracy (*Commission error*), the overall accuracy and the Kappa statistics. The definitions for the performance parameters are as follow (Lilesand et al., 2004; Panda et al., 2009):

Producer's accuracy is computed by dividing the number of samples/pixels correctly classified in a given class by the total number of samples/pixels chosen for that corresponding class. Mathematically, it can be represented as:

$$= \left(x_{ii} / x_{+i} \right) \times 100\%$$

x_{ii} = total number of correct cells/pixels in a class

x_{+i} = sum of the cell/pixel values in the column of error matrix

User's accuracy is computed by dividing the number of correctly classified pixels/samples in a given class by the total number of pixels/samples that are classified in that group/category. It indicates the probability that a pixel classified into a given class actually represents the class on the ground. It is shown mathematically as below:

$$= \left(x_{ii} / x_{i+} \right) \times 100\%$$

x_{ii} = total number of correct cells/pixels in a class

x_{i+} = sum of the cell/pixel values in the row of error matrix

The overall accuracy summarizes the total agreement or disagreement between the maps. In the accuracy assessment of LULC classification data, the *overall accuracy* is computed by dividing the

total number of correctly classified pixels by the total number of reference samples chosen. In general, it can be represented as:

$$= (D/N) \times 100\%$$

D = total number of correctly classified cells as summed along the major diagonal of the error matrix

N = total number of cells/pixels in the error matrix

Kappa statistics is a discrete multivariate parameter which tries to quantify the level of agreement between two maps compared against the null hypothesis that the maps do not differ by chance from a random map. It serves as an indicator of the extent to which the percentage correct values of an error matrix are due to "true" agreement versus "chance" agreement. It can be mathematically represented as:

$$Kappa\ value = \frac{N . \sum_{i=1}^{r} x_{ii} - \sum_{i=1}^{r} (x_{i+} \times x_{+i})}{N^2 - \sum_{i=1}^{r} (x_{i+} \times x_{+i})}$$

r = number of rows in the error matrix

x_{ii} = total number of correctly classified cells/pixels in a class (i.e. value in row i and column i)

x_{i+} = total for row i

x_{+i} = total for column i

N = total number of cells/pixels in the error matrix

Kappa value lies between 0 and 1, where the latter indicates complete agreement. A *Kappa* of 0 suggests that a given classification is no better than a random assignment of pixels. *Kappa* values are characterized into three groupings for accessing the LULC classification accuracy purpose: a value greater than 0.80 represent strong agreement, a value between 0.4 and 0.8 represent moderate agreement and a value below 0.4 represent poor agreement (Congalton, 1996;Ramsewak, 2006). In general, for assessing the degree of agreement of maps comparison, the *Kappa* value range is group into 6 classes as shown below (Landis and Koch, (1977) and Sousa et al., 2002). It indicates that the stronger the agreement between maps, the higher is the value of *Kappa*.

Kappa values	Strength of Agreement
< 0.00	poor
0.00-0.20	slight
0.21-0.40	fair
0.41-0.60	moderate
0.61-0.80	substantial
> 0.81	almost perfect

The degree of agreement or similarity between two maps can be assessed by looking at simple proportion of areas or by measuring it numerically (Sousa et al, 2002). The map comparison results provide the overall value for similarity and their degree of agreement can be expressed in a single value using the "*Overall accuracy*" and "*Kappa statistics*" when the comparison consists of a pairwise comparisons.

Appendix 5: Computed range of soil erodibility for different soil units of the Upper Awash Basin using three different erodibility computation methods

Soil units	*FAO (1975)	Sand %	Silt %	Clay %	Org. C %	Textural unit (USDA)	Soil erodibility (K) value (by method)		
							Williams	Monchareon	Stewart
Calcaric Flubisois	JC	39.6	39.9	20.6	0.65	L	0.313	0.320	0.340
Calcic Xerosols	XK	48.7	29.9	21.6	0.64	L	0.270	0.260	0.340
Chromic Cambisols	BC	40.1	21.5	38.4	1.44	CL	0.202	0.130	0.210
Chromic Luvisols	LC	64.3	12.2	23.5	0.63	SCL	0.189	0.140	0.250
Dystric Cambisols	BD	32.7	30.3	37.1	3.28	CL	0.217	0.170	0.210
Dystric Fluvisols	JD	35.9	39.4	24.8	2.16	L	0.243	0.290	0.290
Dystric Gleysols	GD	18.9	21.8	59.3	2.92	C	0.205	0.070	0.130
Dystric Nitisols	ND	38.9	17.6	43.6	1.57	C	0.183	0.100	0.130
Eutric Cambisols	BE	36.4	37.2	26.4	1.07	L	0.283	0.260	0.340
Eutric Gleysols	GE	42.8	20.4	36.8	1.3	CL	0.203	0.130	0.250
Eutric Nitisols	NE	68.4	10.5	21.2	0.6	SCL	0.178	0.120	0.250
Eutric Vertisols	V	24.6	14.4	61	0.68	C	0.222	0.065	0.130
Haplic Xerosols	XH	54.8	20.6	24.9	0.53	SCL	0.231	0.180	0.250
Leptosols	LP	69.9	10.5	19.5	0.73	SCL	0.175	0.130	0.250
Mollic Andosols	TM	31.2	39.6	29.2	3.95	CL	0.245	0.230	0.210
Orthic Acrisols	AO	53.6	15.8	30.6	2.25	SCL	0.161	0.130	0.210
Orthic Luvisols	LO	76	9.9	14.1	0.41	SL	0.165	0.190	0.240
Orthic Solonchak	ZO	43.2	24.6	32.4	0.4	CL	0.255	0.160	0.250
Pellic Vertisols	VP	25.1	12.2	62.7	0.68	C	0.209	0.050	0.130
Vertic Cambisols	BV	23.3	26	50.7	1.1	C	0.255	0.120	0.130
Vitric Andosols	TV	64.5	26.2	9.3	1.4	SL	0.215	0.290	0.240
Vitric	LV	26.1	27.3	46.7	1.86	C	0.220	0.120	0.130

Soil units	*FAO (1975)	Sand %	Silt %	Clay %	Org. C %	Textural unit (USDA)	Soil erodibility (K) value (by method)		
							Williams	Monchareon	Stewart
Luvisols									
Chromic Vertisols	VC	22.4	24.5	53	0.69	C	0.271	0.103	0.130
		Mean K for Upper Awash Basin					**0.222**	**0.163**	**0.219**

Key: C *Clay*; L *Loam*; CL *Clay loam*; SL *Sandy loam*; SCL *Sandy clay loam*
*FAO (1975): *Nomenclature of soil type according to FAO*

Appendix 6: Physical interpretation of the different NDVI class

Sl. No.	NDVI range (-1 to +1)	Corresponding Cover class	# Rescale range: (0-200)	Explanation and Reference
1	-1- 0.1 (Very low value)	Barren land (areas of rock, sand or snow)	0-110	Values close to 0 indicate 'no vegetation' and close to +1 indicates the highest possible density of green leaves or vegetation
	0.2- 0.4 (Moderate value)	Shrubland or grassland	120-140	(Weier and Herring, 2000)
	0.6-0.8 (High value)	Temperate and tropical rainforests	160-180	
2	< 0	Non-vegetated areas (water bodies, snow, water clouds, etc.)	<100	Value of 0.1 in desert areas and 0.8 in dense forest regions
	0-0.1	Rock and bare soil	100-110	(Wunderle, 2003)
	0.1- 0.8	Vegetated surface	110-180	

 # *The valid data range of -1 to 1 is achieved after scaling by a factor of 10000 according to provided metadata and it has been rescaled to a range of 0-200 using the factor 100*(NDVI+1) to represent the range of fuzzy set for vegetation cover parameter.*

Appendix 7: An example of the feedback on the questionnaire survey on soil erosion risk assessment provided by one of the experts

I. Personal Information

Ivica Milevski, PhD in Geography, BSc. (1995) MSc. (2001); PhD (2006)
Assistant professor at the Institute of Geography, Faculty of Natural Sciences and Mathematics, State University "Ss. Cyril and Methodius"-Skopje, Macedonia. Speciality: Physical geography-Geomorphology; Soil erosion; GIS modelling of soil erosion.

1. Please state your current occupation and position

Current occupation	Position held
University professor	Assistant professor

2. Familiarity and knowledge about the subject matter (scale: 0-5; 0 – unfamiliar and 5- well familiar)

Scale	Please cross (X)
0	
1	
2	
3	
4	
5	X

II. Identification and weighting of the potential parameters influencing soil erosion process in a landscape

1. From your own opinion, ranked accordingly to the given scale (1 to 5), which of the listed parameters is most influential in accessing the soil erosion risk on a regional scale?

Considered Parameters	Scale rating	Weight* (based on importance)
Land use/cover class	5	3.0
NDVI (proxy for vegetation cover)	3	2.0
Rainfall erosivity (rainfall parameter)	3	1.5
Slope (topographic factor)	4	2.5
Soil erodibility (soil factor)	2	1.0
		Total weight: 10

* Note: The total weight after considering all 5 parameters should add up to 10.

2. Please suggest other parameters that are considered to be important for assessing erosion risk which is not considered here, if any.

Profile and plan curvature (or convergence index in SAGA): to determinate sites of erosion or/and accumulation; Slope aspects: there is commonly high differences between south or north aspects; Drainage network density: sometimes show intensity of linear erosion; Road network density: show recent human impact on some soil erosion processes; Protection measures in the catchment (retention walls, engineering etc.); Mean temperatures and temperature fluctuations: may show the rate of weathering and other soil erosion-related issues. All parameters above can be derived by GIS software, such as from SAGA GIS.

3. Considering the literature knowledge and after taking the test site into account, the LULC parameters were classified into 5 classes, shown below:

1. Forest
2. Agriculture
3. Shrubland/Barrenland
4. Grassland
5. Settlement

i) Rank the cover types according to their order of highest potential for erosion risk to lowest potential for erosion risk [i.e. on a scale of 1 (lowest potential) to 5 (highest)].

LULC	*Rank*
Forest	1
Agriculture	5
Shrubland/Barrenland	4
Grassland	2
Settlement	3

* Test site: **Ethiopian Highlands** (tropical climate).

If you have any additional information or opinions, please provide them below:

I work on new approaches on the estimation of soil erosion risk based on the GIS-adopted equation; this provides very good results compared with field measurement and reservoir sedimentation rate. For more details see the related papers in electronic form at http://milevski.50webs.com.

Appendix 8: Mean average soil loss (t/ha/yr) of Italy for each of the provinces as obtained from two different erosion risk maps

ID	Province	Erosion risk map van der Knijff et al., (2002a, b)	Erosion risk map F-WERCAM
1	Sondrio	124.354	78.268
2	Viterbo	5.523	8.474
3	Catanzaro	11.423	21.460
4	Carbonia-Iglesias	5.127	10.953
5	Ravenna	2.239	2.867
6	Bolzano	61.371	66.042
7	Belluno	88.698	35.622
8	Trento	52.538	19.748
9	Verbano Cusio Ossola	35.913	21.605
10	Padua	0.510	0.991
11	Pordenone	34.753	12.796
12	Brescia	18.985	9.001
13	Como	6.210	3.392
14	Lecco	8.115	1.372
15	Varese	2.271	0.872
16	Treviso	3.506	2.017
17	Bergamo	21.852	11.745
18	Vicenza	8.533	2.054
19	Aosta	151.095	72.356
20	Vercelli	19.153	10.714
21	Novara	1.460	0.414
22	Verona	4.888	2.836
23	Trieste	10.395	5.372
24	Udine	37.657	23.480
25	Biella	15.086	3.779
26	Gorizia	2.416	2.598
27	Milan	0.342	0.907
28	Monza	0.881	1.537
29	Turin	36.813	6.892
30	Cremona	0.147	0.479
31	Lodi	0.275	0.474
32	Mantua	0.232	0.757
33	Pavia	3.427	1.756
34	Venecia	0.063	0.538
35	Alessandria	8.696	2.141
36	Piacenza	9.869	4.668
37	Asti	8.083	3.588
38	Parma	8.028	4.265
39	Rovigo	0.058	0.471

ID	Province	Erosion risk map van der Knijff et al., (2002a, b)	Erosion risk map F-WERCAM
40	Reggio nell'Emilia	5.190	4.506
41	Modena	4.298	5.842
42	Cuneo	25.726	3.987
43	Bologna	4.999	4.638
44	Ferrara	0.055	0.624
45	Genoa	12.463	1.080
46	Savona	13.261	4.827
47	Massa-Carrara	10.015	3.026
48	Forli-Cesena	9.462	6.405
49	Florence	5.381	9.306
50	Rimini	8.397	6.646
51	Lucca	6.422	1.303
52	Pistoia	2.421	1.137
53	Imperia	24.526	12.785
54	Prato	3.676	2.480
55	La Spezia	8.029	1.070
56	Pesaro e Urbino	12.649	7.994
57	Pisa	3.964	12.020
58	Arezzo	5.004	2.523
59	Ancona	17.576	11.029
60	Perugia	9.498	6.781
61	Fermo	23.268	60.872
62	Siena	5.376	5.960
63	Macerata	18.363	22.922
64	Grosseto	4.926	4.371
65	Ascoli Piceno	24.594	40.255
66	Terni	7.262	8.743
67	Teramo	23.724	42.147
68	Rieti	11.537	5.353
69	Livorno	11.460	4.694
70	L'Aquila	23.086	27.863
71	Pescara	12.816	21.709
72	Chieti	13.310	16.493
73	Rome	7.191	16.404
74	Foggia	5.321	9.187
75	Campobasso	9.361	12.161
76	Frosinone	14.991	28.233
77	Isernia	9.325	14.868
78	Caserta	11.457	23.147
79	Benevento	15.577	21.919
80	Barletta-Andria-Trani	2.248	3.217
81	Avellino	15.986	11.943
82	Bari	2.447	3.656

ID	Province	Erosion risk map van der Knijff et al., (2002a, b)	Erosion risk map F-WERCAM
83	Potenza	11.244	16.921
84	Sassari	10.237	14.740
85	Olbia-Tempio	8.486	9.205
86	Latina	14.533	27.432
87	Nuoro	12.609	16.376
88	Salerno	12.706	20.346
89	Brindisi	1.247	3.033
90	Napoli	34.426	45.940
91	Taranto	1.740	2.911
92	Oristano	6.245	6.786
93	Matera	10.723	24.772
94	Cosenza	9.749	19.831
95	Lecce	1.834	2.250
96	Ogliastra	13.303	15.388
97	Medio Campidano	5.040	8.450
98	Crotone	10.868	19.067
99	Cagliari	6.513	7.340
100	Vibo Valentia	11.272	24.552
101	Messina	28.917	57.211
102	Reggio di Calabria	21.401	42.320
103	Palermo	31.699	120.328
104	Trapani	8.458	25.034
105	Catania	23.341	21.914
106	Enna	21.175	110.564
107	Caltanissetta	19.993	79.290
108	Ragusa	7.819	14.438
109	Agrigento	18.900	50.211
110	Syracuse	9.249	18.506

CURRICULAM VITAE

Personal Information

Name: Oinam Bakimchandra
Date of Birth: 15.12.1979
Place of Birth: Imphal, Manipur, India
Email ID: bakim143@gmail.com

Educational Background

10/2007-05/2011:   *Doctoral degree*; International Doctoral Program: Environment and Water, ENWAT (Department of Hydraulic Engineering and Water Resource Management, University of Stuttgart, Germany)

06/2004-01/2006:   *Master of Geo-information Science* (specializing in Hazard and Risk Analysis); International Institute of Geo-information & Earth Science, ITC, The Netherlands (in collaboration with Indian Institute of Remote Sensing, Dehradun, India.)

10/2001-06/2003:   *Master of Civil Engineering* (specializing in Construction Technology & Management); Madhav Institute of Technology & Science, (MITS) under Rajiv Gandhi Technical University, Bhopal, M.P., India.

05/1997-07/2001:   *Bachelor of Civil Engineering*; Tripura Engineering College under Tripura University (Presently, National Institute of Technology, NIT-Agartala, India.)

Working/Research Experience

02/2006- 05/2007:   Actively involved as *Research Assistant/Scholar* under the supervision of Professor Nayan Sharma, WRDM, IIT-Roorkee, India in a project "Topographic Analysis and Terrian fly through generation of Kullu Airport runway extension using automated generated DEM" (a Consultancy Project of Airport Authority of India, Kullu, Manalia, India).

List of Publications (Journals/Conferences/Magazines)

1. N. Sharma, B.R.Parida and **B. Oinam**, (2006). Assessment of annual soil erosion rate of Brahmaputra Basin in India using remote sensing and GIS-a comparative analysis of empirical

based models. ***UNESCO-IHP-ISI workshop on "Sediment management in South and South East Asia"***, 24-25 April 2006, AIT campus, Pathumthani, Thailand. (Published in Proceedings of the symposium)

2. N.Sharma, **B.Oinam** and B.R.Parida (2006) Remote Sensing Based Study on Channel Changes and Wetland Ecosystem Dynamics of Brahmaputra River in India. ***"International Conference on Riverine Hydro-ecology: Advance in Research and Applications***": 13-18th August 2006, University of Stirling, UK.

3. B.R.Parida, **B. Oinam**, N. Sharma, Manzul.H and R. Kandwal (2008). Land Surface Temperature Variation with relation to Vegetation Types using MODIS Satellite Data in Gujarat state of India. ***International Journal of Remote Sensing***, Volume 29, Number 14, 2008 , pp. 4219-4235(17) *Link to the article:*
http://www.informaworld.com/smpp/content~db=all~content=a794086605~frm=titlelink

4. Bikash Ranjan Parida and **Bakimchandra Oinam**, (2008). Drought monitoring in India and the Philippines with satellite remote sensing measurements. ***EARSeL eProceedings*** 7, 1/2008. *Link to the article:*
http://www.eproceedings.org/static/vol07_1/07_1_parida1.pdf?SessionID=5460d0f64d07f1c885ca8

5. Ngangbam Romeji and **Bakimchandra Oinam**, (2008). Mapping dynamic change in Phumdi distribution from multi-temporal satellite imagery: An assessment on Loktak Freshwater wetland, Manipur, India; ***XXI ISPRS Congress***, Bejing, China.

6. **Bakimchandra Oinam** (2008) 'One needs not be a Rocket Scientist or a Nuclear Scientist...!' ***Young Geo Professional Magazine***, pp. 4-6, October 2008, Reed Business bv, The Netherlands.

7. **Bakimchandra Oinam** (2009) Geospatial Revolution, Column article on ***GIM International Magazine***, May 2009 edition, The Netherlands.

8. **Bakimchandra Oinam** and Silke Wieprecht (2009) 'Is the immune system of our Blue planet weakening?'***10th IAHR Colloquium,, Social, Economical and Political perspective of water":*** 2nd December 2009, Stuttgart University. (Poster session)

9. Sharma, N., Janauer, G., Mondal, Md. S., **Bakimchandra, O**.(2010) Wetland Ecosystem Dynamics Assessment in the Deepor Beel of Brahmaputra Basin using Geoinformatic Technique. ***Lakes & Reservoirs: Research and Management Journal*** (under review).

10. **Oinam, B**., Walter, M., Scholten, T. and Wieprecht, S., (2011) A Fuzzy Rule Base approach towards Developing and Mapping the Soil Protection Index (SPI): a Case Study on Upper Awash basin in Ethiopian Highlands. Submitted to the Journal of ***Land Degradation and Development*** (under review)

Awards/ Scholarships

- Gold Medalist-2001 in Bachelor of Civil Engineering, Tripura University

- 3 month - ITC Fellowship 2005, for undergoing a short-term course in " GIS and Remote Sensing for Natural Hazards and Risk Assessment, EREG 2.0, ITC, The Netherlands.

- DAAD (Deutscher Akademischer Austausch Dienst) scholarship for undergoing PhD program at University of Stuttgart, Germany. (*Starting June 2007 till dated*)

- Financial supports from Marie Curie Actions program, European Commission (EU) for attending Marie Curie Series of Events: METIER graduate training course at Helsinki in 2008 (Finland) and at Brussel in 2009 (Belgium).

Computer/Software Proficiency

RS and GIS Software : ERDAS imagine, Arc View, Arc GIS 9.2, ILWIS 3.3, ENVI

Soil Erosion Models : GEOWEPP, SWAT, RUSLE, MUSLE, USPED, F-WERCAM

Others Software : MS Office, Adobe Photoshop, SPSS, MatLab
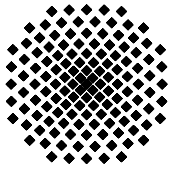
Institut für Wasserbau
Universität Stuttgart

Pfaffenwaldring 61
70569 Stuttgart (Vaihingen)
Telefon (0711) 685 - 64717/64749/64752/64679
Telefax (0711) 685 - 67020 o. 64746 o. 64681
E-Mail: iws@iws.uni-stuttgart.de
http://www.iws.uni-stuttgart.de

Direktoren
Prof. Dr. rer. nat. Dr.-Ing. András Bárdossy
Prof. Dr.-Ing. Rainer Helmig
Prof. Dr.-Ing. Silke Wieprecht

Vorstand *(Stand 01.04.2009)*
Prof. Dr. rer. nat. Dr.-Ing. A. Bárdossy
Prof. Dr.-Ing. R. Helmig
Prof. Dr.-Ing. S. Wieprecht
Jürgen Braun, PhD
Dr.-Ing. H. Class
Dr.-Ing. S. Hartmann
Dr.-Ing. H.-P. Koschitzky
PD Dr.-Ing. W. Marx
Dr. rer. nat. J. Seidel

Emeriti
Prof. Dr.-Ing. habil. Dr.-Ing. E.h. Jürgen Giesecke
Prof. Dr.h.c. Dr.-Ing. E.h. Helmut Kobus, PhD

Lehrstuhl für Wasserbau und
Wassermengenwirtschaft
Leiter: Prof. Dr.-Ing. Silke Wieprecht
Stellv.: PD Dr.-Ing. Walter Marx, AOR

Versuchsanstalt für Wasserbau
Leiter: Dr.-Ing. Sven Hartmann, AOR

Lehrstuhl für Hydromechanik
und Hydrosystemmodellierung
Leiter: Prof. Dr.-Ing. Rainer Helmig
Stellv.: Dr.-Ing. Holger Class, AOR

Lehrstuhl für Hydrologie und Geohydrologie
Leiter: Prof. Dr. rer. nat. Dr.-Ing. András Bárdossy
Stellv.: Dr. rer. nat. Jochen Seidel

VEGAS, **Versuchseinrichtung zur**
Grundwasser- und Altlastensanierung
Leitung: Jürgen Braun, PhD
                Dr.-Ing. Hans-Peter Koschitzky, AD

Verzeichnis der Mitteilungshefte

5 Plate, Erich: *Beitrag zur Bestimmung der Windgeschwindigkeitsverteilung in der durch eine Wand gestörten bodennahen Luftschicht,* und Röhnisch, Arthur; Marotz, Günter: *Neue Baustoffe und Bauausführungen für den Schutz der Böschungen und der Sohle von Kanälen, Flüssen und Häfen; Gestehungskosten und jeweilige Vorteile,* sowie Unny, T.E.: *Schwingungsuntersuchungen am Kegelstrahlschieber,* 1967

6 Seiler, Erich: *Die Ermittlung des Anlagenwertes der bundeseigenen Binnenschiffahrtsstraßen und Talsperren und des Anteils der Binnenschiffahrt an diesem Wert,* 1967

7 *Sonderheft anläßlich des 65. Geburtstages von Prof. Arthur Röhnisch mit Beiträgen von* Benk, Dieter; Breitling, J.; Gurr, Siegfried; Haberhauer, Robert; Honekamp, Hermann; Kuz, Klaus Dieter; Marotz, Günter; Mayer-Vorfelder, Hans-Jörg; Miller, Rudolf; Plate, Erich J.; Radomski, Helge; Schwarz, Helmut; Vollmer, Ernst; Wildenhahn, Eberhard; 1967

8 Jumikis, Alfred: *Beitrag zur experimentellen Untersuchung des Wassernachschubs in einem gefrierenden Boden und die Beurteilung der Ergebnisse,* 1968

9 Marotz, Günter: *Technische Grundlagen einer Wasserspeicherung im natürlichen Untergrund,* 1968

10 Radomski, Helge: *Untersuchungen über den Einfluß der Querschnittsform wellenförmiger Spundwände auf die statischen und rammtechnischen Eigenschaften,* 1968

11 Schwarz, Helmut: *Die Grenztragfähigkeit des Baugrundes bei Einwirkung vertikal gezogener Ankerplatten als zweidimensionales Bruchproblem,* 1969

12 Erbel, Klaus: *Ein Beitrag zur Untersuchung der Metamorphose von Mittelgebirgsschneedecken unter besonderer Berücksichtigung eines Verfahrens zur Bestimmung der thermischen Schneequalität,* 1969

13 Westhaus, Karl-Heinz: *Der Strukturwandel in der Binnenschiffahrt und sein Einfluß auf den Ausbau der Binnenschiffskanäle,* 1969

14 Mayer-Vorfelder, Hans-Jörg: *Ein Beitrag zur Berechnung des Erdwiderstandes unter Ansatz der logarithmischen Spirale als Gleitflächenfunktion,* 1970

15 Schulz, Manfred: *Berechnung des räumlichen Erddruckes auf die Wandung kreiszylindrischer Körper,* 1970

16 Mobasseri, Manoutschehr: *Die Rippenstützmauer. Konstruktion und Grenzen ihrer Standsicherheit,* 1970

17 Benk, Dieter: *Ein Beitrag zum Betrieb und zur Bemessung von Hochwasserrückhaltebecken,* 1970

33   Rueff, Helge: *Untersuchung der schwingungserregenden Kräfte an zwei hinterein-ander angeordneten Tiefschützen unter besonderer Berücksichtigung von Kavita-tion*, 1974

34   Röhnisch, Arthur: *Einpreßversuche mit Zementmörtel für Spannbeton - Vergleich der Ergebnisse von Modellversuchen mit Ausführungen in Hüllwellrohren*, 1975

35   *Sonderheft anläßlich des 65. Geburtstages von Prof. Dr.-Ing. Kurt Petrikat mit Bei-trägen von*: Brombach, Hansjörg; Erbel, Klaus; Flinspach, Dieter; Fischer jr., Ri-chard; Gàl, Attila; Gerlach, Reinhard; Giesecke, Jürgen; Haberhauer, Robert; Haf-ner Edzard; Hausenblas, Bernhard; Horlacher, Hans-Burkhard; Hutarew, Andreas; Knoll, Manfred; Krummet, Ralph; Marotz, Günter; Merkle, Theodor; Miller, Chris-toph; Minor, Hans-Erwin; Neumayer, Hans; Rao, Syamala; Rath, Paul; Rueff, Hel-ge; Ruppert, Jürgen; Schwarz, Wolfgang; Topal-Gökceli, Mehmet; Vollmer, Ernst; Wang, Chung-su; Weber, Hans-Georg; 1975

36   Berger, Jochum: *Beitrag zur Berechnung des Spannungszustandes in rotations-symmetrisch belasteten Kugelschalen veränderlicher Wandstärke unter Gas- und Flüssigkeitsdruck durch Integration schwach singulärer Differentialgleichungen*, 1975

37   Dirksen, Wolfram: *Berechnung instationärer Abflußvorgänge in gestauten Gerin-nen mittels Differenzenverfahren und die Anwendung auf Hochwasserrückhalte-becken*, 1976

38   Horlacher, Hans-Burkhard: *Berechnung instationärer Temperatur- und Wärme-spannungsfelder in langen mehrschichtigen Hohlzylindern*, 1976

39   Hafner, Edzard: *Untersuchung der hydrodynamischen Kräfte auf Baukörper im Tiefwasserbereich des Meeres*, 1977, ISBN 3-921694-39-6

40   Ruppert, Jürgen: *Über den Axialwirbelkammerverstärker für den Einsatz im Was-serbau*, 1977, ISBN 3-921694-40-X

41   Hutarew, Andreas: *Beitrag zur Beeinflußbarkeit des Sauerstoffgehalts in Fließge-wässern an Abstürzen und Wehren*, 1977, ISBN 3-921694-41-8, vergriffen

42   Miller, Christoph: *Ein Beitrag zur Bestimmung der schwingungserregenden Kräfte an unterströmten Wehren*, 1977, ISBN 3-921694-42-6

43   Schwarz, Wolfgang: *Druckstoßberechnung unter Berücksichtigung der Radial- und Längsverschiebungen der Rohrwandung*, 1978, ISBN 3-921694-43-4

44   Kinzelbach, Wolfgang: *Numerische Untersuchungen über den optimalen Einsatz variabler Kühlsysteme einer Kraftwerkskette am Beispiel Oberrhein*, 1978, ISBN 3-921694-44-2

45   Barczewski, Baldur: *Neue Meßmethoden für Wasser-Luftgemische und deren An-wendung auf zweiphasige Auftriebsstrahlen*, 1979, ISBN 3-921694-45-0

62   Kaleris, Vassilios: *Erfassung des Austausches von Oberflächen- und Grundwasser in horizontalebenen Grundwassermodellen*, 1986, ISBN 3-921694-62-0

63   Herr, Michael: *Grundlagen der hydraulischen Sanierung verunreinigter Porengrundwasserleiter*, 1987, ISBN 3-921694-63-9

64   Marx, Walter: *Berechnung von Temperatur und Spannung in Massenbeton infolge Hydratation*, 1987, ISBN 3-921694-64-7

65   Koschitzky, Hans-Peter: *Dimensionierungskonzept für Sohlbelüfter in Schußrinnen zur Vermeidung von Kavitationsschäden*, 1987, ISBN 3-921694-65-5

66   Kobus, Helmut (Hrsg.): *Modellierung des großräumigen Wärme- und Schadstofftransports im Grundwasser*, Tätigkeitsbericht 1986/87 (DFG-Forschergruppe an den Universitäten Hohenheim, Karlsruhe und Stuttgart) 1987, ISBN 3-921694-66-3

67   Söll, Thomas: *Berechnungsverfahren zur Abschätzung anthropogener Temperaturanomalien im Grundwasser*, 1988, ISBN 3-921694-67-1

68   Dittrich, Andreas; Westrich, Bernd: *Bodenseeufererosion, Bestandsaufnahme und Bewertung*, 1988, ISBN 3-921694-68-X, vergriffen

69   Huwe, Bernd; van der Ploeg, Rienk R.: *Modelle zur Simulation des Stickstoffhaushaltes von Standorten mit unterschiedlicher landwirtschaftlicher Nutzung*, 1988, ISBN 3-921694-69-8, vergriffen

70   Stephan, Karl: *Integration elliptischer Funktionen*, 1988, ISBN 3-921694-70-1

71   Kobus, Helmut; Zilliox, Lothaire (Hrsg.): *Nitratbelastung des Grundwassers, Auswirkungen der Landwirtschaft auf die Grundwasser- und Rohwasserbeschaffenheit und Maßnahmen zum Schutz des Grundwassers*. Vorträge des deutsch-französischen Kolloquiums am 6. Oktober 1988, Universitäten Stuttgart und Louis Pasteur Strasbourg (Vorträge in deutsch oder französisch, Kurzfassungen zweisprachig), 1988, ISBN 3-921694-71-X

72   Soyeaux, Renald: *Unterströmung von Stauanlagen auf klüftigem Untergrund unter Berücksichtigung laminarer und turbulenter Fließzustände*, 1991, ISBN 3-921694-72-8

73   Kohane, Roberto: *Berechnungsmethoden für Hochwasserabfluß in Fließgewässern mit überströmten Vorländern*, 1991, ISBN 3-921694-73-6

74   Hassinger, Reinhard: *Beitrag zur Hydraulik und Bemessung von Blocksteinrampen in flexibler Bauweise*, 1991, ISBN 3-921694-74-4, vergriffen

75   Schäfer, Gerhard: *Einfluß von Schichtenstrukturen und lokalen Einlagerungen auf die Längsdispersion in Porengrundwasserleitern*, 1991, ISBN 3-921694-75-2

76   Giesecke, Jürgen: *Vorträge, Wasserwirtschaft in stark besiedelten Regionen; Umweltforschung mit Schwerpunkt Wasserwirtschaft*, 1991, ISBN 3-921694-76-0

92   Emmert, Martin: *Numerische Modellierung nichtisothermer Gas-Wasser Systeme in porösen Medien,* 1997, ISBN 3-921694-92-2

93   Kern, Ulrich: *Transport von Schweb- und Schadstoffen in staugeregelten Fließgewässern am Beispiel des Neckars*, 1997, ISBN 3-921694-93-0, vergriffen

94   Förster, Georg: *Druckstoßdämpfung durch große Luftblasen in Hochpunkten von Rohrleitungen 1997*, ISBN 3-921694-94-9

95   Cirpka, Olaf: *Numerische Methoden zur Simulation des reaktiven Mehrkomponententransports im Grundwasser*, 1997, ISBN 3-921694-95-7, vergriffen

96   Färber, Arne: *Wärmetransport in der ungesättigten Bodenzone: Entwicklung einer thermischen In-situ-Sanierungstechnologie*, 1997, ISBN 3-921694-96-5

97   Betz, Christoph: *Wasserdampfdestillation von Schadstoffen im porösen Medium: Entwicklung einer thermischen In-situ-Sanierungstechnologie*, 1998, ISBN 3-921694-97-3

98   Xu, Yichun: *Numerical Modeling of Suspended Sediment Transport in Rivers*, 1998, ISBN 3-921694-98-1, vergriffen

99   Wüst, Wolfgang: *Geochemische Untersuchungen zur Sanierung CKW-kontaminierter Aquifere mit Fe(0)-Reaktionswänden,* 2000, ISBN 3-933761-02-2

100   Sheta, Hussam: *Simulation von Mehrphasenvorgängen in porösen Medien unter Einbeziehung von Hysterese-Effekten*, 2000, ISBN 3-933761-03-4

101   Ayros, Edwin: *Regionalisierung extremer Abflüsse auf der Grundlage statistischer Verfahren*, 2000, ISBN 3-933761-04-2, vergriffen

102   Huber, Ralf: *Compositional Multiphase Flow and Transport in Heterogeneous Porous Media*, 2000, ISBN 3-933761-05-0

103   Braun, Christopherus: *Ein Upscaling-Verfahren für Mehrphasenströmungen in porösen Medien*, 2000, ISBN 3-933761-06-9

104   Hofmann, Bernd: *Entwicklung eines rechnergestützten Managementsystems zur Beurteilung von Grundwasserschadensfällen*, 2000, ISBN 3-933761-07-7

105   Class, Holger: *Theorie und numerische Modellierung nichtisothermer Mehrphasenprozesse in NAPL-kontaminierten porösen Medien,* 2001, ISBN 3-933761-08-5

106   Schmidt, Reinhard: *Wasserdampf- und Heißluftinjektion zur thermischen Sanierung kontaminierter Standorte*, 2001, ISBN 3-933761-09-3

107   Josef, Reinhold:, *Schadstoffextraktion mit hydraulischen Sanierungsverfahren unter Anwendung von grenzflächenaktiven Stoffen*, 2001, ISBN 3-933761-10-7

124   Hrsg.: Schrenk, Volker; Batereau, Katrin; Barczewski, Baldur; Weber, Karolin und Koschitzky, Hans-Peter: *Symposium Ressource Fläche und VEGAS - Statuskolloquium 2003, 30. September und 1. Oktober 2003,* 2003, ISBN 3-933761-27-1

125   Omar Khalil Ouda: *Optimisation of Agricultural Water Use: A Decision Support System for the Gaza Strip,* 2003, ISBN 3-933761-28-0

126   Batereau, Katrin: *Sensorbasierte Bodenluftmessung zur Vor-Ort-Erkundung von Schadensherden im Untergrund*, 2004, ISBN 3-933761-29-8

127   Witt, Oliver: *Erosionsstabilität von Gewässersedimenten mit Auswirkung auf den Stofftransport bei Hochwasser am Beispiel ausgewählter Stauhaltungen des Oberrheins*, 2004, ISBN 3-933761-30-1

128   Jakobs, Hartmut: *Simulation nicht-isothermer Gas-Wasser-Prozesse in komplexen Kluft-Matrix-Systemen*, 2004, ISBN 3-933761-31-X

129   Li, Chen-Chien: *Deterministisch-stochastisches Berechnungskonzept zur Beurteilung der Auswirkungen erosiver Hochwasserereignisse in Flussstauhaltungen,* 2004, ISBN 3-933761-32-8

130   Reichenberger, Volker; Helmig, Rainer; Jakobs, Hartmut; Bastian, Peter; Niessner, Jennifer: *Complex Gas-Water Processes in Discrete Fracture-Matrix Systems: Upscaling, Mass-Conservative Discretization and Efficient Multilevel Solution,* 2004, ISBN 3-933761-33-6

131   Hrsg.: Barczewski, Baldur; Koschitzky, Hans-Peter; Weber, Karolin; Wege, Ralf: *VEGAS - Statuskolloquium 2004,* Tagungsband zur Veranstaltung am 05. Oktober 2004 an der Universität Stuttgart, Campus Stuttgart-Vaihingen, 2004, ISBN 3-933761-34-4

132   Asie, Kemal Jabir: *Finite Volume Models for Multiphase Multicomponent Flow through Porous Media*. 2005, ISBN 3-933761-35-2

133   Jacoub, George: *Development of a 2-D Numerical Module for Particulate Contaminant Transport in Flood Retention Reservoirs and Impounded Rivers,* 2004, ISBN 3-933761-36-0

134   Nowak, Wolfgang: *Geostatistical Methods for the Identification of Flow and Transport Parameters in the Subsurface,* 2005, ISBN 3-933761-37-9

135   Süß, Mia: *Analysis of the influence of structures and boundaries on flow and transport processes in fractured porous media*, 2005, ISBN 3-933761-38-7

136   Jose, Surabhin Chackiath: *Experimental Investigations on Longitudinal Dispersive Mixing in Heterogeneous Aquifers,* 2005, ISBN: 3-933761-39-5

137   Filiz, Fulya: *Linking Large-Scale Meteorological Conditions to Floods in Mesoscale Catchments,* 2005, ISBN 3-933761-40-9

138 Qin, Minghao: *Wirklichkeitsnahe und recheneffiziente Ermittlung von Temperatur und Spannungen bei großen RCC-Staumauern*, 2005, ISBN 3-933761-41-7

139 Kobayashi, Kenichiro: *Optimization Methods for Multiphase Systems in the Subsurface - Application to Methane Migration in Coal Mining Areas*, 2005, ISBN 3-933761-42-5

140 Rahman, Md. Arifur: *Experimental Investigations on Transverse Dispersive Mixing in Heterogeneous Porous Media,* 2005, ISBN 3-933761-43-3

141 Schrenk, Volker: *Ökobilanzen zur Bewertung von Altlastensanierungsmaßnahmen,* 2005, ISBN 3-933761-44-1

142 Hundecha, Hirpa Yeshewatesfa: *Regionalization of Parameters of a Conceptual Rainfall-Runoff Model,* 2005, ISBN: 3-933761-45-X

143 Wege, Ralf: *Untersuchungs- und Überwachungsmethoden für die Beurteilung natürlicher Selbstreinigungsprozesse im Grundwasser,* 2005, ISBN 3-933761-46-8

144 Breiting, Thomas: *Techniken und Methoden der Hydroinformatik - Modellierung von komplexen Hydrosystemen im Untergrund,* 2006, 3-933761-47-6

145 Hrsg.: Braun, Jürgen; Koschitzky, Hans-Peter; Müller, Martin: *Ressource Untergrund: 10 Jahre VEGAS: Forschung und Technologieentwicklung zum Schutz von Grundwasser und Boden,* Tagungsband zur Veranstaltung am 28. und 29. September 2005 an der Universität Stuttgart, Campus Stuttgart-Vaihingen, 2005, ISBN 3-933761-48-4

146 Rojanschi, Vlad: *Abflusskonzentration in mesoskaligen Einzugsgebieten unter Berücksichtigung des Sickerraumes,* 2006, ISBN 3-933761-49-2

147 Winkler, Nina Simone: *Optimierung der Steuerung von Hochwasserrückhaltebecken-systemen,* 2006, ISBN 3-933761-50-6

148 Wolf, Jens: *Räumlich differenzierte Modellierung der Grundwasserströmung alluvialer Aquifere für mesoskalige Einzugsgebiete,* 2006, ISBN: 3-933761-51-4

149 Kohler, Beate: *Externe Effekte der Laufwasserkraftnutzung,* 2006, ISBN 3-933761-52-2

150 Hrsg.: Braun, Jürgen; Koschitzky, Hans-Peter; Stuhrmann, Matthias: *VEGAS-Statuskolloquium 2006,* Tagungsband zur Veranstaltung am 28. September 2006 an der Universität Stuttgart, Campus Stuttgart-Vaihingen, 2006, ISBN 3-933761-53-0

151 Niessner, Jennifer: *Multi-Scale Modeling of Multi-Phase - Multi-Component Processes in Heterogeneous Porous Media,* 2006, ISBN 3-933761-54-9

152 Fischer, Markus: *Beanspruchung eingeerdeter Rohrleitungen infolge Austrocknung bindiger Böden,* 2006, ISBN 3-933761-55-7

153 Schneck, Alexander: *Optimierung der Grundwasserbewirtschaftung unter Berücksichtigung der Belange der Wasserversorgung, der Landwirtschaft und des Naturschutzes*, 2006, ISBN 3-933761-56-5

154 Das, Tapash: *The Impact of Spatial Variability of Precipitation on the Predictive Uncertainty of Hydrological Models,* 2006, ISBN 3-933761-57-3

155 Bielinski, Andreas: *Numerical Simulation of CO_2 sequestration in geological formations*, 2007, ISBN 3-933761-58-1

156 Mödinger, Jens: *Entwicklung eines Bewertungs- und Entscheidungsunterstützungssystems für eine nachhaltige regionale Grundwasserbewirtschaftung*, 2006, ISBN 3-933761-60-3

157 Manthey, Sabine: *Two-phase flow processes with dynamic effects in porous media - parameter estimation and simulation,* 2007, ISBN 3-933761-61-1

158 Pozos Estrada, Oscar: *Investigation on the Effects of Entrained Air in Pipelines,* 2007, ISBN 3-933761-62-X

159 Ochs, Steffen Oliver: *Steam injection into saturated porous media – process analysis including experimental and numerical investigations*, 2007, ISBN 3-933761-63-8

160 Marx, Andreas: *Einsatz gekoppelter Modelle und Wetterradar zur Abschätzung von Niederschlagsintensitäten und zur Abflussvorhersage, 2007,* ISBN 3-933761-64-6

161 Hartmann, Gabriele Maria: *Investigation of Evapotranspiration Concepts in Hydrological Modelling for Climate Change Impact Assessment*, 2007, ISBN 3-933761-65-4

162 Kebede Gurmessa, Tesfaye: *Numerical Investigation on Flow and Transport Characteristics to Improve Long-Term Simulation of Reservoir Sedimentation*, 2007, ISBN 3-933761-66-2

163 Trifković, Aleksandar: *Multi-objective and Risk-based Modelling Methodology for Planning, Design and Operation of Water Supply Systems*, 2007, ISBN 3-933761-67-0

164 Götzinger, Jens: *Distributed Conceptual Hydrological Modelling - Simulation of Climate, Land Use Change Impact and Uncertainty Analysis*, 2007, ISBN 3-933761-68-9

165 Hrsg.: Braun, Jürgen; Koschitzky, Hans-Peter; Stuhrmann, Matthias: *VEGAS – Kolloquium 2007,* Tagungsband zur Veranstaltung am 26. September 2007 an der Universität Stuttgart, Campus Stuttgart-Vaihingen, 2007, ISBN 3-933761-69-7

166 Freeman, Beau: *Modernization Criteria Assessment for Water Resources Planning; Klamath Irrigation Project, U.S.*, 2008, ISBN 3-933761-70-0

167 Dreher, Thomas: *Selektive Sedimentation von Feinstschwebstoffen in Wechselwirkung mit wandnahen turbulenten Strömungsbedingungen*, 2008, ISBN 3-933761-71-9

168 Yang, Wei: *Discrete-Continuous Downscaling Model for Generating Daily Precipitation Time Series*, 2008, ISBN 3-933761-72-7

169 Kopecki, Ianina: *Calculational Approach to FST-Hemispheres for Multiparametrical Benthos Habitat Modelling,* 2008, ISBN 3-933761-73-5

170 Brommundt, Jürgen: *Stochastische Generierung räumlich zusammenhängender Niederschlagszeitreihen*, 2008, ISBN 3-933761-74-3

171 Papafotiou, *Alexandros: Numerical Investigations of the Role of Hysteresis in Heterogeneous Two-Phase Flow Systems*, 2008, ISBN 3-933761-75-1

172 He, Yi: *Application of a Non-Parametric Classification Scheme to Catchment Hydrology,* 2008, ISBN 978-3-933761-76-7

173 Wagner, Sven: *Water Balance in a Poorly Gauged Basin in West Africa Using Atmospheric Modelling and Remote Sensing Information*, 2008, ISBN 978-3-933761-77-4

174 Hrsg.: Braun, Jürgen; Koschitzky, Hans-Peter; Stuhrmann, Matthias; Schrenk, Volker: *VEGAS-Kolloquium 2008 Ressource Fläche III*, Tagungsband zur Veranstaltung am 01. Oktober 2008 an der Universität Stuttgart, Campus Stuttgart-Vaihingen, 2008, ISBN 978-3-933761-78-1

175 Patil, Sachin: *Regionalization of an Event Based Nash Cascade Model for Flood Predictions in Ungauged Basins*, 2008, ISBN 978-3-933761-79-8

176 Assteerawatt, Anongnart: *Flow and Transport Modelling of Fractured Aquifers based on a Geostatistical Approach,* 2008, ISBN 978-3-933761-80-4

177 Karnahl, Joachim Alexander: *2D numerische Modellierung von multifraktionalem Schwebstoff- und Schadstofftransport in Flüssen*, 2008, ISBN 978-3-933761-81-1

178 Hiester, Uwe: *Technologieentwicklung zur In-situ-Sanierung der ungesättigten Bodenzone mit festen Wärmequellen,* 2009, ISBN 978-3-933761-82-8

179 Laux, Patrick: *Statistical Modeling of Precipitation for Agricultural Planning in the Volta Basin of West Africa,* 2009, ISBN 978-3-933761-83-5

180 Ehsan, Saqib: *Evaluation of Life Safety Risks Related to Severe Flooding*, 2009, ISBN 978-3-933761-84-2

181 Prohaska, Sandra: *Development and Application of a 1D Multi-Strip Fine Sediment Transport Model for Regulated Rivers,* 2009, ISBN 978-3-933761-85-9

182 Kopp, Andreas: *Evaluation of CO$_2$ Injection Processes in Geological Formations for Site Screening,* 2009, ISBN 978-3-933761-86-6

183 Ebigbo, Anozie: *Modelling of biofilm growth and its influence on CO$_2$ and water (two-phase) flow in porous media,* 2009, ISBN 978-3-933761-87-3

184 Freiboth, Sandra: *A phenomenological model for the numerical simulation of multiphase multicomponent processes considering structural alterations of porous media*, 2009, ISBN 978-3-933761-88-0

185 Zöllner, Frank: *Implementierung und Anwendung netzfreier Methoden im Konstruktiven Wasserbau und in der Hydromechanik*, 2009, ISBN 978-3-933761-89-7

186 Vasin, Milos: *Influence of the soil structure and property contrast on flow and transport in the unsaturated zone*, 2010, ISBN 978-3-933761-90-3

187 Li, Jing: *Application of Copulas as a New Geostatistical Tool*, 2010, ISBN 978-3-933761-91-0

188 AghaKouchak, Amir: *Simulation of Remotely Sensed Rainfall Fields Using Copulas*, 2010, ISBN 978-3-933761-92-7

189 Thapa, Pawan Kumar: *Physically-based spatially distributed rainfall runoff modelling for soil erosion estimation*, 2010, ISBN 978-3-933761-93-4

190 Wurms, Sven: *Numerische Modellierung der Sedimentationsprozesse in Retentionsanlagen zur Steuerung von Stoffströmen bei extremen Hochwasserabflussereignissen*, 2011, ISBN 978-3-933761-94-1

191 Merkel, Uwe: *Unsicherheitsanalyse hydraulischer Einwirkungen auf Hochwasserschutzdeiche und Steigerung der Leistungsfähigkeit durch adaptive Strömungsmodellierung*, 2011, ISBN 978-3-933761-95-8

192 Fritz, Jochen: *A Decoupled Model for Compositional Non-Isothermal Multiphase Flow in Porous Media and Multiphysics Approaches for Two-Phase Flow*, 2010, ISBN 978-3-933761-96-5

193 Weber, Karolin (Hrsg.): *12. Treffen junger WissenschaftlerInnen an Wasserbauinstituten*, 2010, ISBN 978-3-933761-97-2

194 Bliefernicht, Jan-Geert: *Probability Forecasts of Daily Areal Precipitation for Small River Basins,* 2011, ISBN 978-3-933761-98-9

195 Hrsg.: Koschitzky, Hans-Peter; Braun, Jürgen: *VEGAS-Kolloquium 2010 In-situ-Sanierung - Stand und Entwicklung Nano und ISCO -,* Tagungsband zur Veranstaltung am 07. Oktober 2010 an der Universität Stuttgart, Campus Stuttgart-Vaihingen*, 2010, ISBN 978-3-933761-99-6*

196 Gafurov, Abror: *Water Balance Modeling Using Remote Sensing Information - Focus on Central Asia,* 2010, ISBN 978-3-942036-00-9

197 Mackenberg, Sylvia: *Die Quellstärke in der Sickerwasserprognose: Möglichkeiten und Grenzen von Labor- und Freilanduntersuchungen,* 2010, ISBN 978-3-942036-01-6

198 Singh, Shailesh Kumar: *Robust Parameter Estimation in Gauged and Ungauged Basins,* 2010, ISBN 978-3-942036-02-3

199 Doğan, Mehmet Onur: *Coupling of porous media flow with pipe flow,* 2011, ISBN 978-3-942036-03-0

200 Liu, Min: *Study of Topographic Effects on Hydrological Patterns and the Implication on Hydrological Modeling and Data Interpolation,* 2011, ISBN 978-3-942036-04-7

201 Geleta, Habtamu Itefa: *Watershed Sediment Yield Modeling for Data Scarce Areas,* 2011, ISBN 978-3-942036-05-4

202 Franke, Jörg: *Einfluss der Überwachung auf die Versagenswahrscheinlichkeit von Staustufen,* 2011, ISBN 978-3-942036-06-1

203 Bakimchandra, Oinam: *Integrated Fuzzy-GIS approach for assessing regional soil erosion risks,* 2011, ISBN 978-3-942036-07-8

Die Mitteilungshefte ab der Nr. 134 (Jg. 2005) stehen als pdf-Datei über die Homepage des Instituts: www.iws.uni-stuttgart.de zur Verfügung.